THESIS

EXPERIMENTAL EVALUATION OF STACK TESTING METHODS FOR ACCURATE VOC MEASUREMENT

Submitted by

Brenna Allison King

Department of Mechanical Engineering

In partial fulfillment of the requirements

For the Degree of Master of Science

Colorado State University

Fort Collins, Colorado

Summer 2019

Master's Committee:

Advisor: Daniel Olsen

Jason Quinn
Ellison Carter

ABSTRACT

EXPERIMENTAL EVALUATION OF STACK TESTING METHODS FOR ACCURATE VOC MEASUREMENT

There are more than 1,400 natural gas compressor stations that utilize large-bore, two-stroke natural gas engines in the United States to transport natural gas through pipelines across the country. Because of the long operating lives associated with these engines, it is important for emissions to be monitored and technology to be improved to ensure the engines are meeting current emissions standards. One emission class that is currently regulated by the Environmental Protection Agency (EPA) is volatile organic compounds (VOCs). VOCs are defined as non-methane, non-ethane hydrocarbons and have negative environmental effects, especially in the formation of ozone and fine particulates that create smog.

The combination of a Gas Chromatograph (GC) and a Flame Ionization Detector (FID) can be used to measure methane, ethane, and VOCs. The use of a GC/FID to quantify hydrocarbon concentration is in compliance with EPA Method 18/25A. In some cases, this approach is mandated by regulatory bodies. The Fourier Transform Infrared Spectrometer (FTIR) can also be used to measure VOCs in engine exhaust gas, following EPA Method 320. However, there is concern that Method 320 is not as accurate as Method 18/25A. The main objective of this research is to provide data and analysis with both measurement methods from different engine types, conditions, and fuel quality to determine whether Method 320 is acceptable for VOC quantification.

Exhaust gas was sampled from engines of different types and configurations: the GMV-4 lean burn testing with open chamber spark ignition, pre-combustion chamber ignition, and high-pressure fuel injection with electronic fuel valves and the Caterpillar 3304 rich burn testing with a three-way catalyst. For the GMV-4 configurations, an ignition timing sweep was performed, including retarding and advancing ignition timing from the nominal 18°aTDC. In addition, fuel ethane and fuel higher hydrocarbons were added to the natural gas fuel supply separately to determine the effects fuel variability has on emissions and engine performance. For the Caterpillar 3304 configuration, only an ignition timing sweep was performed.

It was concluded that the HP 5890 Series II GC utilizing EPA Method 18/25a is the most accurate method for VOC quantification. Both the Gasmet and MKS FTIRs (EPA Method 320) overestimate total VOC concentration compared to the HP GC by approximately 18 percent and 12 percent, respectively. However, in most cases the differences were within uncertainty bounds. A common process currently used for VOC quantification, which subtracts the methane and ethane measurements from the MKS FTIR (utilizing EPA Method 320) from the THC measurement from the Siemens 5-Gas analyzer, is not an accurate method as it creates large uncertainty up to 193 percent and overestimates total VOC concentration by nearly 100 percent relative to the HP GC.

ACKNOWLEDGMENTS

It has been such a privilege to get my master's degree at Colorado State University. Moving more than a thousand miles away from my home in Kentucky was very tough but it has been such a unique and rewarding experience. I am very blessed to have had the opportunity to do research at the Powerhouse Energy Institute where I have gained a lot of hands-on experience and have made life-long friendships.

First off, I would like to thank my advisor, Dr. Daniel Olsen, for taking me on as a grad student and for giving me all the help and guidance I needed throughout my two years here. I want to thank him for all the time and effort he put in for this research as well as for my success. I would like to thank the control room squad at the Powerhouse Energy Institute (Kirk Evans, Mark James, and James Tillotson) for all their help and endless jocularity that made engine testing possible and so much fun. They went above and beyond to setup and work with the analyzers, run the engine, and spend countless hours fixing the engine whenever things went wrong. These guys were such a pleasure to work with and taught me that no matter where you're at or what you're doing, you can always have fun doing it. I would also like to thank Chris Van Roekel for running the Caterpillar engine for nine hours in the summer heat of the engine's lab. Another thank you to Jack MacDonald and Nick Domagala for designing and constructing the ethane and higher hydrocarbon fuel blending systems.

Next, I would like to thank the Pipeline Research Council International project team for funding this research and for the continuous support and guidance throughout the project. I would like to thank Clean Air and Gasmet Technologies for providing the loaner instruments used for testing and for their dedication to making sure the analyzers were running properly and we had

everything we needed. In addition, I would like to thank the people at Analytical Instrument Resource LLC for their assistance in recommissioning the HP 5890 Series II GC.

I would not be who I am today if it weren't for my amazing, wonderful family – both in Kentucky and in Indiana – constantly supporting me and loving me unconditionally. I want to thank my mom and dad especially for supporting and encouraging me during my time here no matter how crazy I sounded when this home-body told them I wanted to move two states away to get my masters. I also want to thank the friends I've made here, who are so dear to me that they have become my family. Included, but not limited to this, is Mac and Pamela (Pamma) Cook who took me under their wing when I moved to Fort Collins and have been there for me in so many ways, especially in the growing of my faith and identity in Christ. For that I am very grateful. I also want to thank the Babazadeh family for loving me as if I have been a part of them for years and giving me the sense of family away from home. They have blessed me in so many ways and continue to do so. Last and most importantly, I would like to give thanks to my God who has been my Rock and my Savior. Without Him, I could not do any of this, and it is my prayer and goal to do it all for His glory.

TABLE OF CONTENTS

DEFINITION OF TERMS

AFR – air-fuel ratio

aTDC – after top dead center

BMEP – brake mean effective pressure

bTDC – before top dead center

BSCO – brake specific carbon monoxide

BSFC – brake specific fuel consumption

BSVOC – brake specific volatile organic compound

CA – crank angle

COV – coefficient of variance

CSU – Colorado State University

CTS – calibration transfer standard

DAQ – data acquisition

EECL – Engines and Energy Conversion Laboratory

EPA – Environmental Protection Agency

FID – flame ionization detector

FTIR – Fourier Transform Infrared

GC – gas chromatograph

GC-MS – gas chromatograph mass spectrometer

HAP – hazardous air pollutant

HC – hydrocarbon

HPFI – high pressure fuel ignition

IMEP – indicated mean effective pressure

LECM – Large Engine Control Module

MDC – minimum detection concentration

MN – methane number

NMHC – non-methane hydrocarbon

NMNEHC – non-methane, non-ethane hydrocarbon

NO_X – nitrous oxides

NSCR – non-selective catalytic reduction

OC – open chamber

PCC – pre-combustion chamber

PM – particulate matter

PP – peak pressure

ppmd – parts per million, dry

PTR-MS – proton transfer reaction mass spectrometry

QA/QC – quality assurance/quality check

RT – retention time

SI – spark ignited

TER – trapped equivalence ratio

THC – total hydrocarbons

TOFMS – time-of-flight mass spectrometry

UHC – unburned hydrocarbon

UHP – ultra high purity

VOC – volatile organic compound

WOT – wide open throttle

CHAPTER 1 – INTRODUCTION

Background

Natural gas engines have been commonly used to power compressors in the transportation of natural gas through pipelines since the 1950's. According to the U.S. Energy Information Administration's 2008 survey, there are more than 1,400 natural gas compressor stations that utilize large-bore, two-stroke natural gas engines in the United States. These natural gas compressor engines are durable, reliable, and could potentially operate for 100 years. Because of the long operating lives associated with these engines, it is important for emissions to be monitored and technology to be improved to ensure the engines are meeting current emissions standards.

An important emission that is of particular interest is a volatile organic compound (VOC). VOCs are defined as non-methane, non-ethane hydrocarbons (NMNEHC). They have negative environmental effects, especially in the formation of ozone and fine particulates that create smog. According to the 2018 Environmental Protection Agency (EPA) CFR Title 40 Part 60 Subpart JJJJ the VOC emission standard for stationary spark ignition internal combustion engines with a maximum engine power greater than 25 hp and less than 500 hp is 1.0 g/hp-hr. The combination of a Gas Chromatograph (GC) and a Flame Ionization Detector (FID) can be used to measure methane, ethane, and VOCs. The use of a GC/FID to quantify hydrocarbon concentration is in compliance with EPA Method 18/25A. In some cases, this approach is mandated by regulatory bodies. The Fourier Transform Infrared Spectrometer (FTIR) can also be used to measure VOCs in engine exhaust gas, following EPA Method 320. However, there is concern that Method 320 is not as accurate as Method 18/25A. The main objective of this research is to provide data and

analysis with both measurement methods from different engine types, conditions, and fuel quality to determine whether Method 320 is acceptable for VOC quantification.

Literature Review

Since the implementation of the Clean Air Act of 1970 by the EPA, regulations and restrictions on air pollutants produced by stationary and mobile sources have been frequently narrowed and redefined. With each amendment, acceptable levels of emissions such as nitrous oxides (NO_X), total hydrocarbons (THC), and particulate matter (PM) are reduced in order to allay negative effects emissions have on the environment as well as the human population. Engines used in various applications have been a significant focus of the EPA in regards to the restrictions on exhaust products from combustion. To ensure air pollutants emitted from engines meet the EPA's regulations, methods need to be developed and verified to accurately monitor the emissions in the exhaust. Common methods utilize gas chromatographs and spectrometers to quantify the exhaust composition. In addition to ensuring acceptable emission levels, new technology and techniques are crucial in reducing the amount of pollutants produced. Technology and techniques such as after-treatment systems, pre-combustion chambers, and enhanced fuel/air mixing have been implemented to contribute to meeting EPA standards. Natural gas fuel composition can impact emission levels from natural gas engines. Not many studies have been conducted in this area, indicating the need for additional research.

Measurement Methods

Volatile organic compounds are regulated due to their hazardous effects on the environment and human health [1, 2]. VOCs are defined as non-methane, non-ethane hydrocarbons and are commonly found in the exhaust of natural gas engines. Generally, aldehydes, which is a class of oxygenated hydrocarbons, are excluded from the VOC class. The EPA and other

organizations have developed methods to quantify VOCs. These methods include the Measurement of Gaseous Organic Compound Emissions by Gas Chromatography (Method 18) [3], the Determination of Total Gaseous Organic Concentration Using a Flame Ionization Analyzer (Method 25A) [4], and the Measurement of Vapor Phase Organic and Inorganic Emissions by Extractive Fourier Transform Infrared Spectroscopy (Method 320) [5].

The GC, which is the instrument used in EPA Method 18, consists of a cylinder for the carrier gas (typically helium, hydrogen, or nitrogen), a flow controller/pressure regulator, an injection port (sample inlet), a column, and a recorder (system software). A sample is moved through the column within the GC by an inert (carrier) gas. A non-volatile solvent is also added to the column inside surface to hinder the sample components based on their distribution coefficient until the different components separate. The separated species within the sample leave the column and are recorded versus time by the detector. The oven temperature is increased in order to move higher hydrocarbons through the column. A pressure regulator is installed at the sample inlet to ensure a uniform pressure and a constant flow rate of the sample. Each component will have a unique retention time (measured by the detector) based on the specific flow rate and temperature [6].

The purpose of EPA Method 18 is to measure gaseous organics emitted from industrial sources using a GC. The components of the sample are further quantified by an analyzer such as a FID, photoionization, or electron capture. Since the components are identified by the comparison of their retention times to those of known components, the GC needs to be calibrated beforehand under similar testing conditions. The method describes the appropriate calibration process. Blanks consisting of hydrocarbon-free air or nitrogen are suggested to be analyzed often to ensure the analyzer has no contaminants. The method goes into detail about how to set up the sampling system

(Figure 1-1). Since the GC cannot analyze samples continuously, additional samples can be collected in bags or flasks. The method discusses the procedure of adding a dilution system before the sample inlet to the GC if concentrations are too high for adequate detector response. Optimal conditions for the GC will need to be determined by the analyst.

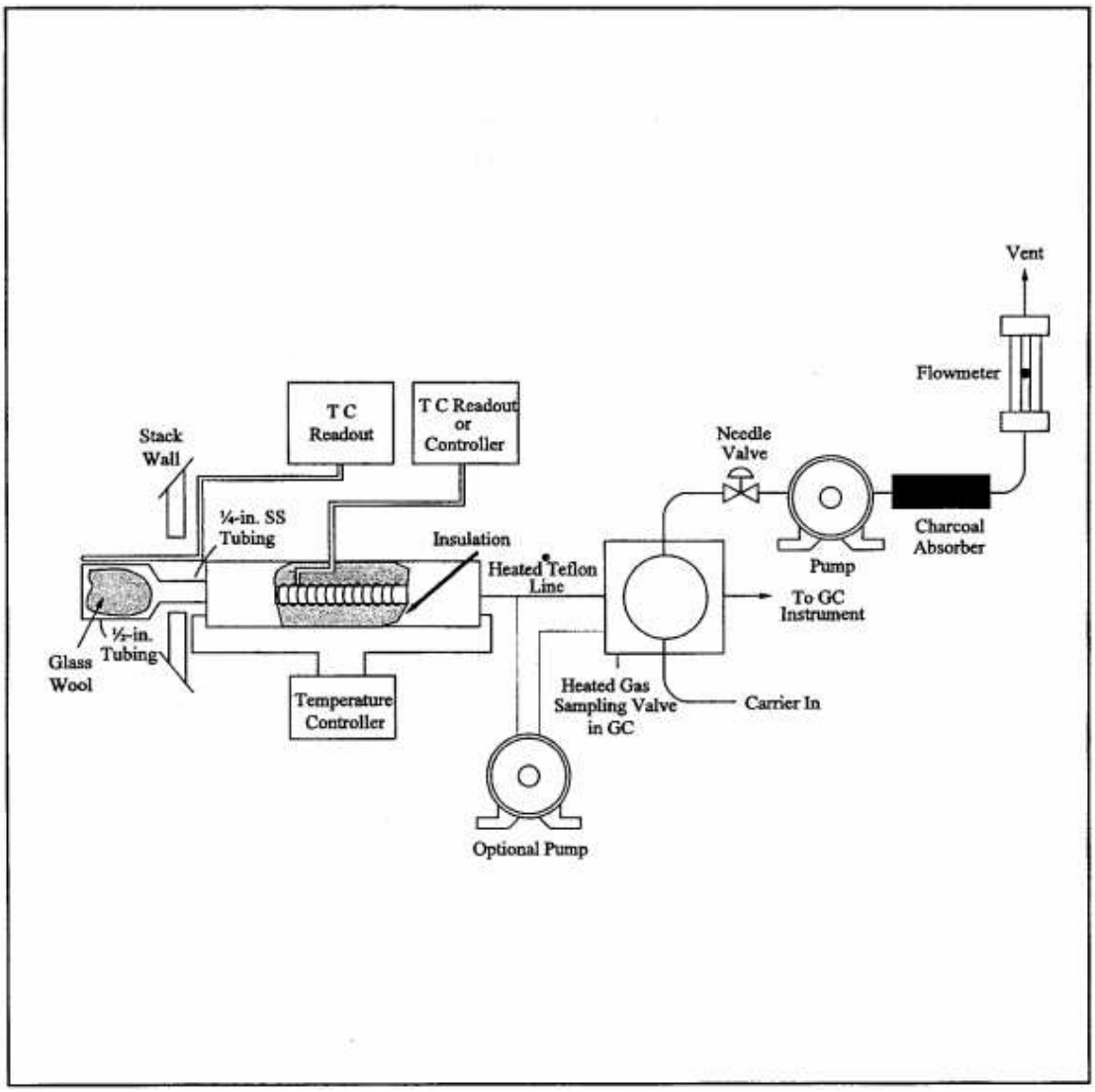

Figure 1-1. Direct interface sampling system from EPA Method 18 [3].

EPA Method 18 is commonly coupled with EPA Method 25A, which focuses on the Flame Ionization Analyzer within a GC that is used to determine total gaseous organic concentration. For this process, hydrogen and air are used as the fuel and oxidizer, respectively, to create a flame

within the FID. A collector electrode with a DC current applied is placed above the flame and measures the conductivity of the flame. The conductivity of hydrogen alone is low but increases with the combustion of the organic compounds in the sample. The current is amplified and detected by the FID, where the amplitude is recorded by the system software. The amplitude versus time data is displayed on the computer with the different species identified and labeled on the graph [6]. EPA Method 25A requires that the sample be heated to greater than 110°C and the detector block be heated to greater than 120°C. Calibration gases are specified to be propane in air or propane in nitrogen, although organic compounds other than propane can be used. The fuel and oxidizer that is recommended is a 40 percent H_2/60 percent N_2 gas mixture and high purity air, respectively. Low-, mid-, and high-level calibration gases are specified as well to verify that the calibration of the analyzer is without significant error caused by drift.

EPA Method 320 describes the use of an FTIR to identify gas components and measure the concentrations. Within a FTIR is a Michelson interferometer, which is the major optical component and consists of a fixed mirror, a moving mirror, and a beam splitter. When infrared light contacts the interferometer and the moving mirror, a signal intensity called an interferogram is produced. Since a sample will absorb certain wavelengths of the light, the interferogram will change and become unique based on the components of the sample as well as the beam splitter and infrared light source. The interferogram is then received by an IR detector. The detector samples the signal in equal increments and a Fourier integral is applied to recover the spectrum from the incremented signal. Characteristics of the sample can be identified from its spectrum. The spectrum of the sample alone can be determined by taking the difference between the spectrums with and without the sample present [7]. EPA Method 320 covers different types of interferences and how to resolve them. The method also goes into detail on what equipment and supplies are

recommended. Three different types of tests are identified: screening, emissions test, and validation. The method further discusses the calibration process and sampling process as well.

VOC Instruments

Many studies that have focused on measuring and analyzing emissions, including VOCs, did so through the use of either a GC or an FTIR. Studies done by Ladd et al. [8, 9], which determined the effects of varying ethane in natural gas fuel on a large-bore engine, used a Nicolet Magna-IR 560 FTIR to measure brake specific VOCs and formaldehyde. Amirante et al. used a GC/FID configuration to analyze all engine exhaust species except for CO, CO_2, and NO_X after varying propane content in the fuel [10]. The studies mentioned above will be discussed in further detail in the next section. Another study that utilized a GC was done by Gilman et al. to characterize the primary VOC emissions from oil and natural gas sources in the Northeastern Colorado region [11]. Specifically, this GC was a custom-built, two-channel gas chromatograph-mass spectrometer (GC-MS). During testing, two unheated, ambient air samples were collected simultaneously for 5 minutes and sent to two separate columns (as opposed to only a single column). One sample entered an Al_2O_3/KCl PLOT column that was ramped from 55 to 150°C in 3.5 min to separate the C_2-C_5 hydrocarbons. The other sample components (C_5-C_{11} hydrocarbons, oxygen, nitrogen, and halogen-containing VOCs) were separated in the other column, which was a semipolar DB-624 capillary column ramped from 38 to 130°C in 11 min. The samples were then analyzed in a linear quadrupole mass spectrometer (Agilent 5973N). The sample acquisition took 5 min and the analysis portion took 25 min. The process repeated every 30 min. The detection limit was typically 0.010 ppbv, the precision limit was 15%, and the accuracy limit was 25%; however, these varied between different compounds.

The GC-MS method that Gilman et al. used for their analysis consists of a capillary column to separate the components within a sample and a mass spectrometer to measure the concentration of each component. There are two types of mass spectrometers: a quadrupole mass spectrometer and a magnetic sector mass spectrometer [12]. A quadrupole mass spectrometer consists of four rods to which a voltage is applied, as well as an ion beam directed through the center of the rods. As a result, an electric field is produced in the space enclosed by the rods. When a compound passes through the center, ions are created by the electric field. Mass separation is achieved by applying DC and AC voltages simultaneously to the rods. In a magnetic sector mass spectrometer, a magnet is used to produce and separate ions according to the ions' mass to charge ratios. The magnetic field forces the ions in a narrow line and guides them into the detector. The detector, in either case, produces a mass spectrum of the sample, which allows individual compounds to be identified. Although the GC-MS method is highly accurate, as seen by the quality of results of Gilman's study, it is also expensive.

In addition to the FTIR and GC/FID, there are currently other instruments on the market that have the capability of measuring VOCs. One of these alternative instruments utilizes the proton transfer reaction mass spectrometry (PTR-MS) method. The PTR-MS method includes a continuous sample that is pumped through a drift tube reactor. The drift tube reactor consists of drift rings that are connected to a resistor network. The rings produce an increasing voltage which results in a homogeneous electric field that is used to transport the ions down the tube, thus eliminating the need for a large pump. A fraction of the VOCs is ionized by exchanging protons with hydronium ions. These hydronium ions are emitted from a hollow cathode discharge in water vapor. As a result, the mass of the product ions conveniently equals the mass of the VOCs plus one. The product ions and reagent are sent to a quadrupole mass spectrometer via an intermediate

chamber. There are no electric fields present within the chamber; therefore, the ions are forced to travel via their kinetic energy alone. The ions separate due to their unique velocities and the arrival time of the ions are measured by the detector, which can then be related to the ion's mass. Advantages to this method are that it allows for high sensitivity and rapid response time as well as not requiring any sample treatment. Despite all of these advantages, however, PTR-MS cannot identify specific VOCs, only the mass of product ions [13].

The company Ionicon specializes in manufacturing instruments utilizing the PTR-MS method. For example, one of Ionicon's products is the PTR-QMS 500. Ionicon claims that the analyzer has a detection limit of less than 1 pptv and that it is the most sensitive commercial PTR-QMS instrument on the market. The company also offers a time of flight modification to the method which increases the resolution for better separation and identification as well as acquiring the entire mass range in split-seconds. TOFWERK, a Swiss company manufacturing analytical instruments using time-of-flight mass spectrometry (TOFMS), also provides a PTR-TOFMS instrument called the Vocus PTR-TOF. The Vocus has a detection limit of less than 1 pptv and has an option for GC coupling.

De Gouw et al. [13] used the PTR-MS method for the measurement of VOCs in the earth's atmosphere. The authors claimed that this method can make up for some of the disadvantages seen using a GC such as the amount of time needed to acquire an adequate sample. The authors used PTR-MS on aircraft for airborne monitoring of VOCs. The method is beneficial on aircraft since it allows for quick, real-time monitoring of VOCs in the atmosphere. During one of their missions, they achieved a cycle time of about 18 seconds. The study concluded that measurements taken by PTR-MS were accurate within 20 percent. The study also coupled a GC with the PTR-MS in order

to identify certain VOC species; however, this method significantly increased the residence time, which the PTR-MS method is meant to reduce.

Clark et al. [14] used the Rosemount Analytical Model 402 as the hydrocarbon analyzer to quantify emissions from a Hercules GTA 3.7 L, 4-cylinder engine. The Rosemount Analytical Model 402 is a contacting conductivity sensor. According to the application data sheet provided by Emerson Process Management, the sensor measures the conductance of an electrolyte solution depending on the concentration of ions in the solution along with the volume of solution where the current flows. The sensor consists of two metal electrodes that are separated by a known distance. The current within the solution is produced when an alternating voltage is applied to the electrodes and the ions in the solution begin to move. The conductance is calculated from the ratio of the current to the voltage. If the area and length of the solution carrying the current is known, the conductance can be related to the concentration of ions in the sample. It can be inferred that the sensor can only measure total ion concentration and cannot identify individual species, however, since Clark et al. only reported total hydrocarbon concentrations and not the individual species.

Another example of a hydrocarbon analyzer is one manufactured by Thermo Scientific called the Model 55i. This analyzer uses the GC method to measure methane and non-methane hydrocarbons in a sample. It utilizes an eight-port, two position rotary valve to inject the sample into the GC column and has a 70-second analysis time. The instrument includes a backflush feature so that direct measurements of non-methane concentrations can be taken as well as direct methane concentrations. Additional special features include automatic flame sensing and ignition, automatic calibration and span checks, and real-time corrections of THC readings. A disadvantage to the Model 55i, however, is that it doesn't speciate ethane from other non-methane compounds;

therefore, an additional analyzer with ethane quantification capabilities would be needed for recording total VOC measurements.

Fuel Composition Effects

It is common for the composition of natural gas fuel to vary in the field. The change in natural gas fuel composition can be due to uncontrolled effects such as the source of the fuel, the season in which the fuel is being used, and the type of processing the gas has undergone. Altering fuel composition could affect engine performance and emissions. Therefore, research in variable natural gas fuel composition is important to determine what the effects are.

A study by Ladd et al. [8] analyzed the effects of varying ethane in fuel on a large bore 2-stroke natural gas engine. The ethane content was varied from 5 to 23%. Testing was conducted using a Cooper Bessemer GMV-4 large bore 2-stroke natural gas engine operated at 500 brake horsepower (bhp). The engine utilized pipeline quality natural gas with an ethane blending system to increase the energy content and decrease the methane number (MN) of the fuel. It was found that even though ethane addition improved combustion stability, which reduced fuel consumption, NO_X levels increased since ethane increased flame speeds and adiabatic flame temperatures. Brake specific carbon monoxide (BSCO) remained constant. However, brake specific volatile organic compounds (BSVOC), mainly ethylene, propylene, and propane, increased from 0.35 to 0.47 g/bhp-hr. Formaldehyde decreased by a relatively small amount from 0.29 to 0.275 g/bhp-hr due to the decrease in methane. Emissions versus ethane volume percentage can be seen in Figure 1-2.

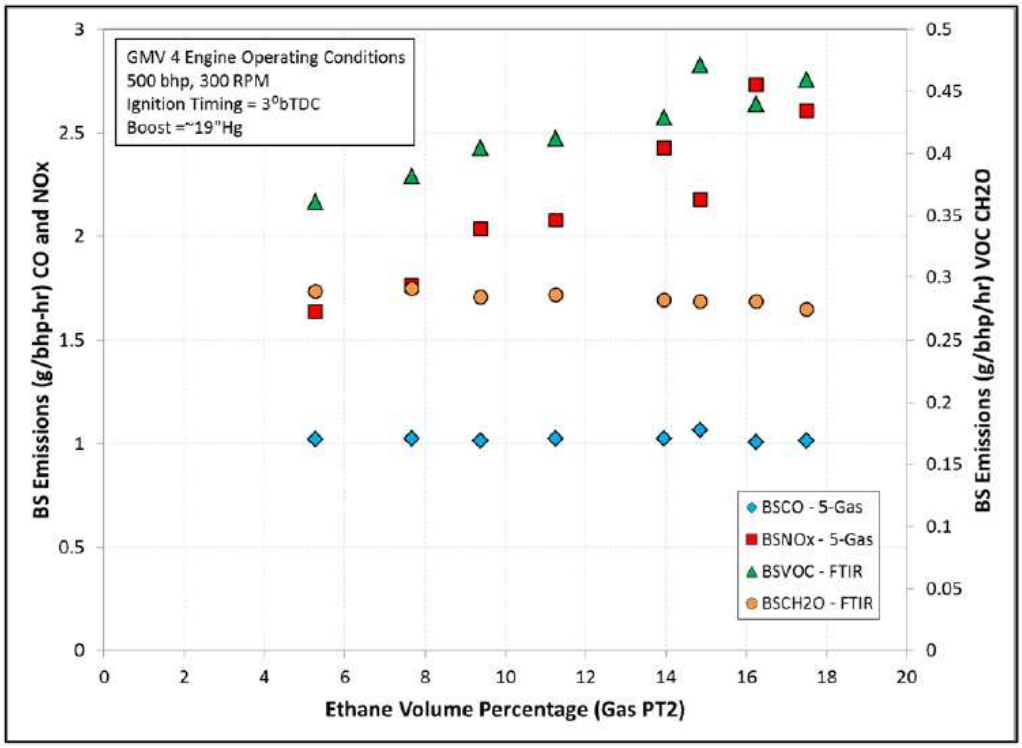

Figure 1-2. Brake specific emissions versus ethane volume percentage at fixed air manifold pressure [8].

Ladd et al. also analyzed past test data from the Engines and Energy Conversion Laboratory in Fort Collins, Colorado to determine the effect of fuel quality on greenhouse emissions such as CO_2, CH_4, and CO_2e (equivalent CO_2) [9]. Data taken from the Cooper Bessemer GMV-4 large bore natural gas engine was the primary source for analysis. Test data indicated that fuel quality had a significant effect on CO_2e emissions. Specifically, higher ethane content, often associated with shale gas, produced more CO_2 while methane emissions remained constant. Syngas (reformed natural gas) was used to fuel the pre-combustion chamber in concentrations of 20% and 100%. The use of this gas extended the lean limit operation which resulted in slightly lower NO_X emissions with no negative effect on combustion stability. In another study testing was performed with constant NO_X levels and constant boost [8]. The authors specifically discussed the portion of testing where ethane content was increased from 9% to 30% to emulate shale gas. The addition of ethane increased CO_2e emissions by 50% due to an increase in CO_2; however, CH_4 emissions

remained constant (Figure 1-3a). CO_2 increased since ethane has a larger C/H ratio than methane. THC and VOC emissions also increased with the addition of ethane. VOC increased due to an increase in propane emissions, despite a decrease in fuel propane (Figure 1-3b). The increase in exhaust propane occurred because there are pathways leading to higher hydrocarbons in the ethane decomposition to acetylene and methane.

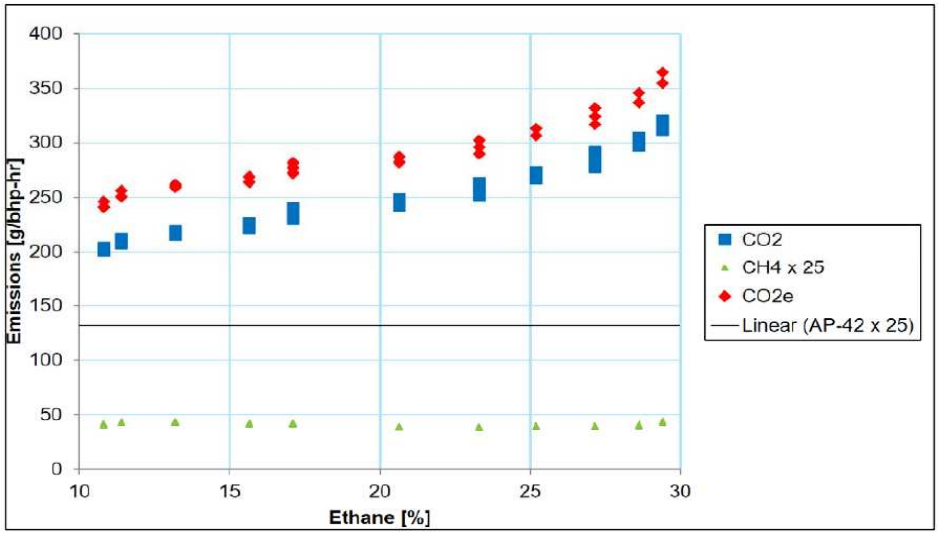

(a)

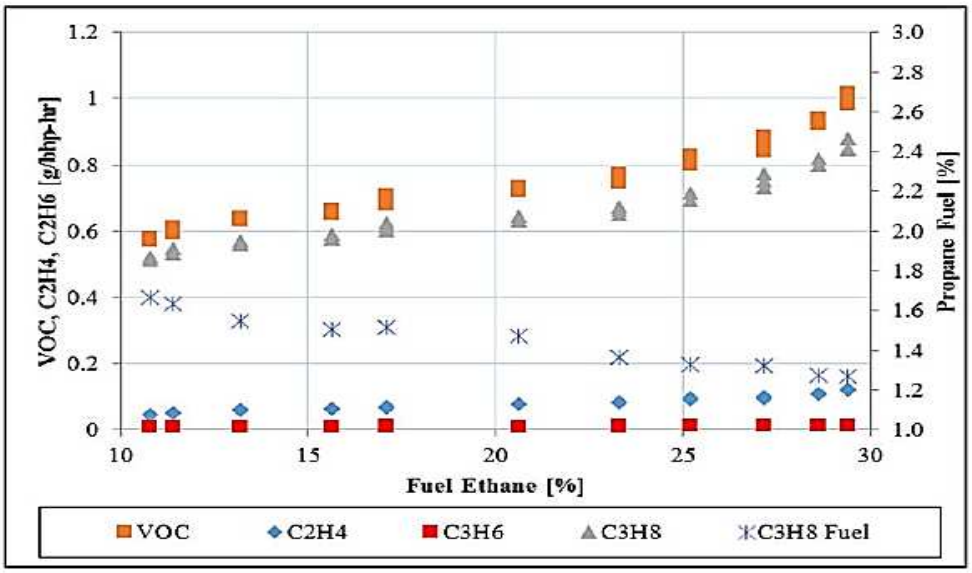

(b)

Figure 1-3. Emissions versus ethane, variable fuel sweep (a) and VOC constituents versus fuel ethane (b) [9].

Amirante et al. [10] altered natural gas by varying amounts of propane and methane. The amounts of propane in methane tested were 10, 20, 30, and 40% by volume. Fuels with 100% propane and 100% methane were tested as well. Tests were performed on a naturally aspirated 4-stroke, single cylinder spark ignited (SI) engine. Results showed that adding more propane to the fuel increased indicated mean effective pressure and reduced peak pressure coefficient of variance, indicating improved combustion stability and efficiency. Propane has a faster burning speed than methane; therefore, there were higher adiabatic flame temperatures during combustion, causing NO_X levels to increase. An increase in NO_X emissions due to a higher content of propane was also supported by Clark et al. [14] who observed high levels of NO_X when a fuel with 100% propane was tested in a Hercules GTA 3.7 L, 4-cylinder engine. The addition of propane also decreased total unburned hydrocarbons (UHCs) and methane emissions (seen in Figure 1-4). Levels of CO_2, however, increased.

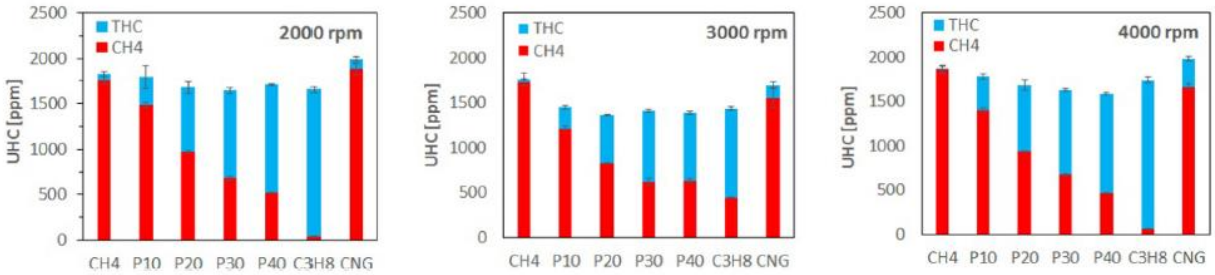

Figure 1-4. TUHC (blue bars) and CH_4 (red bars) emissions for the three different engine speeds investigated [10].

Thiagarajan et al. [15] also studied the impact of varying propane in natural gas on emissions. In addition to varying propane (up to 20% by volume), the authors also varied the amount of nitrogen in the fuel (up to 15% by volume). Fuels were tested on a SI 1987 2.8 L Pontiac V6 engine. Pipeline natural gas was used as the baseline fuel. Running at high propane composition (12 and 20%) for the closed loop method, the engine operated at rich conditions. CO did not depend

on propane fraction as long as an equivalence ratio of one was maintained. THC did not vary significantly with propane fraction as seen in Figure 1-5. Brake specific fuel composition (BSFC) increased with addition of nitrogen since the presence of nitrogen lowered the fuel's heating value. Pre-catalyst NO_X emissions were lower than for baseline natural gas for all nitrogen cases, indicating that nitrogen could have lowered flame temperatures. Pre-catalyst THC and CO emissions appeared to be unaffected by nitrogen addition, yet they increased with nitrogen addition post-catalyst. This was caused by lower NO_X emissions.

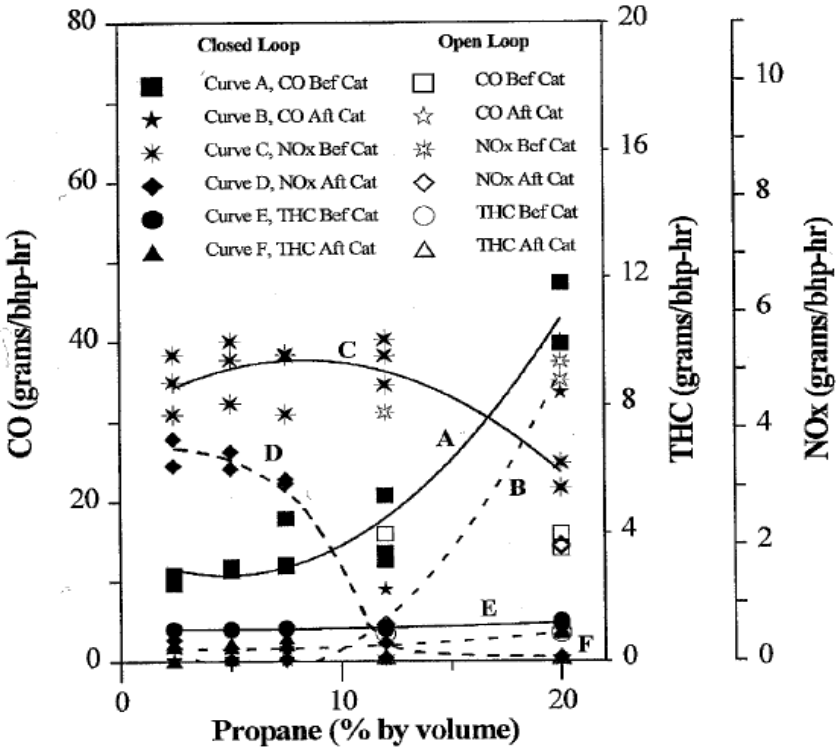

Figure 1-5. Emissions as a function of propane volume fraction at 50 percent WOT and 2000 rpm [15].

A study that varied methane content within natural gas fuel was performed by Feist et al. [16]. In addition to varying the methane content the authors also changed the Wobbe Index of the fuel. A total of eight fuel blends were tested on a 2007 Cummins ISL G, a 2006 Cummins C Gas

Plus, a 2005 John Deere 6081H, a 1998 Cummins C Gas, and a 1999 Detroit Diesel Series 50G TK. The emissions that were measured included THC, non-methane hydrocarbons (NMHC), CO, NO_X, NO_2, PM, and CO_2. After testing different fuel blends, results showed that there was no significant change in performance with the use of various fuel blends in heavy-duty natural gas engines. There was no obvious trend with engine performance for the ISL G engine. All the other engines showed an increase in power output with a decrease in MN and an increase in Wobbe Index. For the cold-start tests, all engines showed an increase in NO_X as MN decreased. NO_X levels also increased with higher Wobbe Index. The increase in NO_X was due to the increase in ethane and propane as a result of the decrease in MN. All engines showed an increase in NMHC as MN decreased. Brake specific NMHC versus MN for all test engines is shown in Figure 1-6. CO emissions showed little variation other than a slight increase as MN decreased with the ISLG, C Gas, and DDC TK engines. Results indicated that BSFC and Wobbe Index number were inversely proportional to each other, mainly due to changes in the energy content of the fuels.

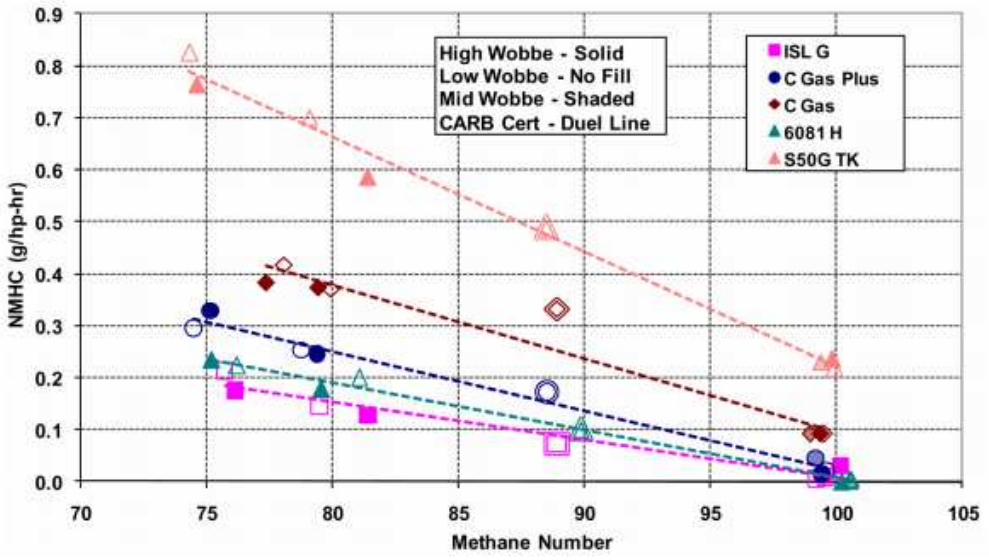

Figure 1-6. Hot-start cycle average brake specific NMHC results versus test fuel methane number for all test engines and fuels [16].

Scope Overview

For the experimental evaluation of stack testing methods for accurate VOC measurements, four instruments will be used, each following the appropriate EPA Method (18/25A or 320). The four analyzers include an HP 5890 Series II GC/FID, a Model No. 2030 FTIR with a liquid nitrogen cooled detector manufactured by MKS Instruments, Inc., a Model 210 FID manufactured by VIG Industries, Inc., and a Gasmet DX4000 FTIR with a Peltier cooled detector. Exhaust will be sampled from engines of different types and configurations. The first engine type/configuration is a lean burn Cooper Bessemer GMV-4 large bore natural gas engine with open chamber ignition. NO_X emissions will be maintained at a constant level of 15 g/bhp-hr. The second type/configuration is the lean burn GMV-4 engine but with pre-chamber ignition and a constant NO_X level of 2 g/bhp-hr. Two other configurations on the GMV-4 lean burn engine have a maintained NO_X level of 0.5 g/bhp-hr with pre-chamber ignition. One configuration utilizes high pressure fuel injection and the other utilizes standard cam-driven low-pressure fuel injection. Last is the rich burn testing on a Caterpillar G3304 engine with a DCL non-selective catalytic reduction (NSCR) system and a constant NO_X level of 2 g/bhp-hr. An ignition timing sweep will be performed for all engines/configurations. Fuel ethane and higher hydrocarbon (C_{3+}) content will be altered for testing on the GMV-4 only, on both open and pre-chamber ignition systems. Ethane will be modified by adding 10 and 20 percent to the nominal amount initially in the fuel. One data point will be taken with the addition of 5 percent higher hydrocarbon (C_{3+}) content in the fuel while the ethane content will remain at the nominal amount. Data taken from the FTIRs and GC/FIDs will be compared to determine whether the FTIR coupled with EPA Method 320 is an acceptable procedure for VOC quantification.

In preparation for testing of the different engine types and configurations, the four analyzers listed above were set up in the control room at CSU's Powerhouse Energy Institute. The control room is located within the engines lab and oversees the testing on engines and records data. The HP 5890 Series II GC was acquired from Analytical Instrument Recycle in 2011 and was re-commissioned for testing. The MKS Instruments Model No. 2030 FTIR had been purchased beforehand and is located in the analyzer room next to the control room. The Model 210 FID manufactured by VIG Industries was loaned by Clean Air and the DX4000 FTIR was loaned by Gasmet. Figure 1-7 is a schematic of the analyzer setup. Required gas bottles for the analyzers were purchased and connected to the appropriate instruments. Gasmet and Clean Air provided support for the setup of the loaner instruments when needed. Along with VOCs, measurements of NO_X, THC, CO, CO_2, and O_2 will also be recorded using a Siemens 5-Gas analyzer.

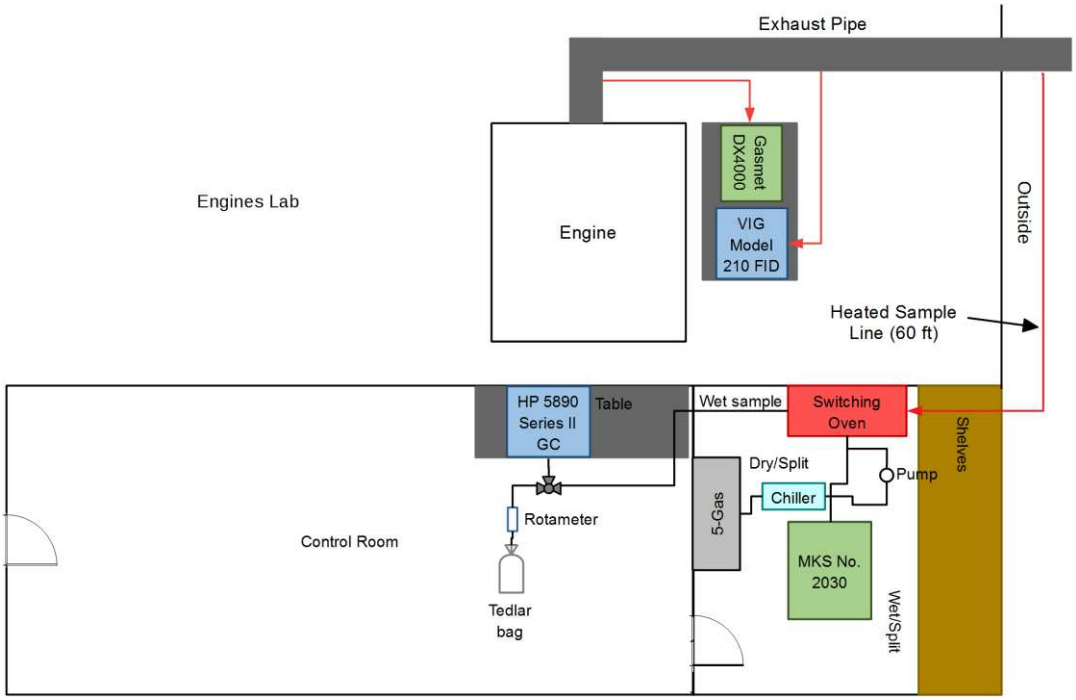

Figure 1-7. Analyzer setup schematic at the EECL. Red lines are the heated lines extracting gas from the exhaust stack to the analyzers.

An ignition timing sweep will be performed for all engine types and configurations. The ignition timing will initially be at 6 degrees before top dead center (°bTDC) below the nominal ignition time for that engine type/configuration. Timing will be increased in increments of 3°bTDC until 6°bTDC above the nominal ignition timing is reached.

In addition to the ignition timing sweep, the ethane and higher hydrocarbon (C_{3+}) content in the fuel will be altered to determine the effects the variation has on emissions. A fuel blending system will be designed and commissioned to inject controlled amounts of the species into the natural gas supply line to the engine. Fuel will be altered for all GMV-4 engine configurations except for the pre-chamber ignition at 0.5 g/bhp-hr. For the variable ethane sweep, an addition of 10%, 20%, and 30% by volume ethane will be added to the baseline natural gas fuel. An addition of 5% by volume higher hydrocarbon content will be added to the baseline fuel for the variable C_{3+} sweep. During this portion of testing ignition timing will be adjusted for optimal location of peak pressure.

All raw data recorded will be reduced and consolidated into one or more spreadsheets. Comparison plots for the four analyzers will be generated for all test points. The impact of fuel composition on the hydrocarbon content of the exhaust will be examined. All emission values will be reported as corrected emissions (parts per million dry basis (ppmvd) @15%O2) and emission rates (lbs/hr and g/bhp).

CHAPTER 2 – TEST MATERIALS AND PROCEDURE

Test Equipment

Engines

Exhaust gas will be sampled from two separate sources. The first source is a lean-burn Cooper-Bessemer GMV-4 large-bore, two-stroke cycle natural gas engine, shown in Figure 2-1. The engine has a rated speed of 300 rpm and a bore and stroke of 14 in (35.6 cm). The GMV-4 was manufactured in the 1940's and is used in compressor station applications to transport natural gas through pipelines across the United States. The GMV-4 has a rated load of 440 bhp (330 bkW), corresponding to a brake mean effective pressure (BMEP) of 67.6 psi (466 kPa), and is loaded with a computer-controlled, water brake dynamometer to provide precise load control.

The GMV-4 uses an Altronic CPU-2000 ignition system and has direct fuel injection, utilizing the original cam-driven mechanically actuated fuel valves; however, Enginuity/Woodward electro-hydraulic high-pressure fuel valves are available whenever HPFI is needed. Air supply for the engine is provided via a turbocharger simulator. The turbocharger simulator consists of a Gardner Denver screw compressor and an automated backpressure valve. Through computer control the air and exhaust manifold pressures can be controlled to simulate any turbocharger set-point within the operating envelope of the supercharger (maximum boost ~30"Hg). Fuel is supplied through one of two compressors: a Copeland Scroll compressor (0-75 psi) or an Ingersoll-Rand piston compressor (75-600 psi). The natural gas composition flowing to the engine was continually monitored and recorded for each test point using a Varian CP-4900 micro gas chromatograph.

Figure 2-1. Cooper-Bessemer GMV-4 at the CSU Engines and Energy Conversion Laboratory (EECL).

The second source is a rich-burn Caterpillar G3304 7.0 L engine, shown in Figure 2-2, which is primarily used for well-head compression. The engine has a rated power of 95 bhp (71 bkW) and a bore and stroke of 4.8 in (121 mm) and 6.0 in (152 mm), respectively. The engine is equipped with a Woodward LECM controller and a DCL International, Inc. 3-way catalyst for automated air/fuel ratio control.

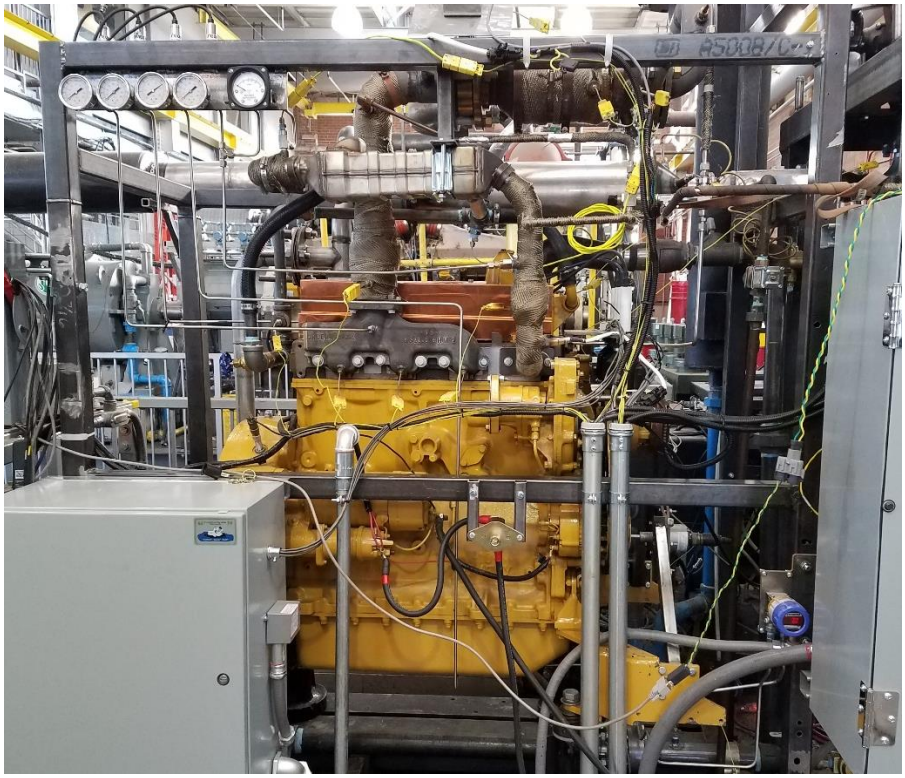

Figure 2-2. Four-stroke rich burn Caterpillar G3304 7.0 L natural gas engine at the EECL.

Fuel Blending System

Ethane and higher hydrocarbon (C3+) contents of the natural gas fuel will be altered separately to determine the effects variable fuel content has on emission composition. The ethane blending system, which has been used previously on research involving fuel composition alterations, was recommissioned for testing. A propane blending system has been used before at the lab, but it has since been deconstructed and the majority of the parts, having been rented, were returned. Therefore, a higher hydrocarbon system had to be designed and constructed. The ethane blending system consists of six liquid ethane bottles connected by a manifold to a pressure regulator. An automated control valve was installed and is managed by LabVIEW in order to alter the flowrate of ethane to the natural gas supply line. After entering the natural gas supply line, the ethane and natural gas fuel travel through a compressor to the engine fuel supply system (Figure

2-3). Figure 2-4 shows the ethane blending system located outside of the EECL. The system consists of six ethane bottles, an automated flow control valve to control the ethane mass flow rate, a flow meter, and a flow control algorithm written in LabVIEW.

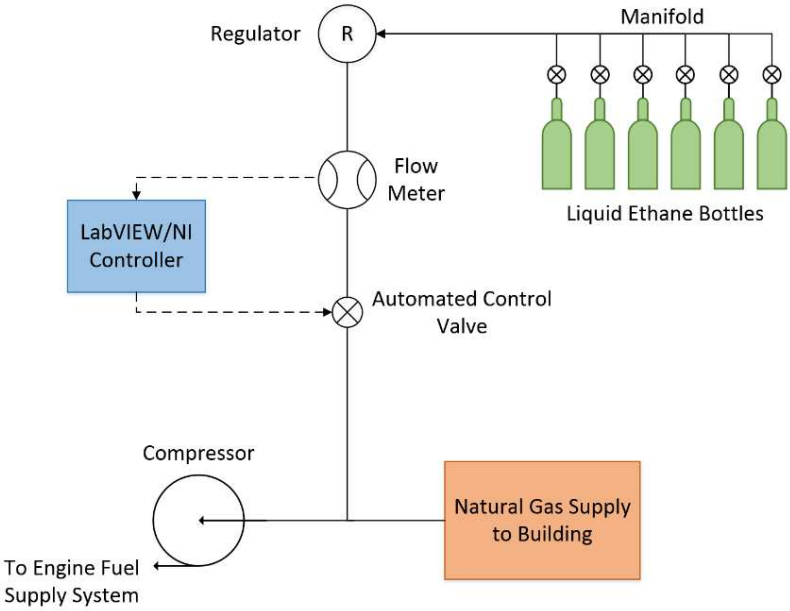

Figure 2-3. Schematic of ethane fuel blending system.

Figure 2-4. Ethane blending system setup.

The higher hydrocarbon blending system is setup in the basement of the EECL. A schematic of the system is shown in Figure 2-5 and the nitrogen and hydrocarbon cylinder setup is shown in Figure 2-6. The higher hydrocarbon blend is stored in a bottle and consists of a propane balance of hexane (1 mol%), i-pentane (2 mol%), n-pentane (2 mol%), n-butane (3 mol%), and i-butane (12 mol%). The higher hydrocarbon bottle is connected to a nitrogen bottle with a pressure relief valve. The liquid blend is injected into the natural gas fuel supply line through a spray nozzle installed in the pipe. The flowrate is controlled by adjusting nitrogen pressure on top of the liquid. The quality of the fuel blending system in adding the correct amount of hydrocarbons into the engine natural gas supply during testing is verified using the Varian CP-4900 micro GC.

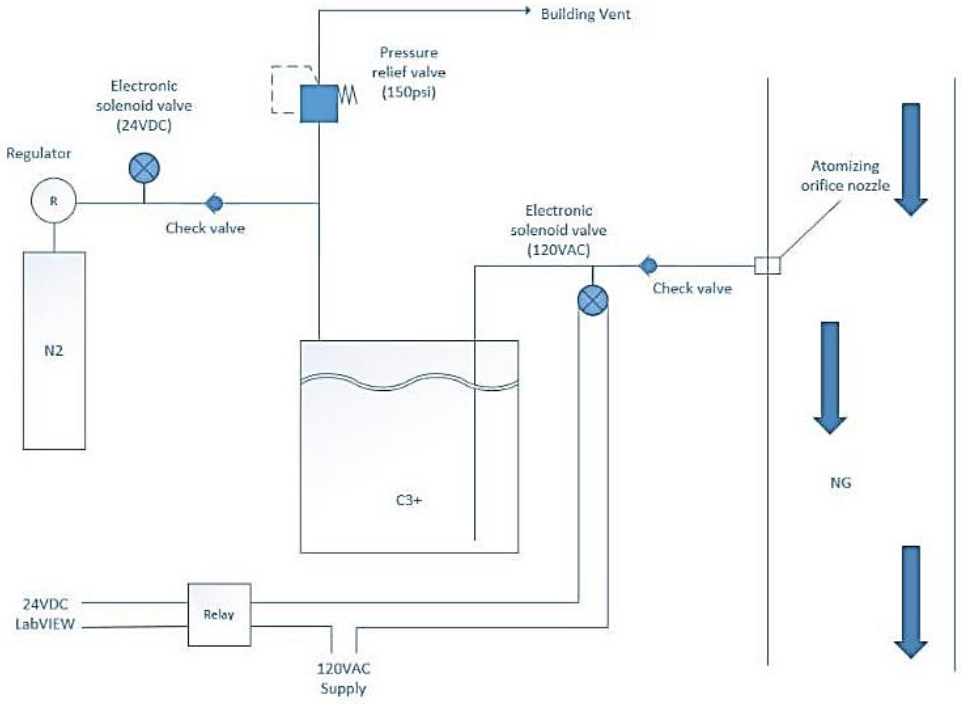

Figure 2-5. Schematic of the higher hydrocarbon fuel blending system.

Figure 2-6. Nitrogen and hydrocarbon cylinder setup in the basement of the EECL.

Sample System

There are three sample probes installed in the engine exhaust stack. One probe supplies exhaust gas to the HP GC and the MKS FTIR. The second probe connects to the VIG FID's sample inlet and the third probe connects to the Gasmet FTIR. Each analyzer requires its own unique sample flowrate and temperature to match that required for the oven or cell where the sample is analyzed. The required sample flowrates and temperatures are shown in Figure 2-7. An Air Dimensions Dia-Vac diaphragm pump is connected before the sample inlet to the VIG FID to maintain the desired flowrate.

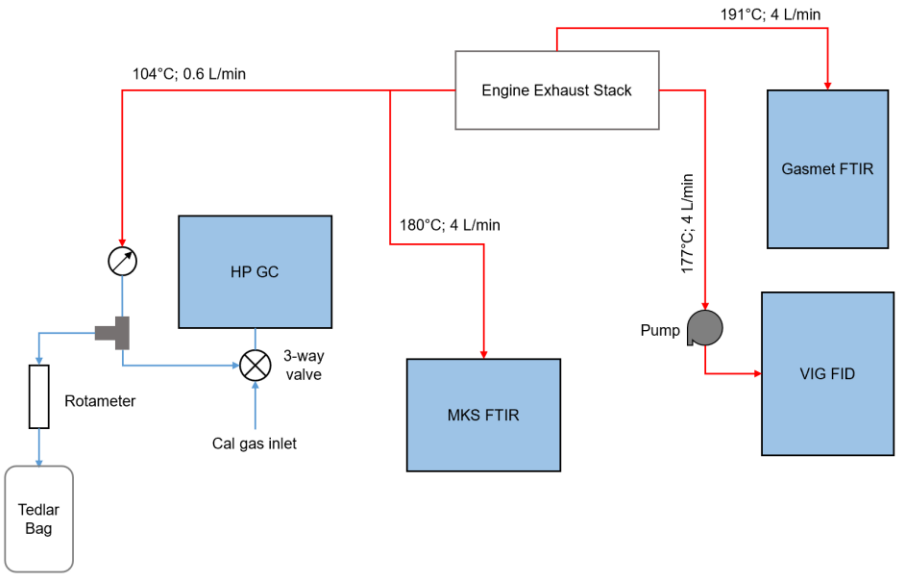

Figure 2-7. Sample system schematic; heated lines are in red.

Analyzers

Four analyzers are set up to measure VOC concentration for comparisons of EPA Methods 320 and 18/25A as follows: a HP 5890 Series II GC, a VIG Model 210 FID, a MKS Instruments Model No. 2030 FTIR, and a Gasmet DX4000 FTIR. The VIG Model 210 FID was loaned by Clean Air and the DX4000 FTIR was loaned by Gasmet. A Siemens 5-Gas analyzer is used to measure CO, CO_2, NO_X, THC and O_2 concentrations. The Siemens 5-Gas analyzer is made up of five different units, the FIDAMAT 6 for THC measurements, the NOXMAT 600 for NO_X measurements, the OXYMAT 6 for O_2 measurements, the two ULTRAMAT 6 units for CO and CO_2 measurements. In addition, an ECOM J2KN Pro Easy analyzer with the capability of measuring NO and NO_2 was lent by Siemens Enginuity to gather data to determine the quality of the instrument.

The HP 5890 Series II GC (shown in Figure 2-8) consists of a HP Plot Q PT capillary column to separate the VOC species as well as an FID to measure the concentration of the individual species. Helium, an inert gas, acts as a carrier to guide the sample through the column.

The column includes a thin film on the inner wall that hinders each specie based on the specie's distribution coefficient until all the VOC species are separated. After the sample travels through the column, it enters the FID. The FID is made up of an electrode with an applied DC voltage located above a hydrogen flame. When hydrocarbons pass through the flame, they produce ions. The concentration of each specie is determined by the magnitude of the current produced as a result of the ions interacting with the voltage at the electrode.

Figure 2-8. HP 5890 Series II GC.

At the start of each run, the oven is at an initial temperature of 60°C. After one minute, a sample of engine exhaust gas is injected into the column. At this time, the oven's temperature is increased 20°C/min until it reaches 200°C. The purpose of the temperature increase is to assist the heavier hydrocarbons in moving through the column at a faster rate, minimizing analysis time. The oven temperature is held at 200°C until the end of the 12-minute run. Sample injection is performed using a Valco 8-port valve. Initially the valve is in Position B, as shown in Figure 2-9, to load a section of sample in the sample loop. Once the valve changes to Position A one minute after the

start of a run, helium enters the loop to guide the sample through the column and into the FID. Figure 2-10 shows a chromatogram of a sample from a custom calibration bottle with concentrations of various hydrocarbons typically found in exhaust from natural gas engines. The components along with their amounts are listed in Table 2-1.

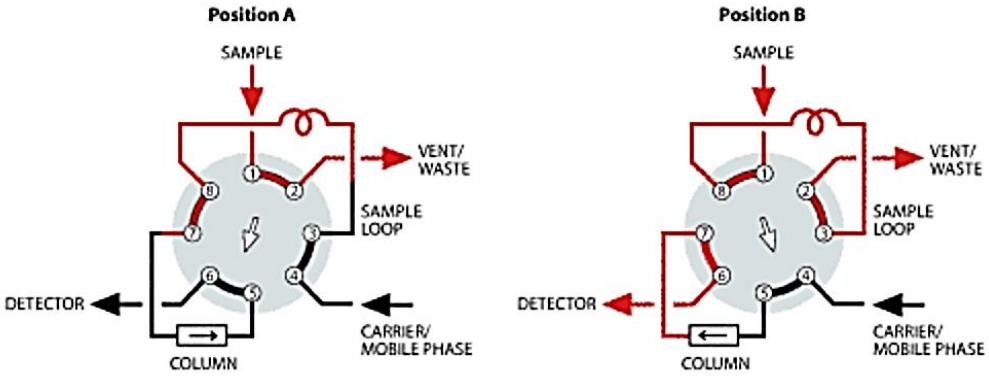

Figure 2-9. Valco Instruments 8-port valve schematic for sample injection in HP GC [17].

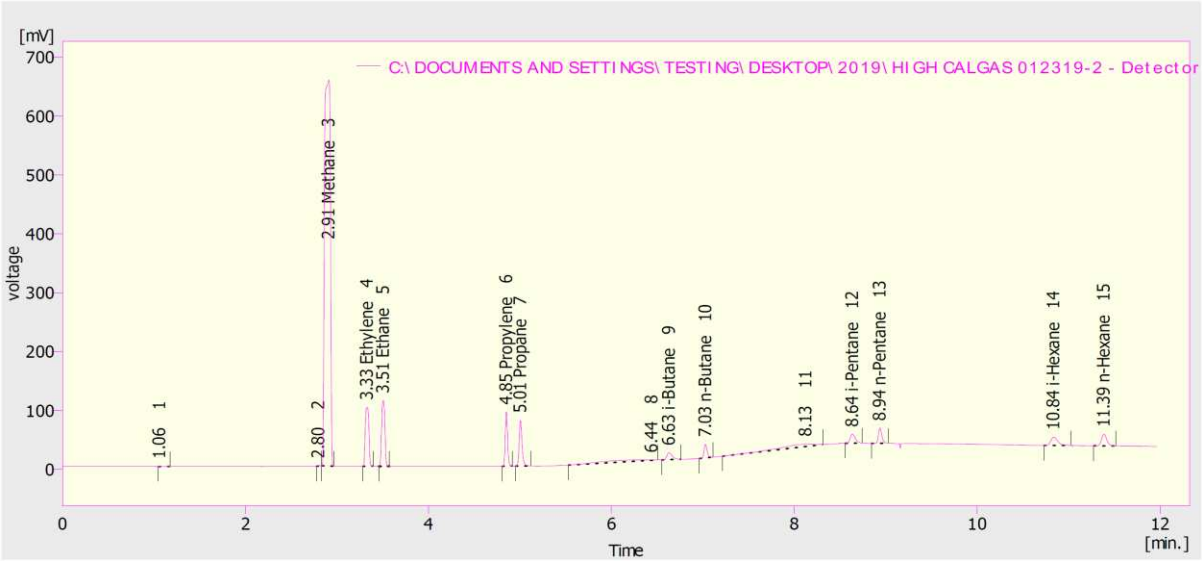

Figure 2-10. Example chromatogram of calibration gas displayed on Clarity software.

The chromatogram was displayed in the Clarity software (version 3.0.6.589) after the run was complete. The lighter hydrocarbons (components with lower numbers of carbon and hydrogen atoms) reach the FID before the heavier hydrocarbons; therefore, the lighter hydrocarbons are

shown on the chromatogram first, reading from left to right. Isomers, such as isobutane and isopentane, travel through the FID before their normal counterparts due to the compactness of their molecular structures. The area under each peak is associated with the concentration of the component the peak represents. The rise in the baseline at around 5.5 minutes is due to the rising oven temperature.

Table 2-1. Custom calibration gas bottle composition.

Component	Amount (ppm)
Methane	1007
Ethylene	50.23
Ethane	50.38
Propylene	20.12
Propane	20.04
i-Butane	4.990
n-Butane	4.960
i-Pentane	4.800
n-Pentane	5.040
i-Hexane	5.290
n-Hexane	5.010

The second analyzer that utilizes EPA Methods 18/25A is the Model 210 FID manufactured by VIG Industries (Figure 2-11). The FID was loaned by the company Clean Air for testing. The instrument consists of two FIDs and a backflush mechanism. One FID measures methane, ethane, and residual (C_{3+}) species at predetermined intervals. The other FID provides a continuous measurement of THCs. Once the sample enters the analyzer, it travels through the first

FID for the continuous measurement of THCs. The sample is then diverted to flow through a GC column toward the second FID to separate methane and ethane from the C_{3+} HCs. After the methane and ethane pass through the second FID, the C_{3+} HCs are back flushed through the column to be analyzed by the first FID [18]. The measurements are displayed in real-time on the screen located on the front face of the analyzer. An NI Instruments DAQ system is connected to the analyzer so the data can be logged in LabVIEW as well.

Figure 2-11. VIG Industries Model 210 FID.

Two FTIRs are used to follow the guidelines specified in EPA Method 320. One FTIR is the MKS Instruments, Inc. Model No. 2030 FTIR (Figure 2-12). When a gas enters the FTIR, an IR beam is sent through the sample. The different components within the sample absorb different wavelengths of the IR beam. The detector picks up the signal and transfers it to the computer where the Multigas software applies a Fourier transform to produce a unique IR spectrum of the gas. According to the Beer-Lambert law, absorbance is directly proportional to the concentration of the

sample gas; therefore, the components of the gas sample are able to be identified with the IR absorption spectrum [19]. For more detailed information on the FTIR spectroscopy process, refer to Ted Moosman's thesis on "FTIR Spectroscopy for 2-Stroke, Lean Burn Gas Engines Emphasizing Low-Level Detection of HAPs" [20]. The MKS FTIR performs real-time analysis of multiple gases simultaneously and accounts for temperature and pressure variations, which the analyzer also measures during operation. The MKS FTIR features a LN_2–cooled detector, a spectral resolution ranging between 0.5 and 16 cm^{-1}, a wavenumber range of 400-5,000 cm^{-1}, an effective spectrometer pathlength of 5.11 m, and mirrors made of nickel-plated aluminum substrate with rugged gold coating.

Figure 2-12. MKS Instruments, Inc. Model No. 2030 FTIR.

The second FTIR used is a DX4000 FTIR manufactured by Gasmet Technologies (Figure 2-13). The instrument is typically used for short term, on site measurements and can simultaneously analyze up to about 50 compounds. The DX4000 features a Peltier-cooled detector, a spectrometer resolution of 8 cm^{-1} or 4 cm^{-1}, and a wave number range of 900 – 4,200 cm^{-1}. The sample cell is made of 100% rhodium coated aluminum, has a fixed pathlength of 5 m, and consists of mirrors that are protected with gold coating. The analyzer uses the Calcmet software to record data.

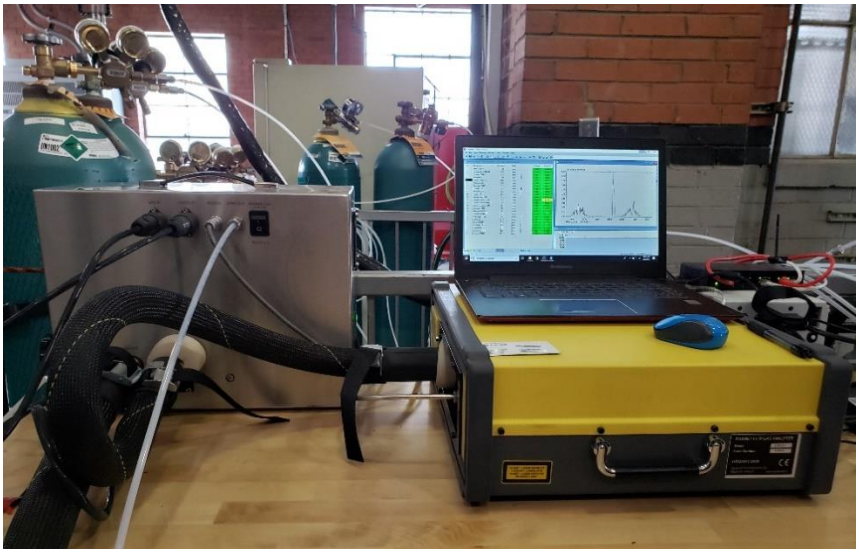

Figure 2-13. Gasmet Technologies DX4000 FTIR.

Tedlar Bag System

The sample manifold (Figure 2-14) involves a heated line that is routed from the exhaust stack to stainless steel tubing that connects to the GC inlet. Downstream of the heated line is a pressure gage to ensure that the sample pressure is held at 10 psi. After the gage a tee was installed to insert a needle valve and a rotameter with a Teflon tube attached to the outlet of the rotameter. The setup is used to fill Tedlar bags with exhaust gas while the engine is running. The rotameter is set to approximately 1 LPM so the bag can be filled with 20L of exhaust gas spanning over a

20-minute period to achieve one representative sample for each data point. The sample manifold and tube leading to the Tedlar bag are wrapped with heat tape to avoid water condensation in the lines.

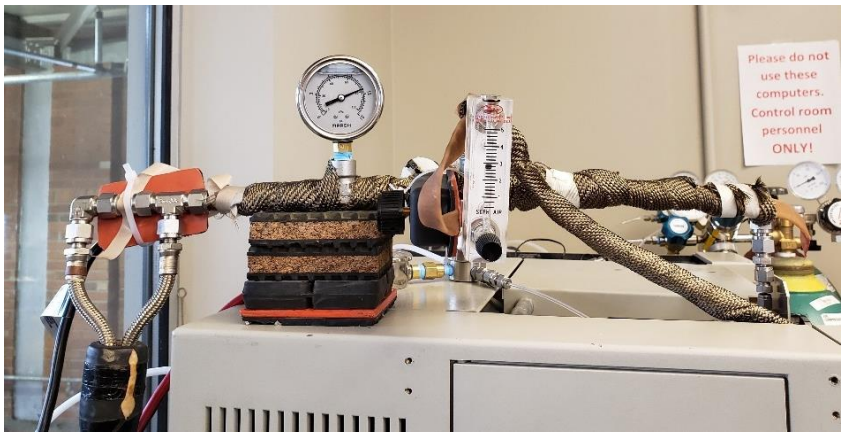

Figure 2-14. Sample manifold and Tedlar bag setup on top of the HP 5890 Series II GC.

Tedlar bags with a maximum capacity of 25L are analyzed within 24-36 hours after they are filled with exhaust gas. When injecting the sample from the Tedlar bag and into the GC, a tube is connected from the port on the bag to the inlet of the sample pump (Figure 2-15) so the sample can be pressurized to 10 psi; a regulator and a gage were installed downstream of the pump to maintain a constant pressure. The tube that connects to the tee in between the gage and regulator leads to the inlet of the GC.

Figure 2-15. Tedlar bag sampling system.

NO_X Sensor Feedback Control

For some data points, NO_X emission levels were controlled via NO_X sensor feedback control instead of TER control to improve NO_X stability during the data points and reduce time required to attain specific NO_X values [8]. The NO_X 5210 system was chosen for NO_X sensor feedback control. The system consists of a display head with a Type T sensor (Figure 2-16a) and a NO_XCANt module (Figure 2-16b) manufactured by ECM. Ladd et al. chose the same system for NO_X sensor feedback control while testing on the GMV-4 and included more detail on the functionality of the sensor compared to alternative NO_X control methods [8]. There are multiple functions of NO_X sensors other than feedback control. Schmitt explained his use of a ceramic NO_X sensor for ammonia injection into a Selective Catalyst Reduction (SCR) system [21]. Gattoni installed a Continental NO_X sensor downstream of a Non-Selective Catalyst Reduction (NSCR) system for feedback air/fuel ratio control for his research on "Advanced Control Techniques and Sensors for Gas Engines with NSCR" [22].

Figure 2-16. NO_X 5210 display box and Type T sensor and NO_XCANt module [23].

Test Procedure

The following tables describe the test matrix used for the program. Each table title includes information on the engine and configuration with which the table is associated. The purpose of

testing with the engine modified to different configurations was to encourage test the performance of the analyzers at different hydrocarbon emissions levels. The table consists of the test day, the data point number, the desired NO_X level, the set location of peak pressure, the fuel composition, and any additional comments.

Testing begins with the GMV-4 engine for the lean burn, open chamber ignition configuration (Table 2-2). Test Day 1 consists of the ignition timing sweep. After starting the engine, ignition timing is adjusted for a location of peak pressure at 18°ATDC, and the NO_X level is maintained at 15 g/bhp-hr. This point is designated as the nominal point for the sweep. After the first data point is complete, NO_X sensor feedback control is turned off and the boost pressure is set to the same value as it was for Data Point 1. The location of peak pressure is set to 15 and 21°aTDC for Data Points 2 and 3, respectively. NO_X sensor control is turned back on to maintain constant NO_X levels for Data Points 4 and 5 at the nominal location of peak pressure (18°aTDC). The second day involves the fuel blending tests on the ethane and higher hydrocarbon content of the natural gas fuel. NO_X sensor control is used for data points that called for nominal fuel composition but is replaced with trapped equivalence ratio (TER) control when adding ethane or higher hydrocarbons.

Table 2-3 describes testing on the GMV-4 engine after pre-combustion chambers are installed. Unlike the open chamber configuration, NO_X is held at 2 g/bhp-hr for the nominal ignition time data points; however, similar to the open chamber configuration, NO_X level is left to vary in order to maintain constant boost pressure when ignition timing is altered. On the next day (Test Day 3), fuel blending is conducted in the same manner as it was for the open chamber configuration.

Table 2-2. Engine/Configuration: GMV-4 Lean Burn, Open Chamber Spark Ignition

Test Day	Data Point	NOx (g/bhp-hr)	Loc. of Peak Pressure (°aTDC)	Fuel Composition	Comments
1	1	15	18	Nominal	Boost control
1	2	Variable	15	"	Set boost at point #1 value.
1	3	Variable	21	"	"
1	4	10	18	"	Boost control
1	5	15	18	"	Boost control
2	6	15	18	Nominal	Boost control
2	7	Variable	Same IT as point #6	Nominal +10% Ethane	Turn on TER control before adding ethane. **Partial data point.**
2	8	Variable	18	Nominal +10% Ethane	Maintain TER control.
2	9	Variable	Same IT as point #6	Nominal +5% C3+	Maintain TER control. **Partial data point.**
2	10	Variable	18	Nominal +5% C3+	Maintain TER control.
2	11	15	18	Nominal	Boost control

Table 2-3. Engine/Configuration: GMV-4 Lean Burn, Pre-chamber Ignition

Test Day	Data Point	NOx (g/bhp-hr)	Loc. of Peak Pressure (°aTDC)	Fuel Composition	Comments
3	12	2	18	Nominal	Boost control
3	13	Variable	15	"	Set boost at point #1 value.
3	14	Variable	21	"	"
3	15	2	18	"	Boost control
4	16	2	18	Nominal	Boost control
4	17	Variable	Same IT as point #17	Nominal +10% Ethane	Turn on TER control before adding ethane. **Partial data point.**
4	18	Variable	18	Nominal +10% Ethane	Maintain TER control.
4	19	Variable	Same IT as point #17	Nominal +5% C3+	Maintain TER control. **Partial data point.**
4	20	Variable	18	Nominal +5% C3+	Maintain TER control.
4	21	2	18	Nominal	Boost control

After testing with the pre-chambers is complete, the Enginuity/Woodward HPFI system will be installed. The HPFI system includes a Woodward Solenoid Operated Gas Admission Valve (SOGAV) 43, a Woodward fuel injector to inject fuel into the main combustion chamber, and an Enginuity gaseous fuel injector for the pre-chamber (Figure 2-17). The HPFI system is controlled by Woodward's Large Engine Control Module (LECM) (Figure 2-18). The same procedure for

the pre-chamber configuration is repeated for HPFI (Table 2-4) during Test Days 5 and 6 except NO_X levels are decreased to 0.5 g/bhp-hr.

Figure 2-17. Enginuity/Woodward HPFI system installed on the GMV-4 engine.

Figure 2-18. Woodward LECM for monitoring HPFI system on the GMV-4 engine.

Table 2-4. Engine/Configuration: GMV-4 Lean Burn, High Pressure Fuel Injection, Pre-chamber Ignition with Electronic Fuel Valves

Test Day	Data Point	NOx (g/bhp-hr)	Loc. of Peak Pressure (°aTDC)	Fuel Composition	Comments
5	22	0.5	18	Nominal	Boost control
5	23	Variable	15	"	Set boost at point #1 value.
5	24	Variable	21	"	"
5	25	0.5	18	"	Boost control
6	26	0.5	18	Nominal	Boost control
6	27	Variable	Same IT as point #17	Nominal +10% Ethane	Turn on TER control before adding ethane. **Partial data point.**
6	28	Variable	18	Nominal +10% Ethane	Maintain TER control.
6	29	Variable	Same IT as point #17	Nominal +5% C3+	Maintain TER control. **Partial data point.**
6	30	Variable	18	Nominal +5% C3+	Maintain TER control.
6	31	0.5	18	Nominal	NOx sensor control

The final round of testing is performed on the Caterpillar G3304 7.0L natural gas engine with a 3-way catalyst for measuring emissions at rich burn conditions. Only an ignition timing sweep is conducted for this round. The target NO_X level is 2.0 g/bhp-hr for the two nominal points but can vary when timing is advanced or retarded 3°aTDC for Data Points 34 and 35.

Table 2-5. Engine/Configuration: Caterpillar 3304 Rich Burn with 3-way Catalyst

Test Day	Data Point	NOx (g/bhp-hr)	Ignition Timing	Fuel Composition	Comments
7	33	2.0	Nominal	Nominal	
7	34	Variable	Nominal -3□	“	
7	35	Variable	Nominal +3□	“	
7	36	2.0	Nominal	“	

Before the start of each test program, leak checks are performed on all sample lines. QA/analyte spike tests and other applicable checks per EPA Method 320 are conducted on both the MKS and Gasmet FTIRs. Composition of the calibration gases for both VIG FID and HP GC analyzers are verified per EPA Method 18/25A.

Before each test day, appropriate quality assurance/checks (QA/QC) are performed for each analyzer. For the FTIRs, this involves recording a spectrum with the appropriate calibration gas. For the FID analyzers, this involves running high-, medium-, and low-level gas standards to verify the accuracy of the calibration file loaded on the analyzers’ software. More detailed explanations of QA/QC procedures per EPA Methods 320 and 18/25A are given in Chapter 3.

At the beginning of each test day, the engine is started and set to desired conditions (ignition timing, AFR, NO_X level, etc.). Once the engine has stabilized (verified through real-time engine data displayed on LabVIEW), data collection is simultaneously taken from each of the four analyzers. Each data point is approximately 40 minutes long. The duration of the data points is determined predominantly by the data collection on the HP GC. Three runs are performed on the

HP GC for each data point. Each run has an analysis time of 12 minutes with approximately two minutes in between runs for the oven to cool down to the initial temperature set by the GC method. The MKS FTIR, Gasmet FTIR, and VIG FID collects data continuously for the duration of the data point; however, 20-minute averages of the data are used for post-processing calculations. A 20-minute sample of the exhaust gas is collected into a 25L Tedlar bag after the first sample is injected into the HP GC. Once a data point is complete, the engine is set to the next data point's conditions and allowed ten minutes to stabilize before data collection begins.

In the middle of the test day, a drift check is performed on the VIG FID and HP GC with the mid-level calibration gas to ensure that the results do not exceed ±3% of the results from the initial calibration check. Once all data points are collected for the test day, the engine is shut down and appropriate QA/QC checks are performed on all analyzers per EPA Methods 320 and 18/25A, including a final drift check on the FID instruments. All QA/QC logbooks recorded for each analyzer during testing are included in Appendix A.

CHAPTER 3 – METHODS AND CALCULATIONS

EPA Method 18

EPA Method 18, titled "Measurement of Gaseous Organic Compound Emissions by Gas Chromatography", was the guideline used for the HP 5890 Series II GC and VIG Model 210 FID analyzers [3]. The method specified that the FID should be fueled with the type of gas recommended by the analyzer manufacturer. Ultra-high purity (UHP) hydrogen was used as the FID fuel for both analyzers. The FID oxidizer was required to be hydrocarbon free air. The carrier gas also had to be hydrocarbon free. Per manufacturer recommendations, UHP helium was used for the HP GC and UHP nitrogen was used for the VIG FID.

Both GC/FID analyzers were calibrated with custom calibration gases. The method stated that a ±1 percent uncertainty for each component within the calibration gas bottle was preferred; however, a ±2 percent uncertainty was also acceptable. The measurements of each component within the calibration gases were required to be within ±5 percent of the concentration listed on the gas bottles to verify the analyzers were calibrated correctly. When sampling during testing, heated lines were maintained at a temperature of 110°C. Care was taken to ensure calibration gases and sample exhaust gas were injected into the analyzers at the same pressure.

Tedlar bags, as recommended by Method 18, were used for collection of exhaust gas during each data point. When filling the Tedlar bags, the method called for a rotameter to monitor the flow rate to ensure that the bag was filled to 80 percent of its full capacity, which equated to 20L of sample for the 25L bags used. The bags were stored in a place where there was no direct sunlight. The method also called for filling and storing the bags at an elevated temperature or diluting the sample to prevent water condensation; however, water was allowed to condense. This was to

emulate sampling procedures performed in the field as well as to analyze the effect water condensation had on VOC measurements when compared to directly injecting the sample into the analyzer. Each bag sample was analyzed three times. After the exhaust gas in the bags were sampled through the HP GC, the bags were filled with UHP nitrogen for 24 hours and then vacuumed to be used for the next round of testing.

EPA Method 25A

EPA Method 25A, titled "Determination of Total Gaseous Organic Concentration Using A Flame Ionization Analyzer" was used in conjunction with EPA Method 18 for the HP GC and VIG FID [4]. Method 25A focused on the process of analyzing a sample using a flame ionization analyzer and how to report the results on a ppm as propane or carbon equivalent basis. The method required that all sample components leading to the analyzer be heated to ≥110°C (220°F) to prevent condensation and the FID detector block be heated to >120°C (250°F). The method stated that the calibration gas should be specifically propane in air or propane in nitrogen, but other organic compounds could be used.

At the beginning of each test day a calibration error test was performed on the GC/FID analyzers using three types of calibration gases: high-, mid-, and low-level. According to the method, the high-level calibration gas consisted of 80-90 percent of the instruments span value or of the concentration expected in the gas sample. The mid-level calibration gas consisted of 45-55 percent and the low-level calibration gas consisted of 25-35 percent. To pass the calibration error test, all measurements for the three calibration gases must be within ±5 percent of the known concentrations listed on the bottles. At the middle and end of the test days, a drift determination check was performed on the analyzers using the mid-level calibration gas. In order for the data collected beforehand to be valid, the results must be within ±3 percent of the bottle concentration.

The checklist used during the test program that included QA/QC checks specified in EPA Method 18/25A can be found in Appendix A.

EPA Method 320

EPA Method 320, which covers the "Measurement of Vapor Phase Organic and Inorganic Emissions by Extractive Fourier Transform Infrared (FTIR) Spectroscopy", was used as the guideline for the MKS Model No. 2030 FTIR and Gasmet DX4000 FTIR [5]. At the beginning of each test program, a leak check was performed on all sampling and analytical systems for the FTIR analyzers. A sample system leak check involved connecting a 0-250 mL flow rate meter on the pump outlet and closing off the exhaust probe inlet. The flow rate measured by the meter could not exceed 200 mL/min. The analytical system was checked for leaks by pressurizing the FTIR cell to a gage pressure of at least 100 mmHg, isolating the pump, and recording the change in pressure after two minutes. The percent leak volume was determined by

$$\%V_L = 50 t_{SS} \frac{\Delta P}{P_{SS}} \tag{3-1}$$

where t_{SS} is the signal integration time, ΔP is the change in pressure, and P_{SS} is the initial pressure. The leak volume could not exceed four percent.

The method called for a calibration transfer standard (CTS) to be completed at the beginning of each test program. Calibration gases were required to have an uncertainty no greater than ±2 percent. The FTIR cell was purged with 10 volumes of CTS gas and the spectrum was recorded. The CTS gas criteria are listed in Method 320. A QA spike was also performed for both FTIRs. The spike/tracer gas used was a blend of 100 ppm formaldehyde and 10 ppm sulfur hexafluoride (SF_6). The gas was introduced at a flowrate that was 10% of the total sample flowrate. The response time (RT) was determined by recording the time the spike took to become constant

after it entered the sample flow. After waiting a duration of two RTs, two spectra were recorded of two independent spiked samples. The two spectra had to be within ±5 percent of the average between the two. The expected concentration of the spiked samples was calculated using

$$CS=DF\times Spike_{dir}+Unspike(1-DF) \tag{3-2}$$

where $Spike_{dir}$ is the concentration of the analyte in the spike standard measured by filling the FTIR cell directly, *Unspike* is the native concentration of analytes in unspiked samples, and *DF* is the dilution factor of the spiked gas, which was required to be ≥10. The dilution factor was calculated using

$$DF=\frac{SF_{6(spk)}}{SF_{6(dir)}} \tag{3-3}$$

where $SF_{6(spk)}$ is the diluted SF_6 concentration measured in a spiked sample and $SF_{6(dir)}$ is the SF_6 concentration measured directly in the undiluted spike gas. This process was completed three times. The average of the spiked concentration had to be between 0.7 and 1.3 times the expected concentration to proceed with testing. At the end of the test day, another CTS spectrum was recorded and could not exceed ±5 percent of the average between the pre- and post-test CTS spectra. The QA/QC checklist following EPA Method 320 used for the test program can be found in Appendix A.

Brake Specific Emissions Calculation

Brake specific NO_X, CO, and VOC emissions were calculated for each data point using equations found in the Code of Federal Regulations Title 40 Chapter 1 Subchapter C Part 60 Subpart JJJJ titled “Standards of Performance for Stationary Spark Ignition Internal Combustion Engines” [24]. The emission rate for NO_X, CO, and VOC in units of g/bhp-hr was calculated using

$$ER = \frac{C_d \times k \times Q}{\dot{W}_b} \quad (3\text{-}4)$$

where C_d is the measured emission concentration in ppm, Q is the stack gas volumetric flow rate, in standard cubic meter per hour, dry basis, and $\dot{W}_b$ is the brake power output of the engine in brake horsepower. The variable k is the conversion constant for ppm of emission to grams per standard cubic meter at 20°C and equates to 1.912×10^{-3} for NO_X, 1.164×10^{-3} for CO, and 1.833×10^{-3} for VOC. The volumetric exhaust flow rate was calculated using the heat input rate of the fuel, the oxygen concentration within the exhaust gas, and multiplied by a factor to convert the volumetric flow rate to a dry basis. The factor was calculated using a programmed Excel spreadsheet created by Air Hygiene International, Inc, following the guidelines specified in the Code of Federal Regulations method.

FID Factors

The area of a peak associated with each compound on a chromatogram isn't always proportional to the concentration of that compound within the sample; therefore, FID correction factors are needed to resolve the discrepancy [6]. FID correction factors (or FID relative sensitivities) are relative to an arbitrary compound; since VOC measurements are typically reported in the field on a propane basis, the base compound is propane. From these FID relative sensitivities, FID factors can be calculated; however, there are multiple ways to calculate a FID factor as will be discussed in this section. The FID factors are then used to convert VOC measurements to a propane basis.

The weight of a compound can be determined using Equation 3-5.

$$W_b = \frac{W_a A_b}{F_{ba} A_a} \tag{3-5}$$

where W_a is the weight of the known compound a (propane), A_b is the measured area of compound b, A_a is the measured area of a, and F_{ba} is the FID relative sensitivity of b relative to a.

Since concentrations are more commonly presented as mole fractions, Equation 3-5 can be converted to a molar basis using the ideal gas law.

$$PV = NR_u T \tag{3-6}$$

where P is pressure, V is volume, N is the number of moles, R_u is the universal gas constant, and T is the absolute temperature. The ideal gas law can also be written using mass.

$$PV = m \frac{R_u}{M} T \tag{3-7}$$

where M is the molecular weight and m is the mass. Equating Equations 3-6 and 3-7 yields

$$m = NM \tag{3-8}$$

Using the fact that weight equals the product of mass and the gravitational constant, Equation 3-5 becomes

$$m_b = \frac{m_a A_b}{F_{ba} A_a} \tag{3-9}$$

Inserting Equation 3-8 into Equation 3-9 and solving for N_b gives

$$\mathrm{N_b} = \frac{\mathrm{N_a A_b M_a}}{\mathrm{F_{ba} A_a M_b}} \tag{3-10}$$

Since concentrations are more commonly reported in units of ppm rather than moles, it is useful to re-write Equation 3-10 in terms of ppm. Performing this conversion and rearranging to solve for F_{ba} yields

$$F_{ba}=\frac{ppm_a M_a A_b}{ppm_b M_b A_a} \tag{3-11}$$

where ppm_a is the measured concentration of compound a in ppm and ppm_b is the measured concentration of compound, b, in ppm. By definition, the equation for an FID factor in terms of ppm is

$$F'_{ba}=\frac{ppm_{ba}}{ppm_b} \tag{3-12}$$

where ppm_{ba} is the measured concentration of compound b relative to compound a in units of ppm. Rearranging to solve for ppm_b and inserting Equation 3-11 after solving for ppm_b gives

$$ppm_b=\frac{ppm_{ba}}{F'_{ba}}=\frac{ppm_a A_b/A_a}{F_{ba} M_b/M_a} \tag{3-13}$$

From Equation 3-13, two subsequent equations can be inferred as follows:

$$ppm_{ba}=ppm_a \frac{A_b}{A_a} \tag{3-14}$$

and

$$F'_{ba}=F_{ba} \frac{M_b}{M_a} \tag{3-15}$$

Equation 3-14 shows that to convert a measurement to a propane basis, the propane measurement is multiplied by the ratio of the area under the peak of the desired specie to the area under the peak of propane. Equation 3-15 shows that the FID factor of a desired specie with respect to propane could be calculated by the FID relative sensitivity of that specie relative to propane multiplied by the ratio of the molecular weights for the specie and propane. An alternative way to calculate FID factor is by plugging Equation 3-14 into Equation 3-12 to get

$$F'_{ba} = \frac{ppm_a A_b}{ppm_b A_a} \tag{3-16}$$

Table 3-1 displays the FID factors calculated using Equation 3-16, as well as the measured concentrations and peak areas used in the calculation. The custom calibration gas was sampled through the HP GC and the peak areas for the desired specie and propane were used for A_b and A_a, respectively. The measured concentration of the specie and propane were used for ppm_b and ppm_a, respectively. These FID factors were used for each of the desired species measured by the analyzers to convert the concentrations to a propane basis.

After collecting data from each of the analyzers, the species were converted to a propane basis using Equation 3-12 rearranged to solve for ppm_{ba}, which yields

$$ppm_{ba} = F'_{ba} ppm_b \tag{3-17}$$

Table 3-1. FID factors calculated from HP GC/FID data.

Species	Concentration (ppm)	Area (mV-s)	F'_{ba}
Methane	1007	2894	0.3427
Ethylene	50.23	275.8	0.6547
Ethane	50.38	279.5	0.6616
Propylene	20.12	163.7	0.9701
Propane	20.04	168.0	1.000
i-Butane	4.990	51.78	1.237
n-Butane	4.960	53.75	1.292
i-Pentane	4.800	62.70	1.558
n-Pentane	5.040	69.51	1.644
i-Hexane	5.290	77.05	1.737
n-Hexane	5.010	82.82	1.971

FID factors were also calculated for measurements taken from the Siemens 5-Gas THC analyzer to convert the measurements from a methane basis to a propane basis. To obtain the FID factors, methane, propane, ethane, and ethylene calibration gases were individually sampled through the 5-Gas analyzer and the measured concentrations were recorded. The FID factors on a methane basis were calculated using Equation 3-12 where ppm_{ba} was the concentration measured by the 5-Gas and ppm_b was the concentration reported on the calibration gas bottle. The FID factors on a propane basis were calculated using

$$F'_{i\text{-}C3H8} = \frac{F'_{i\text{-}CH4}}{F'_{C3H8\text{-}CH4}} \tag{3-18}$$

where $F'i_{\text{-}CH4}$ is the FID factor of a specie relative to methane and $F'_{C3H8\text{-}CH4}$ is the FID factor of propane relative to methane. The FID factors on a propane and methane bases as well as the calibration gas and measured concentrations used in Equation 3-12 are listed in Table 3-2.

Table 3-2. FID factors calculated using data from Siemens 5-Gas THC analyzer.

Species	Calibration Gas Concentration (ppmd)	Measured Concentration (ppmd, as methane)	$F'_{i\text{-}CH4}$	$F'_{i\text{-}C3H8}$
Methane	958.8	970.9	1.000	0.3561
Propane	45.23	127.0	2.808	1.000
Ethane	51.77	97.40	1.881	0.6700
Ethylene	10.33	18.50	1.791	0.6378

Uncertainty

Uncertainty for each of the measurements taken from all analyzers was calculated and reported with the results. The types of uncertainty considered were calibration gas error, random error, minimum detection concentration #1 (MDC#1), linearity, and zero and span. Since VOC concentrations were reported on a dry, propane basis, the total uncertainty of the measurements in ppm are propagated when factoring out the water content in the sample and converting the result to a propane basis.

The calibration gas error was calculated by multiplying the average measurement from a data point by the uncertainty provided on the specification sheet for the standard gas used to calibrate the analyzer. The random error was calculated by taking the standard deviation of the samples recorded for each analyzer. MDC#1 is a method of calculating an uncertainty for FTIR measurements and is published in ASTM method D 6348 [25]. To determine the MDC#1 uncertainty, a zero gas (UHP nitrogen) was sampled through the FTIRs. It was expected that each compound would read a concentration of exactly zero; however, sometimes the FTIR recorded a number approximate to zero. The MDC#1 uncertainty was taken as the measurement reported by the FTIR, whether it was zero or a value close to it. Moosman also calculated MDC#1 when taking FTIR measurements on HAP emissions from natural gas engines and describes the process in more detail in his thesis [20]. The linearity, zero, and span errors are listed on the analyzers' specification

sheets published by their manufacturers. Table 3-3 shows which uncertainty was considered for each analyzer as not all uncertainties were applicable for all analyzers.

Table 3-3. List of uncertainties considered for each analyzer.

Uncertainty Type	HP GC	MKS FTIR	VIG FID	Gasmet FTIR	Siemens 5-Gas
Calibration Error	✓	✓	✓	✓	✓
Random Error	✓	✓	✓	✓	✓
MDC#1		✓		✓	
Linearity Error			✓		✓
Zero & Span Error			✓		✓

Once the concentration measurements were converted to a dry, propane basis, the uncertainties propagated to even greater uncertainties. The raw, wet measurement was converted to a dry, propane basis using

$$ppmd_{C3H8} = \frac{ppmw \cdot F'_{i\text{-}C3H8}}{(1\text{-}ppm_{H2O})} \tag{3-19}$$

where *ppmw* is the raw, wet measurement of a specie in units of ppm, $F'_{i\text{-}C3H8}$ is the FID factor for the specie relative to propane, and ppm_{H2O} is the raw measurement of water taken from the MKS FTIR in units of ppm. The uncertainty associated with the concentration on a dry, propane basis was determined using

$$\delta ppmd_{C3H8} = \sqrt{\left(\frac{\partial ppmd_{C3H8}}{\partial ppmw}\delta ppmw\right)^2 + \left(\frac{\partial ppmd_{C3H8}}{\partial ppm_{H2O}}\delta ppm_{H2O}\right)^2} \tag{3-20}$$

where δppm_{H2O} is the uncertainty in the water concentration measurement from the MKS FTIR, which consists of the random error of the sample, and $\delta ppmw$ is the total uncertainty of the VOC specie measurement which is found by taking the sum of the uncertainties listed in Table 3-2

$$\delta ppmw = \delta ppmw_{cal} + \delta ppmw_{ran} + \delta ppmw_{MDC\#1} + \delta ppmw_{lin} + \delta ppmw_{zs} \tag{3-21}$$

where $\delta ppmw_{cal}$ is the calibration error, $\delta ppmw_{ran}$ is the random error, $\delta ppmw_{MDC\#1}$ is the MDC#1 error, $\delta ppmw_{lin}$ is the linearity error, and $\delta ppmw_{zs}$ is the zero and span error. Taking the partial derivatives in Equation 3-19 yields

$$\delta ppmd_{C3H8} = \sqrt{\left(\frac{F'_{i\text{-}C3H8}}{\left(1\text{-}ppm_{H2O}\right)}\delta ppmw\right)^2 + \left(-\frac{ppmw \cdot F'_{i\text{-}C3H8}}{\left(1\text{-}ppm_{H2O}\right)^2}\delta ppm_{H2O}\right)^2} \tag{3-22}$$

In addition to reporting VOC concentrations on a dry, propane basis, NO_X measurements from the ECOM Pro Easy, MKS FTIR, and Siemens 5-Gas analyzers were reported in terms of ppm dry at 15% O_2. Similar to how the uncertainties of the VOC concentration measurements were compounded when converting units, the uncertainties of the NO_X measurements were also propagated when normalized to 15% O_2. The conversion from units of ppmd to ppmd@15%O_2 was made using

$$ppmd@15\%O_2 = \frac{ppmd(20.9\text{-}15)}{20.9\text{-}\%O_2} \tag{3-23}$$

where *ppmd* is the dry measurement of an individual VOC concentration and $\%O_2$ is the volumetric percent of oxygen in the exhaust sample measured by the Siemens 5-Gas analyzer. Since the MKS FTIR required a wet sample, the uncertainty of the wet-to-dry conversion had to be incorporated

as well for the MKS measurements. The uncertainty of the NO_X concentration measurement in terms of ppmd@15%O_2 was calculated using

$$\delta ppmd@15\%O_2 = \sqrt{\left(\frac{\partial ppmd@15\%O_2}{\partial ppmd}\delta ppmd\right)^2 + \left(\frac{\partial ppmd@15\%O_2}{\partial \%O_2}\delta \%O_2\right)^2} \qquad (3\text{-}24)$$

where $\delta ppmd$ is the uncertainty of the raw, dry concentration measurement reported by the analyzers and is a sum of the uncertainty types considered for each analyzer listed in Table 3-2. The uncertainty of the %O_2 measurement is denoted $\delta\%O_2$ and is the sum of the uncertainties considered for the Siemens 5-Gas analyzer (OXYMAT 6). Taking the partial derivatives in Equation 3-23 gives

$$\delta ppmd@15\%O_2 = \sqrt{\left(\frac{5.9}{20.9-\%O_2}\delta ppmd\right)^2 + \left(-\frac{5.9ppmd}{(20.9-\%O_2)^2}\delta \%O_2\right)^2} \qquad (3\text{-}25)$$

CHAPTER 4 – ANALYZER/METHOD COMPARISON

VOC Concentration Results

The concentrations of the individual VOC compounds reported from each analyzer taken during Data Point 1 for the GMV-4 lean burn, open chamber spark ignition configuration is shown in Figure 4-1. It is important to note that while monitoring the engine using a LabVIEW VI, NO_X was calculated in real time using an atom balance method and was used to adjust boost for the specified target NO_X level, in this case 15 g/bhp-hr; however, processing the data afterward and following EPA Method 19 to calculate brake specific NO_X did not always yield a NO_X level close to the desired target. In this case, the NO_X emission was calculated to be 11.9 g/bhp-hr for Data Point 1. For all following data points, the EPA Method 19 calculation for NO_X emission will be reported, even though engine conditions were adjusted to reach the desired NO_X level specified by the test plan during testing. In addition, TER control and NO_X sensor feedback control were not available during most of the test program; therefore, boost control was used to maintain the target NO_X level. TER was calculated using equations discussed in papers on comparing the tracer gas method and perfect mixing method [26, 27] and was 0.58 for this data point.

The MKS reported similar concentrations to the HP GC for ethylene and propylene. According to the HP GC data, the highest contributor to the VOC concentration was propane. The HP GC reported very little higher hydrocarbons; n-butane is shown having the maximum concentration of 4.64 ppmd, as propane and there were no i-hexane or n-hexane detected. The MKS FTIR, Gasmet FTIR, and the VIG FID reported propane and higher hydrocarbons as a single output, denoted by the term “C3+”, and can be seen on the very right of the plot in Figure 4-1. The Gasmet FTIR reported a similar ethylene concentration to the HP GC and was within ±3 percent

of the VIG FID and MKS FTIR for the C_{3+} measurement. The VIG FID reported a C_{3+} concentration 5 percent higher than the MKS FTIR. A sample chromatogram taken from the HP GC during this data point is shown in Figure 4-2.

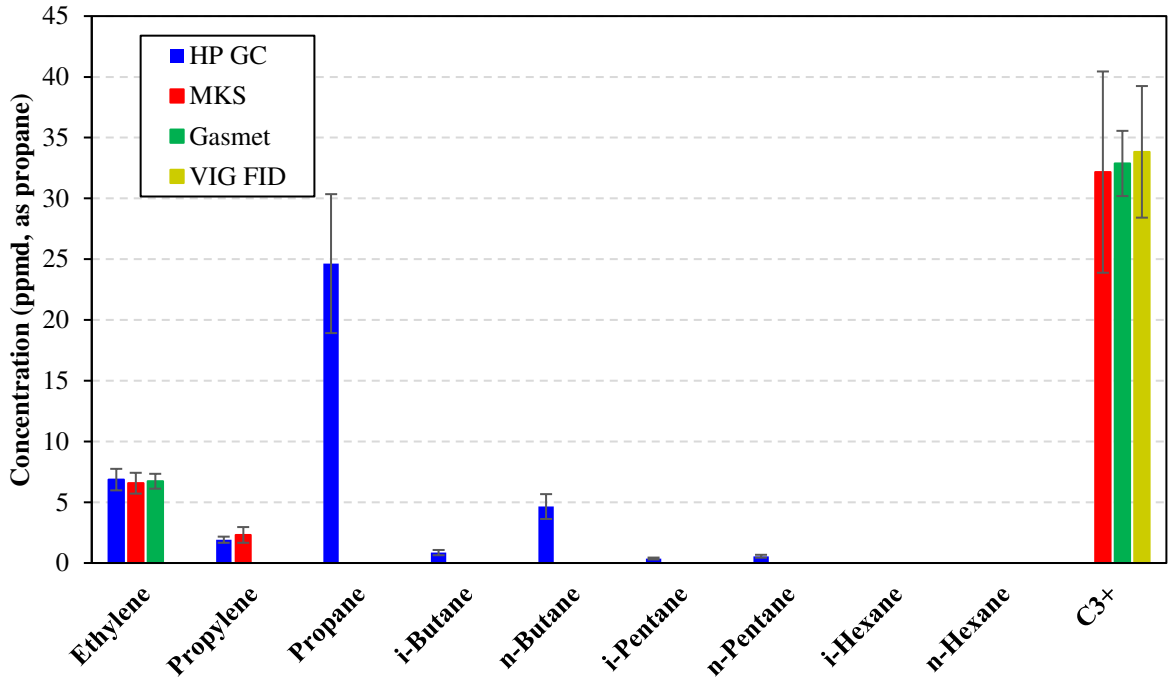

Figure 4-1. Individual VOC concentrations reported from each analyzer during Data Point 1.

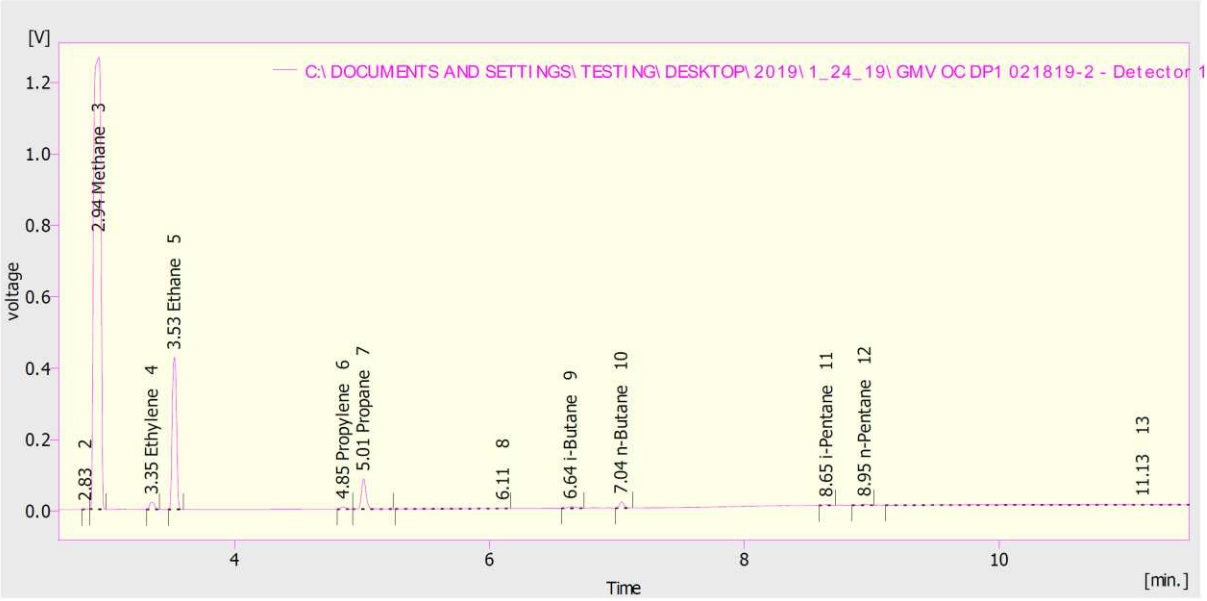

Figure 4-2. Sample chromatogram depicting response peaks detected by the HP GC during Data Point 1.

The chromatogram depicts response peaks for each of the VOC species as well as methane and ethane. The methane peak, located at a time of 2.94 min, has the largest peak area, indicating that methane makes up most of the exhaust gas hydrocarbons. Ethane appears to have the second largest peak area and propane has the third. The butanes and pentanes contribute very little to exhaust hydrocarbons compared to the lighter hydrocarbons and there is no iso-hexane or n-hexane peak areas detected by the FID. The plot comparing different methods for calculating total VOC concentration for Data Point 1 is shown in Figure 4-3.

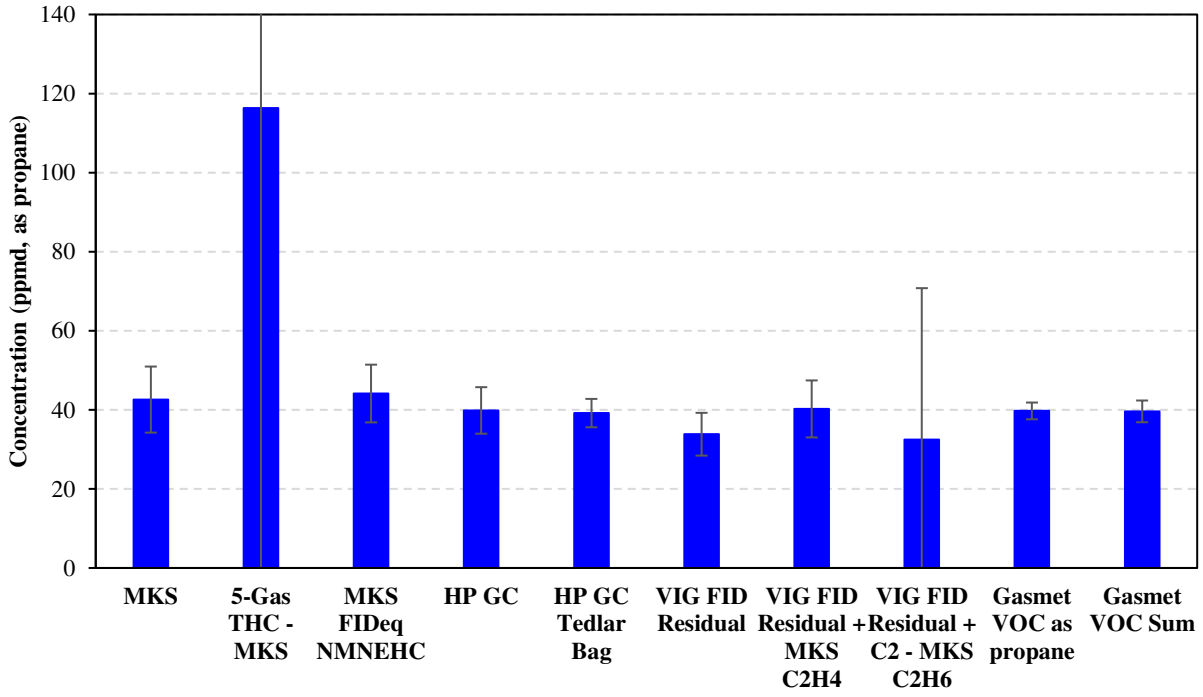

Figure 4-3. Total VOC concentrations reported using different analyzers/methods for Data Point 1. Note that the uncertainty for "5-Gas THC – MKS" is ±285 ppmd, as propane.

The "MKS" method seen on the plot is the addition of the individual VOC concentrations. The "5-Gas THC – MKS" method is carried out by taking the THC concentration measurement from the Siemens 5-Gas analyzer and subtracting the methane and ethane concentrations reported by the MKS; this method yields the largest total VOC concentration among all the methods as well as the largest uncertainty. This large uncertainty arises because the method involves evaluating the

difference of two large numbers, THC and the sum CH4+C2H6, to compute a smaller number (VOCs). The "MKS FIDeq NMNEHC" is a measurement reported by the MKS FTIR software and is calculated using the same process as the "MKS" method; however slightly different FID factors are used. The total VOC concentration using the "MKS FIDeq NMNEHC" measurement is higher than the "MKS" measurement, but only by 3.6 percent.

The "HP GC" method is the addition of each VOC measurement performed by direct extraction of an exhaust gas sample; three samples are analyzed and averaged for each data point. The "HP GC Tedlar Bag" is the addition of each VOC measurement taken from an exhaust gas sample stored in a Tedlar bag, which is analyzed 24-36 hours after filling the bag. During each data point the Tedlar bag sampling rate is controlled to a steady flow such that the bag is filled over the data point period. The resulting total VOC concentration from the Tedlar bag was 1.7 percent lower than the total VOC concentration for the direct extraction of the exhaust gas into the HP GC. The results from the direct extraction method of the HP GC is the most accurate instrument used for this test program. The HP GC is the most accurate because each VOC is separately calibrated and performed daily. Furthermore, instrument linearity and drift checks are performed per Method 18/25a. The procedures for the other instruments each have some but not all the steps performed for the HP GC. The FID is sensitive enough to detect low levels (~0.05 ppm) of individual VOCs without interference from other exhaust constituents. Comparing the HP GC direct extraction vs. Tedlar bag sampling techniques, direct extraction is expected to be more accurate since there is no opportunity for VOC species absorption in condensed water.

The measurement taken from the residual channel of the VIG FID is denoted by "VIG FID Residual." This measurement only consists of higher hydrocarbons (C_{3+}) and excludes ethylene, which is defined as a VOC. Because of this, the total VOC concentration from this method is

significantly lower than the total VOC concentrations from the "MKS" and "HP GC" methods. To correct this, the ethylene measurement from the MKS FTIR is added to the VIG FID residual measurement to get the total VOC concentration, denoted by "VIG FID Residual + MKS C2H4." Another method to calculate total VOC concentration using the VIG FID is to add the residual and C2 measurements and subtract the ethane measurement from the MKS FTIR ("VIG FID Residual + C2 – MKS C2H6"). This method yields the lowest total VOC concentration of all the methods and a significantly large uncertainty (±38.3 ppmd, as propane). The second to the last method is labeled as "Gasmet VOC as Propane" in the Gasmet software, Calcmet, and is the individual measurement that the Gasmet FTIR reports, which sums the total VOC species and applies FID factors specified by the manufacturer. The total VOC measurement calculated from this method is less than 1 percent lower than the HP GC's measurement. The last method, "Gasmet VOC Sum", is the addition of each VOC reported by the Gasmet FTIR, which yields a total VOC concentration very similar to the HP GC. Since the FID factors used by Gasmet Technologies and the FID factors calculated using the method discussed in Chapter 3 are slightly different, the total VOC concentrations from the two Gasmet methods may be different, but never greater than 1 percent.

The concentrations of the individual VOC compounds reported from each analyzer taken during Data Point 7 for the GMV-4 lean burn, open chamber spark ignition configuration is shown in Figure 4-4. For this data point, the NO_X level was 12.5 g/bhp-hr, TER was 0.56, and there was a 10 mol% addition of ethane to the natural gas fuel supply. The Gasmet FTIR and MKS FTIR measured an ethylene concentration 9 percent higher than the HP GC. Otherwise, the trends comparing the individual VOC concentrations among the analyzers are similar to those seen in the plot shown for Data Point 1. The plot comparing different methods for calculating total VOC concentration for Data Point 7 is shown in Figure 4-5.

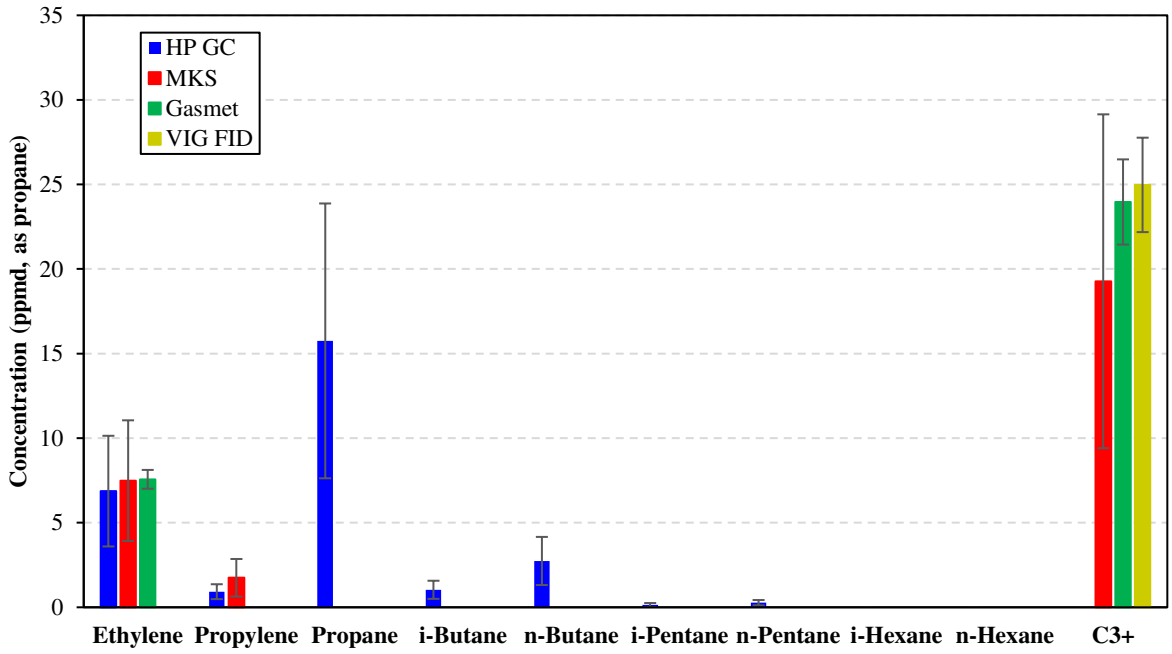

Figure 4-4. Individual VOC concentrations reported from each analyzer during Data Point 7.

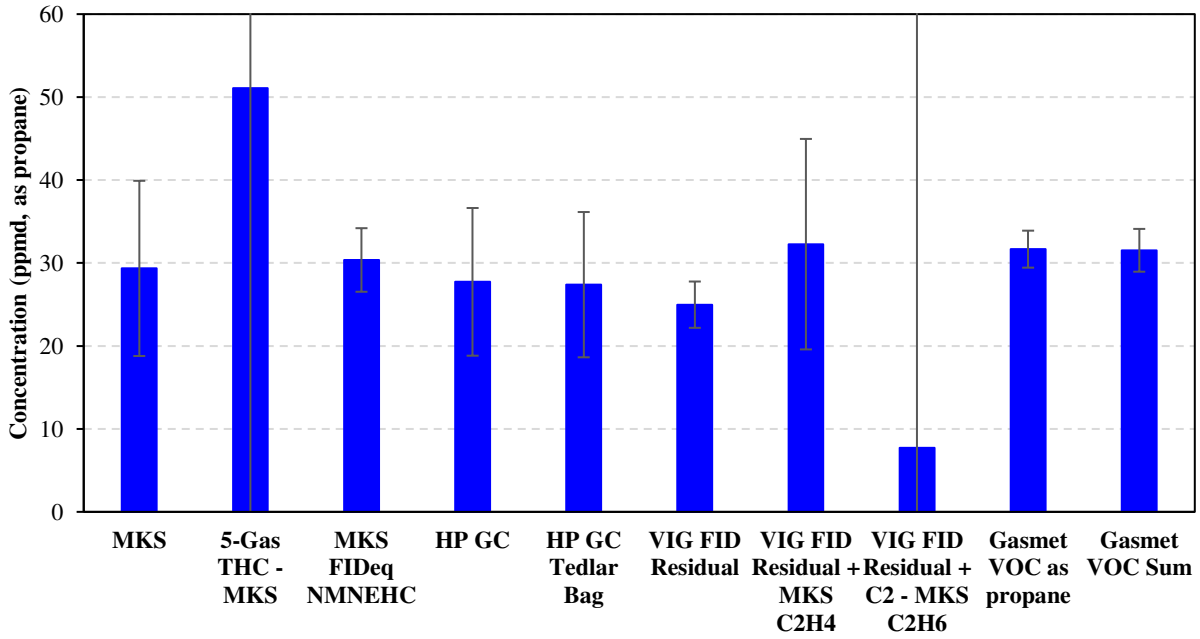

Figure 4-5. Total VOC concentrations reported using different analyzers/methods for Data Point 7. Note that the uncertainty for "5-Gas THC – MKS" is ±258 ppmd, as propane and the uncertainty for "VIG FID Residual + C2 – MKS C2H6" is ±133 ppmd, as propane.

With the addition of 10 mol% ethane in the natural gas fuel, there was a 44 percent decrease in the total VOC concentration, according to the HP GC measurements. The total VOC measurement

calculated using the "VIG FID Residual + C2 – MKS C2H6" method differed from the HP GC by approximately 72 percent, as opposed to the 18 percent difference seen for Data Point 1. The uncertainty of the measurement for this method was also significantly larger for Data Point 7. The Gasmet methods reported, on average, a total VOC concentration approximately 14 percent higher than the HP GC. The trends among the remaining methods did not vary greatly from those seen for Data Point 1.

The concentrations of the individual VOC compounds reported from each analyzer taken during Data Point 9/10 for the GMV-4 lean burn, open chamber spark ignition configuration is shown in Figure 4-6. No boost or IT adjustments were necessary between Data Points 9 and 10 so they were combined and recorded at the same engine conditions. For this data point, the NO_X level was 10.8 g/bhp-hr, TER was 0.59, and there was a 5 mol% addition of higher hydrocarbons (C_{3+}) to the natural gas fuel supply.

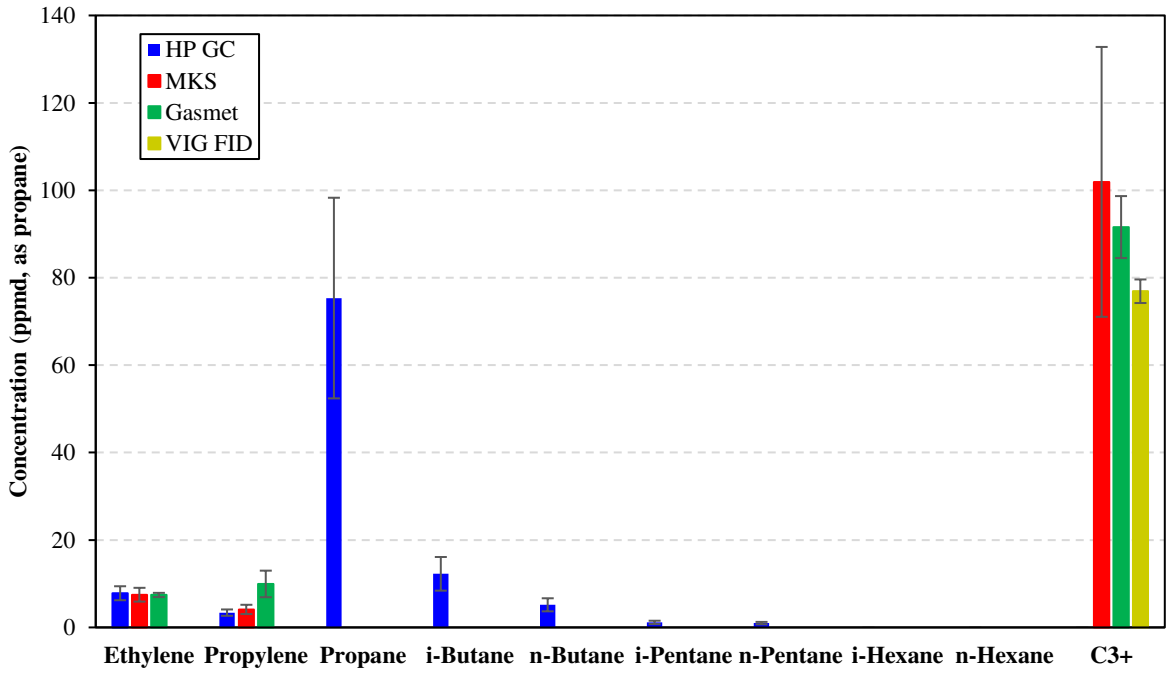

Figure 4-6. Individual VOC concentrations reported from each analyzer during Data Point 9/10.

The ethylene concentration measured by the Gasmet FTIR is similar to the HP GC but the Gasmet FTIR reported a significantly higher propylene concentration. Unlike the previous data points discussed, the MKS FTIR and Gasmet FTIR measured significantly higher than the VIG FID for the C_{3+} concentration. The plot comparing different methods for calculating total VOC concentration for Data Point 9/10 is shown in Figure 4-7.

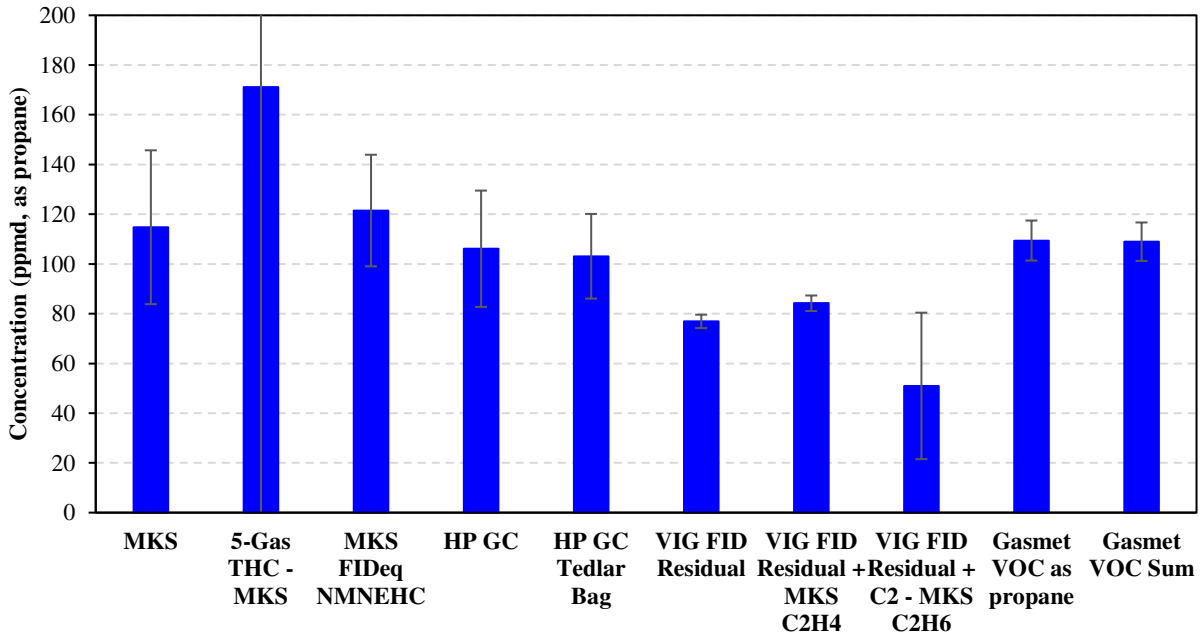

Figure 4-7. Total VOC concentrations reported using different analyzers/methods for Data Point 9/10. Note that the uncertainty for "5-Gas THC – MKS" is ±172 ppmd, as propane.

According to the HP GC data, there was an increase of total VOC concentration by 166 percent compared to the nominal point (Data Point 1). No other significant variation among the analyzer/method comparison occurred compared to Data Point 1.

The individual VOC and total VOC concentration plots for the remaining data points within the GMV-4 lean burn, open chamber (OC) spark ignition configuration (i.e. Data Points 2, 3, 4, 6, 8, and 11) did not show significant variation in total VOC concentration or significant change in the trends for the analyzer/method comparison than the nominal Data Point 1 or what has been previously discussed; therefore, the plots showing the results of these data points are not presented

here. They are provided in Appendix B. The chromatograms taken from the HP GC can also be seen in Appendix B.

The concentrations of the individual VOC compounds reported from each analyzer recorded during Data Point 12 for the GMV-4 lean burn, pre-combustion chamber (PCC) ignition configuration are shown in Figure 4-8. The NO_X level was 1.03 g/bhp-hr, TER was 0.49, and this data point was one of the nominal data points for this engine configuration. Note that there are no results shown for the Gasmet FTIR. The analyzer was lent to another company between testing on the OC and PCC configurations. After two weeks, the analyzer was returned, and testing was resumed for the PCC configuration. Unfortunately, after testing for the PCC configuration was complete and the engine was configured, it was noticed that the software library had been modified so that no spectra was saved, and the library was saved under the same name and version number. Because of this, there is no Gasmet FTIR data for the PCC configuration. The issue was discovered and resolved before testing began on the HPFI configuration. Saving the spectra was critical because VOC method development for the Gasmet FTIR was carried out in parallel with testing. Final processing of the spectra was not performed until after the test program was concluded.

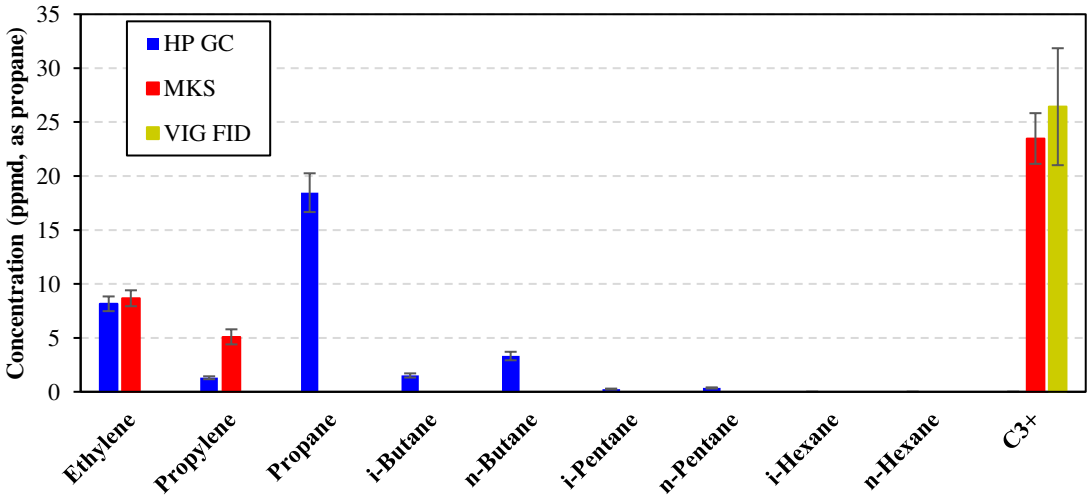

Figure 4-8. Individual VOC concentrations reported from each analyzer during Data Point 12.

The MKS FTIR measurement of ethylene is comparable to the HP GC measurement; however, the MKS FTIR reported a significantly higher amount of propylene than the HP GC. The VIG FID measured 12.6 percent higher than the MKS FTIR in C_{3+} concentrations. The chromatogram taken from the HP GC during Data Point 12 is shown in Figure 4-9.

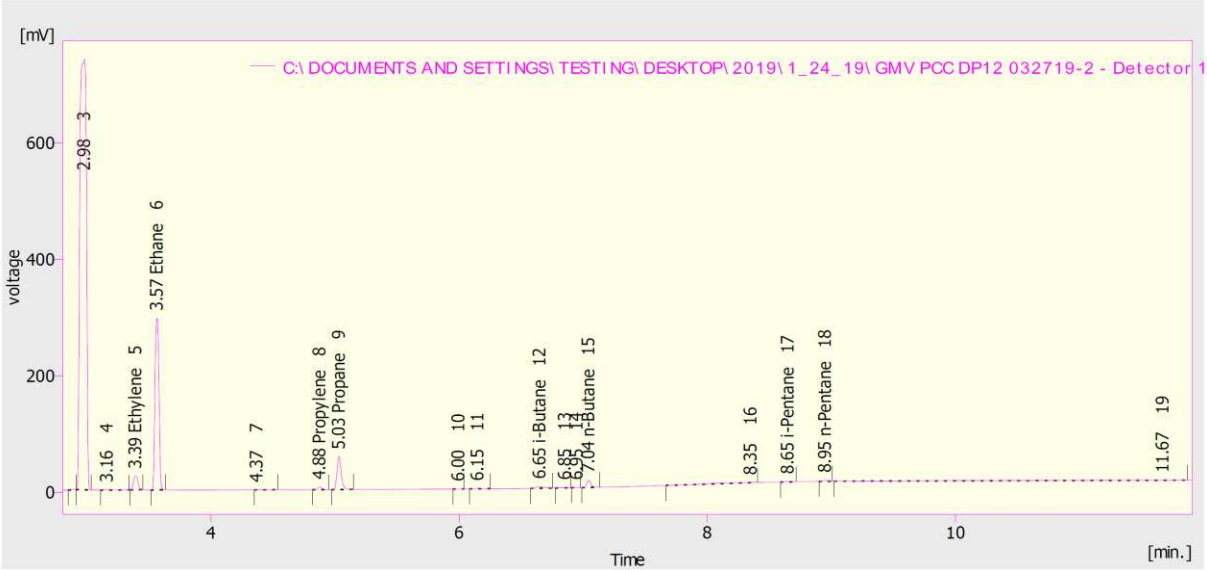

Figure 4-9. Sample chromatogram depicting response peaks detected by the HP GC during Data Point 12.

Like the chromatogram shown for Data Point 1 (Figure 4-2), the methane peak area is the largest area shown on the chromatogram; however, the area is almost half of the methane peak area for Data Point 1, implying that the methane concentration is about half that for Data Point 1. Again, very small peak areas were detected by the FID for butane and pentane and no hexane peak areas were measured. The plot comparing different methods for calculating total VOC concentration for Data Point 12 is shown in Figure 4-10.

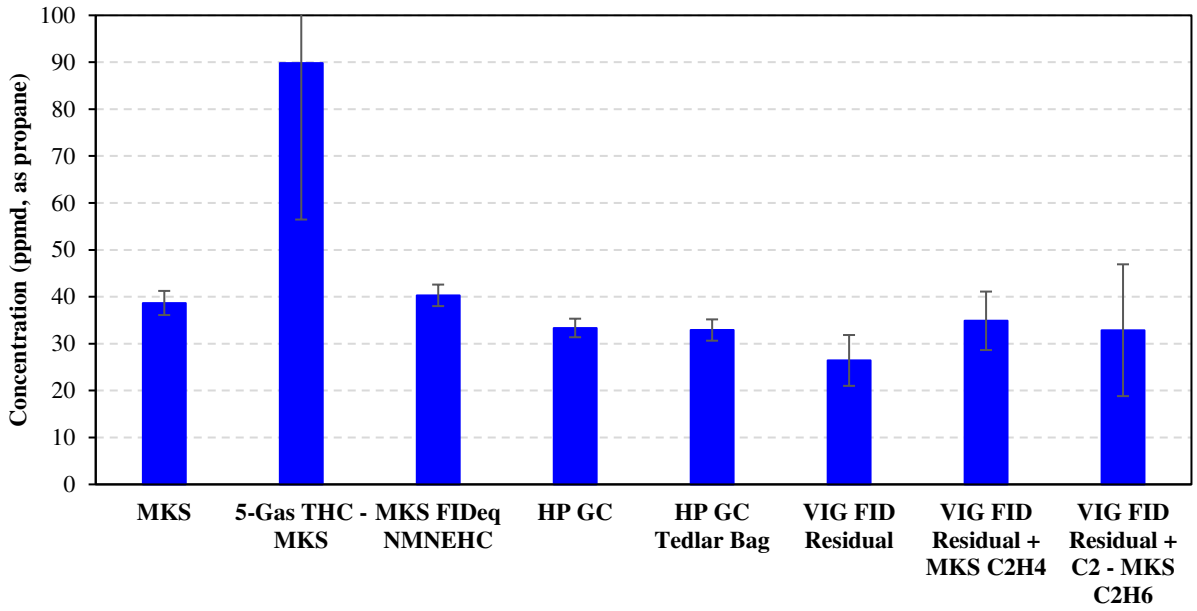

Figure 4-10. Total VOC concentrations reported using different analyzers/methods for Data Point 12. Note that the uncertainty for "5-Gas THC – MKS" is ±33.4 ppmd, as propane.

The total VOC concentration calculated from the "MKS" method is lower than the total VOC concentration calculated by the "MKS FIDeq NMNEHC" method; however, the difference is small (<10 percent). The "MKS" calculation of total VOC concentration is 16.0 percent larger than the "HP GC" calculation. The "HP GC" and "HP GC Tedlar Bag" calculations are similar, with the "HP GC" calculation being slightly higher. The "VIG FID" method calculated a total VOC concentration lower than the "HP GC" method; however, when the MKS ethylene measurement is added in the "VIG FID Residual + MKS C2H4", the total VOC concentration becomes comparable to the "HP GC" calculation. Subtracting the MKS ethane measurement from the sum of the VIG FID's C2 and residual measurements also produces a similar VOC concentration to the "HP GC" calculation. The "5-Gas THC – MKS" produced the largest total VOC concentration along with the largest uncertainty.

The concentrations of the individual VOC compounds reported from each analyzer taken during Data Point 13 for the GMV-4 lean burn, PCC ignition configuration is shown in Figure 4-

11. For this data point, ignition timing was advanced from 18°aTDC to 13°aTDC, the NO_X level was 1.48 g/bhp-hr, and TER was 0.47. The MKS reported an ethylene measurement similar to the HP GC; however, the MKS measured a propylene concentration significantly larger than the HP GC. The plot comparing different methods for calculating total VOC concentration for Data Point 13 is shown in Figure 4-12.

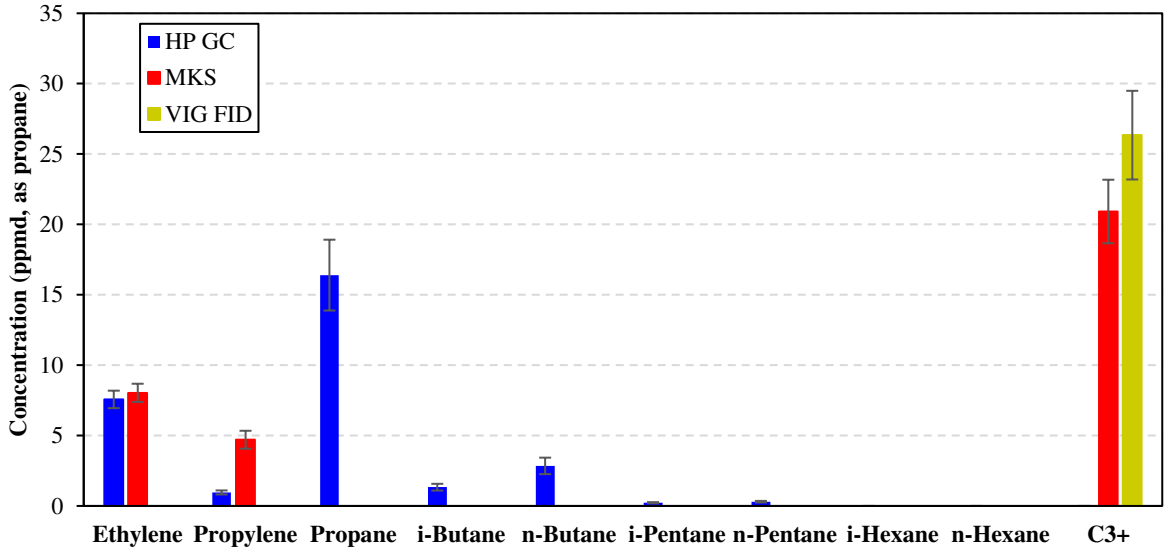

Figure 4-11. Individual VOC concentrations reported from each analyzer during Data Point 13.

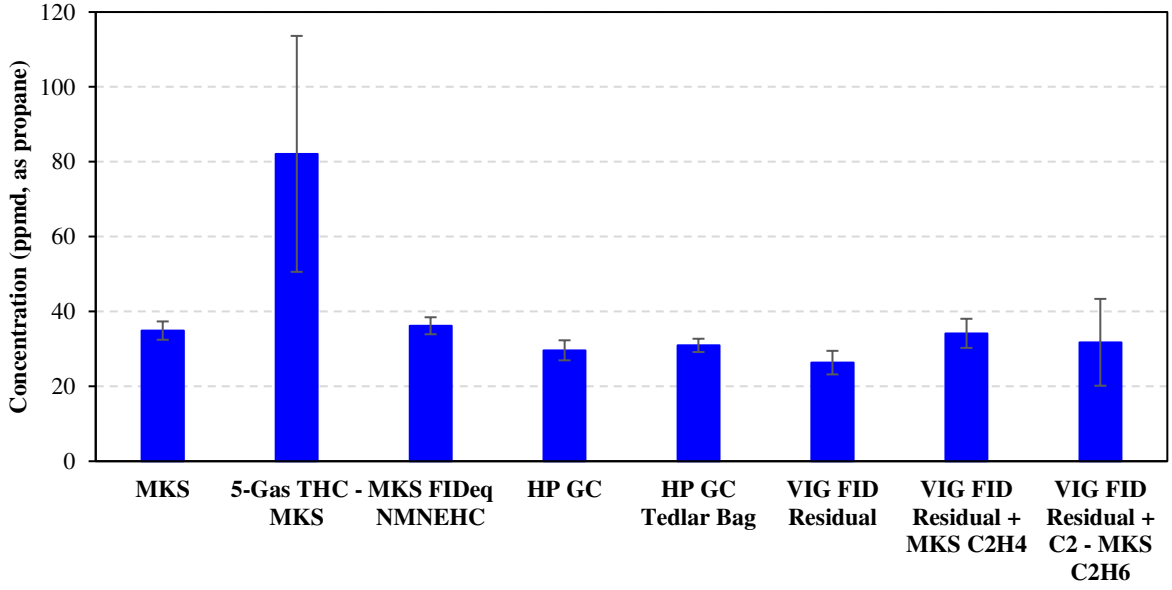

Figure 4-12. Total VOC concentrations reported using different analyzers/methods for Data Point 13.

According to the HP GC, the total VOC concentration decreased 11 percent compared to the nominal data point; however, the comparisons between the methods remain consistent with those seen for the nominal data point.

The concentrations of the individual VOC compounds reported from each analyzer taken during Data Point 20/21 for the GMV-4 lean burn, pre-combustion chamber ignition configuration is shown in Figure 4-13. For this data point, 5 mol% of higher hydrocarbons was added to the nominal fuel composition, the NO_X level was 1.00 g/bhp-hr, and TER was 0.47. The MKS FTIR and VIG FID reported similar C_{3+} concentrations. The plot comparing different methods for calculating total VOC concentration for Data Point 20/21 is shown in Figure 4-14.

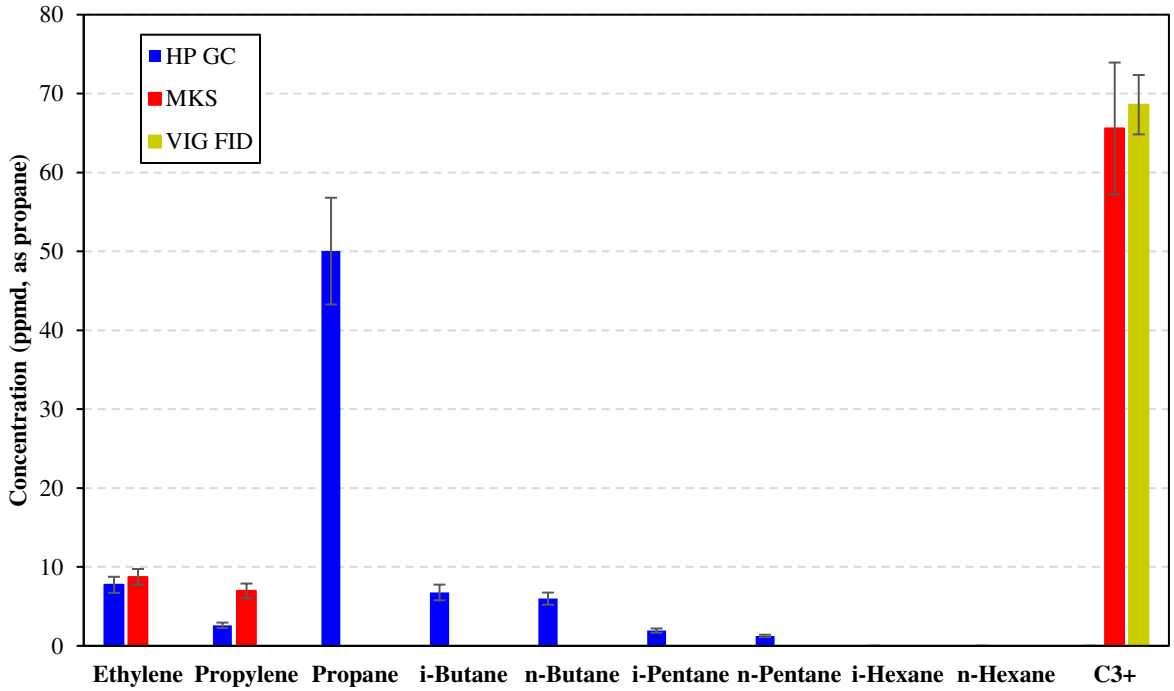

Figure 4-13. Individual VOC concentrations reported from each analyzer during Data Point 20/21.

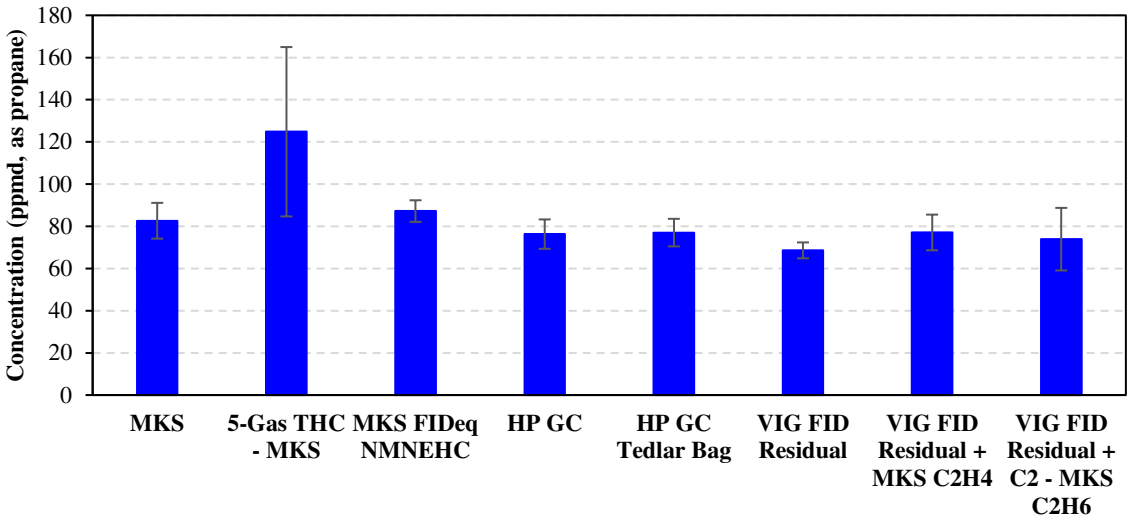

Figure 4-14. Total VOC concentrations reported using different analyzers/methods for Data Point 20/21.

The HP GC data shows the total VOC concentration increased 129 percent compared to the nominal data point. The "HP GC Tedlar Bag" calculation for the total VOC concentration was larger than the "HP GC" calculation but only by 1 percent.

The individual VOC and total VOC concentration plots for the remaining data points within the GMV-4 lean burn, PCC ignition configuration (i.e. Data Points 14, 17, and 18/19) did not show significant variation in total VOC concentration or significant change in the trends for the analyzer/method comparison than the nominal Data Point 12 or what has been previously discussed. Consequently, the plots showing the results of these data points are shown in Appendix B.

The concentrations of the individual VOC compounds reported from each analyzer taken during Data Point 27 for the GMV-4 lean burn, HPFI PCC ignition with electronic fuel valves configuration is shown in Figure 4-15. The NO_X level was 0.47 g/bhp-hr, TER was 0.44, and this data point was the nominal data point with an ignition timing of 18°aTDC and nominal fuel composition.

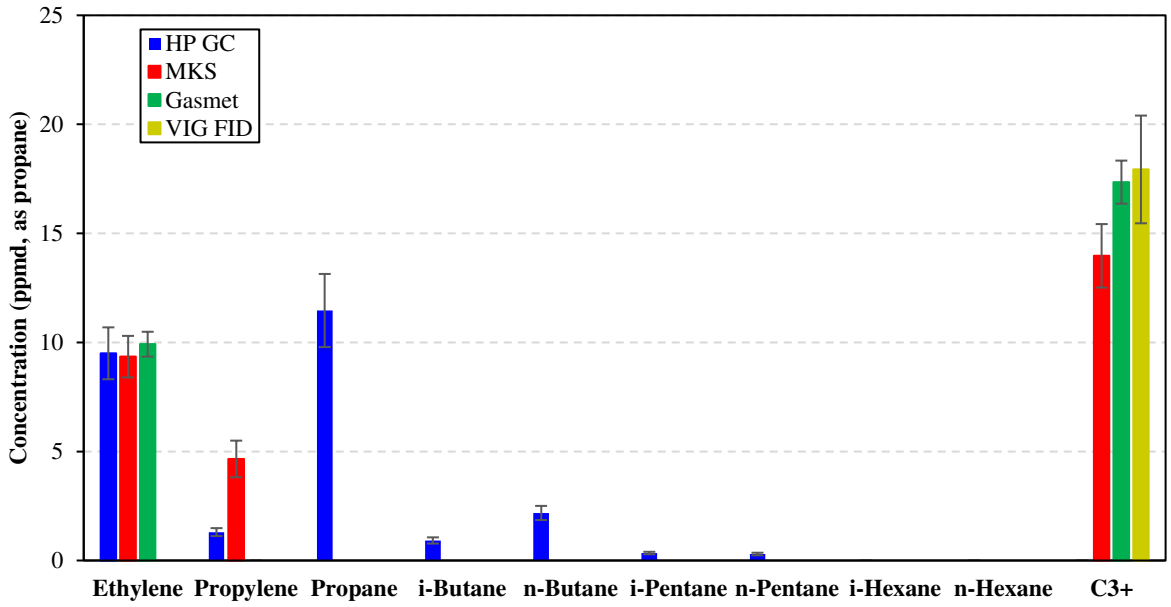

Figure 4-15. Individual VOC concentrations reported from each analyzer for Data Point 27.

Again, as in the previous configuration, the MKS FTIR measured a propylene concentration significantly higher than the HP GC; however, it reported an ethylene concentration within 5 percent of the HP GC measured concentration. The Gasmet FTIR also measured an ethylene concentration similar to the HP GC, only 4.4 percent higher. The MKS FTIR reported greater than 24 percent lower in C_{3+} concentration than the Gasmet FTIR and VIG FID. The plot comparing different methods for calculating total VOC concentration for Data Point 27 is shown in Figure 4-16. The MKS FTIR reported a total VOC concentration measurement 11.2 percent higher than the HP GC. The total VOC concentration measured from the Tedlar bag was 11.4 percent lower than the direct extraction measurement; this difference is larger than what was reported for the previous data points.

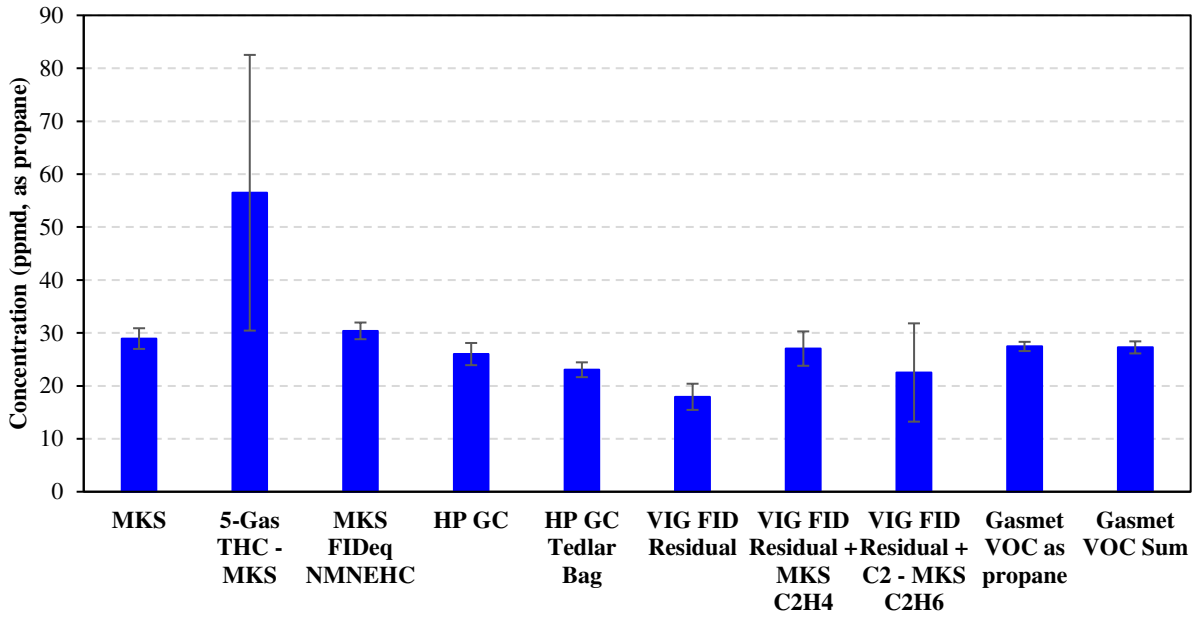

Figure 4-16. Total VOC concentrations reported using different analyzers/methods for Data Point 27.

The individual VOC and total VOC concentration plots for the remaining data points within the GMV-4 lean burn, HPFI PCC ignition with electronic fuel valves configuration (i.e. Data Points 23, 24, 25, 28/29, 30/31, and 32) did not show significant variation in total VOC concentration or significant change in the trends for the analyzer/method comparison than the nominal Data Point 27 or what has been previously discussed, so the plots showing the results of these data points are shown in Appendix B. The chromatograms taken from the HP GC are also included in Appendix B.

The concentrations of the individual VOC compounds reported from each analyzer taken during Data Point 33 for the Caterpillar 3304 rich burn with a 3-way catalyst configuration is shown in Figure 4-17. The NO_X level was 1.20 g/bhp-hr and the equivalence ratio was 1.01, stoichiometric. This data point was at nominal conditions with an ignition timing of 30°bTDC and nominal fuel composition.

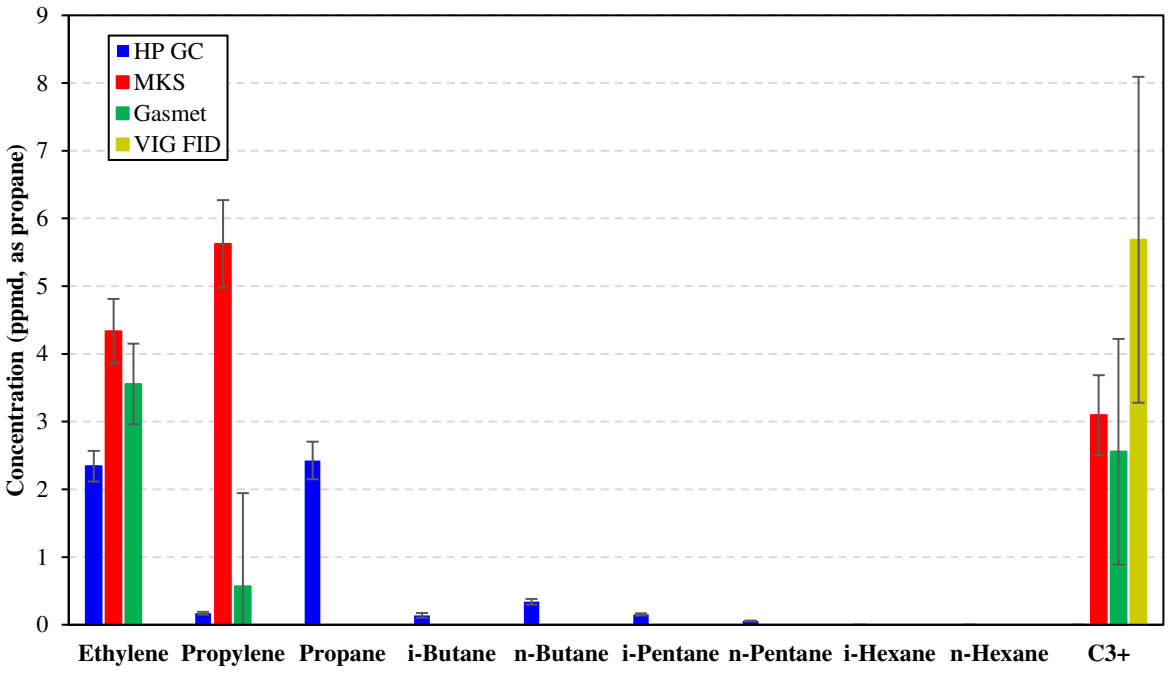

Figure 4-17. Individual VOC concentrations reported from each analyzer for Data Point 33.

The Gasmet and MKS FTIRs reported significantly higher concentrations of ethylene and propylene than the HP GC and the MKS FTIR measured much higher than the Gasmet FTIR. The Gasmet FTIR also measured significantly higher propane than the HP GC. The chromatogram taken from the HP GC for this data point is shown in Figure 4-18.

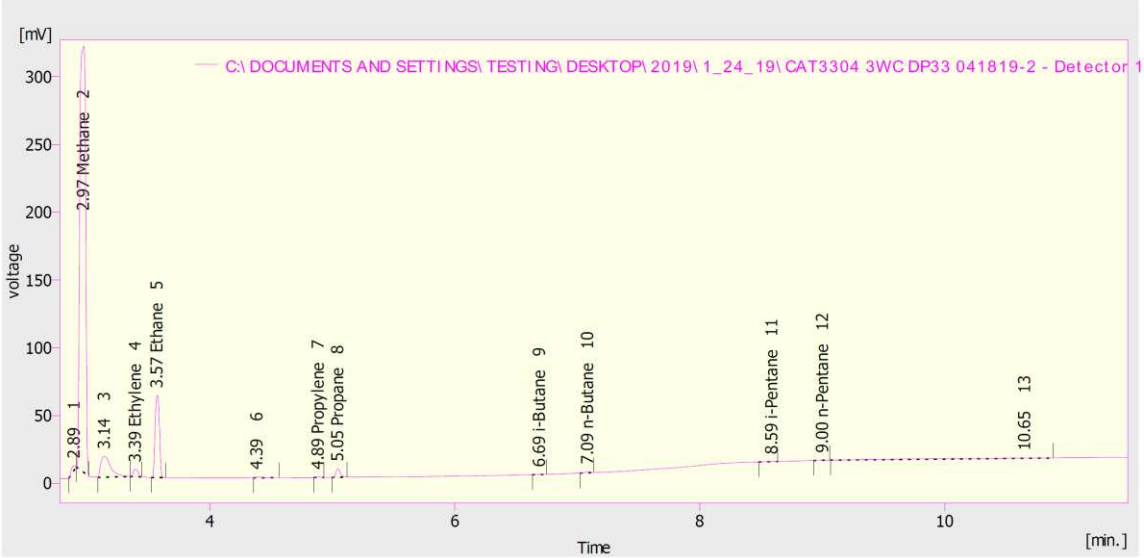

Figure 4-18. Sample chromatogram depicting response peaks detected by the HP GC during Data Point 33.

The HP GC chromatogram shows very small peak areas for propylene and propane; the areas are smaller than those shown for these species on the chromatograms from previous data points taken during testing on the GMV-4 engine since the exhaust gas is sampled downstream of the three-way catalyst, which oxidizes exhaust VOCs. The peak areas for butane and pentane are almost non-detectable. The plot comparing different methods for calculating total VOC concentration for Data Point 33 is shown in Figure 4-19.

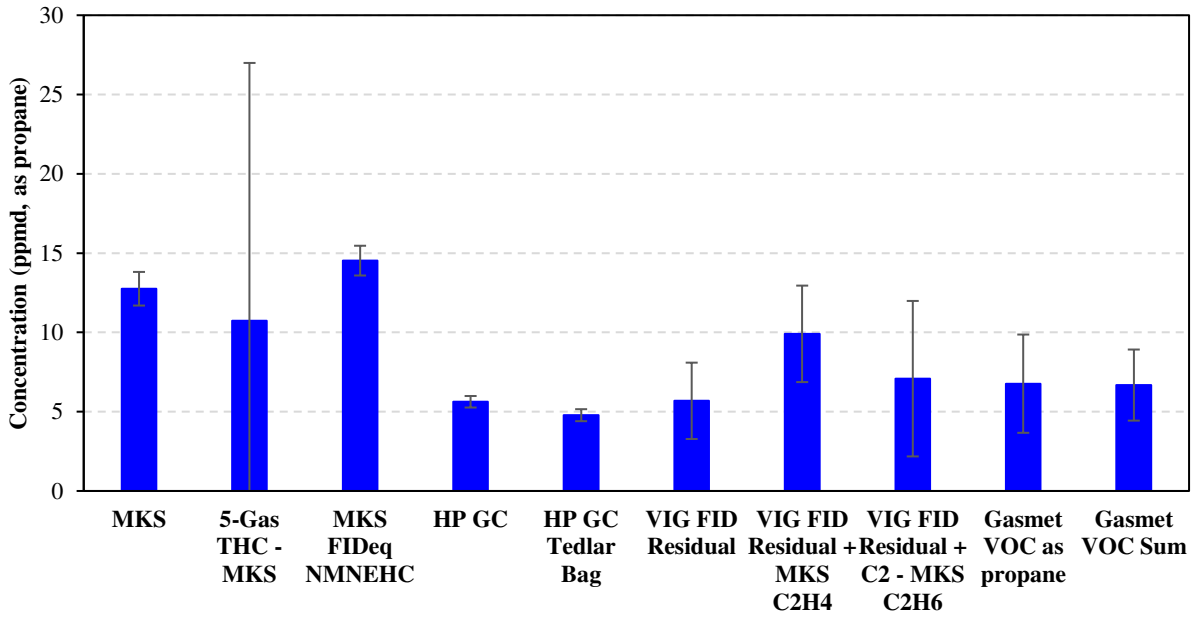

Figure 4-19. Total VOC concentrations reported using different analyzers/methods for Data Point 33.

The Gasmet FTIR measured 20 percent higher than the HP GC in total VOC concentration. The "5-Gas THC – MKS" method yielded a calculated total VOC concentration less than the MKS FTIR; however, the total VOC concentration was still 90.6 percent larger than the HP GC. The individual VOC and total VOC concentration plots for the remaining data points within the Caterpillar 3304 rich burn with a three-way catalyst configuration (i.e. Data Points 34, 35, 36, and 37) did not show significant variation in total VOC concentration or significant change in the trends for the analyzer/method comparison than the nominal Data Point 33; therefore, the plots

showing the results of these data points as well as the HP GC chromatograms are shown in Appendix B.

An average of the total VOC concentrations for each analyzer in units of ppmd, as propane as well as g/bhp-hr was taken over all the data points for the GMV-4 and Caterpillar 3304 engines, separately. An average was also calculated for the uncertainty of each analyzer/method. Average relative measurement differences were calculated for each analyzer to quantify the accuracy of each method relative to the HP GC. The standard deviation of each method among the data points was calculated as well. The results of each parameter among the data points for the GMV-4 engine is shown in Table 4-1. The "Gasmet VOC as propane" and "Gasmet Sum" results for data points where there were no saved spectra from the Gasmet FTIR were excluded from the averages, but the rest of the methods were included in the averages.

Table 4-1. Averages of total VOC concentrations calculated from each analyzer/method among all data points for the GMV-4 engine configurations.

	MKS	5-Gas THC-MKS	MKS FIDeq NMNEHC	HP GC	HP GC Tedlar Bag	VIG Residual	VIG FID Residual + MKS C2H4	VIG FID Residual + C2 - MKS C2H6	Gasmet VOC as propane	Gasmet Sum
VOC (ppmd as propane)	41.5	71.9	43.4	37.4	36.5	30.0	38.3	28.6	38.4	38.2
VOC Uncertainty (% of ppmd as propane)	15.8	193	9.13	14.4	12.5	12.2	17.9	175	4.33	5.50
VOC (g/bhp-hr)	0.567	0.990	0.593	0.510	0.498	0.410	0.527	0.397	34.2	34.0
Relative Measurement Difference (%)	12.2	99.9	17.2	0	-1.94	-19.5	6.30	-23.0	18.8	17.9
Std dev of Relative Measurement Difference (%)	7.65	51.8	7.96	0	7.88	10.3	13.3	31.8	23.3	21.7

For the GMV-4 engine configurations, the “HP GC Tedlar Bag” yielded on average almost two percent less than the HP GC. This difference is small compared to the measurement uncertainty. The second most accurate method is the “VIG FID Residual + MKS C2H4” with a 6.30 percent difference relative to the HP GC. The MKS method generally produced total VOC concentrations similar to the HP GC; the “MKS FIDeq NMNEHC” method gave slightly less accurate results than MKS. The “Gasmet VOC as propane” and “Gasmet VOC Sum” methods tended to overestimate total VOCs by an average of 18.8 percent and 17.9 percent, respectively. The “VIG Residual” channel tended to underestimate total VOC concentrations by nearly 20 percent. The “VIG FID Residual + C2 – MKS C2H6” also underestimated total VOCs by an even greater amount of 23.0 percent. On the other hand, the “5-Gas THC – MKS” method yielded significantly higher total VOC concentrations than the HP GC by approximately 100 percent (e.g. higher by a factor of 2). The results of each parameter among the data points for the Caterpillar 3304 engine is shown in Table 4-2.

For the Caterpillar 3304 data, the “HP GC Tedlar Bag” and “VIG Residual” methods were the most accurate compared to the HP GC; the “HP GC Tedlar Bag” method tended to underestimate total VOC concentrations by approximately 13 percent and the “VIG Residual” method generally overestimated total VOCs by 9.5 percent. The remaining methods yielded significantly higher total VOC concentrations relative to the HP GC. According to the HP GC, brake specific VOCs for the Caterpillar 3304 engine configuration was less than any of the GMV-4 configurations. To see the calculations of the parameters listed in Table 4-1 and Table 4-2 for each data point, refer to Appendix B.

Table 4-2. Averages of total VOC concentrations calculated from each analyzer/method among all data points for the Caterpillar 3304 engine configurations.

	MKS	5-Gas THC-MKS	MKS FIDeq NMNEHC	HP GC	HP GC Tedlar Bag	VIG Residual	VIG FID Residual + MKS C2H4	VIG FID Residual + C2 - MKS C2H6	Gasmet VOC as propane	Gasmet Sum
VOC (ppmd as propane)	12.5	13.7	14.3	5.45	4.74	5.95	10.1	7.05	8.74	8.52
VOC Uncertainty (% of ppmd as propane)	8.42	122	6.62	7.24	7.89	39.2	29.1	78.1	19.8	16.4
VOC (g/bhp-hr)	0.036	0.040	0.041	0.016	0.014	0.017	0.029	0.020	0.025	0.025
Relative Measurement Difference (%)	130	152	163	0.00	-12.9	9.46	85.9	29.6	60.1	56.0
Std dev of Relative Measurement Difference (%)	3.39	35.2	4.25	0.00	2.12	6.93	7.67	5.49	36.6	34.0

For VOC quantification, individual VOC species up to C_6 were reported; however, it may not be necessary to quantify some of the heavier hydrocarbons. The individual VOC and HP GC chromatograms illustrate that butane and pentane do not contribute significantly to the total exhaust gas composition. For most data points, i-hexane or n-hexane are not detected by the HP GC FID. This is true even when significant quantities of these species are added to the fuel (i.e. C_{3+} blending). It may only be necessary to quantify VOCs up to C_4 or C_5 and still be within 10 percent of the total VOC concentration if hydrocarbons up to C_6 were included. To investigate this, the total VOC concentration was calculated for every data point, first including all hydrocarbons up to C_6, then excluding C_{6+}, C_{5+}, C_{4+}, and C_{3+}. The percent relative difference was calculated to determine the accuracy of each alternate total VOC calculation. The percent relative difference of each total VOC calculation for each data point is shown in Table 4-3.

Table 4-3. Percent relative difference of each alternate total VOC calculation for each data point.

Data Point	Total VOC - C_{6+} (%)	Total VOC - C_{5+} (%)	Total VOC - C_{4+} (%)	Total VOC - C_{3+} (%)
1	0.00	-2.33	-14.1	-73.7
2	0.00	-2.28	-17.2	-82.3
3	0.00	-2.04	-14.2	-64.5
4	0.00	-1.87	-14.8	-71.9
6	0.00	-2.04	-17.6	-71.9
7	0.00	-1.47	-13.8	-66.9
8	0.00	-1.37	-13.2	-54.6
9/10	0.00	-2.01	-16.8	-87.0
11	0.00	-1.51	-14.6	-69.9
12	0.00	-1.81	-14.8	-66.1
13	0.00	-1.78	-14.4	-65.8
14	0.00	-3.66	-17.2	-58.0
17	0.00	-4.04	-19.7	-69.6
18/19	0.00	-3.75	-17.9	-58.9
20/21	0.00	-4.17	-17.4	-82.9
23	0.00	-2.84	-14.2	-53.9
24	0.00	-2.78	-14.0	-52.0
25	0.00	-1.77	-11.3	-48.6
27	0.00	-2.46	-12.2	-51.5
28/29	0.00	-1.91	-9.73	-40.7
30/31	0.00	-3.42	-15.4	-71.3
32	0.00	-2.76	-12.9	-52.0
33	0.00	-3.70	-8.84	-49.1
34	0.00	-0.02	-9.14	-51.3
35	0.00	-0.67	-8.77	-47.7
36	0.00	-0.63	-9.44	-50.3
37	0.00	-0.33	-8.26	-49.9
Average	**0.00**	**-2.20**	**-13.8**	**-61.6**

The last row of Table 4-3 is the average of the percent relative differences for each total VOC calculation among all the data points. Propane contributes a great deal to the exhaust gas composition; thus, excluding propane and higher hydrocarbons produces a large relative difference, about 62 percent. Excluding C_{4+} from the total VOC concentration yields a lower relative difference than excluding C_{3+}; however, the difference is still significant with the maximum difference being 19.7 percent for Data Point 17. Excluding C_{5+} on the other hand

produces total VOC concentrations very similar to the total VOC concentration that includes C_{5+}; the maximum relative difference, which occurs at Data Point 17, is still within 5 percent of the total VOC concentration including C_{6+} and the average relative different is roughly 2 percent.

EPA Method 18 Tedlar Bag Results

The guidelines within EPA Method 18 were followed when filling and sampling Tedlar bags except for the allowance of water condensation after the bag was filled as well as sampling from the bag at room temperature since this is a common procedure performed in the field. During the last day of the GMV-4 testing with the HPFI system installed, two extra Tedlar bags were filled with exhaust gas for Data Point 31. The first Tedlar bag sample was filled with wet exhaust gas and was measured in different time intervals with each subsequent interval having an increased amount of time. The first sample was measured through the HP GC one hour after the bag was filled, the next sample was one day, then one week, and the last sample was taken one month after the bag was filled. The individual VOC concentrations measured by the HP GC for each time interval is shown in Figure 4-20.

The lighter hydrocarbons, which contribute to most of the exhaust gas composition, trended downward with increasing time between when the Tedlar bag was filled and when the exhaust gas was sampled through the HP GC. After one week, the ethylene and propylene concentrations decrease by 12 percent and 31 percent, respectively. For propane, the difference becomes significant after one month, underestimating the concentration by 18 percent. The concentration differences for the C_{4+} hydrocarbons also do not become significantly different until approximately one month after the sample is filled into the Tedlar bag.

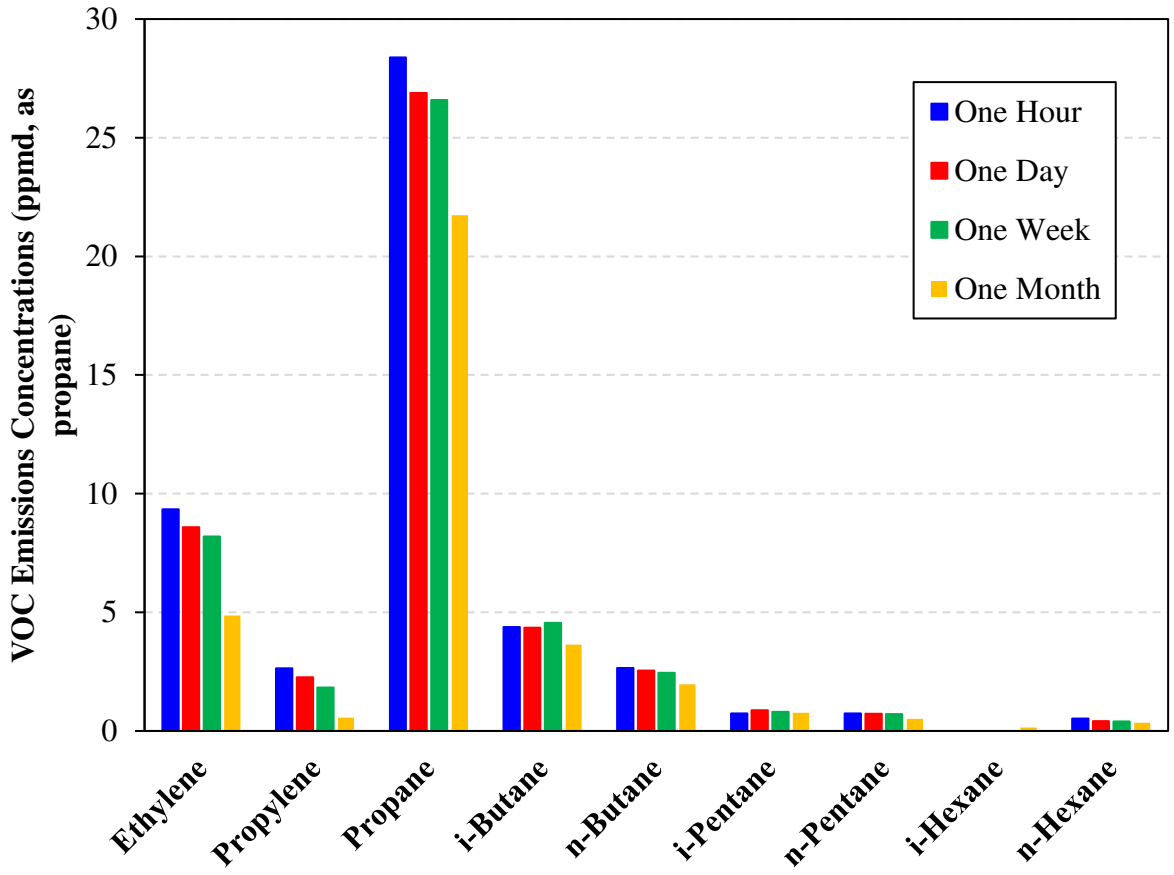

Figure 4-20. Individual VOC concentrations measured by the HP GC sampled from a Tedlar bag at different time intervals after the bag was filled with wet exhaust gas.

The second extra Tedlar bag that was filled during Data Point 31 was filled with dry exhaust gas. The exhaust gas was routed through a chiller upstream of the sample inlet to the Siemens 5-gas analyzer, which requires a dry sample, and splits from the inlet via a ball valve to the Tedlar bag. This Tedlar bag along with another Tedlar bag filled with a wet sample were analyzed in the HP GC 24-36 hours after the data point was taken. The individual VOC concentrations measured from the wet and dry samples are shown in Figure 4-21.

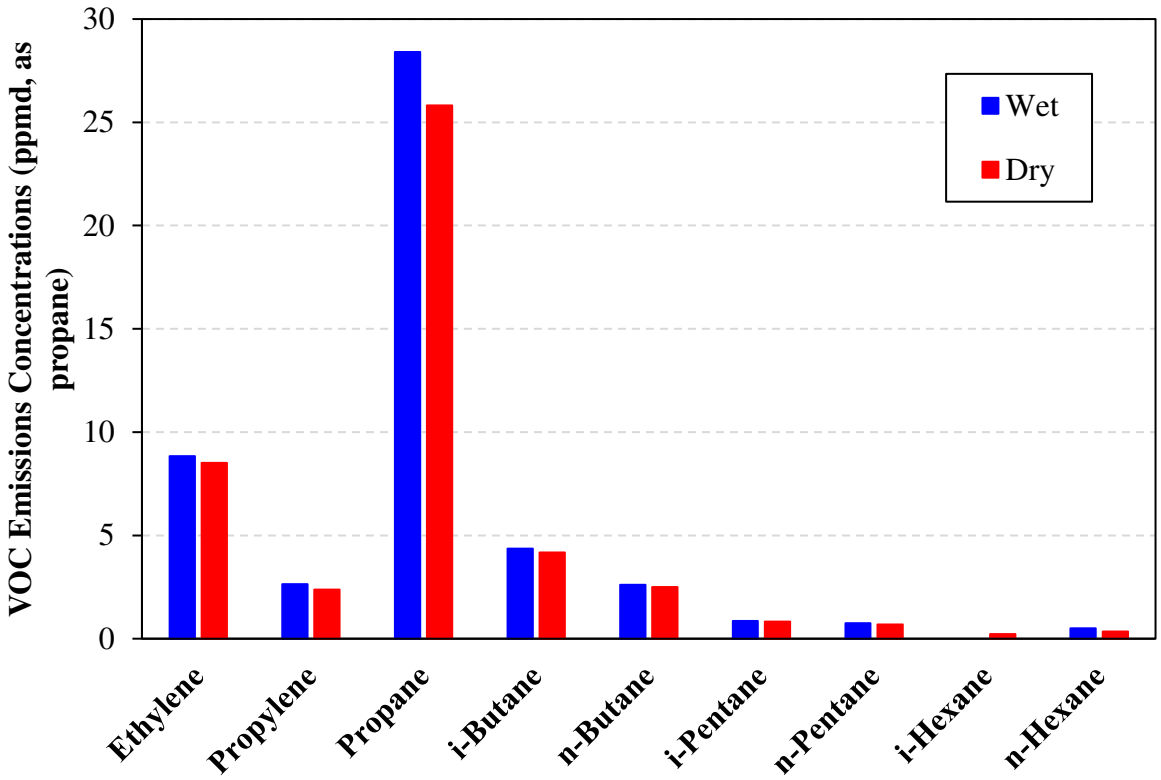

Figure 4-21. Individual VOC concentrations measured by the HP GC taken from Tedlar bags consisting of wet and dry exhaust gas samples.

Note that the unit for the concentration of each VOC is ppmd, as propane. To make this conversion for the wet sample, the water concentration was re-calculated based on a room temperature of 70°F and the assumption that the Tedlar bag was saturated (vapor pressure was calculated to be 0.361 psia with an ambient pressure of 12.2 psia). The re-calculated water concentration was then factored out for each compound. Each VOC was measured lower for the dry sample than for the wet sample. The dry sample contained approximately 3.5 percent less ethylene, 9.8 percent less propylene, and 9.2 percent less propane than the wet sample. The HP GC detected a trace amount of i-hexane in the dry sample; however, the concentration was around 0.2 ppmd, as propane and can be considered negligible.

While filling the Tedlar bag with hot exhaust gas during testing, water condensation was clearly seen forming a film and large droplets on the inner surface of the bag (Figure 4-22). What

was interesting was that approximately 30 minutes later it appeared that the water droplets, which were large and easily seen right after filling, had dispersed throughout the bag and were undetectable (Figure 4-23). It is assumed that over time the droplets redistribute over the inside surface as a thin layer. This occurred every time a Tedlar bag was filled with wet exhaust gas.

Figure 4-22. Tedlar bag showing water condensation on the inner surface immediately after exhaust gas was filled.

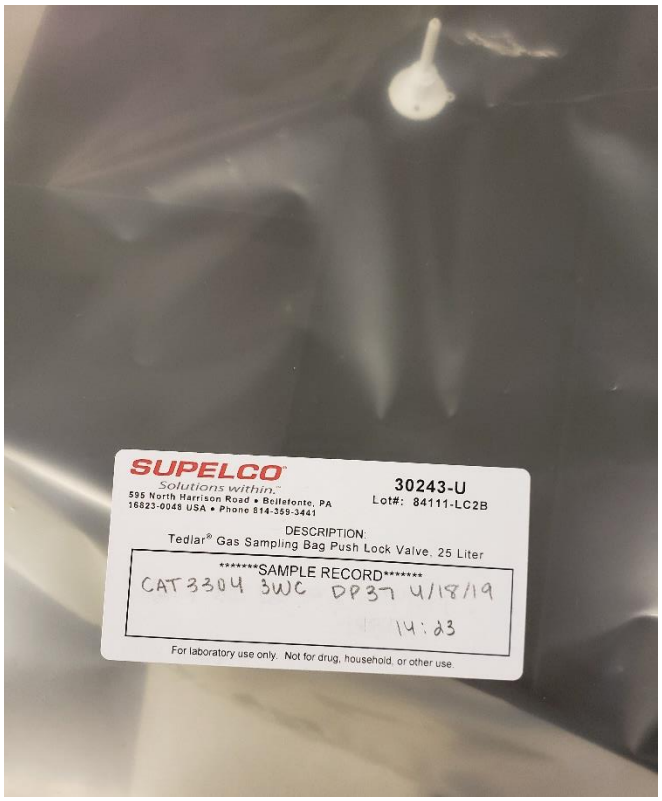

Figure 4-23. Tedlar bag showing dispersed, unnoticeable water droplets approximately 30 minutes after exhaust gas was filled.

Alternate GC/FID with C_{3+} Backflush

The measurement of total VOC concentration using a GC/FID analyzer could be improved by incorporating a column capable of separating ethylene from ethane and a backflush mechanism. This may require only using helium as the carrier gas, eliminating nitrogen as an alternate option. In this alternate analyzer, the sample will enter a short column where the C_{3+} hydrocarbons are separated from the lighter hydrocarbons. The lighter hydrocarbons (i.e. methane, ethylene, and ethane) will exit the short column first and enter a longer column for the three individual compounds to separate. This flow path is shown in Figure 4-24. Meanwhile, with the separated C_{3+} hydrocarbons trapped within the short column, a rotary valve will actuate from Position 1 to Position 2 as shown in Figure 4-25 to backflush the flow of the individual C_{3+} hydrocarbons back through the short column. This will re-combine the higher hydrocarbons before they enter the FID,

which will allow the FID to measure a total C_{3+} hydrocarbon measurement. After the C_{3+} hydrocarbons pass through the FID and exit the analyzer, the separated methane, ethylene, and ethane will travel through the short column and enter the FID where the methane, ethylene, and ethane concentration measurements will be recorded. A schematic of the flow of exhaust gas through the analyzer before and after the rotary valve changes position is shown in Figure 4-24. This GC/FID analyzer would be able to quantify individual VOC concentrations accurately and would require a shorter analysis runtime of approximately four minutes as opposed to 12 minutes when the HP GC is used.

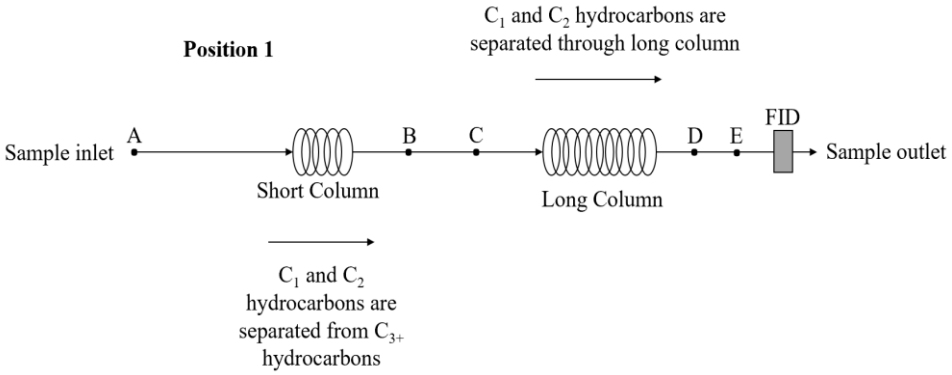

Figure 4-24. Schematic of sample flow of proposed GC/FID analyzer when the rotary valve is in its initial position.

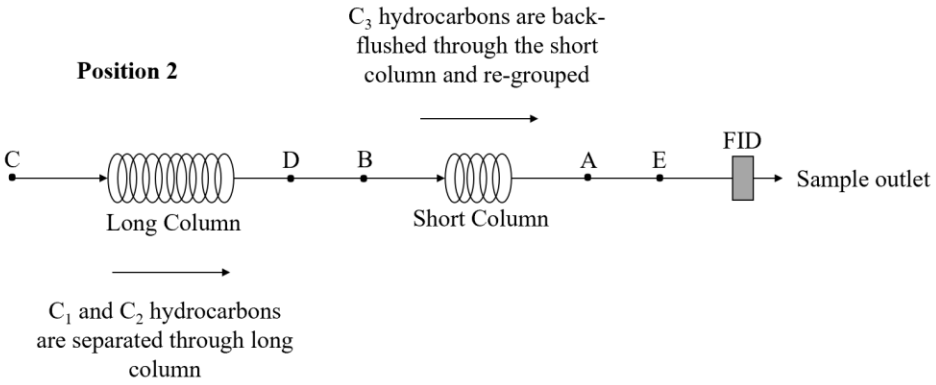

Figure 4-25. Schematic of sample flow of proposed GC/FID analyzer after the rotary valve changes position.

Discussion

The HP GC/FID utilizing EPA Method 18/25a is the most feasible and accurate method for VOC quantification. The HP GC produces a chromatogram with peaks designating each VOC hydrocarbon as well as methane and ethane; therefore, the HP GC can provide information on how much a single hydrocarbon contributes to the total VOC concentration within a sample of exhaust gas. The Tedlar bag process following EPA Method 18 as well as common field procedures of allowing water to condense at room temperature is also a feasible and accurate way to sample exhaust gas. This is supported by the plots showing the total VOC concentrations for each data point as well as Table 4-1 where the Tedlar bag measured on average 1.9 percent less total VOCs than direct extraction of the exhaust sample, which is an insignificant amount. When water condenses in a sample of exhaust gas, it tends to absorb hydrocarbons. Alkenes are more soluble in water than their alkane-counterparts and the solubility of hydrocarbons tend to decrease with the increase in carbon number, so ethylene and propylene are the most vulnerable for absorption in water [28, 29]. This causes the Tedlar bag method to consistently measure less total VOCs than when the exhaust gas is heated and directly extracted to the HP GC. The plot comparing individual VOC concentrations between wet and dry exhaust gas samples taken during Data Point 31 (Figure 4-21) suggests that water absorbs every VOC to some degree; however, this cannot be validated since the uncertainty of the HP GC and the variability of the compositions between the two separate exhaust gas samples can also have an effect on the decrease of VOC content in the dry sample. In Table 4-1, the uncertainty of the Tedlar bag measurement was on average 12.5 percent for the GMV-4 data, which also contributes greatly to the discrepancy between the wet and dry sample. There was an increase of approximately 115 percent water concentration in the exhaust between the GMV-4 engine at nominal conditions and the Caterpillar 3304 engine at nominal conditions;

therefore, there was more water to absorb VOCs for the Tedlar bags containing exhaust gas from the Caterpillar 3304 engine than the Tedlar bags containing the exhaust gas from the GMV-4 engine. This is shown in Table 4-2 where the Tedlar bag method underestimated the total VOC concentration on an average of 13 percent compared to the heated, direct injected method for the HP GC.

The MKS and Gasmet FTIRs tended to overestimate total VOC concentration compared to the HP GC, as suggested by the percent relative differences in Table 4-1 and Table 4-2. The Gasmet FTIR measured on average 7 percent higher total VOC concentration than the MKS FTIR for the data points taken on the GMV-4 engine; however, the MKS FTIR measured more than twice the concentration of total VOC than the Gasmet FTIR for the Caterpillar 3304 data. Because of this, no conclusion can be made on whether a N_2-cooled FTIR (MKS) provides more accurate results than a Peltier-cooled FTIR (Gasmet). The Gasmet FTIR yields lower uncertainties of total VOC measurements (about 5 percent for the GMV-4 data) than the MKS FTIR (nearly 16 percent for the GMV-4 data). Both FTIRs largely overestimated ethylene and propylene concentrations for the Caterpillar data points, as seen in Figure 4-17. Comparing the HP GC chromatograms from the nominal Data Points 1 and 12 on the GMV-4 engine (Figures 4-2 and 4-9) to the HP GC chromatogram for nominal Data Point 33 on the Caterpillar engine (Figure 4-18), there is no significant difference in the peak areas for ethylene and propylene. This indicates that there was no drastic change in propylene and ethylene concentrations between the lean burn and rich burn configurations. Furthermore, the FTIRs' overestimation of these hydrocarbons is speculated to be caused by an interference of some kind occurring within the sample cell during analysis. It is important to note that there was a decrease of approximately 97 percent of brake specific VOCs between the GMV-4 engine testing and the Caterpillar 3304 engine testing; therefore, smaller

concentrations were measured for the Caterpillar rich burn data points and uncertainties along with resolutions of the analyzers could have had a greater contribution to the discrepancy of the results.

The "MKS FIDeq NMNEHC" method consistently yielded similar total VOC concentrations to the "MKS" method but overestimated more than the "MKS" method compared to the HP GC direct extraction method. The difference in the FID factors used by MKS Instruments in its FIDeq NMNEHC calculation and the FID factors calculated using the methods described in Chapter 3 is the cause of the slight discrepancy between the two MKS methods. The same explanation contributes to the difference between the "Gasmet VOC as propane" and "Gasmet VOC Sum" methods. Since the "Gasmet VOC Sum" method utilizes the same FID factors as the "HP GC" method, this method is slightly more accurate to the HP GC than the "Gasmet VOC as propane" method.

According to the results from the GMV-4 engine testing listed in Table 4-1, "VIG FID Residual + MKS C2H4" is the second most accurate method to the HP GC in calculating total VOC concentration, with an average relative difference of 6.3 percent. The "VIG FID Residual" method does not include all VOCs in its calculation of total VOC concentration since the residual channel only consists of C_{3+} hydrocarbons and excludes ethylene. To resolve this, the ethylene measurement from the MKS FTIR is added to the residual measurement and proved to be very accurate to the HP GC. The alternative method, called "VIG FID Residual + C2 – MKS C2H6", which takes the sum of the residual and C2 measurements and subtracts the ethane measurement from the MKS FTIR, is not accurate and consistently underestimated total VOC concentration as well as producing large uncertainty. The large uncertainty was due to the addition and subtraction of large numbers (i.e. the VIG FID residual, C2, and MKS ethane) to result in a small number (i.e. the total VOC concentration), where the uncertainties associated with the large numbers are

significant in proportion to the total VOC concentration. This trend is also seen for the "5-Gas THC – MKS" method, which is the most inaccurate method. The method, which is very commonly used in the field for total VOC quantification, takes the THC measurement from the Siemens 5-Gas analyzer and subtracts the methane and ethane measurements from the MKS FTIR. Again, these measurements are very large in proportion to the total VOC concentration, which results in large uncertainties (193 percent for the GMV-4 data) and very inaccurate calculations; the method nearly doubled the total VOC concentration for the GMV-4 data points.

It was speculated that quantifying total VOC concentration including hydrocarbons up to C_6 was not necessary since hexane and higher hydrocarbons do not contribute significantly to the total VOC concentration and therefore could be omitted from the calculation. The percent differences listed in Table 4-3 suggest C_{5+} hydrocarbons could be excluded from the total VOC quantification and still result in a concentration well within 5 percent of the concentration including C_{6+} hydrocarbons; however, excluding C_{4+} hydrocarbons decrease the total VOC concentration by approximately 14 percent. In regard to using the HP GC/FID, excluding the quantification of C_{5+} hydrocarbons is very beneficial in that a sample can be analyzed at approximately 75 percent of the chromatogram runtime required by the current method.

CHAPTER 5 – IMPACT OF FUEL COMPOSITION VARIABILITY ON EMISSIONS CONCENTRATIONS AND ENGINE PERFORMANCE

Fuel Composition Variability Results

The HP GC chromatogram taken during Data Point 23 for the GMV-4 lean burn, HPFI PCC ignition with electronic fuel valves configuration is shown in Figure 5-1. The EPA Method 19 NO_X calculation was 0.36 g/bhp-hr, which was maintained using boost control during testing, and TER was 0.46. Data Point 23 was one of the nominal points taken for the HPFI configuration, which consisted of fueling the engine with the nominal natural gas composition and setting the location of PP at 18°aTDC.

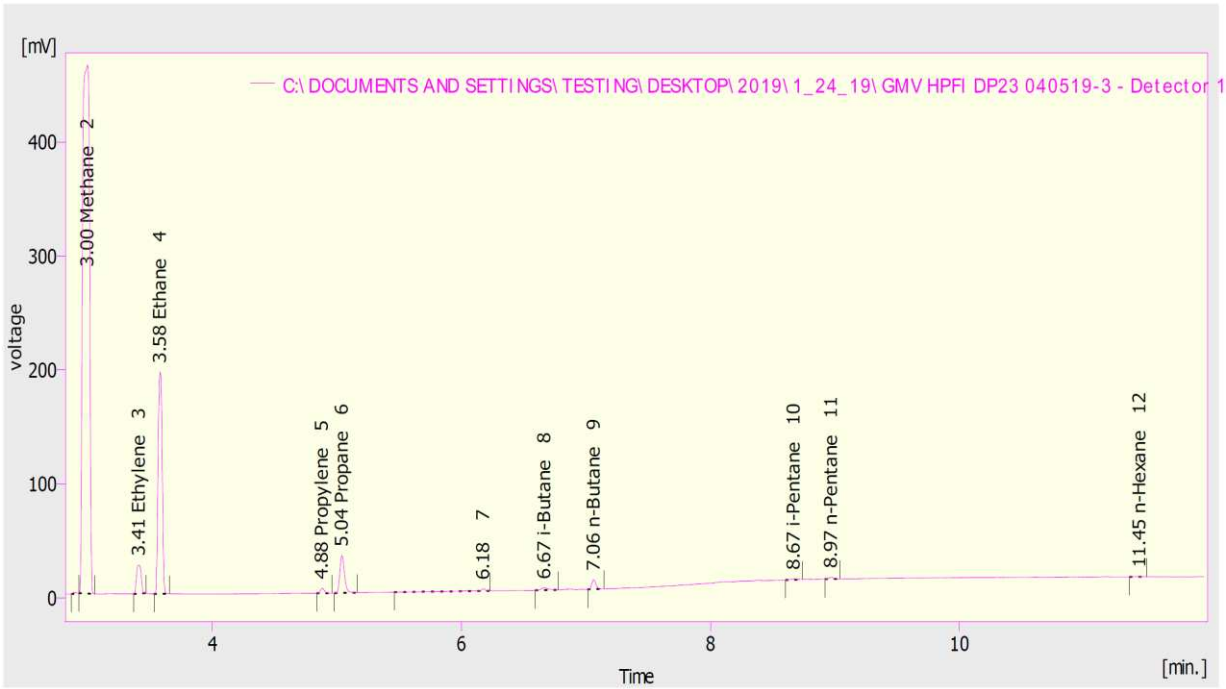

Figure 5-1. HP GC chromatogram taken during Data Point 23 for the GMV-4 lean burn HPFI PCC ignition with electronic fuel valves configuration.

The area of each peak corresponds to the concentration of the associated hydrocarbon in the exhaust gas sample. Focusing on VOCs, propane has the largest peak area and ethylene has the second largest peak area. The remaining higher hydrocarbons have very small peak areas and the

HP GC detected no signal for i-hexane. The concentration for each hydrocarbon shown in the chromatogram above – in units of ppmw –is listed in Table 5-1. This table was generated by the Clarity software and includes the response and retention time as well as the concentration for each hydrocarbon detected by the FID.

Table 5-1. Table produced by the HP GC Clarity software showing results of the exhaust gas sampled during Data Point 23.

	Reten. Time [min]	Response [mV-min]	Amount [ppmw]	Amount [%]	Peak Type	Compound Name
2	3.00	1790	654	85.3	Ordnr	Methane
3	3.41	64.3	12.2	1.60	Ordnr	Ethylene
4	3.58	449	85.3	11.1	Ordnr	Ethane
5	4.88	9.37	1.16	0.200	Ordnr	Propylene
6	5.04	84.6	10.7	1.40	Ordnr	Propane
8	6.67	8.29	0.806	0.100	Ordnr	i-Butane
9	7.06	19.2	1.79	0.200	Ordnr	n-Butane
10	8.67	2.97	0.240	0.000	Ordnr	i-Pentane
11	8.97	4.12	0.196	0.000	Ordnr	n-Pentane
C10	10.9	N/A	N/A	N/A	N/A	i-Hexane
12	11.4	0.765	0.0490	0.000	Ordnr	n-Hexane

Ethylene had the largest concentration among the VOCs with a concentration of 12.2 ppmw. Propane, which was the second largest compound in the VOCs, had a concentration of 10.7 ppmw. Even though the propane peak area was larger than the ethylene peak area shown in Figure 5-1, ethylene had a larger concentration due to the different response factors that were applied to either compound by the Clarity software. Relatively small amounts of the higher hydrocarbons were measured; the n-hexane concentration was almost zero.

Approximately 10 percent fuel ethane was added to the nominal fuel composition for the same configuration during Data Point 28/29. Boost control was utilized for maintaining constant

NO_X, which was calculated to be 0.38 g/bhp-hr and TER was 0.42. The HP GC chromatogram taken during Data Point 28/29 is shown in Figure 5-2.

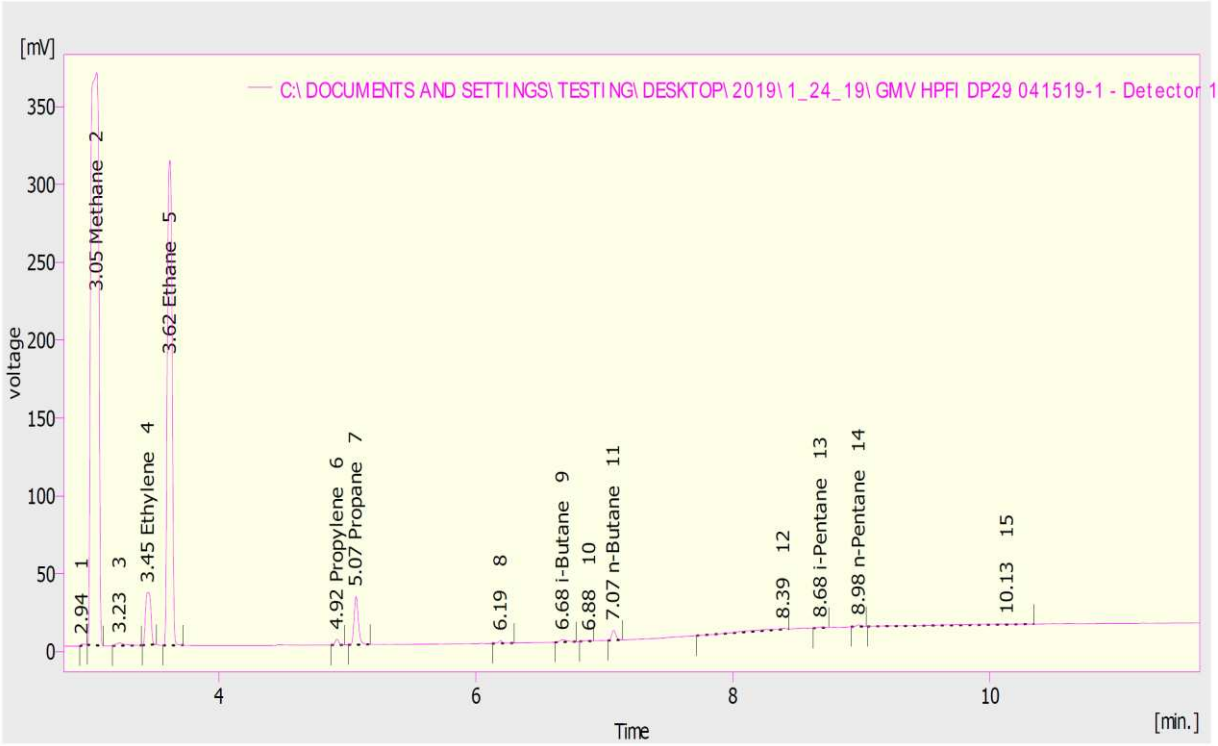

Figure 5-2. HP GC chromatogram taken during Data Point 28/29 for the GMV-4 lean burn HPFI PCC ignition with electronic fuel valves configuration.

Compared to the HP GC chromatogram for Data Point 23 with nominal fuel composition, the ethane peak shows a significant increase in magnitude. No i-hexane or n-hexane peaks were detected by the FID. The concentration for each hydrocarbon shown in the chromatogram above – in units of ppmw – is listed in Table 5-2, which was produced by the Clarity software.

The ethane concentration increased approximately 78.3 percent compared to Data Point 23. There was also an increase in ethylene by 50.8 percent. The propane concentration decreased significantly compared to the nominal data point. There was a 13.3 percent decrease in methane concentration. Methane is a significant greenhouse gas and emissions are beginning to be more

closely monitored so it is important to note the change of the emission concentration with fuel variability.

Table 5-2. Table produced by the HP GC Clarity software showing results of the exhaust gas sampled during Data Point 28/29.

	Reten. Time [min]	Response [mV-min]	Amount [ppmw]	Amount [%]	Peak Type	Compound Name
2	3.05	1560	567	75.7	Ordnr	Methane
4	3.45	97.3	18.4	2.50	Ordnr	Ethylene
5	3.62	806	152	20.3	Ordnr	Ethane
6	4.92	7.48	0.986	0.100	Ordnr	Propylene
7	5.07	70.9	8.93	1.20	Ordnr	Propane
9	6.68	5.71	0.566	0.100	Ordnr	i-Butane
11	7.07	14.4	1.34	0.200	Ordnr	n-Butane
13	8.68	2.12	0.171	0.000	Ordnr	i-Pentane
14	8.98	2.92	0.145	0.000	Ordnr	n-Pentane
C10	10.9	N/A	N/A	N/A	N/A	i-Hexane
C11	11.4	N/A	N/A	N/A	N/A	n-Hexane

The HP GC chromatogram for Data Point 30/31 for the HPFI, PCC configuration is shown in Figure 5-3. For this data point, approximately five percent of fuel C_{3+} hydrocarbons were added to the nominal natural gas fuel. At this time, NO_X sensor feedback control was functional and was used to maintain the target NO_X level. The EPA Method 19 calculation for NO_X was 0.35 g/ bhp-hr. TER was calculated to be 0.45. No significant change in the magnitude of the ethylene peak occurred between this data point and the nominal data point. On the other hand, there was a noticeable increase in the magnitude of the propane peak as well as the magnitudes of the C_4 and C_5 peaks. Like the nominal data point, there was no i-hexane peak detected and the n-hexane peak was very small, almost undetectable. The concentration for each hydrocarbon shown in the chromatogram above – in units of ppmw – is listed in Table 5-3.

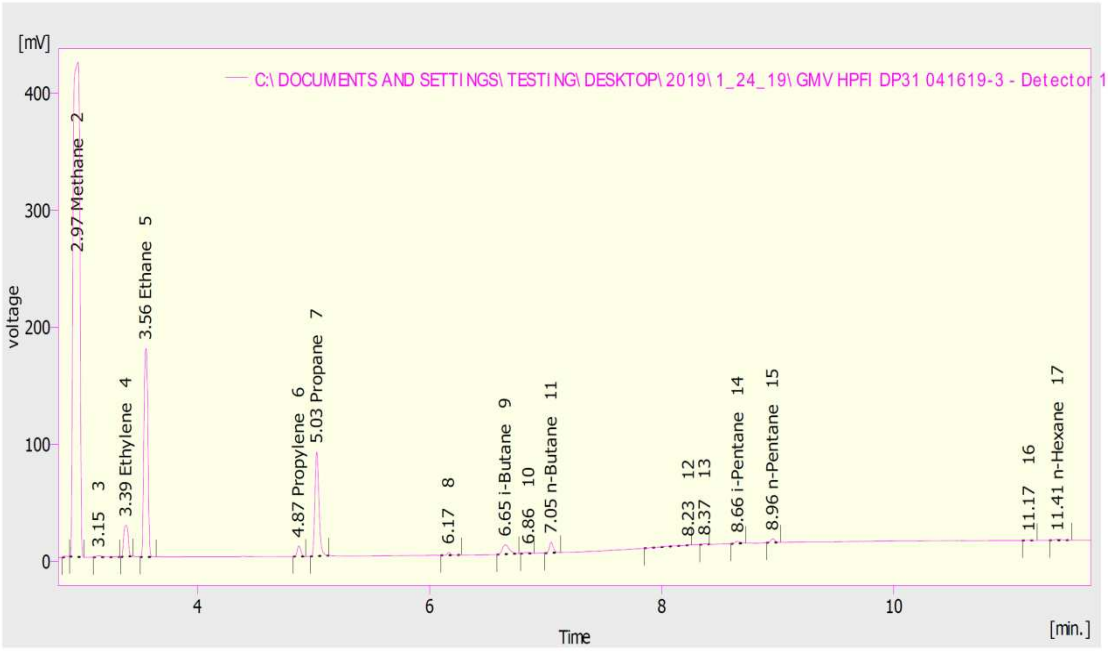

Figure 5-3. HP GC chromatogram taken during Data Point 30/31 for the GMV-4 lean burn HPFI PCC ignition with electronic fuel valves configuration.

Table 5-3. Table produced by the HP GC Clarity software showing results of the exhaust gas sampled during Data Point 30/31.

	Reten. Time [min]	Response [mV-min]	Amount [ppmw]	Amount [%]	Peak Type	Compound Name
2	2.97	1670	580	82.3	Ordnr	Methane
4	3.39	70.7	12.9	1.80	Ordnr	Ethylene
5	3.56	422	76.6	10.9	Ordnr	Ethane
6	4.87	19.7	2.48	0.400	Ordnr	Propylene
7	5.03	216	26.4	3.70	Ordnr	Propane
9	6.65	33.5	3.37	0.500	Ordnr	i-Butane
11	7.05	21.1	1.96	0.300	Ordnr	n-Butane
14	8.66	6.56	0.529	0.100	Ordnr	i-Pentane
15	8.96	8.24	0.425	0.100	Ordnr	n-Pentane
C10	10.8	N/A	N/A	N/A	N/A	i-Hexane
17	11.4	3.64	0.201	0.000	Ordnr	n-Hexane

There was a decrease in methane concentration by about 11 percent compared to the nominal data point. The ethylene and ethane concentrations did not change significantly with the addition of fuel C_{3+} hydrocarbons. Propylene, however, increased approximately 114 percent and the propane concentration increased 147 percent. The C_{4+} concentration increased a total of 111 percent, but i-

hexane was not detected by the FID for either Data Point 23 or Data Point 30/31. The remaining data points consisting of fuel composition variability for all configurations (i.e. Data Points 7, 8, 9/10, 18/19, and 20/21) show similar trends as discussed above. The HP GC chromatograms and individual VOC concentration plots can be seen in Appendix B.

Destruction efficiencies of hydrocarbons that existed in both the natural gas fuel and the exhaust gas (i.e. methane, ethane, propane, i/n-butane, i/n-pentane, and n-hexane) were calculated for each data point taken on the GMV-4 engine. The destruction efficiency of each hydrocarbon was found using

$$\eta_{dest,i} = 1 - \frac{x_{i,exh}\,\dot{m}_{exh}}{x_{i,f}\,\dot{m}_f} \tag{5-1}$$

where $x_{i,exh}$ is the mass fraction of the hydrocarbon in the exhaust, $\dot{m}_{exh}$ is the mass flow rate of the exhaust, $x_{i,f}$ is the mass fraction of the hydrocarbon in the natural gas fuel, and $\dot{m}_f$ is the mass flow rate of the fuel. The mass fraction of each hydrocarbon was calculated using

$$x_i = y_i \frac{M_i}{M_{mix}} \tag{5-2}$$

where y_i is the mole fraction of the hydrocarbon in the fuel (measured by the fuel Micro GC) or the exhaust (measured by the HP GC), M_i is the molecular weight of the hydrocarbon, and M_{mix} is the molecular weight of the exhaust gas or fuel mixture. A table with the destruction efficiency for each hydrocarbon for each data point taken on both the GMV-4 Caterpillar 3304 engines can be seen in Appendix B. An average of the destruction efficiency for each hydrocarbon was calculated among data points that were taken during nominal conditions and among data points that involved fuel blending. Table 5-4 lists the average destruction efficiencies.

Table 5-4. Average destruction efficiencies of hydrocarbons among data points with same fuel composition for the GMV-4 configuration only.

Condition	Methane (%)	Ethane (%)	Propane (%)	i-Butane (%)	n-Butane (%)	i-Pentane (%)	n-Pentane (%)	n-Hexane (%)
Nominal	95.2	95.5	96.6	97.5	96.9	98.4	98.5	100
+10% ethane	95.7	96.0	97.0	97.8	97.1	98.7	98.6	100
+5% C_{3+}	95.5	95.8	96.9	97.0	97.2	98.1	98.7	100

Methane consistently had the lowest destruction efficiency compared to the other hydrocarbons. The destruction efficiency tended to increase for hydrocarbons with more carbon and hydrogen atoms; n-hexane, the heaviest of the hydrocarbons listed in Table 5-4, had a destruction efficiency of 100 percent for each fuel composition type. A 100 percent destruction efficiency for n-hexane implies that all n-hexane molecules were combusted during the combustion event. In general, there was no significant variability in destruction efficiency with changing fuel composition. The addition of 10 percent fuel ethane yielded the largest destruction efficiency for methane, ethane, propane, i-butane, and i-pentane. The fuel composition with +5 percent C_{3+} hydrocarbons produced the largest destruction efficiency for n-butane and n-pentane but produced the lowest destruction efficiency for i-butane and i-pentane. The average destruction efficiency calculated from the nominal fuel composition data was not the highest for any of the hydrocarbons. The nominal fuel composition condition yielded the lowest destruction efficiency for methane, ethane, propane, n-butane, and n-pentane.

In addition to the steady-state data points where the fuel composition was varied by either an increase of 10 percent fuel ethane or 5 percent fuel C_{3+} hydrocarbons, sweeps were performed using each fuel blending system. These sweeps occurred during the last day of GMV-4 testing after all steady-state data points were taken for the HPFI configuration. The sweeps started with the nominal fuel composition and increasing fuel ethane or fuel C_{3+} until the maximum

concentration allowed by the fuel blending system was reached. For the fuel ethane blending sweep, the fuel ethane concentration started from 12.4 mol% and increased to 27.9 mol% and the fuel C_{3+} concentration increased from 2.56 mol% to 13.3 mol% during the fuel higher hydrocarbon sweep. The target NO_X emissions level was controlled using NO_X sensor feedback during both fuel blending sweeps.

After each increase in fuel ethane or fuel C_{3+} to the natural gas supply, the fuel GC chromatogram, which updated every two minutes, was monitored until at least two consequent chromatograms measured similar concentrations. When there were at least two chromatograms showing similar fuel compositions, steady-state was assumed, and two minutes of data were collected before the process was repeated. The data collected for each iteration consisted of combustion and engine DAQ parameters as well as MKS FTIR and Siemens 5-gas emissions concentrations. The coefficient of variance of the indicated mean effective pressure (COV IMEP) and the coefficient of variance of the peak pressure (COV of PP) measured during each iteration for the fuel ethane sweep are shown in Figure 5-4. Each parameter was averaged among the four cylinders of the GMV-4 engine. The COV IMEP remained constant with the addition of fuel ethane; however, the COV PP decreased roughly 17 percent between the nominal and maximum fuel ethane concentrations. The 0-10%, 50%, and 10-90% burn durations as well as the location of PP recorded for the fuel ethane sweep are shown in Figure 5-5.

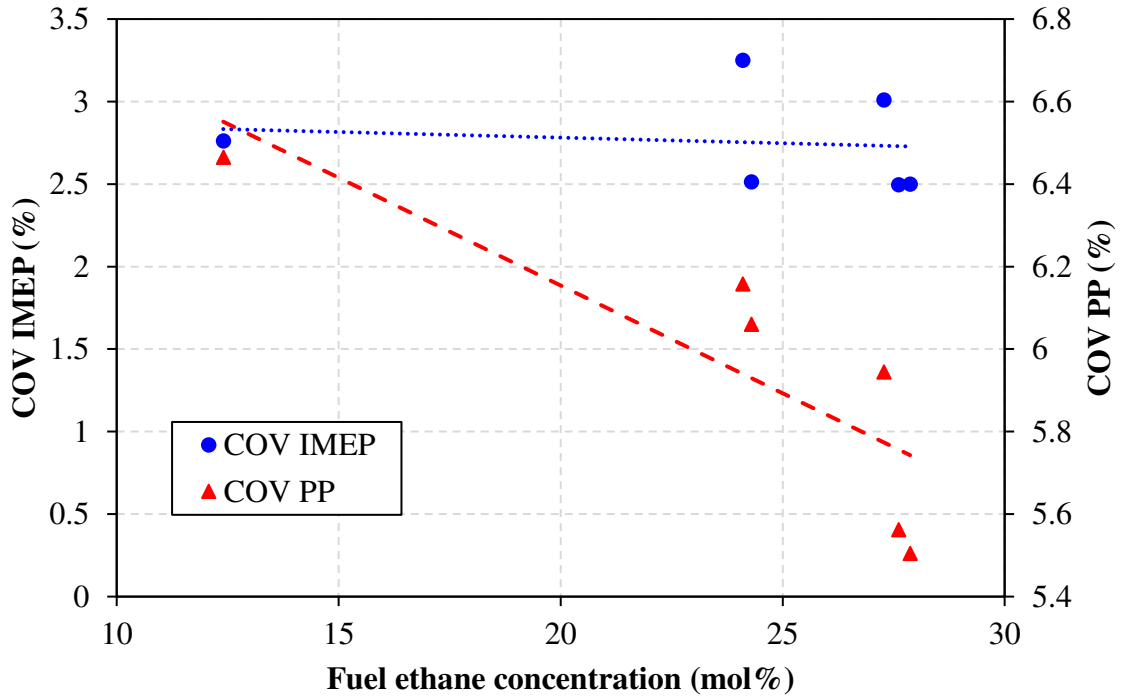

Figure 5-4. COV IMEP and COV PP versus fuel ethane concentration during fuel ethane sweep for the HPFI GMV-4 configuration.

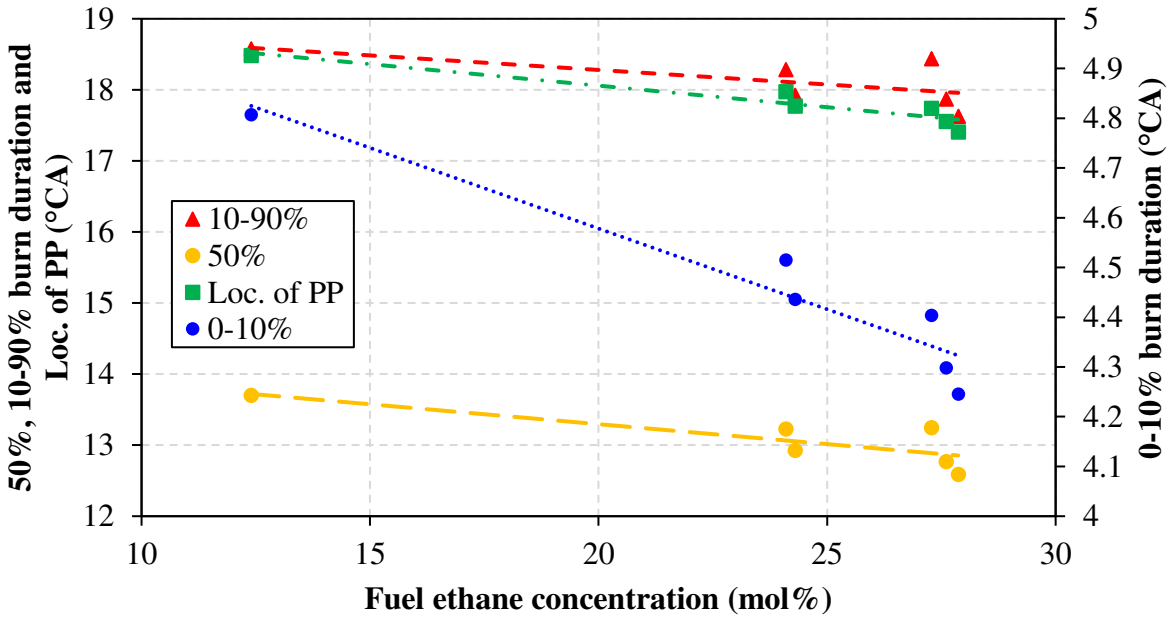

Figure 5-5. 0-10%, 50%, 10-90% burn durations and average location of PP versus fuel ethane concentration during fuel ethane sweep for the HPFI GMV-4 configuration.

The 0-10%, 50%, and 10-90% burn durations trend downward with the addition of fuel ethane; however, the change was not significant. The location of PP also remained constant with a slight downward trend when fuel ethane was added. The TER was calculated for each iteration and is shown in Figure 5-6.

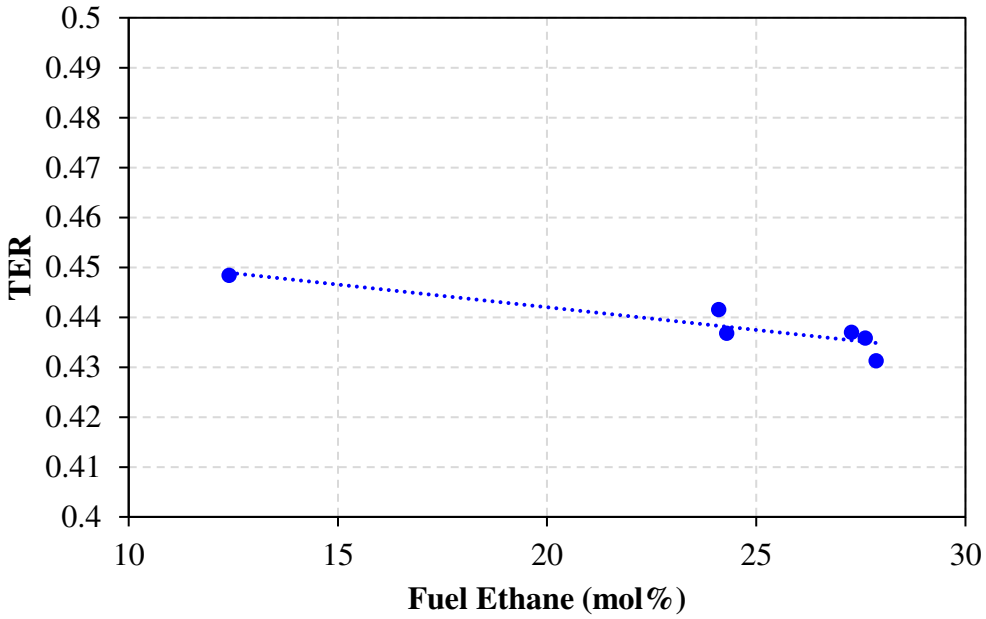

Figure 5-6. TER versus fuel ethane concentration during fuel ethane sweep for the HPFI GMV-4 configuration.

There was no significant change in TER between the nominal fuel ethane content and the maximum concentration tested for the sweep; the TER only decreased a slight amount of approximately 3.8 percent. The exhaust NO_X, formaldehyde (CH_2O), and CO concentrations measured by the MKS FTIR and converted to units of ppmd at 15 percent O_2 are shown in Figure 5-7.

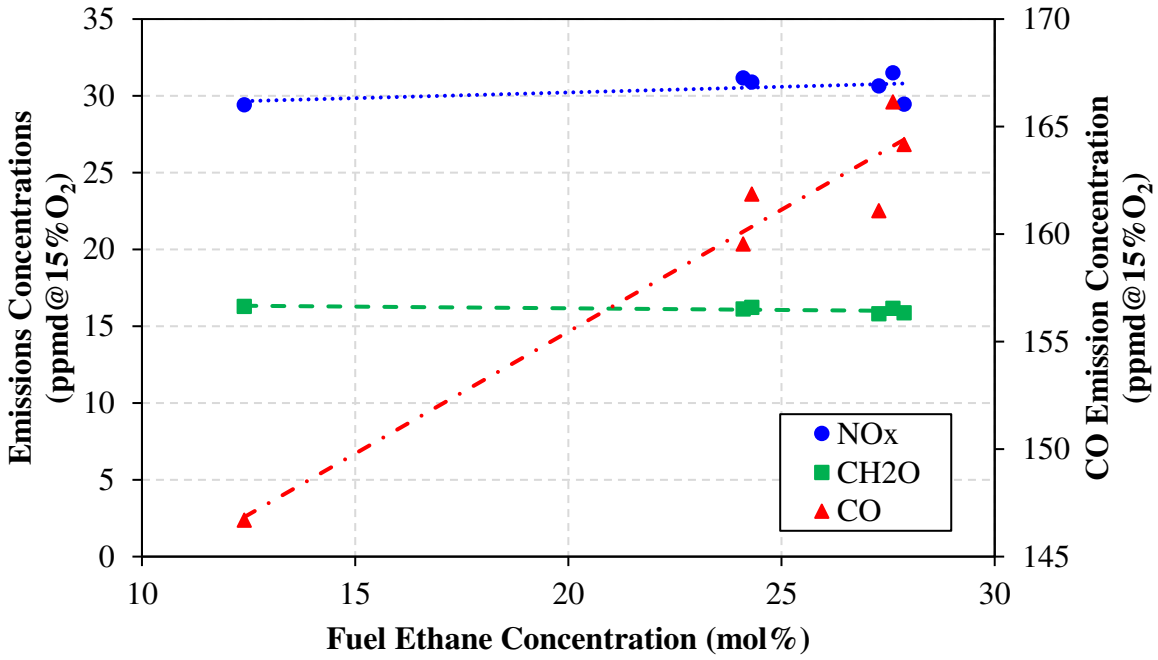

Figure 5-7. Exhaust NO_X, CH_2O, and CO concentrations taken from the MKS FTIR versus fuel ethane concentration during fuel ethane sweep for the HPFI GMV-4 configuration.

NO_X and formaldehyde emissions remained at steady concentrations of 30.5 ppmd@15%O_2 and 16.1 ppmd@15%O_2, respectively, with the addition of fuel ethane to the natural gas fuel; however, CO emissions increased significantly from 146 ppmd@15%O_2 to 166 ppmd@15%O_2. Emissions concentrations for total VOCs, ethylene, ethane, propylene, and C_{3+} hydrocarbons measured by the MKS FTIR are shown in Figure 5-8. The exhaust ethylene concentration increased 60 percent with the addition of fuel. Exhaust ethane increased by an even greater amount (113 percent). On the other hand, propylene and C_{3+} hydrocarbons decreased slightly with the addition of fuel ethane. Overall, the total VOC concentration in the exhaust gas increased, but only by 4.5 percent. The COV of IMEP and COV of PP versus fuel C_{3+} concentration for the C_{3+} hydrocarbon sweep is shown in Figure 5-9.

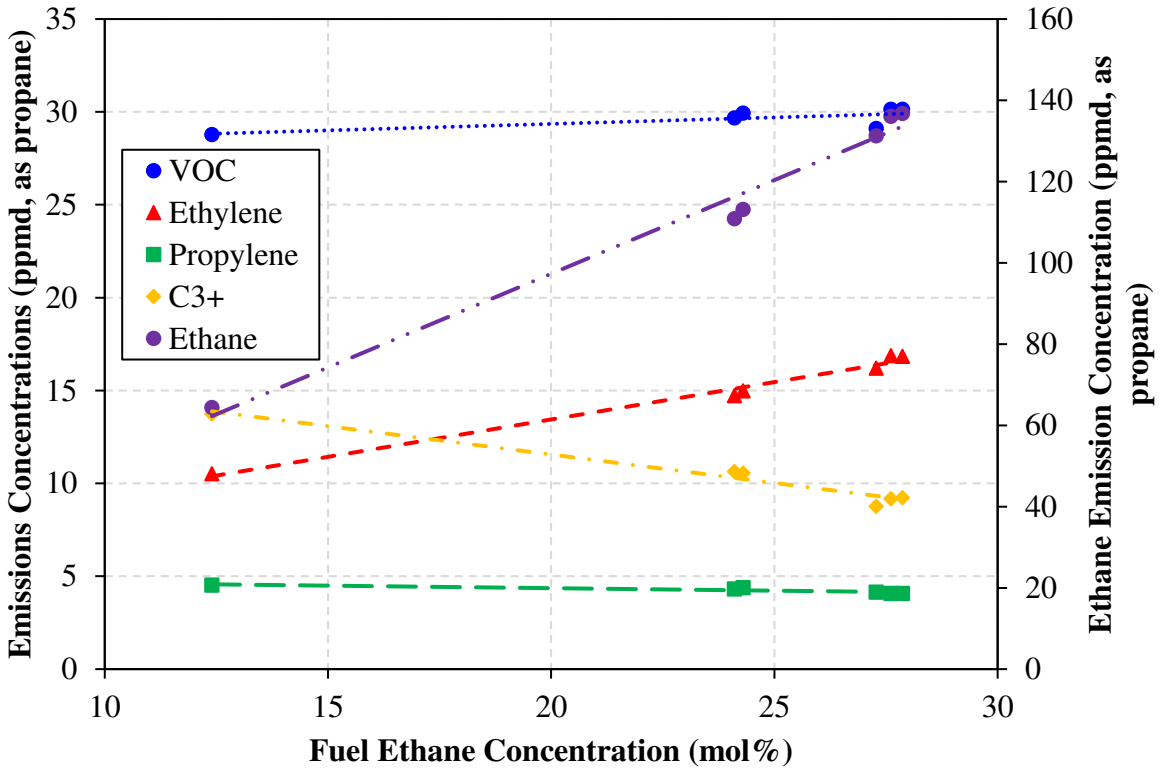

Figure 5-8. Exhaust NO_X, CH_2O, and CO concentrations taken from the MKS FTIR versus fuel ethane concentration during fuel ethane sweep for the HPFI GMV-4 configuration.

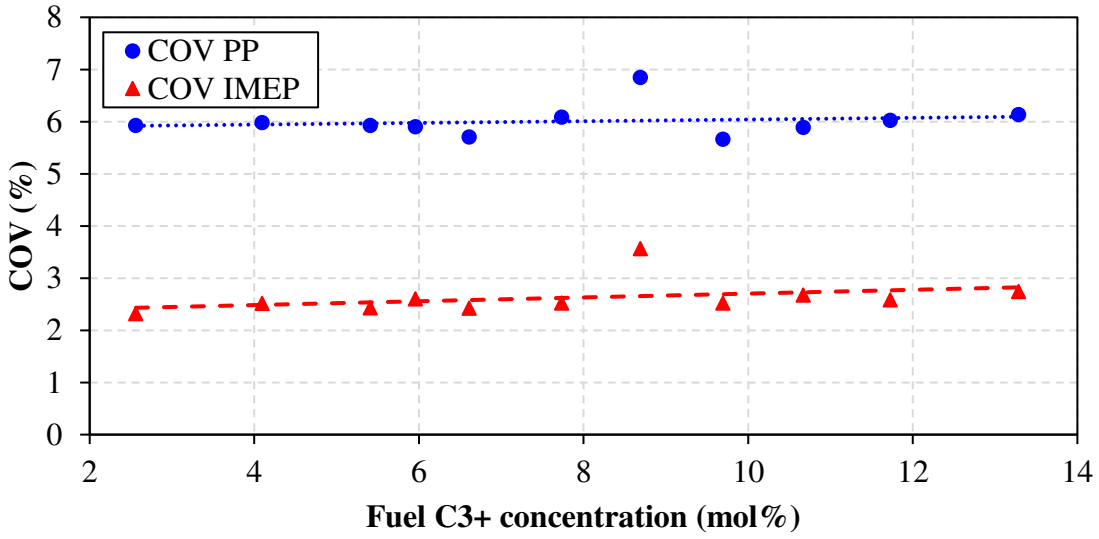

Figure 5-9. COV IMEP and COV PP versus fuel C_{3+} concentration during fuel C_{3+} hydrocarbon sweep for the HPFI GMV-4 configuration.

Increasing C_{3+} hydrocarbon concentration in the natural gas fuel did not have a significant effect on COV of IMEP and COV of PP. On average, the COV of IMEP remained steady at around 2.7 and the COV of PP was 6. The 0-10%, 50%, and 10-90% burn durations as well as the location of PP recorded for the fuel C_{3+} hydrocarbon sweep are shown in Figure 5-10.

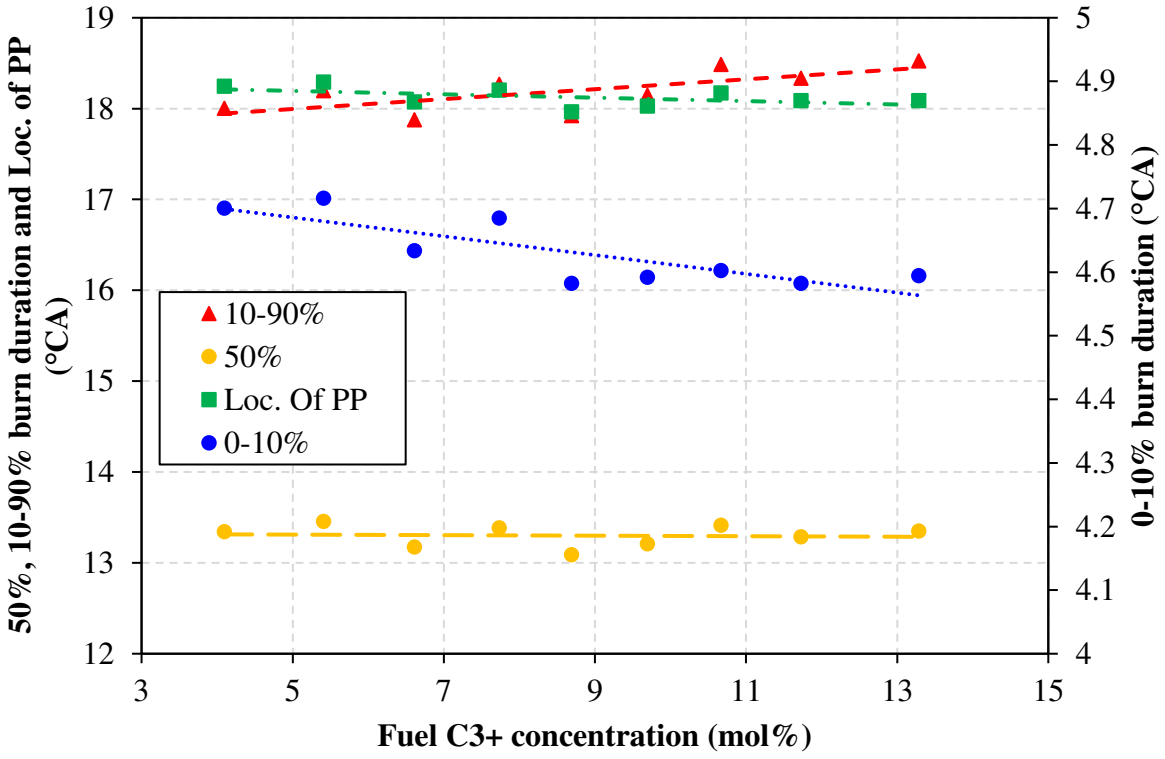

Figure 5-10. 0-10%, 50%, 10-90% burn durations and average location of PP versus fuel C_{3+} concentration during fuel C_{3+} hydrocarbon sweep for the HPFI GMV-4 configuration.

There was no significant variability in any of the burn durations shown above or in the location of PP with the increase in fuel C_{3+} hydrocarbons. On average, the 0-10% burn duration was 4.6°CA, the 50% burn duration was 13.3°CA, the 10-90% burn duration was 18.2°CA, and the location of PP was 18.1°CA. The TER was calculated for each iteration and is shown in Figure 5-11.

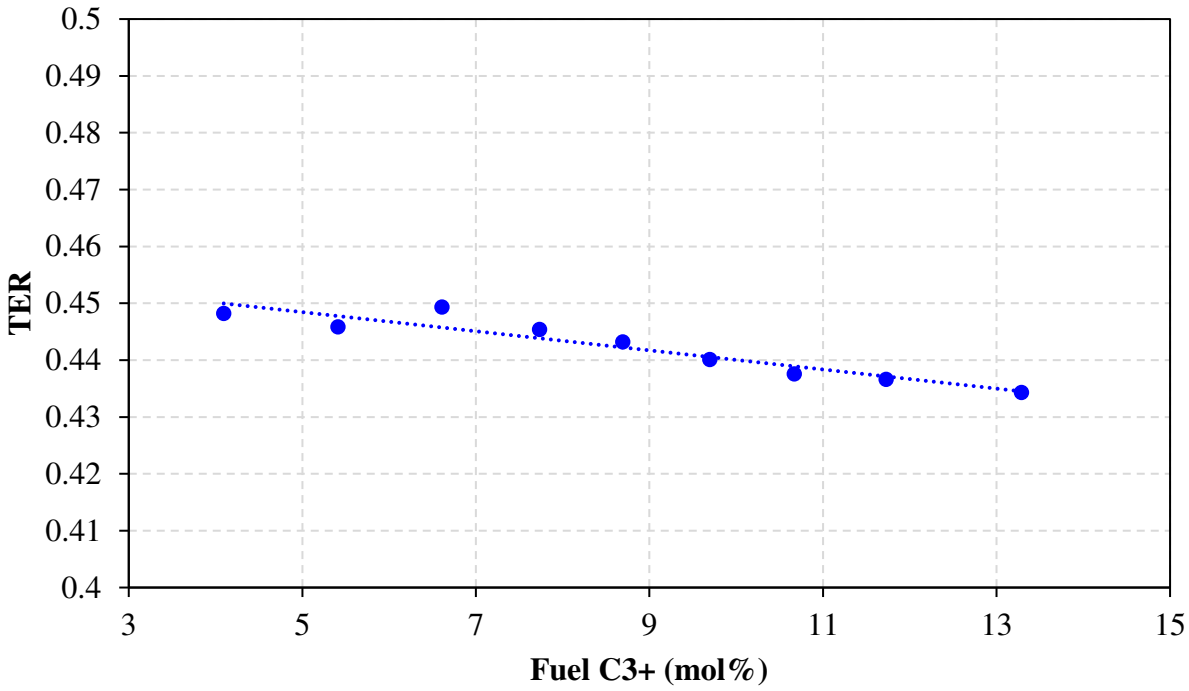

Figure 5-11. TER versus fuel C_{3+} concentration during fuel C_{3+} hydrocarbon sweep for the HPFI GMV-4 configuration.

No significant change of TER occurred with the addition of fuel C_{3+} hydrocarbons; it decreased approximately 3.1 percent from the beginning to the end of the sweep. The exhaust NO_X, formaldehyde, and CO concentrations measured by the MKS FTIR and converted to units of ppmd at 15 percent O_2 are shown in Figure 5-12. Exhaust NO_X concentration did not vary significantly with the increase of fuel C_{3+} hydrocarbons since it was maintained at a constant level using NO_X sensor feedback control. Exhaust CO concentration increased about 18 percent. Formaldehyde emission increased from 16.3 ppmd@15%O_2 to 18.6 ppmd@15%O_2 during the sweep. Emissions concentrations for total VOCs, ethylene, ethane, propylene, and C_{3+} hydrocarbons measured by the MKS FTIR are shown in Figure 5-13.

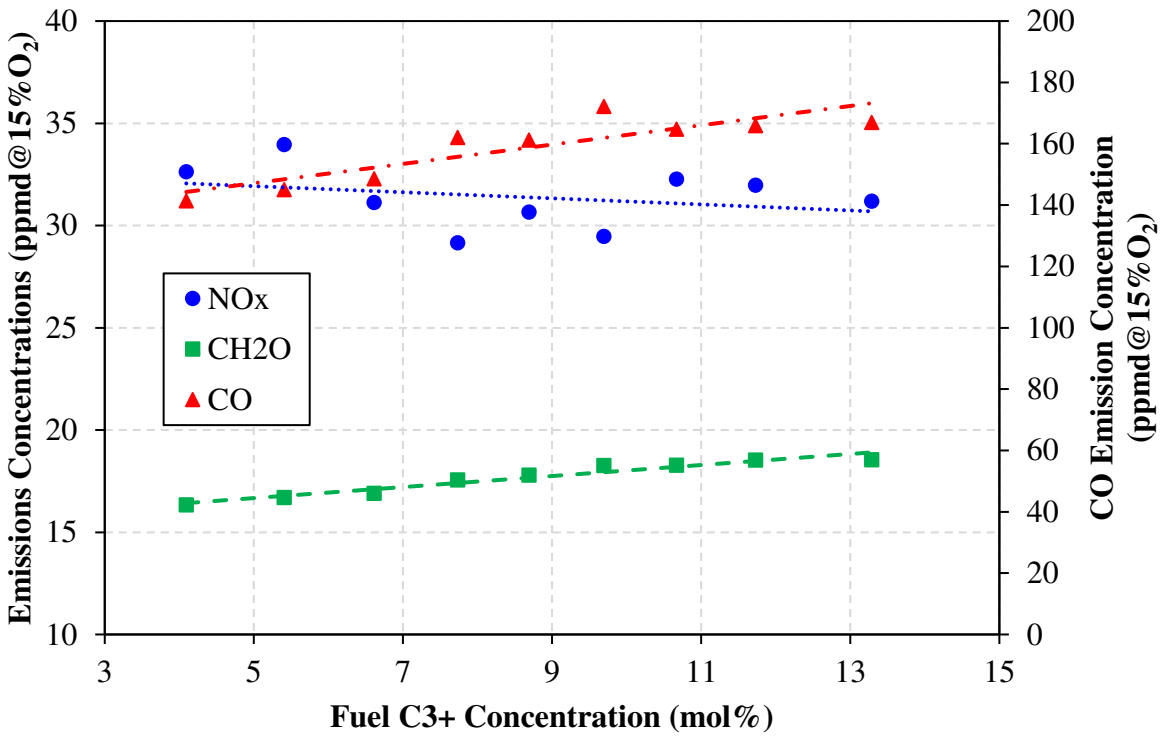

Figure 5-12. Exhaust NO_X, CH_2O, and CO concentrations taken from the MKS FTIR versus fuel C_{3+} concentration during fuel C_{3+} hydrocarbon sweep for the HPFI GMV-4 configuration.

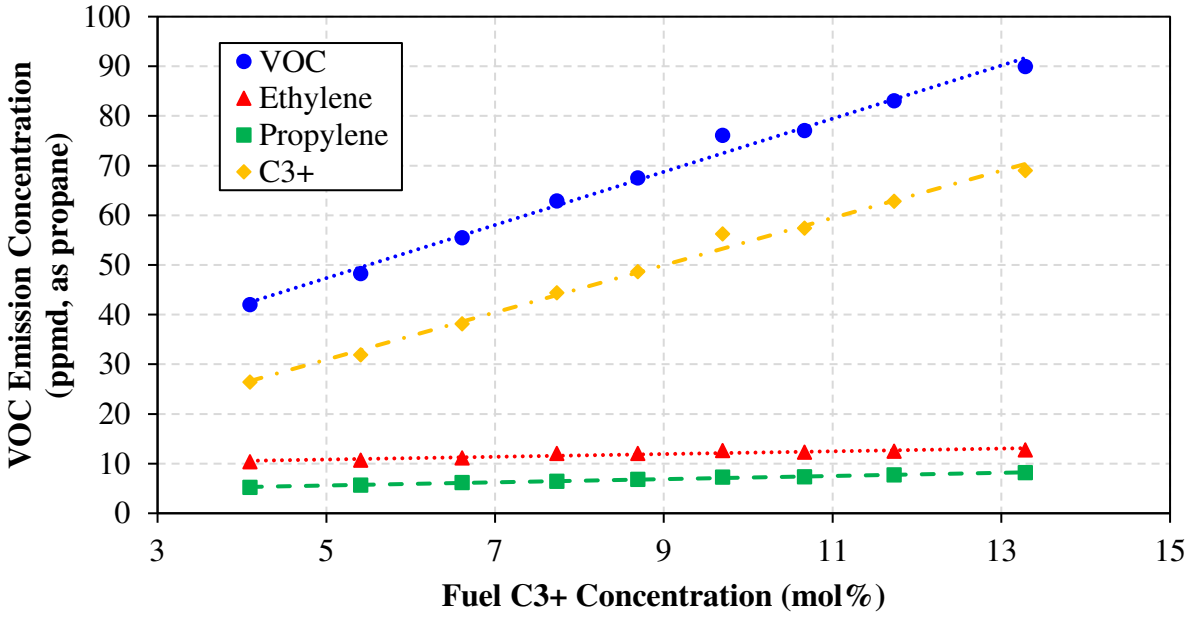

Figure 5-13. Exhaust NO_X, CH_2O, and CO concentrations taken from the MKS FTIR versus fuel C_{3+} concentration during fuel C_{3+} hydrocarbon sweep for the HPFI GMV-4 configuration.

All hydrocarbons shown in Figure 5-13 increased significantly with the addition of fuel C_{3+} hydrocarbons. Exhaust ethylene and propylene concentrations increased 23 percent and 56 percent, respectively, from the beginning to the end of the sweep. Exhaust C_{3+} hydrocarbons increased the largest in concentration (161 percent). Overall, the total VOC concentration increased from 42.0 ppmd, as propane to 89.9 ppmd, as propane (114 percent) when fuel C_{3+} concentration increased 10.7 mol%.

Discussion

Fuel composition variability has noticeable effects on exhaust gas concentration and engine performance. The addition of 10 percent fuel ethane significantly increased the ethylene and ethane concentrations but there was a decrease in propane concentration as well as the higher hydrocarbon concentration during the combustion event. As fuel ethane increased 10 mol%, fuel C_{3+} hydrocarbons decreased an average of 16.8 mol% and the destruction efficiencies of the higher hydrocarbons also increased compared to the nominal fuel composition data, indicating that a higher fraction of fuel C_{3+} was combusted. These trends result in a decrease of higher hydrocarbon concentration in the exhaust gas with added fuel ethane. Equations 5-3 to 5-8 reaction pathways that occur during the combustion of ethane [30, 31].

$$C_2H_6 + H \leftrightarrow C_2H_5 + H_2 \quad (5\text{-}3)$$

$$C_2H_6 + O \leftrightarrow C_2H_5 + OH \quad (5\text{-}4)$$

$$C_2H_6 + OH \leftrightarrow C_2H_5 + H_2O \quad (5\text{-}5)$$

$$C_2H_6 + CH_3 \leftrightarrow C_2H_5 + CH_4 \quad (5\text{-}6)$$

The ethyl radical is very unstable and reacts quickly to form ethylene.

$$C_2H_5 + M \leftrightarrow C_2H_4 + H + M \quad (5\text{-}7)$$

$$C_2H_5 + O_2 \leftrightarrow C_2H_4 + HO_2 \quad (5\text{-}8)$$

Since ethylene is a product of combusting ethane, an increase in fuel ethane will increase ethylene emissions, which increases the total VOC concentration. The exhaust ethane concentration more than doubled with the addition of 10 percent fuel ethane, implying that there was significant ethane slip since the destruction efficiency for ethane increased half of a percent compared to the nominal data. The addition of fuel ethane also produced higher destruction efficiencies overall than the addition of C_{3+} hydrocarbons or running the engine with nominal fuel composition. When pure ethane is combusted at 1 atm with air (79 percent N_2, 21 percent O_2) at stoichiometric conditions, the resulting adiabatic flame temperature is 2259 K, which is 33 K higher than the combustion of methane at the same conditions [32]. The higher flame temperature provides additional energy for more fuel higher hydrocarbons to undergo reactions during combustion, increasing the destruction efficiencies.

The fuel ethane sweep data was consistent with the results from the steady-state data points. As the fuel ethane concentration increased 16 mol%, exhaust ethylene and ethane increased 60 percent and 113 percent, respectively, but there was a decrease in propylene and C_{3+} hydrocarbons by 10 percent and 33 percent, respectively. The resulting large increase in exhaust ethylene concentration causes the total VOC concentration to increase significantly; however, the decrease in propylene and C_{3+} counteracted this leading to only a slight increase in total VOCs. The combustion of ethane leads to a higher adiabatic flame temperature and, therefore, produces enough energy to react with and break down the heavier hydrocarbons, which consist of a greater number of C-H bonds, which are weaker than C-C bonds; C-H bonds have a dissociation energy

of 337 kJ/mol and C-C bonds have a dissociation energy of 607 kJ/mol [33]. The dissociation energy of a hydrocarbon generally decreases with higher number of C-H bonds; thus, methane had the lowest destruction efficiency due to having the greatest dissociation energy of 431 kJ/mol while butane and pentane had higher destruction efficiencies due to lower dissociation energies (360 kJ/mol and 418 kJ/mol, respectively) [33]. The addition of fuel ethane during the sweep did not significantly change the formaldehyde or NO_X emissions since NO_X sensor feedback control was active but significantly increased CO emissions. This is likely due to the increase of carbon content with the addition of ethane in the fuel, which increases the amount of CO formed during combustion; the amount of carbon increased from 119 mol to 132 mol between the nominal composition (12.4 mol% ethane) and the maximum ethane composition (27.9 mol% ethane).

The overall engine performance improved with the addition of fuel ethane. Although the COV IMEP remained relatively constant as fuel ethane concentration increased, the COV PP decreased significantly. Since ethane has a lower bond dissociation energy than methane (410 kJ/mol as opposed to 431 kJ/mol [33]), fuel with higher ethane content is more easily combustible, which improves combustion stability. The location of PP advanced slightly from 18.5°CA to 17.5°CA with the increase of fuel ethane. The hotter flame temperature resulting from the higher fuel ethane content caused the engine to operate at a leaner TER (seen in Figure 5-6) to compensate for the increase in NO_X that would occur. There were no significant changes in the 0-10%, 50%, or 10-90% burn durations; however, there was a slight decrease in each. For methane burning in air at a stoichiometric AFR and at standard temperature and pressure, the flame speed is 40 cm/s. For ethane burning in air at the same conditions, the flame speed is 43 cm/s [32]. Because ethane has a faster flame speed than methane, an addition of fuel ethane would cause the fuel to burn quicker and the burn durations to decrease.

Adding 5 percent C_{3+} hydrocarbons to the natural gas fuel increased propylene, propane, and C_{4+} exhaust concentrations greater than 100 percent. The fuel C_{3+} hydrocarbon sweep data supported this result with a 56 percent increase in propylene concentration and a 24 percent increase in ethylene when 13 mol% of higher hydrocarbons were added. The main products of propane combustion are methane, ethylene, and propylene so there is an increase in these VOCs when fuel propane is added [34]. The increase in the exhaust hydrocarbons increased the total VOC concentration by 114 percent. Like with the addition of fuel ethane, the addition of fuel C_{3+} hydrocarbons significantly increased CO emissions due to the higher fraction of carbon atoms in the fuel. NO_X levels remained steady since NO_X sensor feedback control was active; however, there was a decrease in TER, which is indicative of compensation for a NO_X concentration increase. The addition of higher hydrocarbons did contribute to better destruction efficiencies than the nominal fuel composition but not as much as the addition of fuel ethane. The destruction efficiencies for i-butane and i-pentane were the lowest among all the fuel composition types.

Adding higher hydrocarbons to the natural gas fuel did not affect overall engine performance. The COV PP decreased less than one percent and the COV IMEP decreased only eight percent, implying no disadvantage or benefit towards combustion stability. The 0-10%, 50%, and 10-90% burn durations increased less than two percent with the increase in fuel C_{3+} content, likely due to the faster flame speed of propane than methane (44 cm/s for propane burning in air at a stoichiometric AFR and standard conditions [30]). One benefit of increased C_{3+} concentration in the fuel, on the other hand, is that the higher flame temperatures did allow the engine to run on a leaner TER to prevent an increase in NO_X emissions.

CHAPTER 6 – CONCLUSION AND FUTURE WORK

Conclusion

Exhaust gas from the GMV-4 and Caterpillar 3304 natural gas compressor engines was sampled through four separate analyzers comparing EPA Method 320 and EPA Method 18/25a to determine whether EPA Method 320 is an acceptable process for VOC quantification. The four analyzers were the HP 5890 Series II GC and VIG Industries Model 210 FID, utilizing EPA Method 18/25a, as well as the liquid N_2-cooled MKS Instruments No. 2030 FTIR and Peltier-cooled Gasmet Technologies DX4000 FTIR, utilizing EPA Method 320.

The GMV-4 engine testing consisted of different configurations, each targeting a unique NO_X emission level to achieve emission composition variability. The first configuration was the OC ignition with a target NO_X level of 15 g/bhp-hr. The second configuration tested was with PCC installed and a maintained NO_X level of 2 g/bhp-hr. The final configuration tested on the GMV-4 consisted of an HPFI system with PCC ignition and electronic fuel valves, which achieved a NO_X level of 0.5 g/bhp-hr. For each GMV-4 configuration an ignition timing sweep was performed, starting at the nominal ignition timing of 18°aTDC. Ignition timing was advanced and retarded 5°CA for final ignition timings of 13°aTDC and 23°aTDC, respectively, and held at steady-state for data collection.

Two data points were taken for each GMV-4 configuration with the addition of 10 mol% ethane and 5 mol% higher hydrocarbons separately added to the natural gas fuel supply to determine the impact fuel composition variability has on emission concentration and engine performance. In addition, fuel ethane and fuel higher hydrocarbon sweeps were performed on the last day of GMV-4 testing with the HPFI configuration where the molar concentration of each was

increased from the nominal value to the maximum amount allowed by each blending system. For the fuel ethane sweep, fuel ethane concentration was increased from 12.4 mol% to 27.9 mol%. For the fuel higher hydrocarbon sweep, fuel C_{3+} hydrocarbon concentration was increased from 2.56 mol% to 13.3 mol%.

The last configuration for the test program was the rich burn test with a three-way catalyst on the Caterpillar 3304 natural gas compressor engine. Exhaust gas was sampled from the exhaust stack downstream of the three-way catalyst. Only an ignition timing sweep was performed for this configuration. A data point was taken at steady-state with an ignition timing at the nominal 30°bTDC, then timing was advanced and retarded 4°CA for final ignition timings of 26°bTDC and 34°bTDC, respectively.

Before and after each test day as well as each engine test program (i.e. the GMV-4 and Caterpillar 3304 engines) a quality assurance/quality check (QA/QC) was performed for each analyzer per the appropriate EPA method guidelines. During each data point, engine DAQ data, including measurements from the Siemens 5-Gas analyzer, and combustion data were recorded and monitored. Spectra were continuously recorded from the MKS FTIR and the Gasmet FTIR and emissions concentrations were recorded from the VIG FID. Twenty-minute averages of data from each instrument was taken for post-processing. Three separate samples of heated, wet exhaust gas were injected into the HP GC during a data point. In addition, a Tedlar bag was filled with the exhaust gas while allowing water to condense within the bag to be analyzed in the HP GC 24-36 hours after the data point was taken. To compare each analyzer/method, individual VOC concentrations as well as total VOC concentrations were calculated and plotted for each data point. Various engine performance parameters and emissions concentrations were plotted for the fuel ethane and fuel C_{3+} hydrocarbon sweeps and steady-state data points.

From the results provided for the analyzer/method comparison, it was concluded that

- The HP 5890 Series II GC utilizing EPA Method 18/25a is the most accurate and feasible process for VOC quantification.
    - The HP GC provides individual VOC concentration for hydrocarbons up to C_6.
    - Each individual hydrocarbon can be calibrated to the correct response factor before collecting data.
- A common process currently used for VOC quantification, which subtracts the methane and ethane measurements from the MKS FTIR from the THC measurement from the Siemens 5-Gas analyzer, is not an accurate method as it creates large uncertainty up to 193 percent and overestimates total VOC concentration by nearly 100 percent relative to the HP GC. The large uncertainty associated with this method makes it unacceptable for VOC quantification.
- The use of Tedlar bags to sample exhaust gas can yield similar VOC concentration measurements to the direct extraction method for the HP GC.
    - Water can condense in the bag, as is practiced in the field; the wet sample from the Tedlar bag yields the most accurate results to the direct extraction of the exhaust gas into the HP GC than any other method considered for this research; the method underestimated the total VOC concentration less than two percent.
    - Since water condensation within the bag is allowed, storing and analyzing the Tedlar bags at an elevated temperature is not necessary.
    - A Tedlar bag can be analyzed up to 24-36 hours after being filled and result in similar VOC concentration measurements to the direct extraction method for the HP GC; after one week, the ethylene and propylene measurements decrease by 12

percent and 31 percent, respectively. After one month the propane concentration decreases 18 percent.

  - Removing the water content from the exhaust gas via a chiller before injecting the sample into the Tedlar bag underestimates the total VOC concentration by a small amount of about seven percent as water tends to absorb hydrocarbons during condensation in the chiller.

- The "VIG FID Residual + MKS C2H4" method is the second most accurate method to the direct extraction of exhaust gas to the HP GC.
  - The residual measurement reported by the VIG FID is not sufficient for VOC quantification since it only includes C_{3+} hydrocarbons and excludes ethylene.
  - The alternate method "VIG FID Residual + C2 – MKS C2H6" is not an accurate method of measuring total VOC concentration; this method tends to report total VOC concentrations 23 percent lower than the HP GC.
- Both the Gasmet and MKS FTIRs (EPA Method 320) overestimate total VOC concentration compared to the HP GC (EPA Method 18/25A) by approximately 18 percent and 12 percent, respectively.
  - However, the differences between the methods are within uncertainty bounds in most cases.
  - Consequently, Methods 320 is deemed an acceptable method for VOC quantification.
- Including C_{5+} hydrocarbons when quantifying total VOC concentration in natural gas engine exhaust is not needed; eliminating C_{5+} hydrocarbons decreases the total VOC concentration by only 2.2 percent.

- Excluding the measurement of C_{5+} hydrocarbons reduces the analysis time by 25 percent when using the HP GC.

The steady-state data points taken after the addition of 10 mol% ethane to the natural gas fuel as well as the fuel ethane sweep showed that

- Exhaust propane and C_{4+} hydrocarbon concentrations decreased about 33 percent due to the 17 percent decrease of fuel C_{3+} hydrocarbon molar concentration when fuel ethane was added during the sweep.
- The molar concentration of fuel ethane increased 10 percent, which resulted in a 113 percent increase in exhaust ethane during sweep due to ethane slip.
- Ethylene, which is a product of ethane combustion, increased 60 percent in concentration between the nominal fuel ethane and maximum fuel ethane compositions.
- The increase in exhaust ethylene and ethane concentration along with the decrease in C_{3+} hydrocarbon concentration caused the total VOC concentration to increase a small amount of 4.5 percent.
- Overall engine performance improved; COV of PP decreased 15 percent, indicating improved combustion stability.

The steady-state data points taken after the addition of 5 mol% C_{3+} hydrocarbons to the natural gas fuel as well as the fuel C_{3+} hydrocarbon sweep showed that

- Higher hydrocarbon content in the exhaust increased 161 percent during the sweep, which greatly increased the total VOC concentration by 114 percent.
- Engine performance was not affected.

- COV PP and COV IMEP increased 2.7 percent and 9.2 percent, respectively, during the C_{3+} hydrocarbon sweep.
- The 0-10%, 50%, and 10-90% burn durations differed less than three percent during the C_{3+} hydrocarbon sweep.

Future Work

Ideas for future work include

- additional testing on the GMV-4 natural gas engine and quantifying VOC concentration in the exhaust gas using the four different analyzers at the following conditions
  - a lower target NO_X level of 0.2 g/bhp-hr.
  - an increase of the GMV-4 engine's BMEP to 82 psi at an increased engine speed of 330 rpm (110 percent of the rated speed).
- a condensed version of this thesis as a White Paper focusing on the method comparison results and conclusions.
- constructing the proposed alternate GC/FID analyzer with the C_{3+} backflush mechanism.
- determining a unique factor for each VOC based on its reactivity in the formation of ozone in the earth's atmosphere. For the results from this test program, all VOCs were assumed equal in their potential of creating ozone in the earth's atmosphere; however, this is not the case since each individual VOC has a unique reactivity in the formation of ozone [35]. To compensate for this, a factor for each VOC can be applied to normalize the total VOC concentration based on its significance in forming smog in the environment.

REFERENCES

[1] Kampa, M., & Castanas, E. (2008). Human health effects of air pollution. *Environmental pollution*, 151(2), 362-367.

[2] Ware, J. H., Spengler, J. D., Neas, L. M., Samet, J. M., Wagner, G. R., Coultas, D.,& Schwab, M. (1993). Respiratory and irritant health effects of ambient volatile organic compounds: the Kanawha County Health Study. *American Journal of Epidemiology*, 137(12), 1287-1301.

[3] EPA Method 18, *Measurement of Gaseous Organic Compound Emissions by Gas Chromatography*. U.S. EPA, Washington D.C., December 1971, 36 FR 24877

[4] EPA Method 25A, *Determination of Total Gaseous Organic Concentration Using a Flame Ionization Analyzer*. U.S EPA, Washington D.C., December 1971, 36 FR 24877

[5] EPA Method 320, *Measurement of Vapor Phase Organic and Inorganic Emissions by Extractive Fourier Transform Infrared (FTIR) Spectroscopy*. U.S EPA, Washington D.C., December 1992, 57 FR 61992

[6] MacNair, H. M., & Bonelli, E. J. (1968). *Basic Gas Chromatography* (5th ed.). Walnut Creek, CA: Varian Aerograph.

[7] Bates, J. B. (1976). Fourier transform infrared spectroscopy. *Science, 191*(4222), 31-37.

[8] Ladd, John, Neuner, Benjamin, Olsen, Daniel B. (2016). Variable fuel composition air fuel ratio control of lean burn engines. *Pipeline Research Council International, Inc.*

[9] Ladd, John, Stevens, Mary, Olsen, Daniel B. (2016). Methane Reduction Data Analysis for 2-Stroke Lean Burn Natural Gas Engines. *Pipeline Research Council International, Inc.*

[10] Amirante, R., Distaso, E., Di Iorio, S., Sementa, P., Tamburrano, P., Vaglieco, B. M., & Reitz, R. D. (2017). Effects of natural gas composition on performance and regulated, greenhouse gas and particulate emissions in spark-ignition engines. *Energy Conversion and Management*, *143*, 338-347.

[11] Gilman, J. B., Lerner, B. M., Kuster, W. C., & De Gouw, J. A. (2013). Source signature of volatile organic compounds from oil and natural gas operations in northeastern Colorado. *Environmental science & technology*, *47*(3), 1297-1305.

[12] Karasek, F., & Clement, R. (2012). *Basic Gas Chromatography-Mass Spectrometry: Principles and Techniques*. Amsterdam: Elsevier Science.

[13] de Gouw, J., & Warneke, C. (2007). Measurements of volatile organic compounds in the earth's atmosphere using proton-transfer-reaction mass spectrometry. Mass spectrometry reviews, 26(2), 223-257.

[14] Clark, N., Mott, G., Atkinson, C., deJong, R. et al., "Effect of Fuel Composition on the Operation of a Lean Burn Natural Gas Engine," SAE Technical Paper 952560, 1995,https://doi.org/10.4271/952560

[15] Thiagarajan, Siva, Midkiff, K. Clark, Bell, Stuart R., Green, Michael N. (1994). Investigation of fuel composition effects on a natural gas fueled spark-ignited engine. *ASME Natural Gas and Alternative Fuels for Engines,* 41-51

[16] Michael D. Feist, Mike Landau and Ed Harte. The effect of fuel composition on performance and emissions of a variety of natural gas engines. *SAE International Journal of Fuels and Lubricants*. Vol. 3, No. 2 (2010), pp. 100-117

[17] CUSTOMER SERVICE. (n.d.). Retrieved January 16, 2019, from https://www.vici.com/support/app/app22.php

[18] VIG Industries, Inc. Model 210 FID NMEHC Hydrocarbon Analyzer. (n.d.). Retrieved from http://www.vigindustries.com/m210.htm

[19] George, W. O., & McIntyre, P. S. (1987). *Infrared Spectroscopy*. Chichester: Wiley.

[20] Moosman, T. G. (2005). FTIR Spectroscopy for 2-Stroke, Lean Burn Gas Engines Emphasizing Low-Level Detection of HAPs (Doctoral dissertation, Colorado State University).

[21] Schmitt, J. C. (2010). *Selective catalytic reduction: testing, numeric modeling, and control strategies* (Master thesis, Colorado State University. Libraries).

[22] Gattoni, J. (2012). *Advanced control techniques and sensors for gas engines with NSCR* (Master thesis, Colorado State University. Libraries).

[23] ECM. (2017). NOx 5210t. Retrieved from http://www.ecm-co.com/product.asp?5210t

[24] Subpart JJJJ—Standards of Performance for Stationary Spark Ignition Internal Combustion Engines. (n.d.). Retrieved from https://www.ecfr.gov/cgi-bin/text-idx?node=sp40.7.60.jjjj#sg40.8.60_14230.sg106

[25] *Standard Test Method for Determination of Gaseous Compounds by Extractive Direct Interface Fourier Transform Infrared (FTIR) Spectroscopy*. ASTM International, ASTM D 6348-03, 2003.

[26] Willson, B. D., & Mitchell, C. E. (2002). Development of the tracer gas method for large bore natural gas engines—part I: method validation.

[27] Olsen, D. B., Hutcherson, G. C., Willson, B. D., & Mitchell, C. E. (2002). Development of the tracer gas method for large bore natural gas engines—part II: measurement of scavenging parameters. *Journal of engineering for gas turbines and power*, 124(3), 686-694.

[28] Shinoda, K. O. Z. O., & Fujihira, M. (1968). The analysis of the solubility of hydrocarbons in water. *Bulletin of the chemical society of Japan, 41*(11), 2612-2615.

[29] Tsonopoulos, C. (2001). Thermodynamic analysis of the mutual solubilities of hydrocarbons and water. *Fluid Phase Equilibria, 186*(1-2), 185-206.

[30] Waly, M. M. Y., Li, S. C., & Williams, F. A. (1999, June). Experimental and numerical studies of two-stage ethane-air flames. In *ASME 1999 International Gas Turbine and Aeroengine Congress and Exhibition* (pp. V002T02A013-V002T02A013). American Society of Mechanical Engineers.

[31] Blanquart, G., Pepiot-Desjardins, P., & Pitsch, H. (2009). Chemical mechanism for high temperature combustion of engine relevant fuels with emphasis on soot precursors. *Combustion and Flame, 156*(3), 588-607.

[32] Turns, S. R. (2012). *An Introduction to Combustion: Concepts and Applications* (3rd ed.). NY: McGraw-Hill Companies.

[33] Dean, J. A. (1999). *Lange's Handbook of Chemistry* (15th ed.). McGraw-Hill.

[34] Jachimowski, C. J. (1984). Chemical kinetic reaction mechanism for the combustion of propane. *Combustion and flame, 55*(2), 213-224.

[35] Carter, W. P. (1994). Development of ozone reactivity scales for volatile organic compounds. *Air & waste, 44*(7), 881-899

APPENDIX A: QA/QC

EPA Method 25A Check List

THC (Method 25A)

General

Beginning of the Test Program

- ☐ Place probe at least 8 diameters downstream and 2 diameters upstream from any flow disturbance.
- ☐ Make sure there are 12 traverse points for a diameter greater than 24 in. or 8 traverse points for a diameter between 12 and 24 in.
- ☐ Make sure no traverse points are within 1 in. of stack wall for diameter greater than 24 in. If less than 24 in., make sure no traverse points are within 0.5 in of stack wall.
- ☐ Make sure the analyzers minimum detectable limits are less that 2% of span.
- ☐ Make sure the calibration gases are[3]:
  - -Low-level: 25-35% of the span
  - -Mid-level: 45-55% of the span
  - -High-Level: 80-90% of the span.
- ☐ Make sure the calibration gases used are propane, or other organic compounds (e.g. CH4), in N2.

Beginning of Each Day

- ☐ Ensure all sampling components leading to the analyzer are heated to a temperature that is greater than or equal to 220°F including the sample lines.
- ☐ Make sure the FID is heated to a temperature that is greater than 250°F.[16]
- ☐ Zero and calibrate the instrument according to manufacturer's procedures.[4]
- ☐ Perform a Calibration Error Test making sure calibration error is less than ± 5% of the calibrated gas values.[5]

Before/After Each Data Point

- ☐ Calibrate the analyzers according to the manufacturers instructions.
- ☐ Determine the Drift making sure it is no greater than ± 3% of the span for the zero drift and calibration drift.[11]

Figure A-1. QA/QC checklist for the GC/FID analyzers following EPA Method 18/25a.

FTIR Procedures Check List for Method 320

Start of Test Program	End of Test Program	Start of Each Test Day	End of Each Test Day
☐ Perform leak check of the sampling system.	☐ Inspect sample spectra.	☐ Calibration Transfer Standard. Evacuate the gas cell to ≤5 mmHg absolute pressure, and fill the FTIR cell to atmospheric pressure with the CTS gas.	☐ Perform QA and analyte spikes.
☐ Perform analyte spiking procedure.	☐ Perform analyte spiking procedure.	☐ Perform QA and analyte spikes.	☐ Verify that the sampling and instrumental parameters were appropriate for the conditions encountered.
☐ Perform QA Spike.	☐ _____	☐ _____	☐ Compare the pre- and post-test CTS spectra.
☐ _____	☐ _____	☐ _____	☐ Inspect the sample spectra immediately after the run to verify that the gas matrix composition was close to the expected (assumed) gas matrix.
☐ _____	☐ _____	☐ _____	☐ _____
☐ _____	☐ _____	☐ _____	☐ _____
☐ _____	☐ _____	☐ _____	☐ _____

Figure A-2. QA/QC checklist for the FTIR analyzers following EPA Method 320.

Cal Gas Check; 2/18/19

HP GC High Level; 9:15

Compound	Actual concentration (ppm)	HP GC Measurement (ppm)	Difference (%)
Methane	1007	988.571	-1.83
Ethylene	50.23	49.211	-2.03
Ethane	50.38	49.512	-1.72
Propylene	20.12	19.452	-3.32
Propane	20.04	19.659	-1.90
i-Butane	4.99	1.975	-60.4
n-Butane	4.96	4.786	-3.51
i-Pentane	4.8	2.496	-48.0
n-Pentane	5.04	2.569	-49.0
i-Hexane	5.29	5.237	-1.00
n-Hexane	5.01	3.39	-32.3

HP GC Mid Level Propane Check; 9:35

Compound	Actual concentration (ppm)	HP GC Measurement 1 (ppm)	Difference (%)
Propane	13.92	14.543	4.48

HP GC Low Level Propane Check; 9:50

Compound	Actual concentration (ppm)	HP GC Measurement 1 (ppm)	Difference (%)
Propane	8.87	8.765	-1.18

Drift Checks

Check	Time	HP GC Measurement (ppm)	Difference (%)
Mid-day 1	16:35	13.727	-5.61
Mid-day 2			-100.00

Figure A-3. High-, mid-, low-calibration, and drift checks on the HP GC during Day 1 on the GMV-4 engine OC configuration.

Cal Gas Check; 2/19/19

HP GC High Level; 8:40

Compound	Actual concentration (ppm)	HP GC Measurement (ppm)	Difference (%)
Methane	1007	986.005	-2.08
Ethylene	50.23	49.146	-2.16
Ethane	50.38	49.385	-1.97
Propylene	20.12	19.164	-4.75
Propane	20.04	19.451	-2.94
i-Butane	4.99	4.036	-19.1
n-Butane	4.96	4.768	-3.87
i-Pentane	4.8	2.545	-47.0
n-Pentane	5.04	2.566	-49.1
i-Hexane	5.29	5.354	1.21
n-Hexane	5.01	3.419	-31.8

HP GC Mid Level Propane Check; 9:45

Compound	Actual concentration (ppm)	HP GC Measurement 1 (ppm)	Difference (%)
Propane	13.92	13.71	-1.51

HP GC Low Level Propane Check; 10:00

Compound	Actual concentration (ppm)	HP GC Measurement 1 (ppm)	Difference (%)
Propane	8.87	8.67	-2.25

Drift Checks

Check	Time	HP GC Measurement (ppm)	Difference (%)
Mid-day	15:25	14.006	2.16
End of day	17:10	13.751	0.30

Figure A-4. High-, mid-, low-calibration, and drift checks on the HP GC during Day 2 on the GMV-4 engine OC configuration.

Cal Gas Check; 2/20/19

HP GC High Level; 9:20

Compound	Actual concentration (ppm)	HP GC Measurement (ppm)	Difference (%)
Methane	1007	975.422	-3.14
Ethylene	50.23	48.506	-3.43
Ethane	50.38	48.833	-3.07
Propylene	20.12	15.027	-25.3
Propane	20.04	19.198	-4.20
i-Butane	4.99	4.013	-19.6
n-Butane	4.96	4.753	-4.17
i-Pentane	4.8	2.537	-47.1
n-Pentane	5.04	2.537	-49.7
i-Hexane	5.29	4.927	-6.86
n-Hexane	5.01	3.013	-39.9

HP GC Mid Level Propane Check; 9:40

Compound	Actual concentration (ppm)	HP GC Measurement 1 (ppm)	Difference (%)
Propane	13.92	14.028	0.77

HP GC Low Level Propane Check; 10:00

Compound	Actual concentration (ppm)	HP GC Measurement 1 (ppm)	Difference (%)
Propane	8.87	8.634	-2.66

Drift Checks

Check	Time	HP GC Measurement (ppm)	Difference (%)
Mid-day	14:15	14.12	0.66
End of day	17:15	14.022	-0.04

Figure A-5. High-, mid-, low-calibration, and drift checks on the HP GC during Day 3 on the GMV-4 engine OC configuration.

Cal Gas Check; 2/21/19

HP GC High Level; 9:20

Compound	Actual concentration (ppm)	HP GC Measurement (ppm)	Difference (%)
Methane	1007	989.771	-1.71
Ethylene	50.23	49.163	-2.12
Ethane	50.38	49.618	-1.51
Propylene	20.12	17.576	-12.6
Propane	20.04	19.661	-1.89
i-Butane	4.99	5.179	3.79
n-Butane	4.96	3.954	-20.3
i-Pentane	4.8	2.213	-53.9
n-Pentane	5.04	1.584	-68.6
i-Hexane	5.29	4.132	-21.9
n-Hexane	5.01	4.449	-11.2

HP GC Mid Level Propane Check; 9:40

Compound	Actual concentration (ppm)	HP GC Measurement 1 (ppm)	Difference (%)
Propane	13.92	13.913	-0.05

HP GC Low Level Propane Check; 10:00

Compound	Actual concentration (ppm)	HP GC Measurement 1 (ppm)	Difference (%)
Propane	8.87	9.941	12.07

Drift Checks

Check	Time	HP GC Measurement (ppm)	Difference (%)
Mid-day	14:15	13.829	-0.60
End of day	15:20	14.06	1.06

Figure A-6. High-, mid-, low-calibration, and drift checks on the HP GC during Day 4 on the GMV-4 engine OC configuration.

Cal Gas Check; 3/27/19

HP GC High Level; 9:30

Compound	Actual concentration (ppm)	HP GC Measurement (ppm)	Difference (%)
Methane	1007	975.105	-3.17
Ethylene	50.23	48.641	-3.16
Ethane	50.38	48.891	-2.96
Propylene	20.12	18.08	-10.1
Propane	20.04	19.241	-3.99
i-Butane	4.99	4.318	-13.5
n-Butane	4.96	4.239	-14.5
i-Pentane	4.8	2.224	-53.7
n-Pentane	5.04	2.421	-52.0
i-Hexane	5.29	4.761	-10.0
n-Hexane	5.01	3.852	-23.1

HP GC Mid Level Propane Check; 9:50

Compound	Actual concentration (ppm)	HP GC Measurement 1 (ppm)	Difference (%)
Propane	13.92	13.829	-0.65

HP GC Low Level Propane Check; 10:10

Compound	Actual concentration (ppm)	HP GC Measurement 1 (ppm)	Difference (%)
Propane	8.87	8.74	-1.47

Drift Checks

Check	Time	HP GC Measurement (ppm)	Difference (%)
Mid-day	14:50	13.626	-1.47
End of day	16:30	13.592	-1.71

Figure A-7. High-, mid-, low-calibration, and drift checks on the HP GC during Day 1 on the GMV-4 engine PCC configuration.

Cal Gas Check; 3/28/19

HP GC High Level; 9:40

Compound	Actual concentration (ppm)	HP GC Measurement (ppm)	Difference (%)
Methane	1007	996.646	-1.03
Ethylene	50.23	49.346	-1.76
Ethane	50.38	50.233	-0.29
Propylene	20.12	17.876	-11.2
Propane	20.04	20.347	1.53
i-Butane	4.99	4.406	-11.7
n-Butane	4.96	4.793	-3.37
i-Pentane	4.8	5.182	7.96
n-Pentane	5.04	2.647	-47.5
i-Hexane	5.29	5.24	-0.95
n-Hexane	5.01	4.235	-15.5

HP GC Mid Level Propane Check; 10:00

Compound	Actual concentration (ppm)	HP GC Measurement 1 (ppm)	Difference (%)	Comments
Propane	13.92	14.581	4.75	

HP GC Low Level Propane Check; 10:20

Compound	Actual concentration (ppm)	HP GC Measurement 1 (ppm)	Difference (%)	Comments
Propane	8.87	8.891	0.24	

Drift Checks

Check	Time	HP GC Measurement (ppm)	Difference (%)	Comments
Mid-day	14:20	13.579	-2.45	Drift was greater than 3% (6.87%) but is within 5% (2.45%) of actual value, therefore accepte
End of day	17:05	13.35	-4.09	Drift was greater than 3% (8.44%) but is within 5% (4.09%) of actual value, therefore accepte

Figure A-8. High-, mid-, low-calibration, and drift checks on the HP GC during Day 2 on the GMV-4 engine PCC configuration.

Cal Gas Check; 4/5/19

HP GC High Level; 9:20

Compound	Actual concentration (ppm)	HP GC Measurement (ppm)	Difference (%)
Methane	1007	1005.222	-0.18
Ethylene	50.23	49.421	-1.61
Ethane	50.38	50.348	-0.06
Propylene	20.12	19.13	-4.92
Propane	20.04	20.019	-0.10
i-Butane	4.99	4.761	-4.59
n-Butane	4.96	4.854	-2.14
i-Pentane	4.8	4.802	0.04
n-Pentane	5.04	3.124	-38.0
i-Hexane	5.29	5.197	-1.76
n-Hexane	5.01	5.093	1.66

HP GC Mid Level Propane Check; 9:35

Compound	Actual concentration (ppm)	HP GC Measurement 1 (ppm)	Difference (%)
Propane	13.92	14.194	1.97

HP GC Low Level Propane Check; 9:50

Compound	Actual concentration (ppm)	HP GC Measurement 1 (ppm)	Difference (%)
Propane	8.87	8.907	0.42

Drift Checks

Check	Time	HP GC Measurement (ppm)	Difference (%)
Mid-day	14:50	14.211	0.12
End of day	16:20	14.195	0.01

Figure A-9. High-, mid-, low-calibration, and drift checks on the HP GC during Day 1 on the GMV-4 engine HPFI configuration.

Cal Gas Check; 4/15/19

HP GC High Level; 9:20

Compound	Actual concentration (ppm)	HP GC Measurement (ppm)	Difference (%)
Methane	1007	1013.211	0.62
Ethylene	50.23	49.795	-0.87
Ethane	50.38	50.747	0.73
Propylene	20.12	19.311	-4.02
Propane	20.04	20.151	0.55
i-Butane	4.99	4.907	-1.66
n-Butane	4.96	4.89	-1.41
i-Pentane	4.8	4.982	3.79
n-Pentane	5.04	3.157	-37.4
i-Hexane	5.29	5.329	0.74
n-Hexane	5.01	4.791	-4.37

HP GC Mid Level Propane Check; 9:45

Compound	Actual concentration (ppm)	HP GC Measurement 1 (ppm)	Difference (%)
Propane	13.92	14.147	1.63

HP GC Low Level Propane Check; 10:00

Compound	Actual concentration (ppm)	HP GC Measurement 1 (ppm)	Difference (%)
Propane	8.87	9.1	2.59

Drift Checks

Check	Time	HP GC Measurement (ppm)	Difference (%)
Mid-day	14:05	14.033	-0.81
End of day	16:10	13.918	-1.62

Figure A-10. High-, mid-, low-calibration, and drift checks on the HP GC during Day 2 on the GMV-4 engine HPFI configuration.

Cal Gas Check; 4/16/19

HP GC High Level; 9:15

Compound	Actual concentration (ppm)	HP GC Measurement (ppm)	Difference (%)
Methane	1007	1020.195	1.31
Ethylene	50.23	50.278	0.10
Ethane	50.38	51.152	1.53
Propylene	20.12	20.813	3.44
Propane	20.04	20.362	1.61
i-Butane	4.99	5.072	1.64
n-Butane	4.96	4.938	-0.44
i-Pentane	4.8	4.941	2.94
n-Pentane	5.04	3.369	-33.2
i-Hexane	5.29	5.543	4.78
n-Hexane	5.01	5.206	3.91

HP GC Mid Level Propane Check; 9:45

Compound	Actual concentration (ppm)	HP GC Measurement 1 (ppm)	Difference (%)
Propane	13.92	13.972	0.37

HP GC Low Level Propane Check; 9:50

Compound	Actual concentration (ppm)	HP GC Measurement 1 (ppm)	Difference (%)
Propane	8.87	9.168	3.36

Drift Checks

Check	Time	HP GC Measurement (ppm)	Difference (%)
Mid-day	12:30	9.238	0.76
End of day	14:05	9.317	1.63

Figure A-11. High-, mid-, low-calibration, and drift checks on the HP GC during Day 3 on the GMV-4 engine HPFI configuration.

Cal Gas Check; 4/18/19

HP GC High Level; 9:05

Compound	Actual concentration (ppm)	HP GC Measurement (ppm)	Difference (%)
Methane	1007	1006.11	-0.09
Ethylene	50.23	49.339	-1.77
Ethane	50.38	49.503	-1.74
Propylene	20.12	19.45	-3.33
Propane	20.04	19.492	-2.73
i-Butane	4.99	5.071	1.62
n-Butane	4.96	4.895	-1.31
i-Pentane	4.8	4.909	2.27
n-Pentane	5.04	3.311	-34.3
i-Hexane	5.29	5.132	-2.99
n-Hexane	5.01	4.964	-0.92

HP GC Mid Level Propane Check; 9:35

Compound	Actual concentration (ppm)	HP GC Measurement 1 (ppm)	Difference (%)
Propane	13.92	13.613	-2.21

HP GC Low Level Propane Check; 9:50

Compound	Actual concentration (ppm)	HP GC Measurement 1 (ppm)	Difference (%)
Propane	8.87	8.831	-0.44

Drift Checks

Check	Time	HP GC Measurement (ppm)	Difference (%)
Mid-day	13:25	8.958	1.44
End of day	15:40	8.702	-1.46

Figure A-12. High-, mid-, low-calibration, and drift checks on the HP GC during Day 1 on the Caterpillar 3304 engine rich burn with three-way catalyst configuration.

Siemens 5-Gas Analyzer Logbook

5-Gas High Level; 8:35

Compund	Actual concentration (ppm)	5-Gas Measurement (ppm)	Difference (%)
Methane	958.8	959.1	0.03

5-Gas Mid Level Methane Check; 9:10

Compound	Actual concentration (ppm)	5-Gas Measurement (ppm)	Difference (%)
Methane	504.4	492.1	-2.44

5-Gas Low Level Methane Check; 9:15

Compound	Actual concentration (ppm)	5-Gas Measurement (ppm)	Difference (%)
Methane	249.6	245.5	-1.64

Figure A-13. High-, mid-, and low-calibration checks on the Siemens 5-Gas analyzer during Day 1 on the GMV-4 engine OC configuration.

5-Gas High Level; 8:30

Compund	Actual concentration (ppm)	5-Gas Measurement (ppm)	Difference (%)
Methane	958.8	965.4	0.69

5-Gas Mid Level Methane Check; 8:30

Compound	Actual concentration (ppm)	5-Gas Measurement (ppm)	Difference (%)
Methane	504.4	501.4	-0.59

5-Gas Low Level Methane Check; 8:30

Compound	Actual concentration (ppm)	5-Gas Measurement (ppm)	Difference (%)
Methane	249.6	250.0	0.16

Drift Checks

Check	Time	5-Gas Measurement (ppm)	Difference (%)
End of day	16:50	501.5	0.02

Figure A-14. High-, mid-, low- calibration, and drift checks on the Siemens 5-Gas analyzer during Day 2 on the GMV-4 engine OC configuration.

5-Gas High Level; 10:00

Compund	Actual concentration (ppm)	5-Gas Measurement (ppm)	Difference (%)
Methane	958.8	958.5	-0.03

5-Gas Mid Level Methane Check; 10:00

Compound	Actual concentration (ppm)	5-Gas Measurement (ppm)	Difference (%)
Methane	504.4	504.1	-0.06

5-Gas Low Level Methane Check; 10:00

Compound	Actual concentration (ppm)	5-Gas Measurement (ppm)	Difference (%)
Methane	249.6	251.3	0.68

Figure A-15. High-, mid-, and low-calibration checks on the Siemens 5-Gas analyzer during Day 3 on the GMV-4 engine OC configuration.

5-Gas High Level; 10:00

Compund	Actual concentration (ppm)	5-Gas Measurement (ppm)	Difference (%)
Methane	958.8	964.9	0.64

5-Gas Mid Level Methane Check; 10:00

Compound	Actual concentration (ppm)	5-Gas Measurement (ppm)	Difference (%)
Methane	504.4	500.3	-0.81

5-Gas Low Level Methane Check; 10:00

Compound	Actual concentration (ppm)	5-Gas Measurement (ppm)	Difference (%)
Methane	249.6	249.5	-0.04

Drift Checks

Check	Time	5-Gas Measurement (ppm)	Difference (%)
End of day	15:05	505.5	1.04

Figure A-16. High-, mid-, and low-calibration checks on the Siemens 5-Gas analyzer during Day 4 on the GMV-4 engine OC configuration.

5-Gas High Level; 9:00

Compund	Actual concentration (ppm)	5-Gas Measurement (ppm)	Difference (%)
Methane	958.8	946.1	-1.32

5-Gas Mid Level Methane Check; 9:00

Compound	Actual concentration (ppm)	5-Gas Measurement (ppm)	Difference (%)
Methane	504.4	499.2	-1.03

5-Gas Low Level Methane Check; 9:00

Compound	Actual concentration (ppm)	5-Gas Measurement (ppm)	Difference (%)
Methane	249.6	248.8	-0.32

Drift Checks

Check	Time	5-Gas Measurement (ppm)	Difference (%)
End of day	17:00	501.1	0.38

Figure A-17. High-, mid-, low-calibration, and drift checks on the Siemens 5-Gas analyzer during Day 1 on the GMV-4 engine PCC configuration.

5-Gas High Level; 8:50

Compund	Actual concentration (ppm)	5-Gas Measurement (ppm)	Difference (%)
Methane	958.8	957.9	-0.09

5-Gas Mid Level Methane Check; 8:50

Compound	Actual concentration (ppm)	5-Gas Measurement (ppm)	Difference (%)
Methane	504.4	502.2	-0.44

5-Gas Low Level Methane Check; 8:50

Compound	Actual concentration (ppm)	5-Gas Measurement (ppm)	Difference (%)
Methane	249.6	250.6	0.40

Drift Checks

Check	Time	5-Gas Measurement (ppm)	Difference (%)
End of day	16:50	499.7	-0.50

Figure A-18. High-, mid-, low-calibration, and drift checks on the Siemens 5-Gas analyzer during Day 2 on the GMV-4 engine PCC configuration.

5-Gas High Level; 8:55

Compund	Actual concentration (ppm)	5-Gas Measurement (ppm)	Difference (%)
Methane	958.8	960.6	0.19

5-Gas Mid Level Methane Check; 8:55

Compound	Actual concentration (ppm)	5-Gas Measurement (ppm)	Difference (%)
Methane	504.4	501.2	-0.63

5-Gas Low Level Methane Check; 8:55

Compound	Actual concentration (ppm)	5-Gas Measurement (ppm)	Difference (%)
Methane	249.6	250.0	0.16

Drift Checks

Check	Time	5-Gas Measurement (ppm)	Difference (%)
End of day	16:20	499.4	-0.36

Figure A-19. High-, mid-, low-calibration, and drift checks on the Siemens 5-Gas analyzer during Day 1 on the GMV-4 engine HPFI configuration.

5-Gas High Level; 10:00

Compund	Actual concentration (ppm)	5-Gas Measurement (ppm)	Difference (%)
Methane	958.8	957.1	-0.18

5-Gas Mid Level Methane Check; 10:0

Compound	Actual concentration (ppm)	5-Gas Measurement (ppm)	Difference (%)
Methane	504.4	506.0	0.32

5-Gas Low Level Methane Check; 10:00

Compound	Actual concentration (ppm)	5-Gas Measurement (ppm)	Difference (%)
Methane	249.6	251.5	0.76

Drift Checks

Check	Time	5-Gas Measurement (ppm)	Difference (%)
End of day	16:50	496.9	-1.80

Figure A-20. High-, mid-, low-calibration, and drift checks on the Siemens 5-Gas analyzer during Day 2 on the GMV-4 engine HPFI configuration.

5-Gas High Level; 8:20

Compund	Actual concentration (ppm)	5-Gas Measurement (ppm)	Difference (%)
Methane	958.8	950.5	-0.87

5-Gas Mid Level Methane Check; 8:20

Compound	Actual concentration (ppm)	5-Gas Measurement (ppm)	Difference (%)
Methane	504.4	499.1	-1.05

5-Gas Low Level Methane Check; 8:20

Compound	Actual concentration (ppm)	5-Gas Measurement (ppm)	Difference (%)
Methane	249.6	249.7	0.04

Drift Checks

Check	Time	5-Gas Measurement (ppm)	Difference (%)
End of day	17:05	494.2	-0.98

Figure A-21. High-, mid-, low-calibration, and drift checks on the Siemens 5-Gas analyzer during Day 3 on the GMV-4 engine HPFI configuration.

5-Gas High Level; 8:45

Compund	Actual concentration (ppm)	5-Gas Measurement (ppm)	Difference (%)
Methane	958.8	970.2	1.19

5-Gas Mid Level Methane Check; 8:45

Compound	Actual concentration (ppm)	5-Gas Measurement (ppm)	Difference (%)
Methane	504.4	505.5	0.22

5-Gas Low Level Methane Check; 8:45

Compound	Actual concentration (ppm)	5-Gas Measurement (ppm)	Difference (%)
Methane	249.6	252.1	1.00

Drift Checks

Check	Time	5-Gas Measurement (ppm)	Difference (%)
End of day	15:25	502.4	-0.61

Figure A-21. High-, mid-, low-calibration, and drift checks on the Siemens 5-Gas analyzer during Day 1 on the Caterpillar 3304 engine HPFI configuration.

Sample QA/QC for the VIG Model 210 FID following EPA Method 18/25a guidelines

Line	Date	Time	SpectrumFile	LibraryFile	Methane CH4	Unit	Compensation	Residual
GC Calibration Gas Results				***Actual Cal Gas Bottle Values ->***	***1007***			
0	2/14/2019	11:07:55		PRCI_VOCs_MH_11022019.LIB	915	ppm	wet	0.0127
0	2/14/2019	11:11:35		PRCI_VOCs_MH_11022019.LIB	916.2	ppm	wet	0.0127
VIG 50 PPM Gas Results				***Actual Cal Gas Bottle Values ->***	***50.0***	***ppm***		
0	2/14/2019	11:45:59		PRCI_VOCs_MH_11022019.LIB	49	ppm	wet	0.0002
VIG 84 PPM Gas Results				***Actual Cal Gas Bottle Values ->***	***83.8***	***ppm***		
0	2/14/2019	11:52:31		PRCI_VOCs_MH_11022019.LIB	84.4	ppm	wet	0.0009
VIG 25 PPM Gas Results				***Actual Cal Gas Bottle Values ->***	***25.0***	***ppm***		
0	2/14/2019	11:59:29		PRCI_VOCs_MH_11022019.LIB	24.9	ppm	wet	0.0001

Line	Formaldehyde CHOH	Unit	Compensation	Residual	Ethylene C2H4	Unit	Compensation	Residual	Propylene	Unit	Compensation	Residual
GC Calibration Gas Results	***0***				***50.23***				***20.12***			
0	0.1	ppm	wet	0.0001	49.9	ppm	wet	0.0004	51.71	ppm	wet	0.0205
0	0	ppm	wet	0.0001	49.3	ppm	wet	0.0006	18.98	ppm	wet	0.0004
VIG 50 PPM Gas Results												
0	0	ppm	wet	0.0001	0.1	ppm	wet	0.0004	0	ppm	wet	0.0005
VIG 84 PPM Gas Results												
0	0	ppm	wet	0.0001	0	ppm	wet	0.0002	1.18	ppm	wet	0.0005
VIG 25 PPM Gas Results												
0	0.1	ppm	wet	0.0001	0.1	ppm	wet	0.0001	0.04	ppm	wet	0.0003

Line	Sulfur hexafluoride	Unit	Compensation	Residual	Acetaldehyde	Unit	Compensation	Residual	Acetylene C2H2	Unit	Compensation	Residual
GC Calibration Gas Results	***0***				***0***				***0***			
0	0	ppm	wet	0.0006	0	ppm	wet	0.0006	0	ppm	wet	0.0003
0	0	ppm	wet	0.0005	0	ppm	wet	0.0006	0	ppm	wet	0.0002
VIG 50 PPM Gas Results												
0	0	ppm	wet	0.0005	0	ppm	wet	0.0001	0	ppm	wet	0.0001
VIG 84 PPM Gas Results												
0	0	ppm	wet	0.0006	0.1	ppm	wet	0.0002	0	ppm	wet	0.0001
VIG 25 PPM Gas Results												
0	0.01	ppm	wet	0.0005	0	ppm	wet	0.0001	0	ppm	wet	0.0002

Line	Ethane C2H6	Unit	Compensation	Residual	Propane C3H8	Unit	Compensation	Residual	Hexane C6H14	Unit	Compensation	Residual
GC Calibration Gas Results	***50.38***				***20.04***				***5.01***			
0	47.4	ppm	wet	0.0007	18.2	ppm	wet	0.0011	0	ppm	wet	0.011
0	45.6	ppm	wet	0.0007	23.8	ppm	wet	0.0009	0	ppm	wet	0.0038
VIG 50 PPM Gas Results	***50.0***	***ppm***			***50.0***	***ppm***						
0	48.4	ppm	wet	0.0001	49.1	ppm	wet	0.0002	0	ppm	wet	0.0003
VIG 84 PPM Gas Results	***84.3***	***ppm***			***84.4***	***ppm***						
0	82.5	ppm	wet	0.0003	86.9	ppm	wet	0.0005	0	ppm	wet	0.0009
VIG 25 PPM Gas Results	***25.0***	***ppm***			***24.9***	***ppm***						
0	24.7	ppm	wet	0.0001	26.1	ppm	wet	0.0001	0	ppm	wet	0.0001

Line	Nitrous oxide N2O	Unit	Compensation	Residual	Nitrogen dioxide NO2	Unit	Compensation	Residual	Nitrogen monoxide NO	Unit	Compensation	Residual
GC Calibration Gas Results	***0***				***0***							
0	0	ppm	wet	0.0001	5.2	ppm	wet	0.0007	0	ppm	wet	0.0001
0	0	ppm	wet	0.0001	0	ppm	wet	0.0007	0	ppm	wet	0.0002
VIG 50 PPM Gas Results												
0	0	ppm	wet	0.0001	1.6	ppm	wet	0.0001	0	ppm	wet	0.0001
VIG 84 PPM Gas Results												
0	0	ppm	wet	0.0001	2.1	ppm	wet	0.0002	0	ppm	wet	0.0001
VIG 25 PPM Gas Results												
0	0	ppm	wet	0.0001	1	ppm	wet	0.0001	0	ppm	wet	0.0001

Line	Carbon monoxide CO	Unit	Compensation	Residual	Ammonia NH3	Unit	Compensation	Residual	Sulfur dioxide SO2	Unit	Compensation	Residual
GC Calibration Gas Results	***0***				***0***							
0	0.5	ppm	wet	0.0001	0.1	ppm	wet	0.0004	0.2	ppm	wet	0.0033
0	0	ppm	wet	0.0001	0	ppm	wet	0.0004	1.4	ppm	wet	0.0035
VIG 50 PPM Gas Results												
0	0	ppm	wet	0.0001	0	ppm	wet	0.0001	0.2	ppm	wet	0.0001
VIG 84 PPM Gas Results												
0	0	ppm	wet	0.0001	0	ppm	wet	0.0001	0.3	ppm	wet	0.0002
VIG 25 PPM Gas Results												
0	0	ppm	wet	0.0002	0.1	ppm	wet	0.0002	0.1	ppm	wet	0.0001

Line	Carbon dioxide CO2	Unit	Compensation	Residual	Water vapor H2O	Unit	Compensation	Residual	Methanol	Unit	Compensation	Residual
GC Calibration Gas Results	***0***				***0***							
0	0	vol-%	wet	0.0001	0	vol-%	wet	0.0002	0	ppm	wet	0.0004
0	0	vol-%	wet	0.0001	0	vol-%	wet	0.0001	0	ppm	wet	0.0004
VIG 50 PPM Gas Results												
0	0	vol-%	wet	0.0001	0	vol-%	wet	0.0001	0	ppm	wet	0.0002
VIG 84 PPM Gas Results												
0	0	vol-%	wet	0.0001	0	vol-%	wet	0.0001	0	ppm	wet	0.0002
VIG 25 PPM Gas Results												
0	0	vol-%	wet	0.0001	0	vol-%	wet	0.0002	0.07	ppm	wet	0.0002

Line	Butane C4H10	Unit	Compensation	Residual	Isobutane C4H10	Unit	Compensation	Residual	Isopentane	Unit	Compensation	Residual
GC Calibration Gas Results	***4.96***				***4.99***				***4.8***			
0	0	ppm	wet	0.0058	5.54	ppm	wet	0.0008	4.23	ppm	wet	0.001
0	0	ppm	wet	0.0196	5.43	ppm	wet	0.0006	0.61	ppm	wet	0.001
VIG 50 PPM Gas Results												
0	0	ppm	wet	0.0023	0	ppm	wet	0.0003	0	ppm	wet	0.0009
VIG 84 PPM Gas Results												
0	0	ppm	wet	0.0077	0.21	ppm	wet	0.0003	0	ppm	wet	0.0058
VIG 25 PPM Gas Results												
0	0.12	ppm	wet	0.0001	0	ppm	wet	0.0001	0	ppm	wet	0.0011

Line	Isohexane C6H14	Unit	Compensation	Residual	Pentane C5H12	Unit	Compensation	Residual	Status
GC Calibration Gas Results	***5.29***				***5.04***				
0	1.9	ppm	wet	0.0008	17.91	ppm	wet	0.0009	Error
0	3.78	ppm	wet	0.0006	17.22	ppm	wet	0.0008	OK
VIG 50 PPM Gas Results									
0	0	ppm	wet	0.0004	0.02	ppm	wet	0.0001	OK
VIG 84 PPM Gas Results									
0	0	ppm	wet	0.0005	0.05	ppm	wet	0.0004	OK
VIG 25 PPM Gas Results									
0	0	ppm	wet	0.0004	0.57	ppm	wet	0.0001	OK

Measurement	Value	Units	Closest Spectra	Units
Average Exhaust SF6	0.119	ppm		
Average Exhaust Form	15.97667	ppm		
MKS Direct SF6	9.48	ppm	?	
MKS Direct Form	562.2	ppm	500	ppm
Gasmet Direct SF6	10.05182	ppm	10	ppm
Gasmet Direct Form	1129.836	ppm	45	ppm
Average Spike SF6	0.975	ppm		
Average Spike Form	65.61	ppm		
Calculation Using Only Gasmet				
DF (Dilution Factor)	0.096997			
CS (Expected Concentration)	124.0181	ppm		
Error	52.90%			
Calculation Using MKS Direct Values				
DF (Dilution Factor)	0.102848			
CS (Expected Concentration)	68.9589	ppm		
Error	95.14%			

Figure A-22. QA/QC spike check performed for the Gasmet FTIR and MKS FTIR before the GMV-4 OC ignition configuration.

Measurement	Value	Units	Closest Spectra	Units
Average Exhaust SF6	0.119	ppm		
Average Exhaust Form	15.97667	ppm		
MKS Direct SF6	9.48	ppm	?	
MKS Direct Form	562.2	ppm	500	ppm
Gasmet Direct SF6	10.05182	ppm	10	ppm
Gasmet Direct Form	1129.836	ppm	45	ppm
Average Spike SF6	0.975	ppm		
Average Spike Form	65.61	ppm		
Calculation Using Only Gasmet				
DF (Dilution Factor)	0.096997			
CS (Expected Concentration)	124.0181	ppm		
Error	52.90%			
Calculation Using MKS Direct Values				
DF (Dilution Factor)	0.102848			
CS (Expected Concentration)	68.9589	ppm		
Error	4.86%			
Measurement	**Value**	**Units**	**Closest Spectra**	**Units**
Average Exhaust SF6	0.24	ppm		
Average Exhaust Form	10	ppm		
MKS Direct SF6	9.947	ppm	?	
MKS Direct Form	873.1	ppm	500	ppm
Gasmet Direct SF6	9.6	ppm	10	ppm
Gasmet Direct Form	2878	ppm	45	ppm
Average Spike SF6	0.97	ppm		
Average Spike Form	130	ppm		
Calculation Using Only Gasmet				
DF (Dilution Factor)	0.101042			
CS (Expected Concentration)	299.7875	ppm		
Error	56.64%			

Calculation Using MKS Direct Values		
DF (Dilution Factor)	0.101042	
CS (Expected Concentration)	97.20906	ppm
Error	-33.73%	

Figure A-23. QA/QC spike check performed for the Gasmet FTIR and MKS FTIR before the GMV-4 PCC ignition configuration.

APPENDIX B: ANALYZER/METHOD COMPARISON

Analyzer/Method Comparison Plots for Individual and Total VOC Measurements

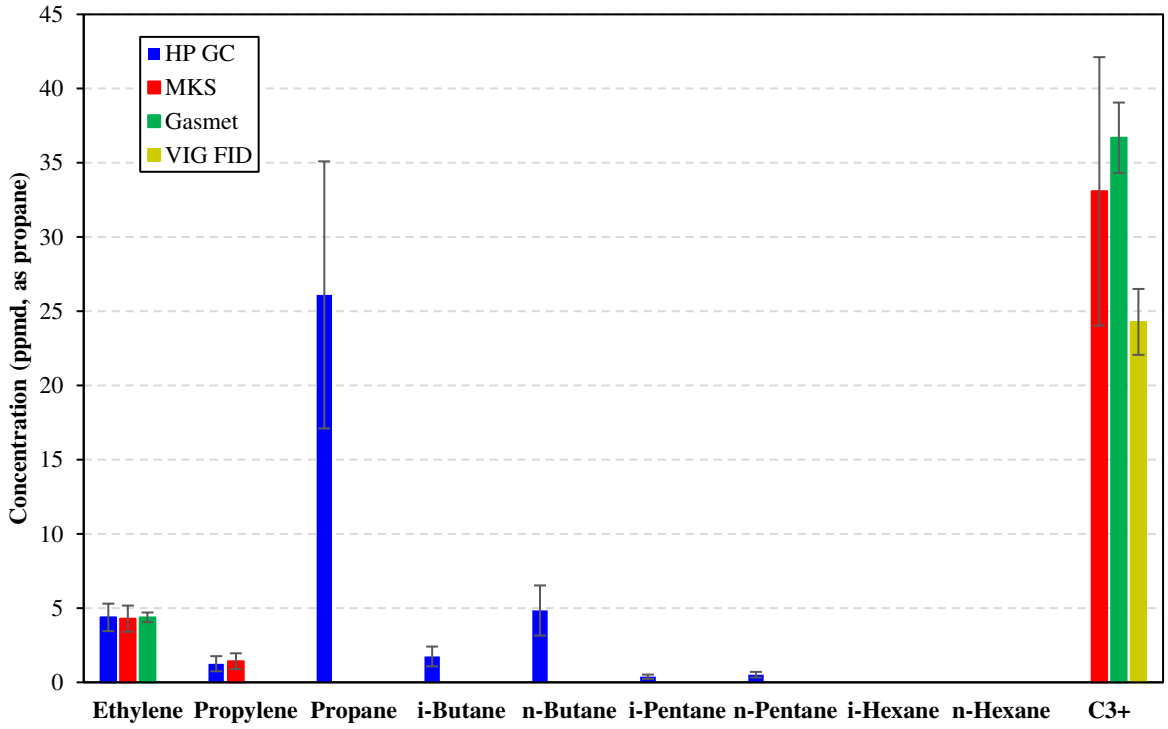

Figure B-1. Individual VOC concentrations reported from each analyzer during Data Point 2 for the GMV-4 lean burn open chamber configuration. NO_X was 10.6 g/bhp-hr and TER was 0.56.

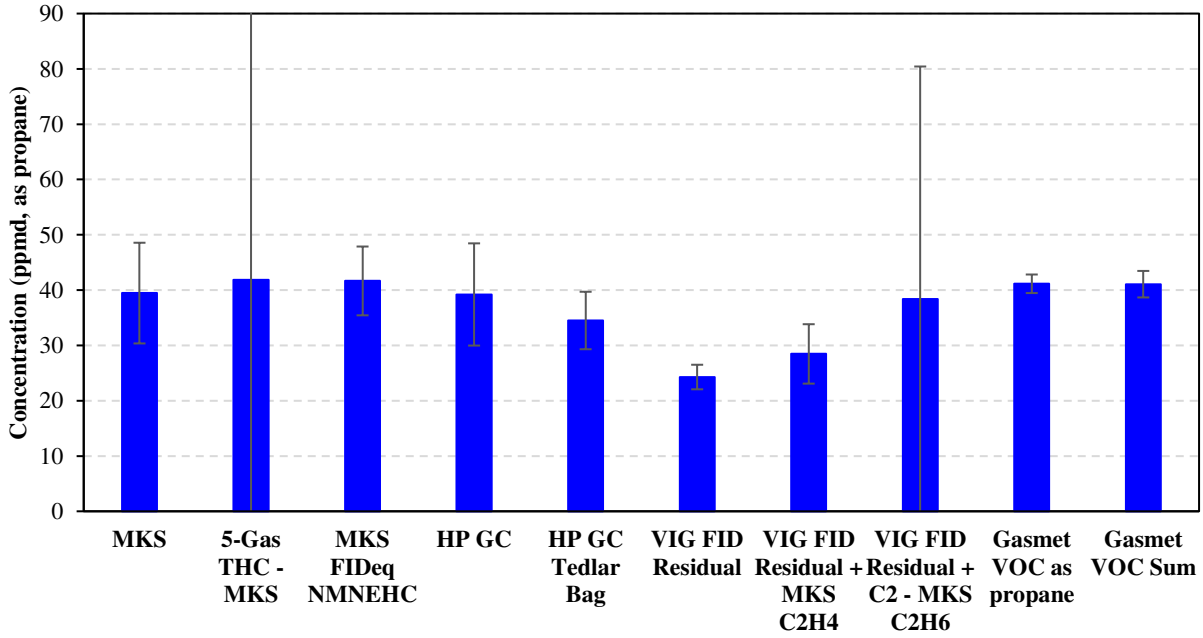

Figure B-2. Total VOC concentrations reported using different analyzers/methods for Data Point 2. Note that the uncertainty for "5-Gas THC – MKS" is ±176.6 ppmd, as propane.

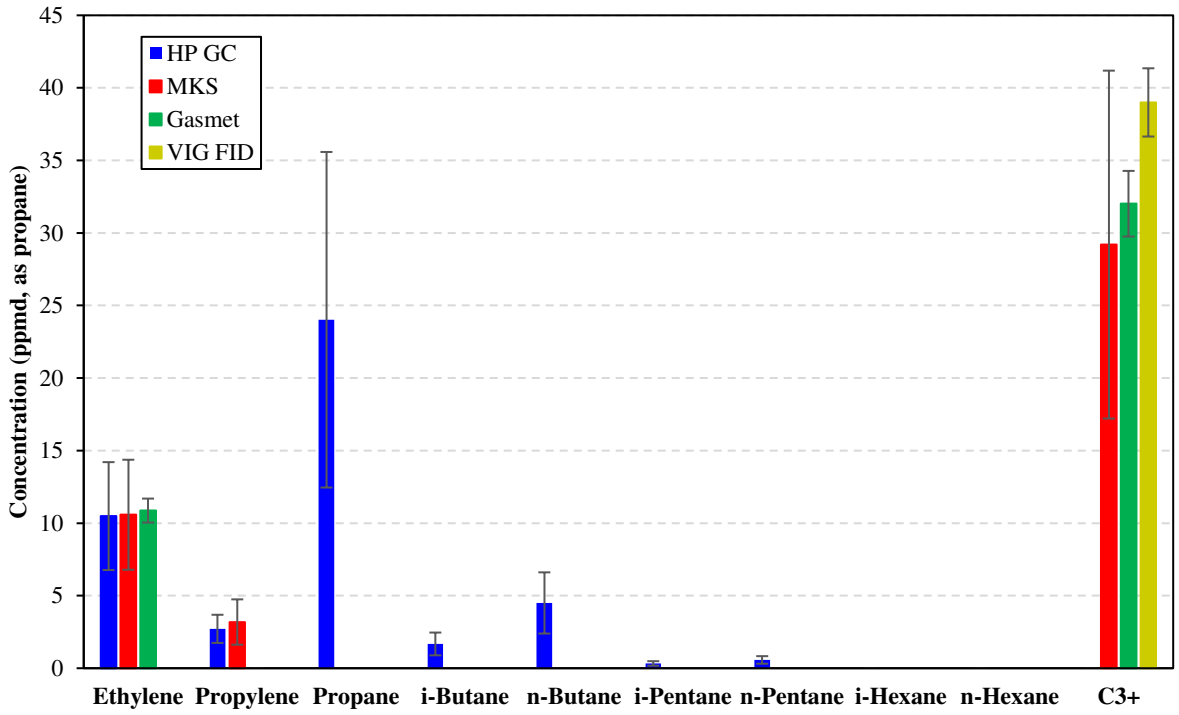

Figure B-3. Individual VOC concentrations reported from each analyzer during Data Point 3 for the GMV-4 lean burn open chamber configuration. NO_X was 9.77 g/bhp-hr and TER was 0.60.

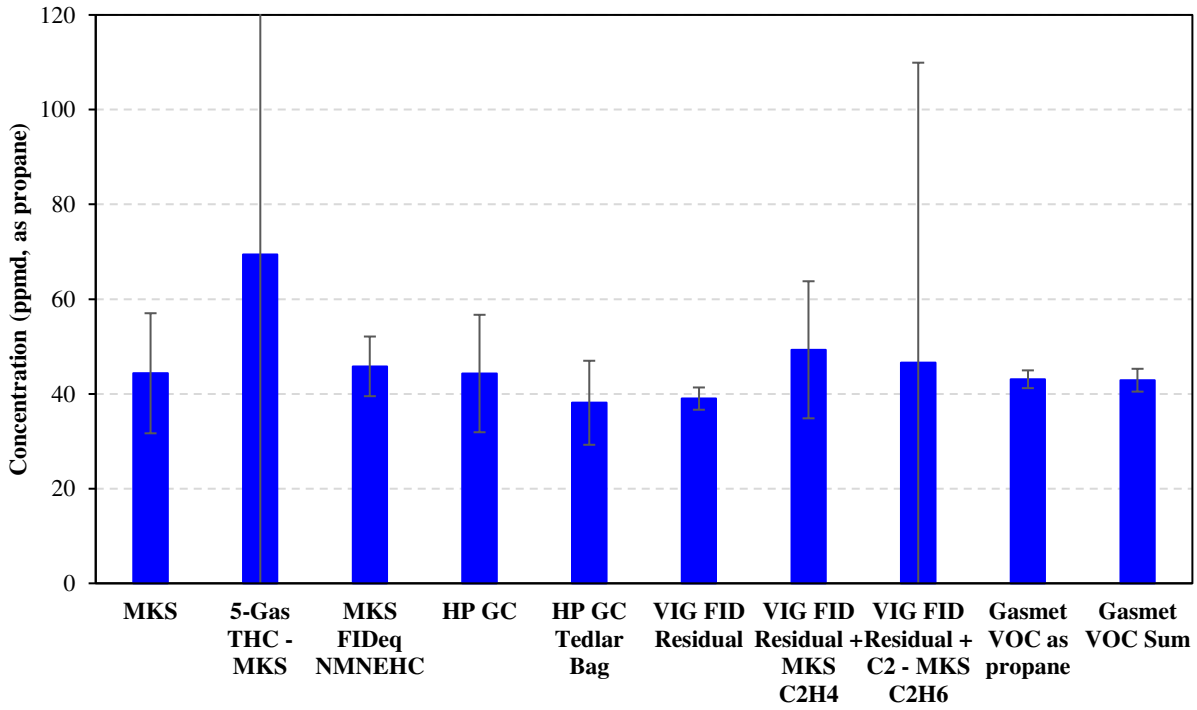

Figure B-4. Total VOC concentrations reported using different analyzers/methods for Data Point 3. Note that the uncertainty for "5-Gas THC – MKS" is ±234.6 ppmd, as propane.

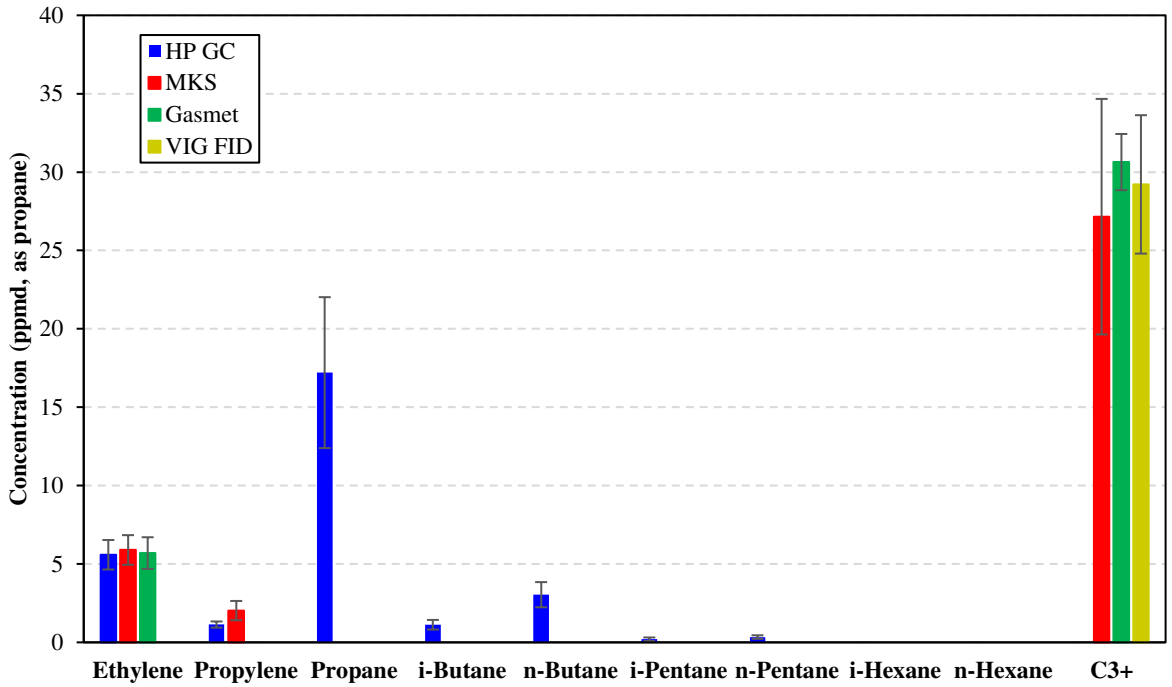

Figure B-5. Individual VOC concentrations reported from each analyzer during Data Point 4 for the GMV-4 lean burn open chamber configuration. NO_X was 6.68 g/bhp-hr and TER was 0.55.

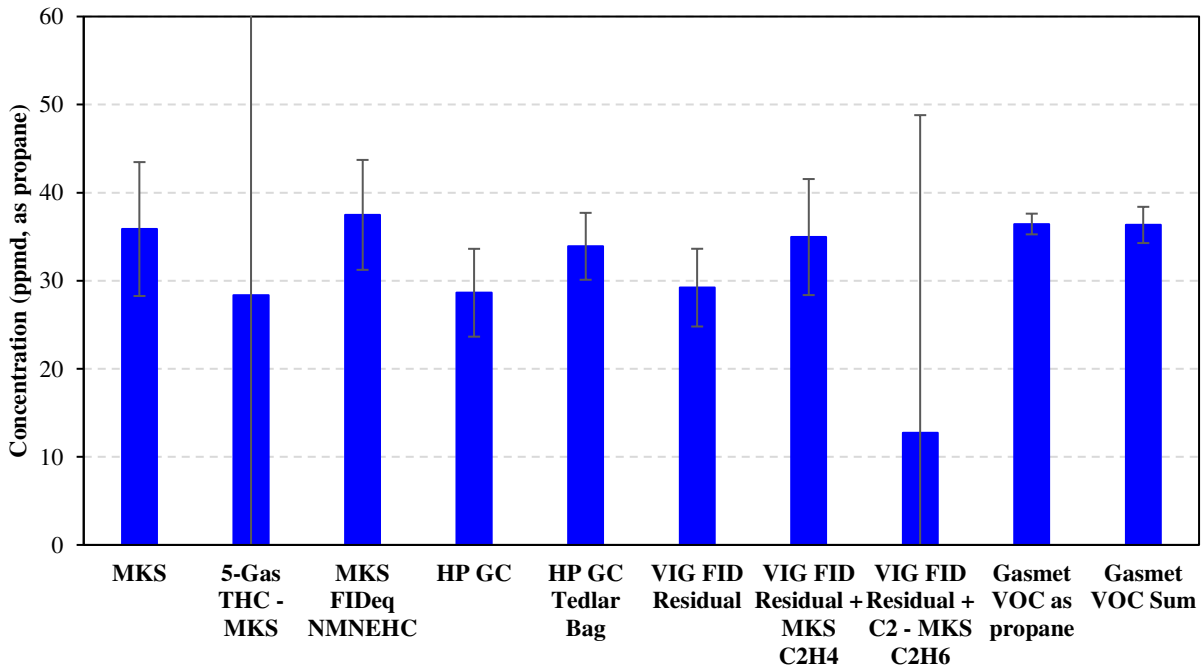

Figure B-6. Total VOC concentrations reported using different analyzers/methods for Data Point 4. Note that the uncertainty for "5-Gas THC – MKS" is ±179.5 ppmd, as propane.

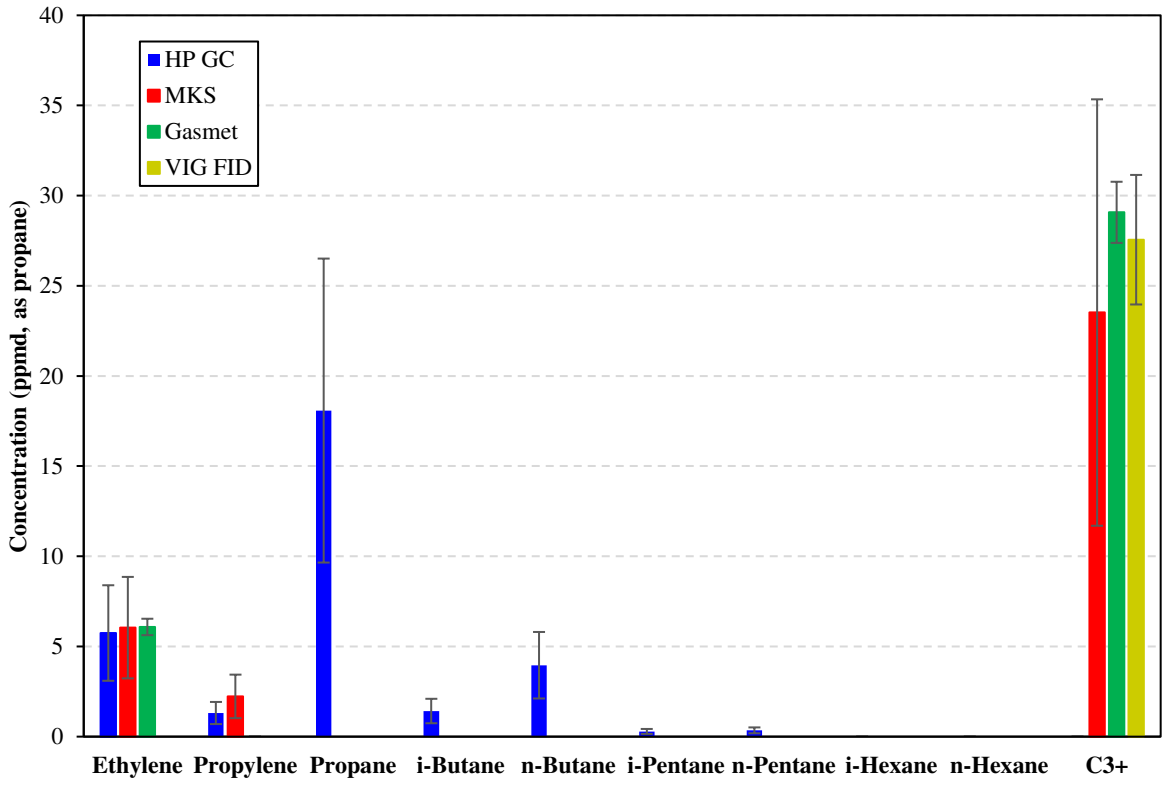

Figure B-7. Individual VOC concentrations reported from each analyzer during Data Point 6 for the GMV-4 lean burn open chamber configuration. NO_X was 14.0 g/bhp-hr and TER was 0.59.

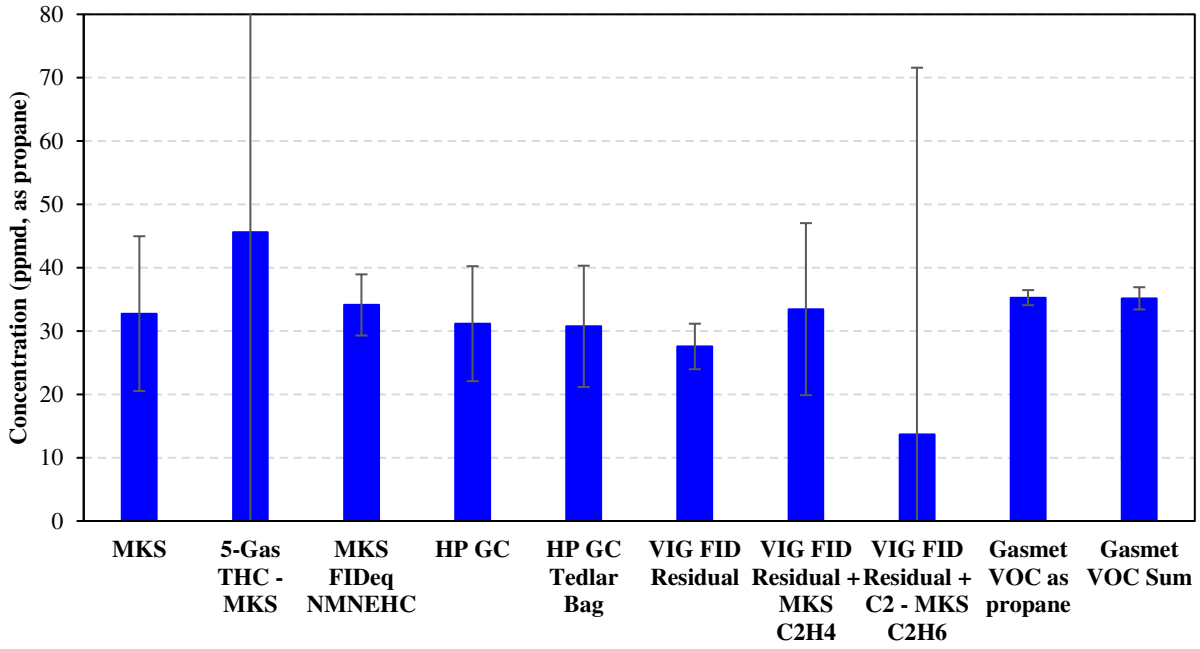

Figure B-8. Total VOC concentrations reported using different analyzers/methods for Data Point 6. Note that the uncertainty for "5-Gas THC – MKS" is ±321.6 ppmd, as propane.

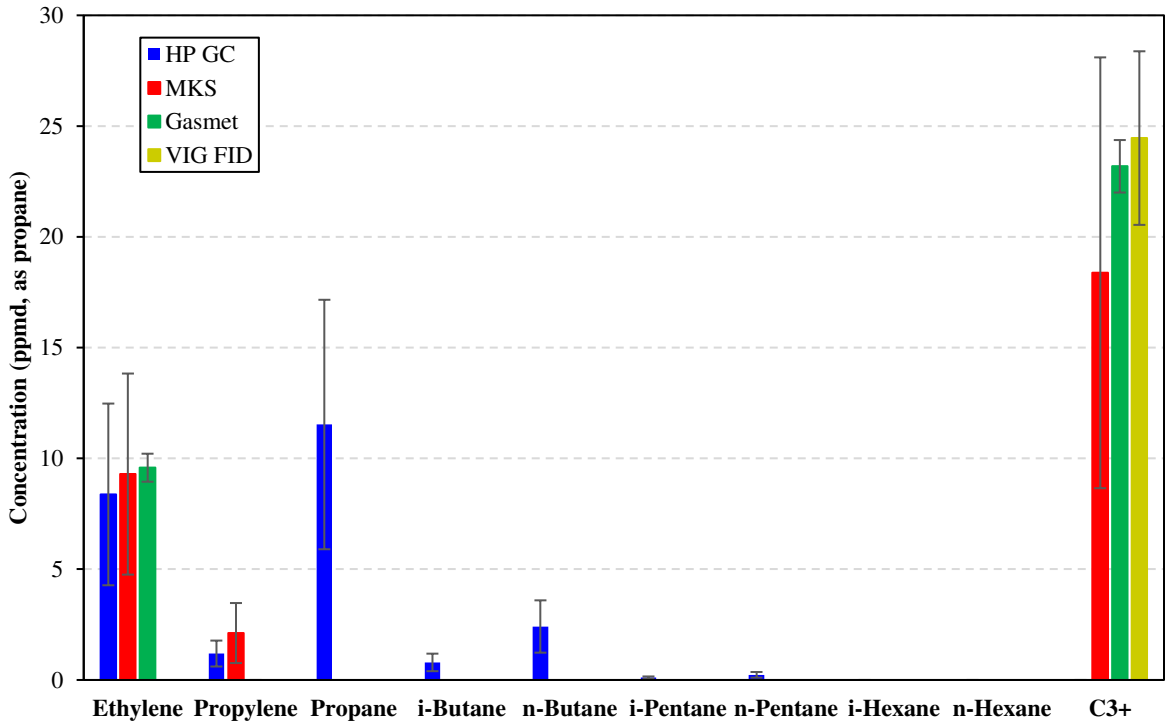

Figure B-9. Individual VOC concentrations reported from each analyzer during Data Point 8 for the GMV-4 lean burn open chamber configuration. NO_X was 12.4 g/bhp-hr and TER was 0.58.

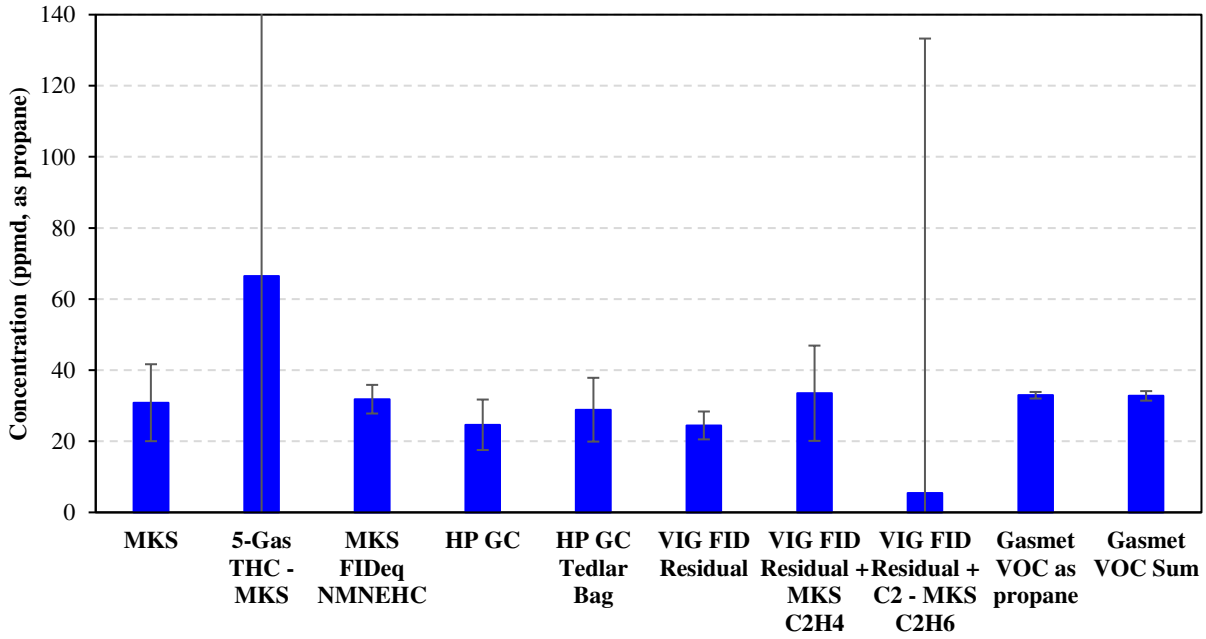

Figure B-10. Total VOC concentrations reported using different analyzers/methods for Data Point 8. Note that the uncertainty for "5-Gas THC – MKS" is ±280.6 ppmd, as propane.

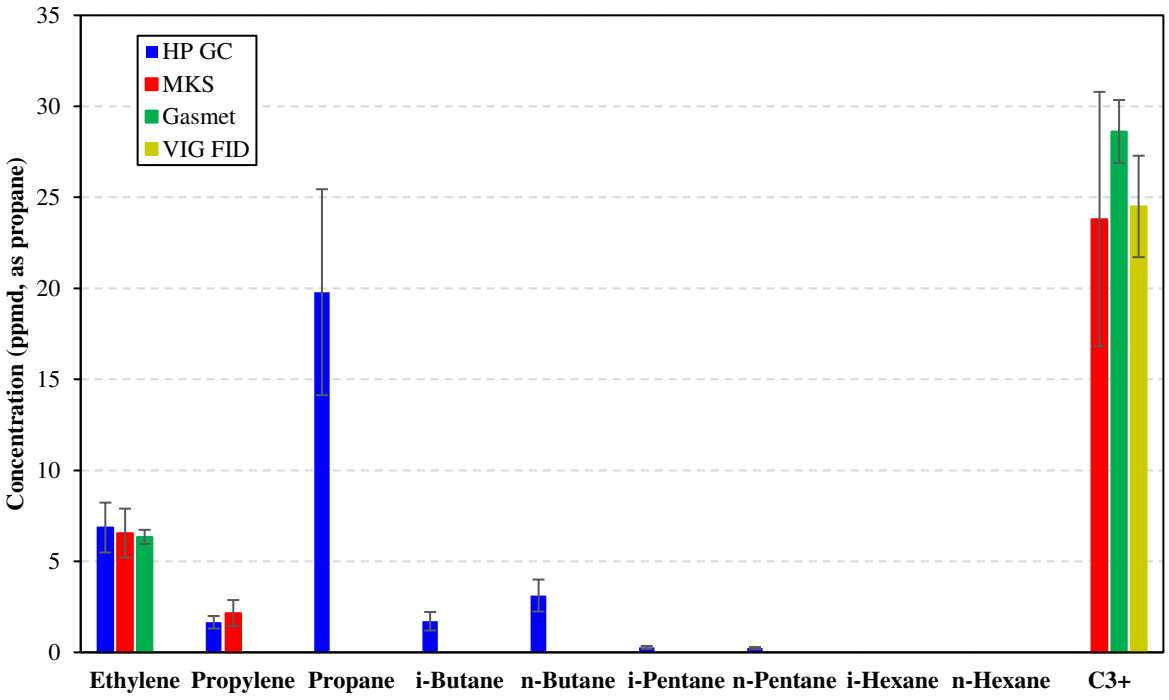

Figure B-11. Individual VOC concentrations reported from each analyzer during Data Point 11 for the GMV-4 lean burn open chamber configuration. NO_X was 10.7 g/bhp-hr and TER was 0.60.

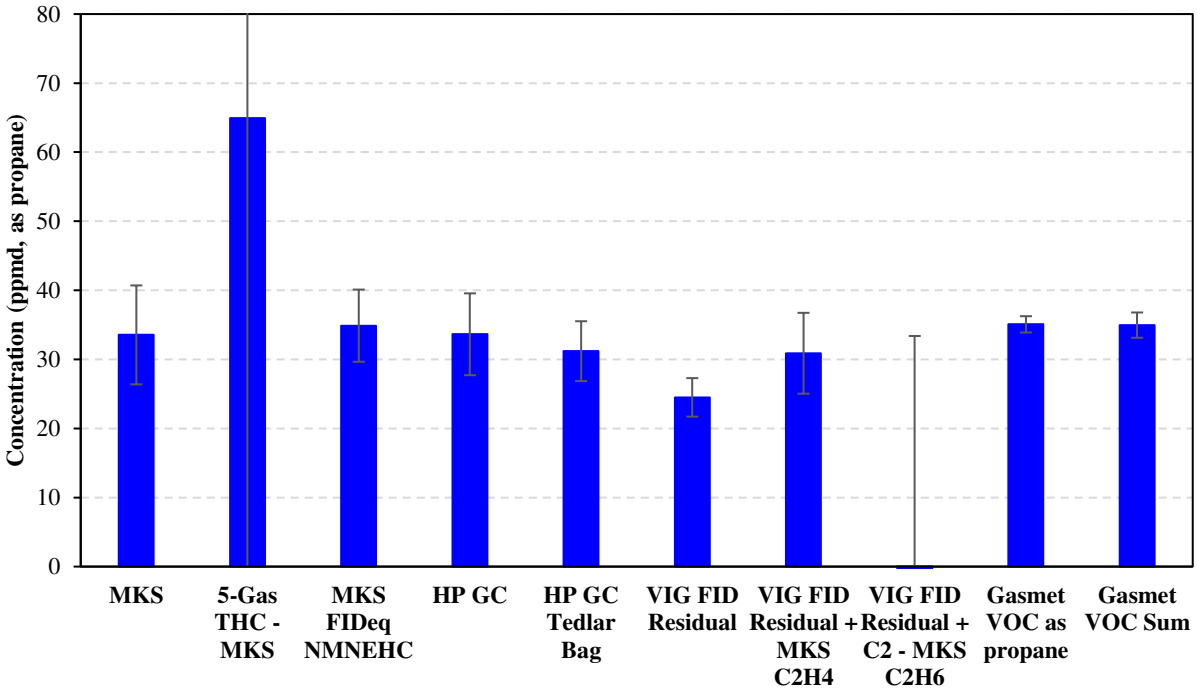

Figure B-12. Total VOC concentrations reported using different analyzers/methods for Data Point 11. Note that the uncertainty for "5-Gas THC – MKS" is ±172.0 ppmd, as propane.

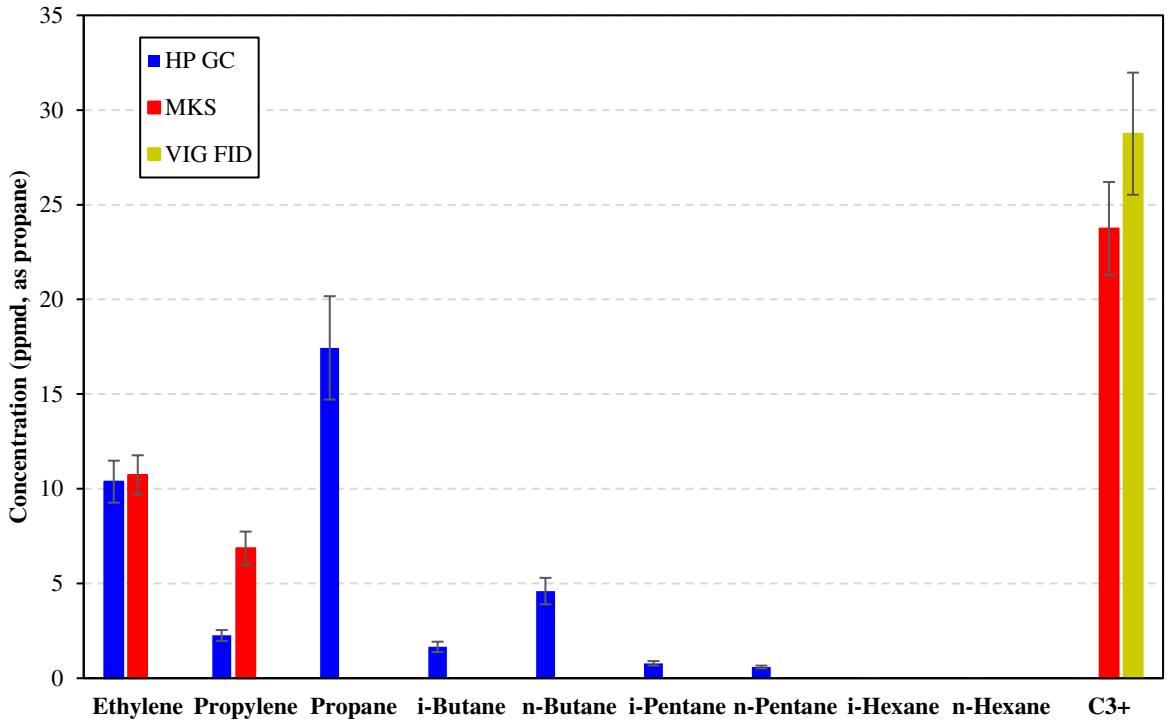

Figure B-13. Individual VOC concentrations reported from each analyzer during Data Point 14 for the GMV-4 lean burn PCC configuration. NO_X was 1.55 g/bhp-hr and TER was 0.52.

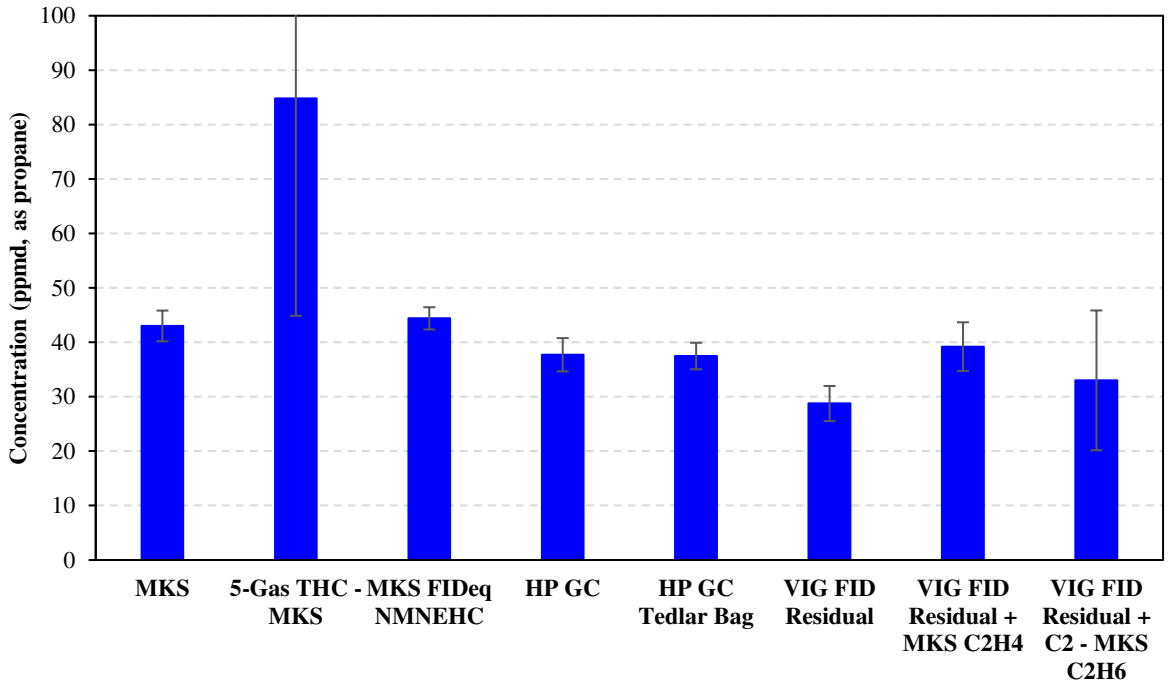

Figure B-14. Total VOC concentrations reported using different analyzers/methods for Data Point 14. Note that the uncertainty for "5-Gas THC – MKS" is ±39.9 ppmd, as propane.

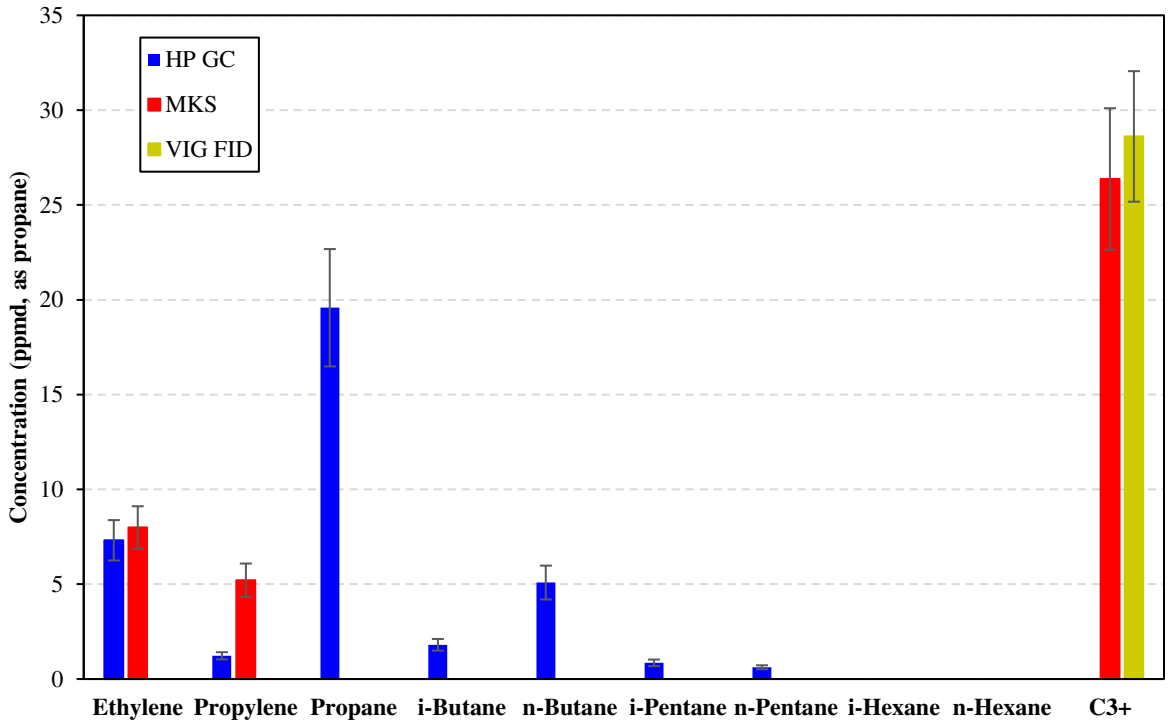

Figure B-15. Individual VOC concentrations reported from each analyzer during Data Point 17 for the GMV-4 lean burn PCC configuration. NO_X was 1.09 g/bhp-hr and TER was 0.48.

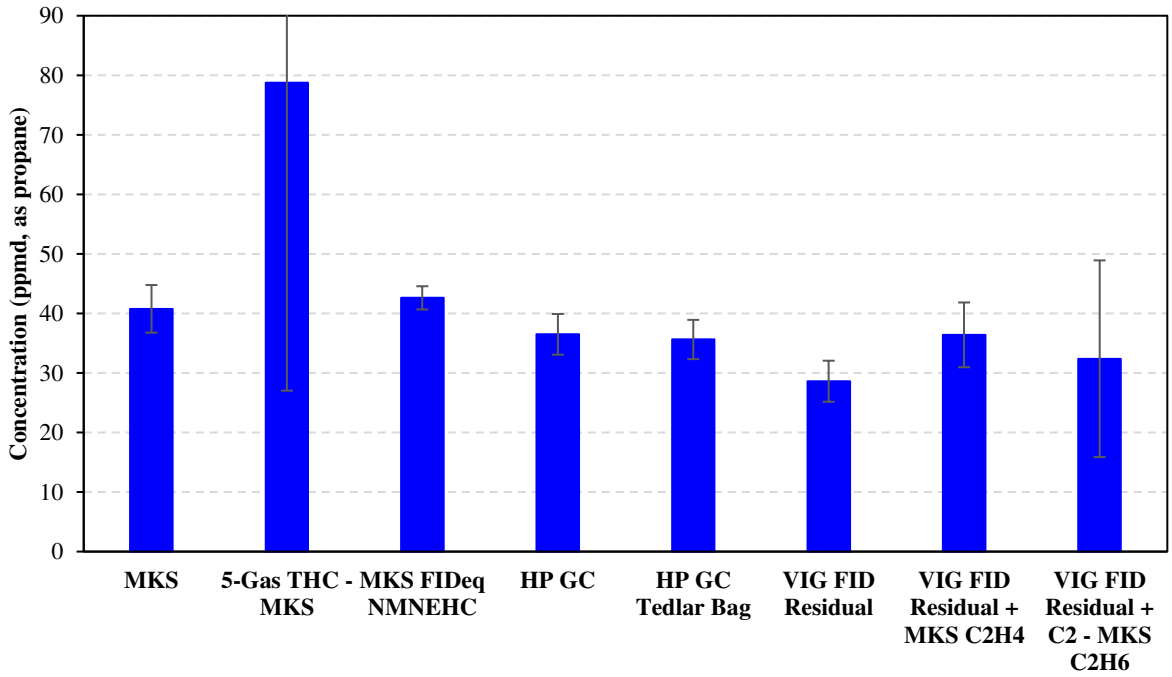

Figure B-16. Total VOC concentrations reported using different analyzers/methods for Data Point 17. Note that the uncertainty for "5-Gas THC – MKS" is ±51.7 ppmd, as propane.

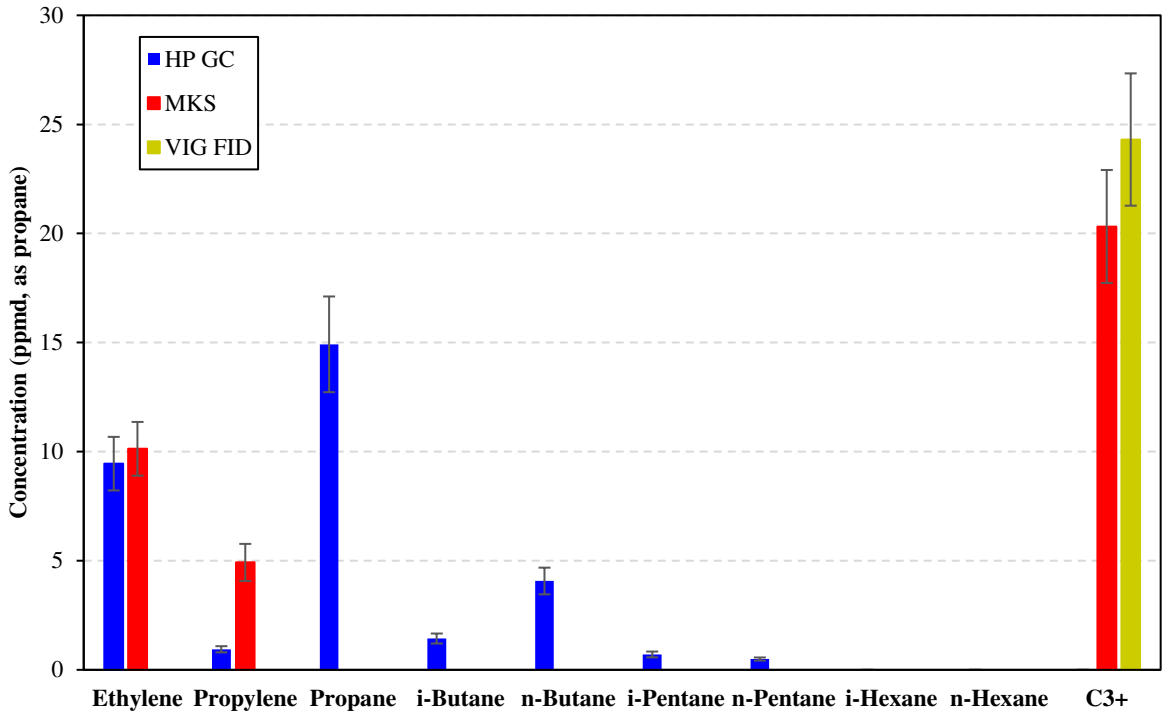

Figure B-17. Individual VOC concentrations reported from each analyzer during Data Point 18/19 and TER was 0.47.

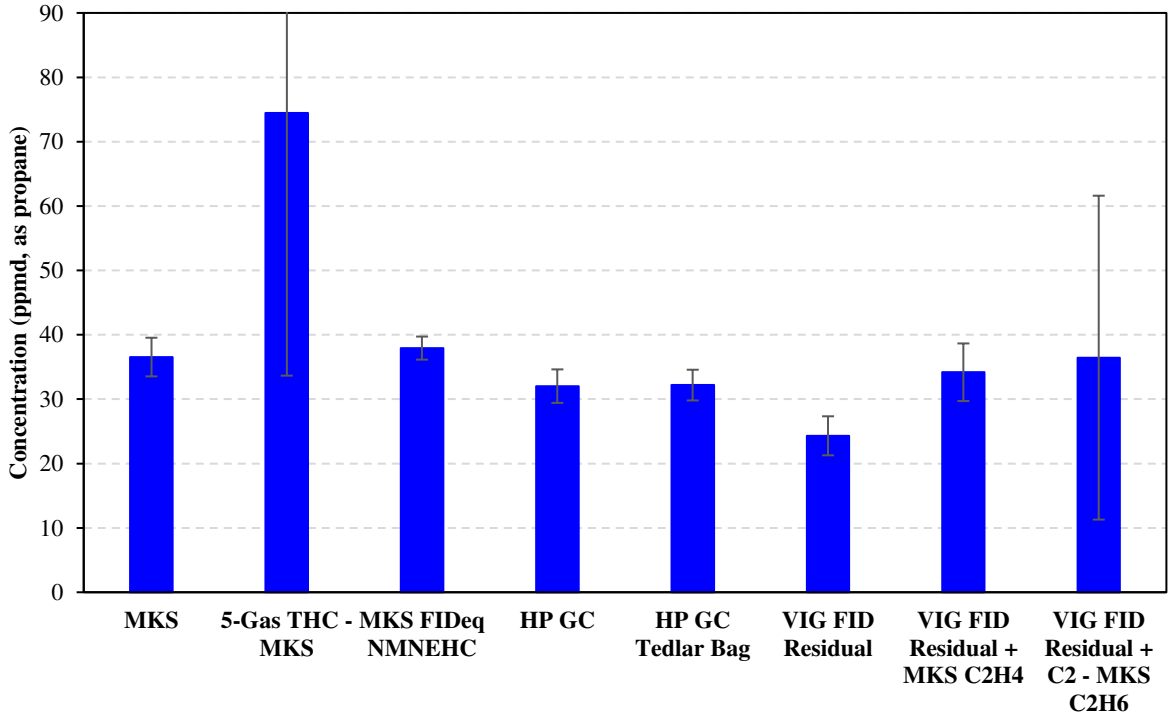

Figure B-18. Total VOC concentrations reported using different analyzers/methods for Data Point 18/19. Note that the uncertainty for "5-Gas THC – MKS" is ±40.8 ppmd, as propane.

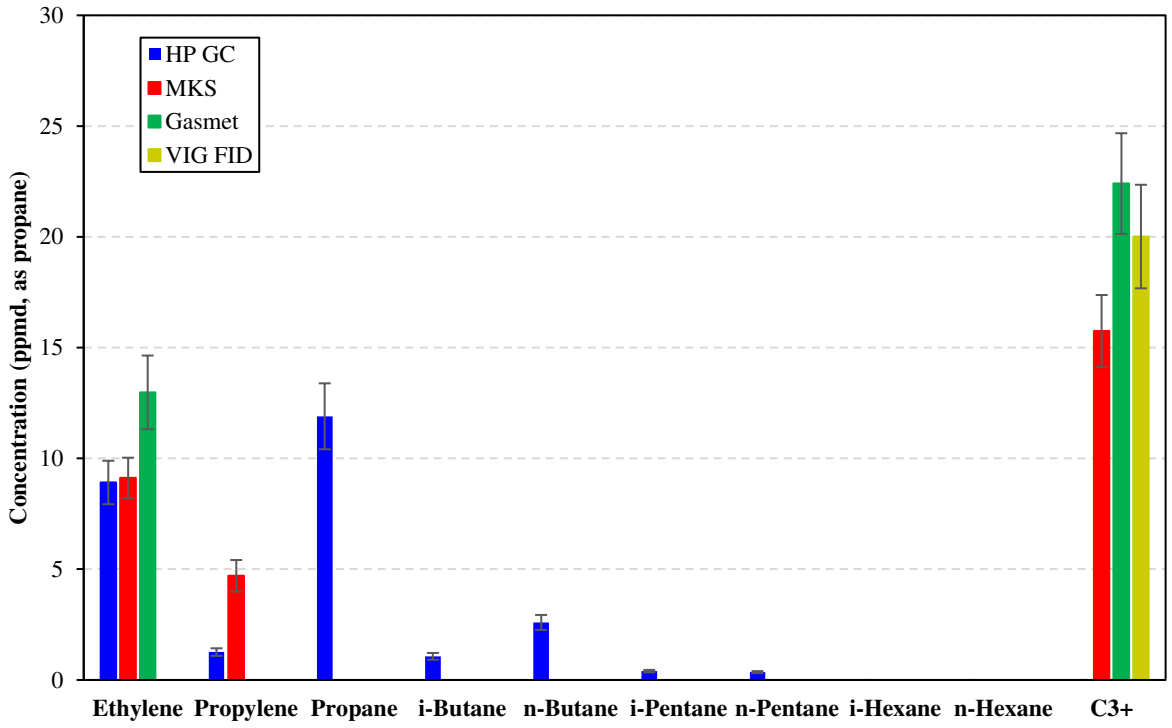

Figure B-19. Individual VOC concentrations reported from each analyzer during Data Point 23 for the GMV-4 lean burn HPFI PCC ignition configuration. NO_X was 0.36 g/bhp-hr and TER was 0.46.

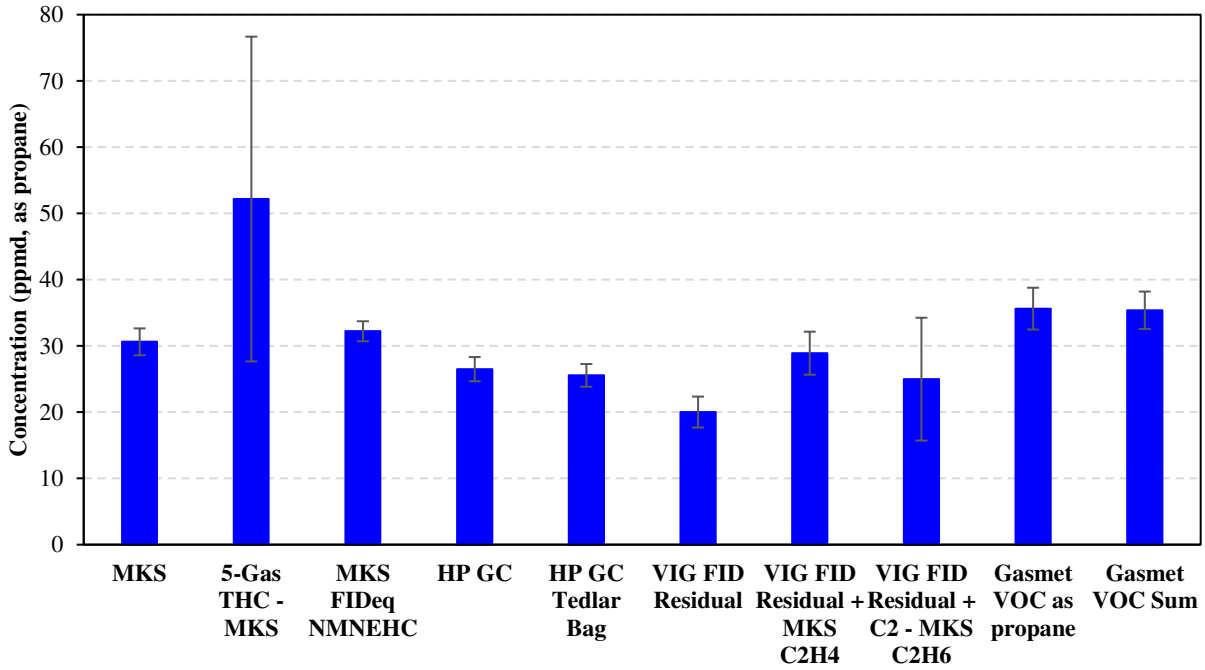

Figure B-20. Total VOC concentrations reported using different analyzers/methods for Data Point 23.

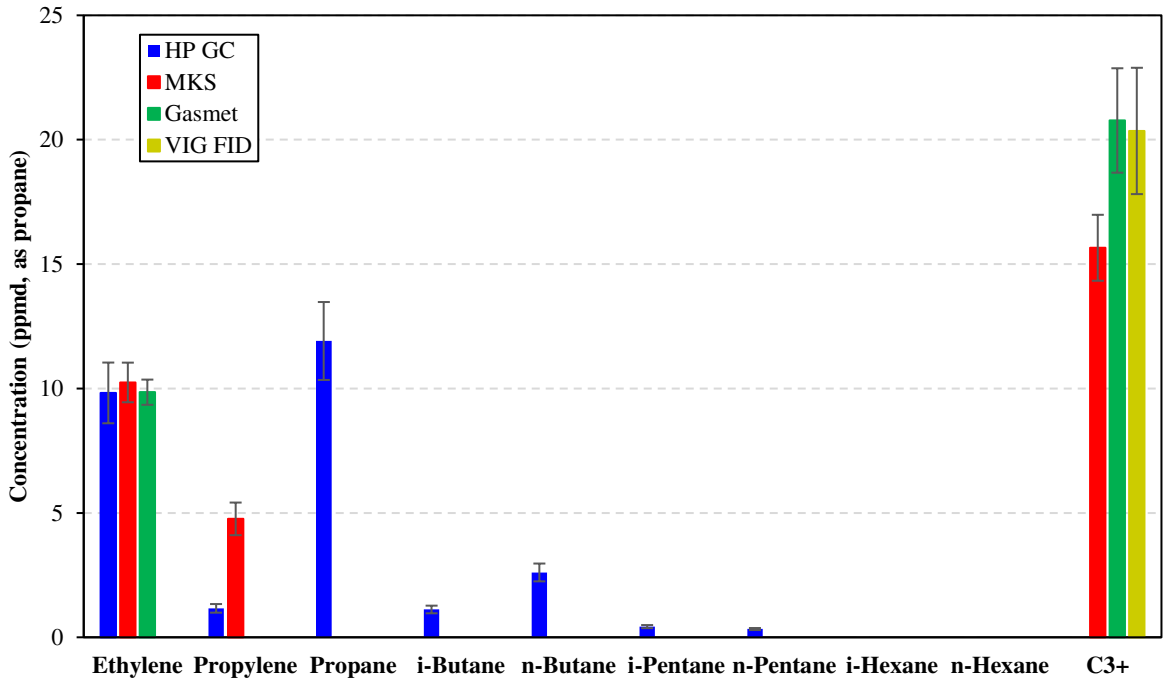

Figure B-21. Individual VOC concentrations reported from each analyzer during Data Point 24 for the GMV-4 lean burn HPFI PCC ignition configuration. NO_X was 0.50 g/bhp-hr and TER was 0.44.

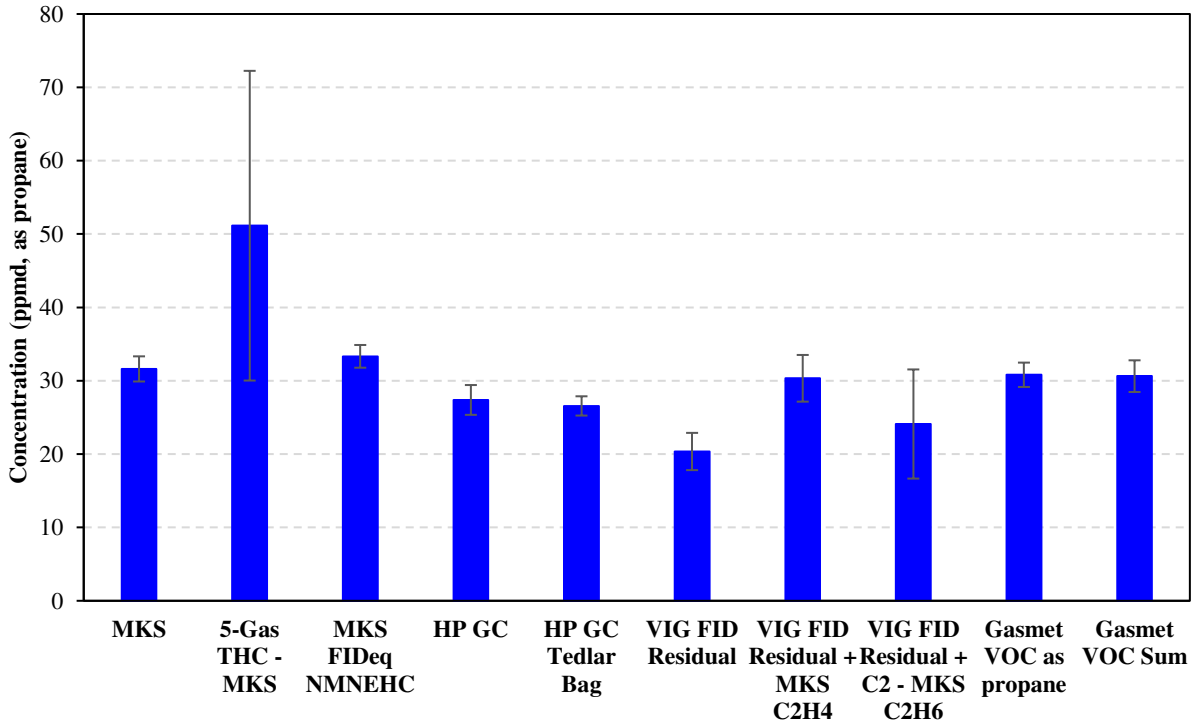

Figure B-22. Total VOC concentrations reported using different analyzers/methods for Data Point 24.

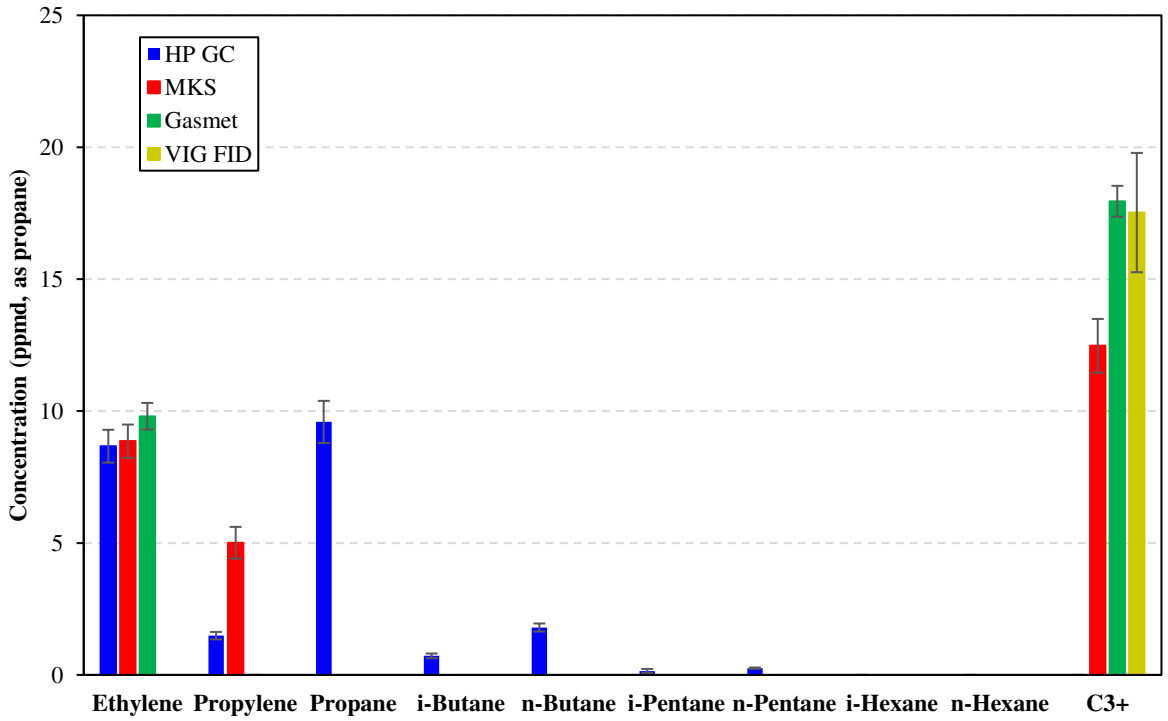

Figure B-23. Individual VOC concentrations reported from each analyzer during Data Point 25 for the GMV-4 lean burn HPFI PCC ignition configuration. NO_X was 0.79 g/bhp-hr and TER was 0.46.

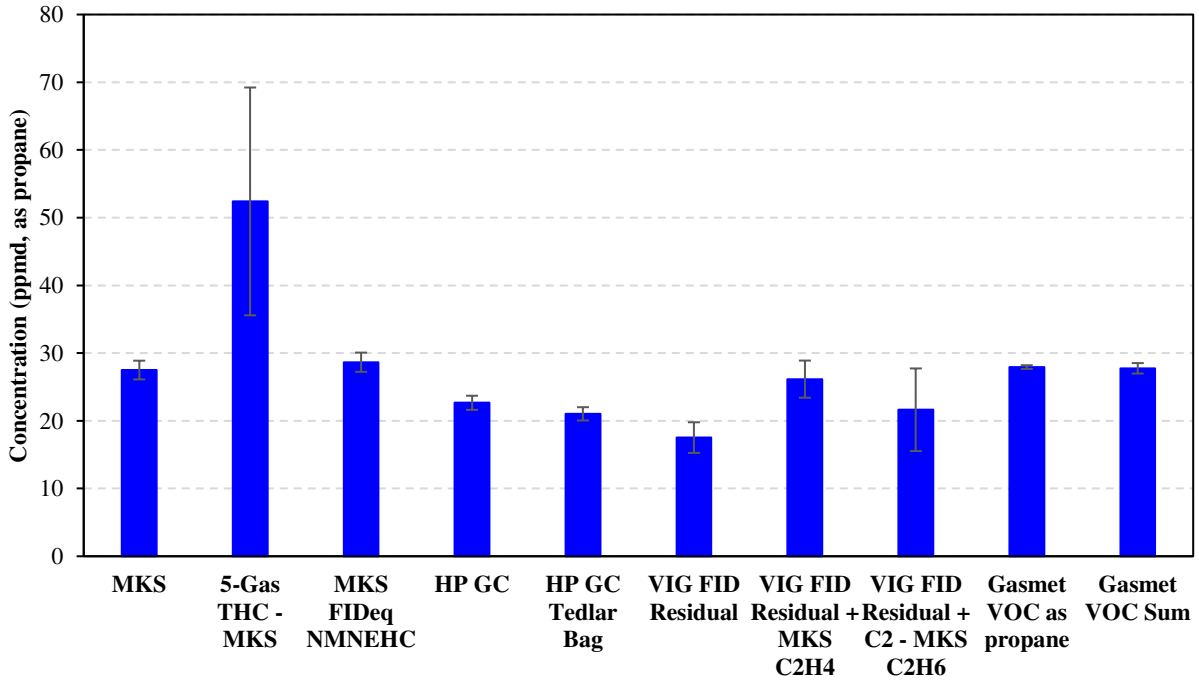

Figure B-24. Total VOC concentrations reported using different analyzers/methods for Data Point 25.

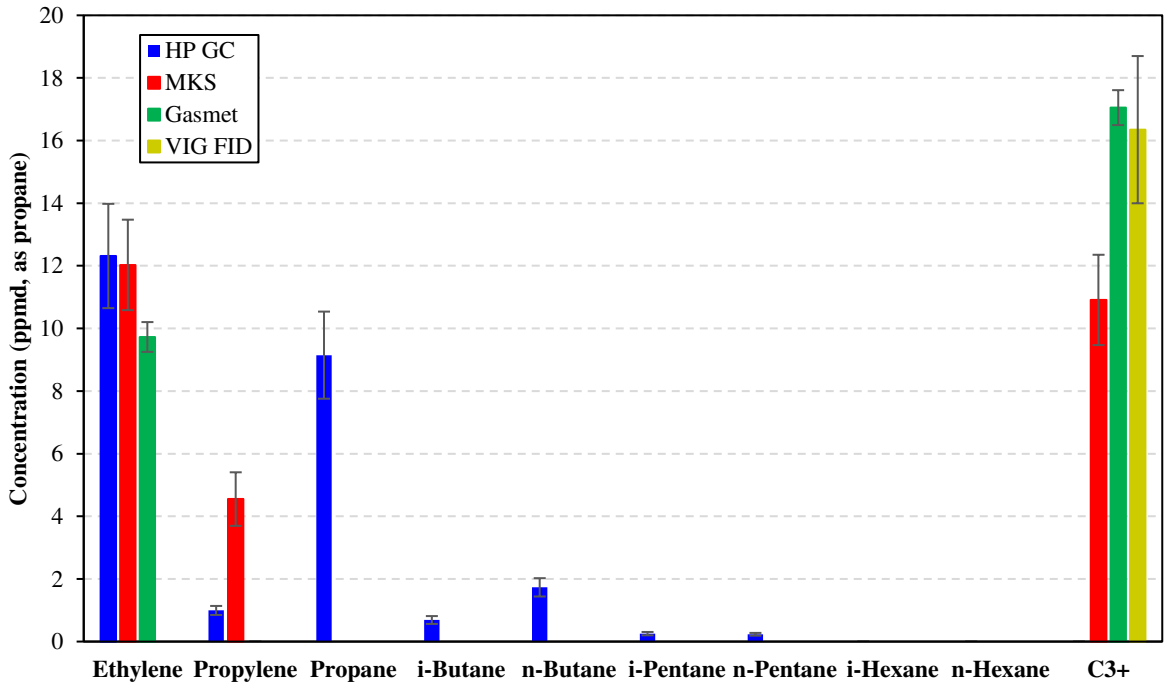

Figure B-25. Individual VOC concentrations reported from each analyzer during Data Point 28/29 for the GMV-4 lean burn HPFI PCC ignition configuration. NO_X was 0.38 g/bhp-hr and TER was 0.42.

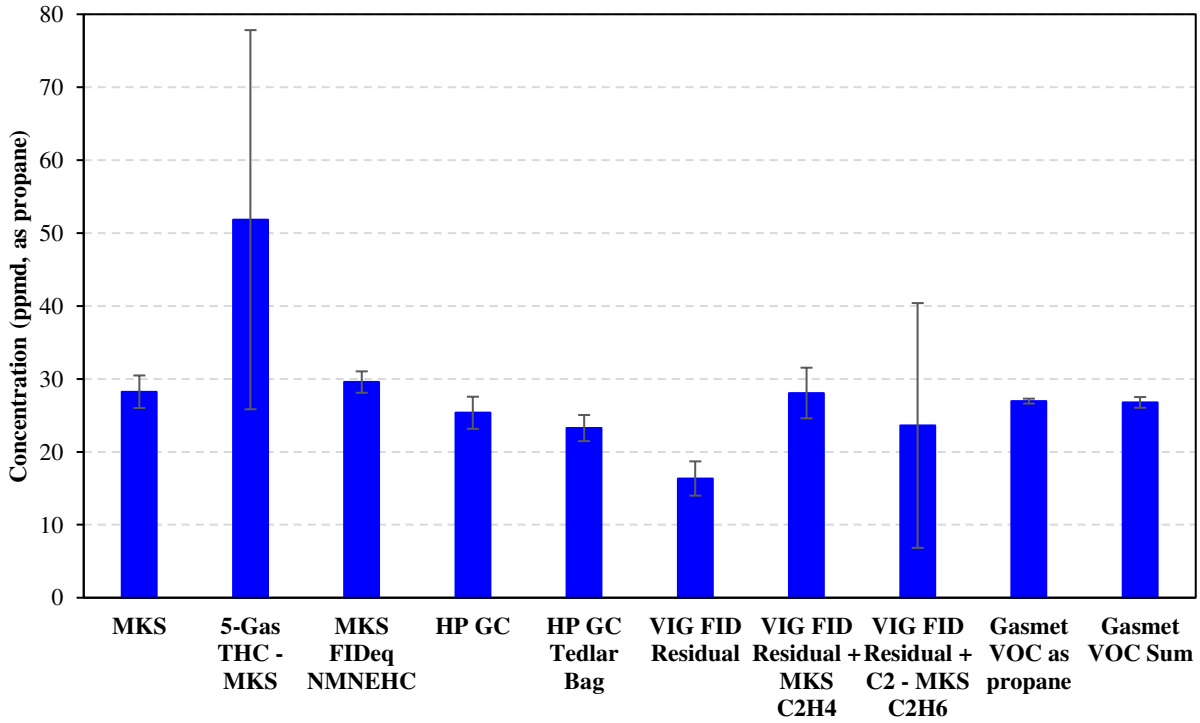

Figure B-26. Total VOC concentrations reported using different analyzers/methods for Data Point 28/29.

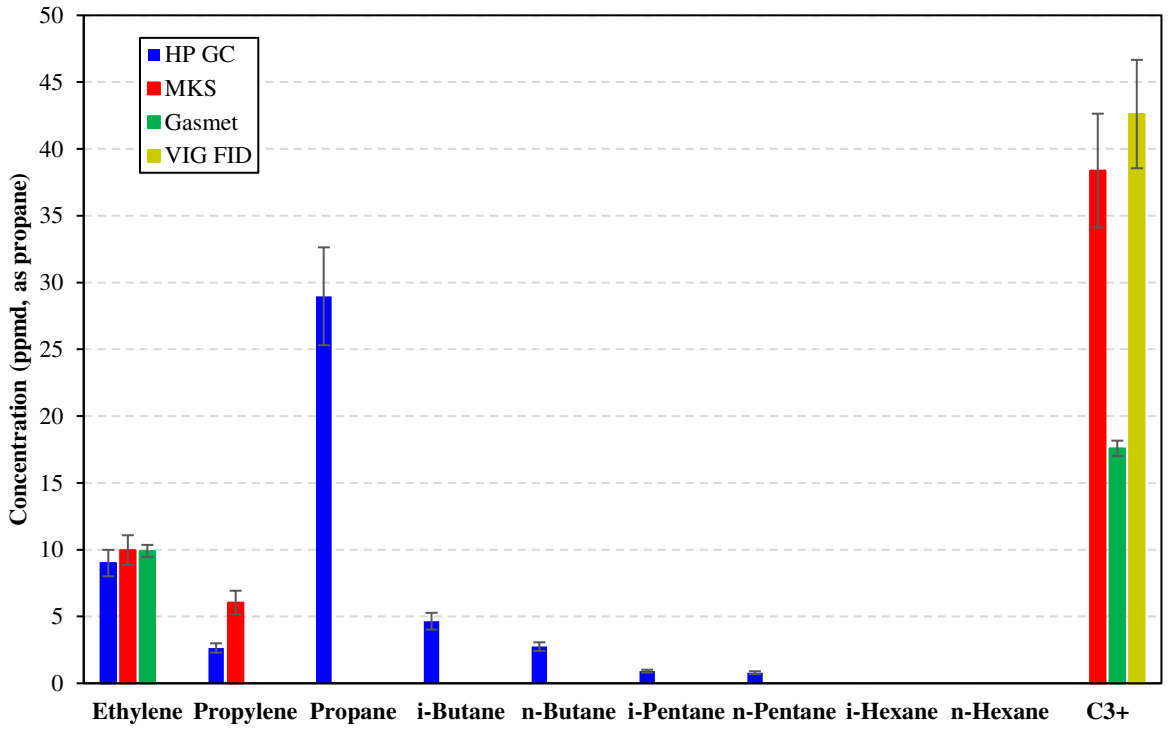

Figure B-27. Individual VOC concentrations reported from each analyzer during Data Point 30/31 for the GMV-4 lean burn HPFI PCC ignition configuration. NO_X was 0.35 g/bhp-hr and TER was 0.45.

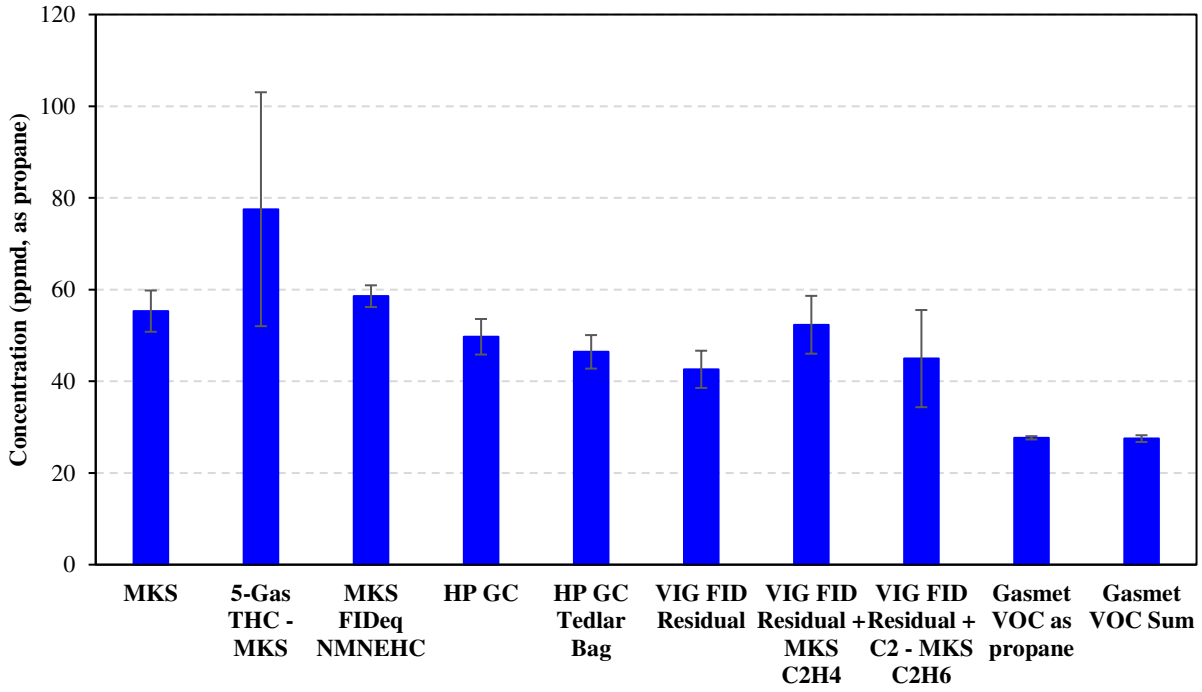

Figure B-28. Total VOC concentrations reported using different analyzers/methods for Data Point 30/31.

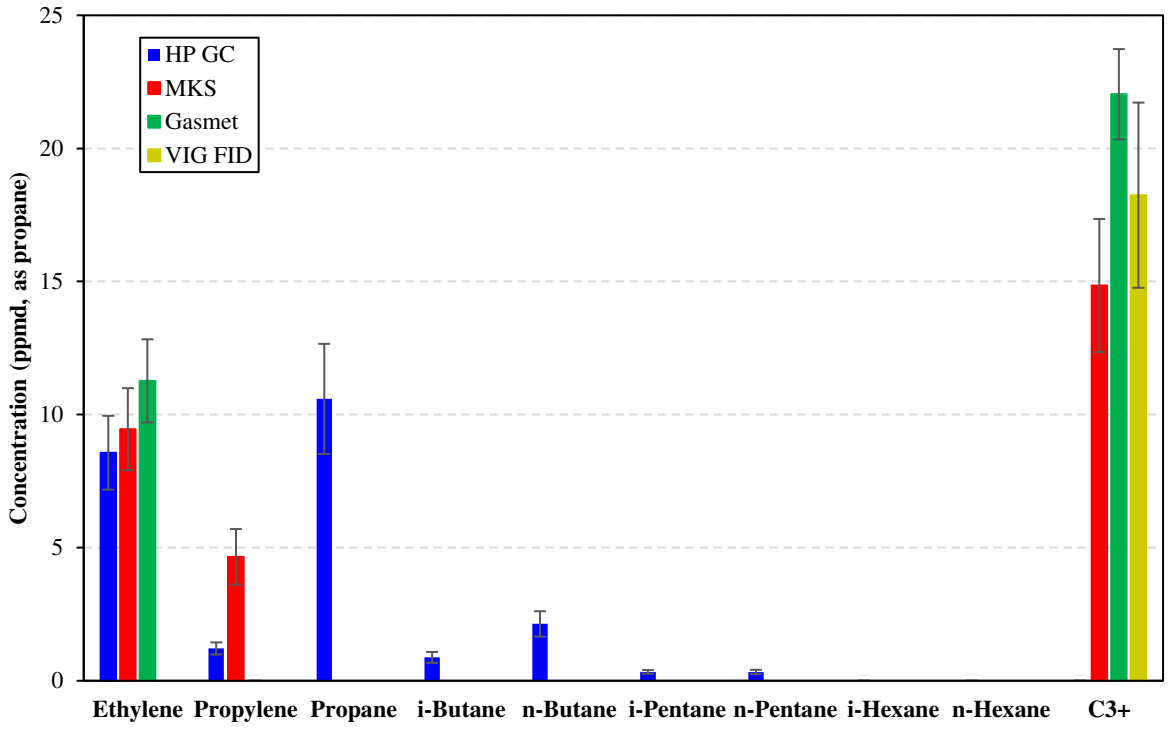

Figure B-29. Individual VOC concentrations reported from each analyzer during Data Point 32 for the GMV-4 lean burn HPFI PCC ignition configuration. NO_X was 0.30 g/bhp-hr and TER was 0.46.

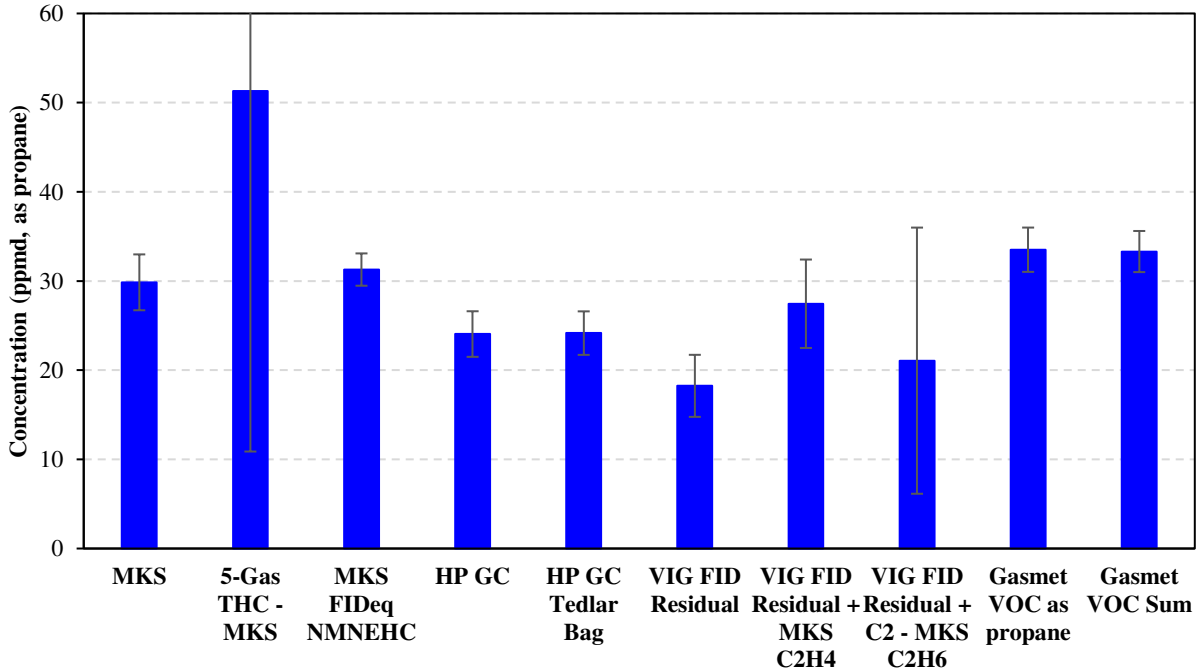

Figure B-30. Total VOC concentrations reported using different analyzers/methods for Data Point 32. Note that the uncertainty for "5-Gas THC – MKS" is ±40.4 ppmd, as propane.

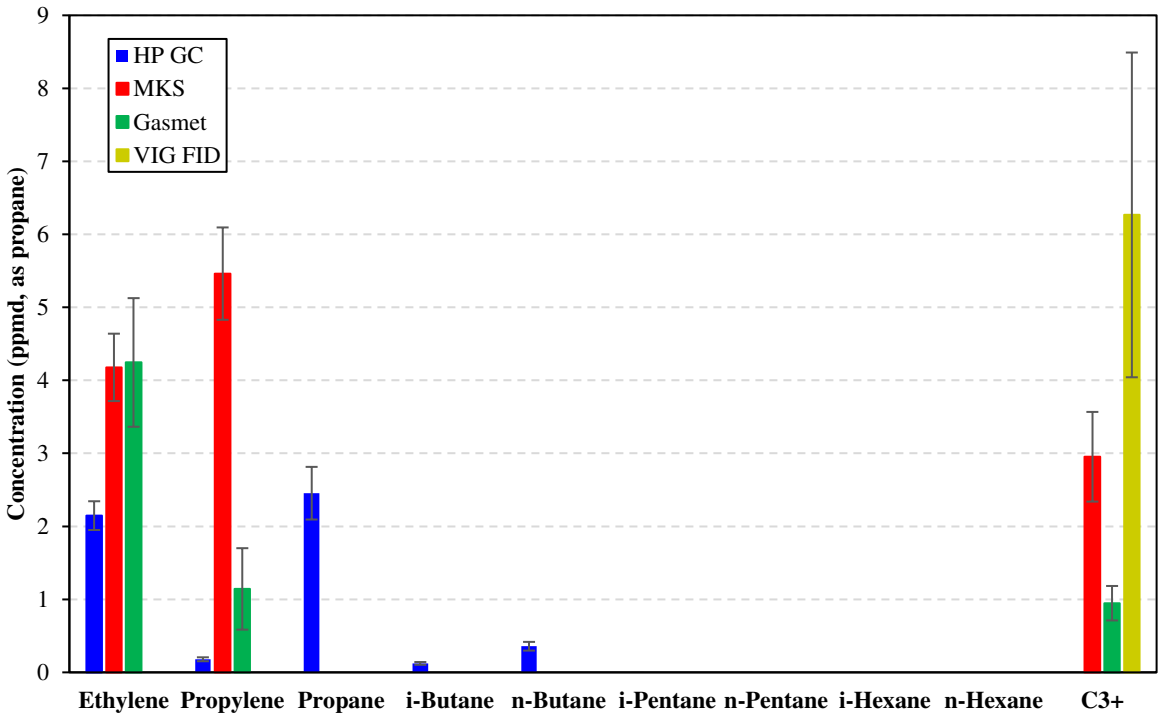

Figure B-31. Individual VOC concentrations reported from each analyzer during Data Point 34 for the Caterpillar 3304 with 3-way catalyst configuration. NO_X was 1.35 g/bhp-hr and ϕ was 1.00.

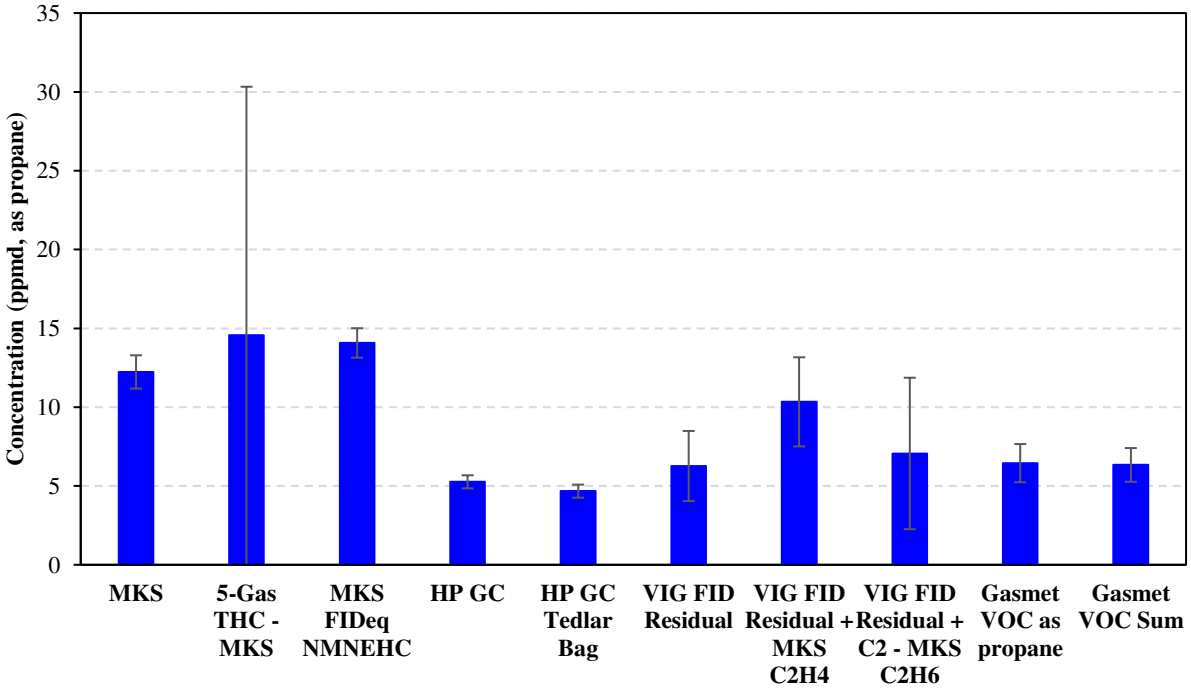

Figure B-32. Total VOC concentrations reported using different analyzers/methods for Data Point 34.

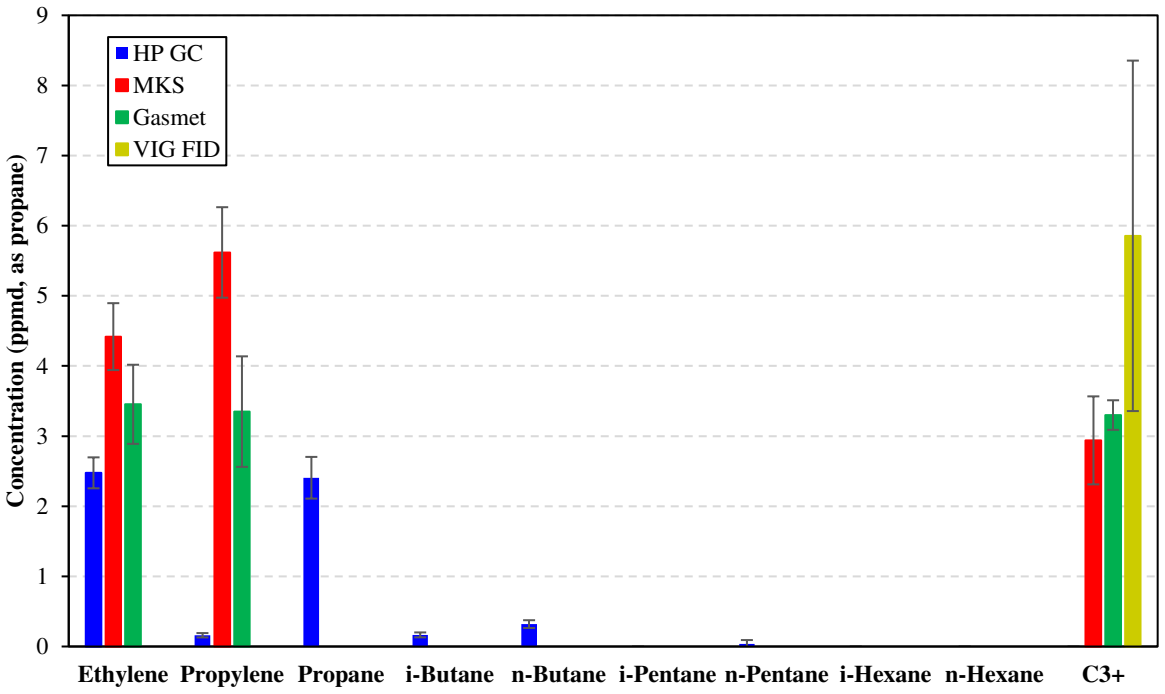

Figure B-33. Individual VOC concentrations reported from each analyzer during Data Point 35 for the Caterpillar 3304 with 3-way catalyst configuration. NO_X was 1.14 g/bhp-hr ϕ was 1.01.

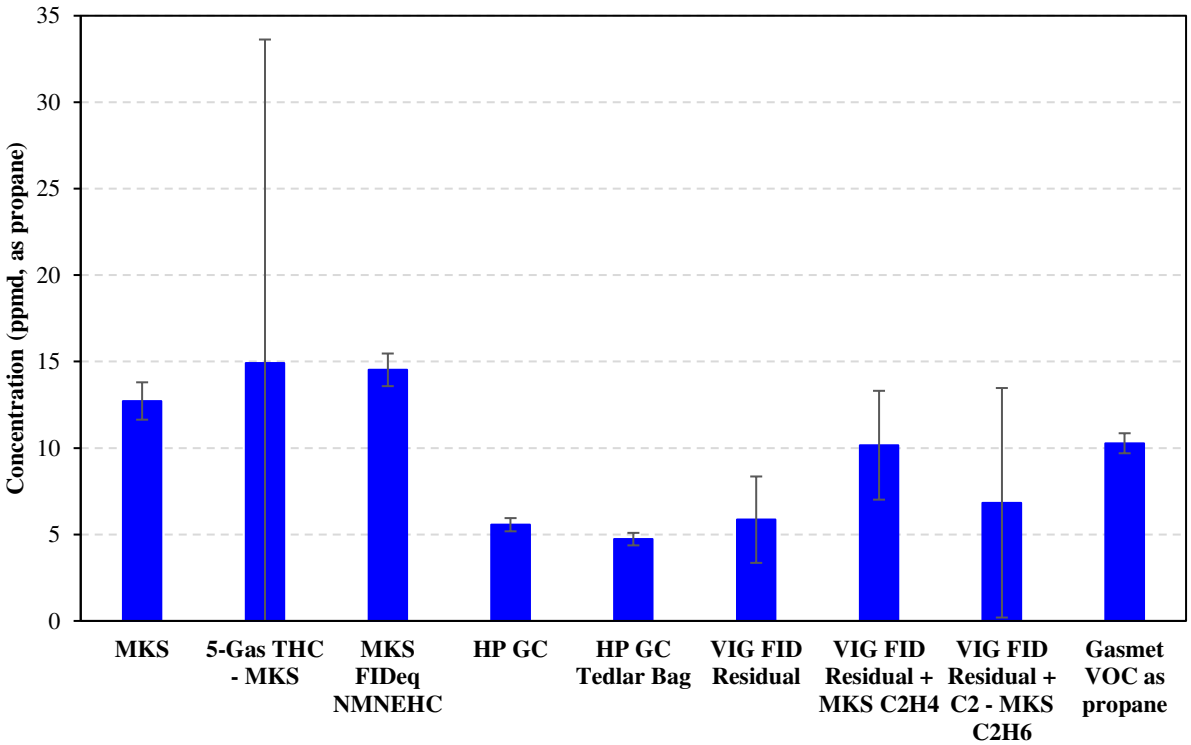

Figure B-34. Total VOC concentrations reported using different analyzers/methods for Data Point 35.

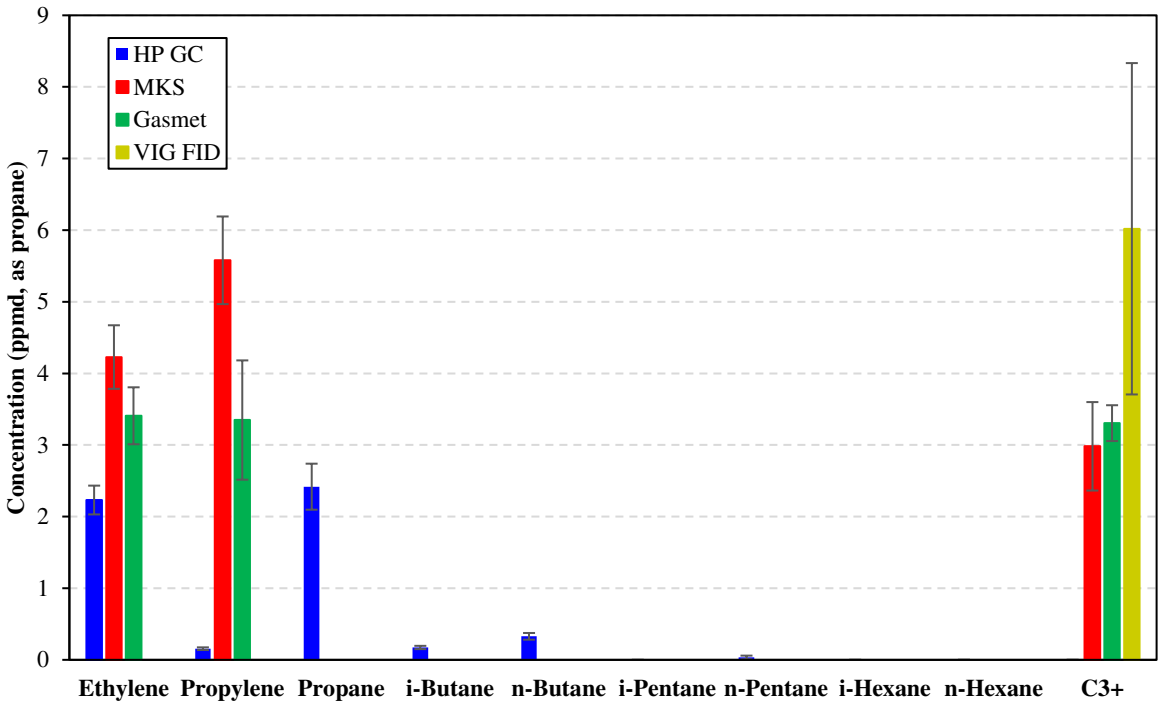

Figure B-35. Individual VOC concentrations reported from each analyzer during Data Point 36 for the Caterpillar 3304 with 3-way catalyst configuration. NO_X was 1.26 g/bhp-hr and ϕ was 1.01.

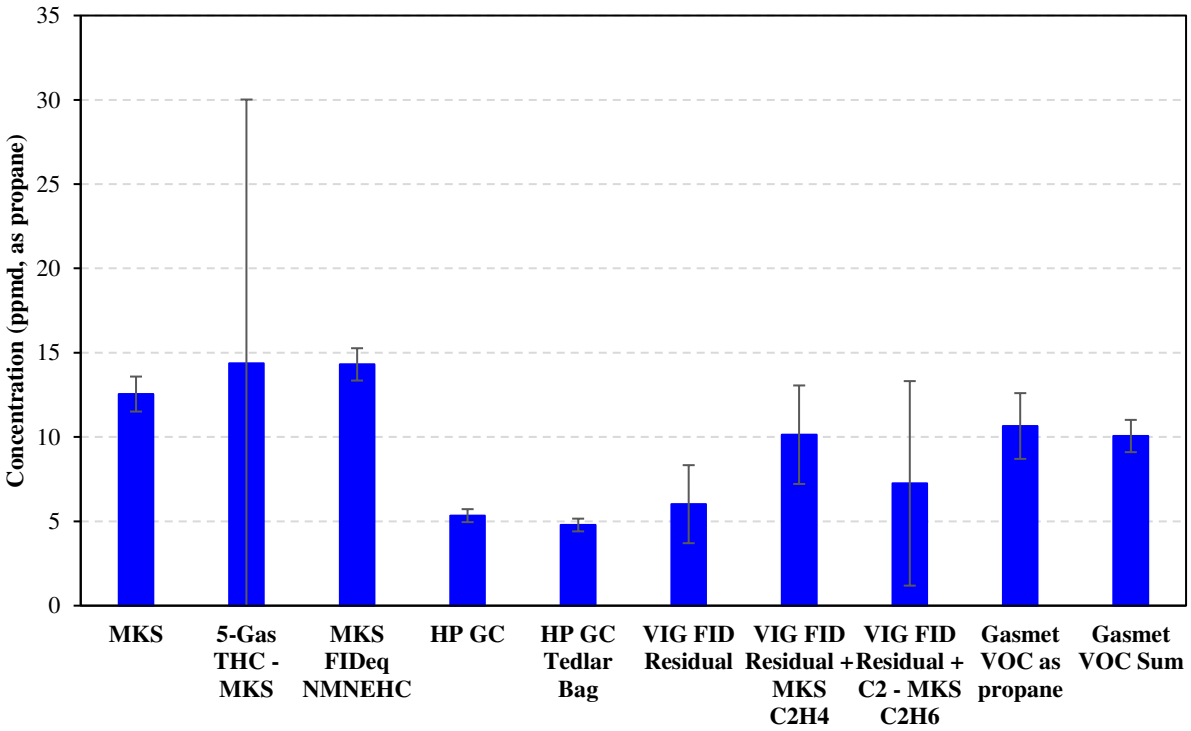

Figure B-36. Total VOC concentrations reported using different analyzers/methods for Data Point 36.

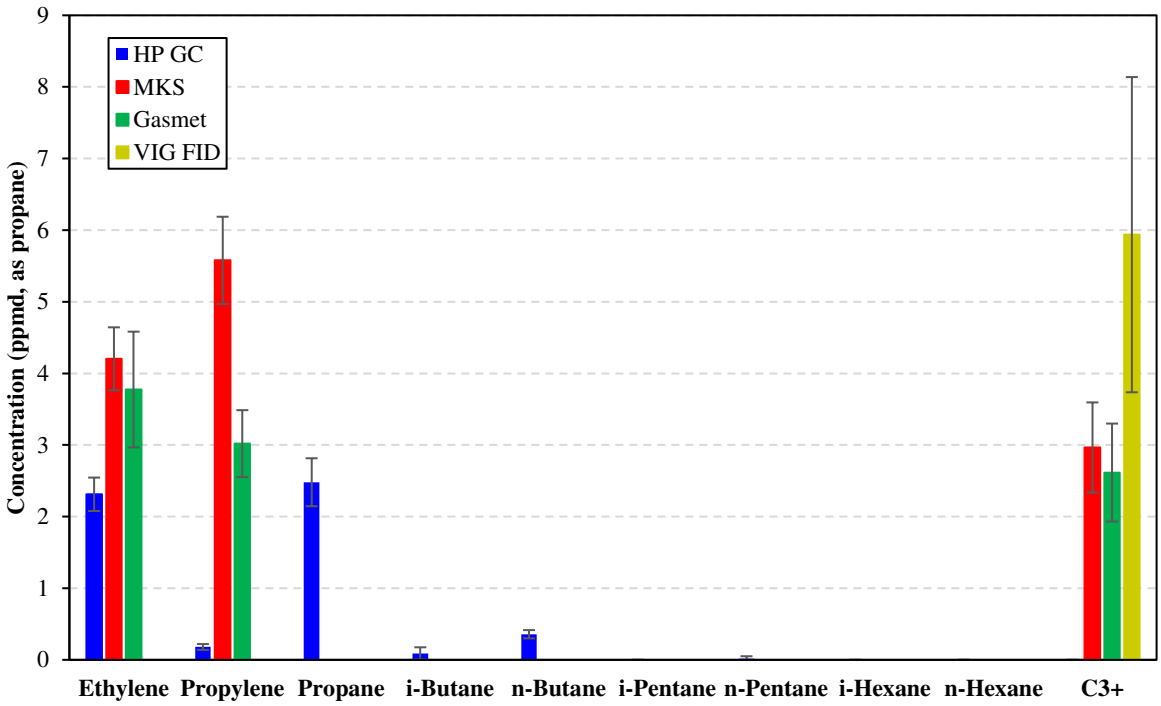

Figure B-37. Individual VOC concentrations reported from each analyzer during Data Point 37 for the Caterpillar 3304 with 3-way catalyst configuration. NO_X was 1.26 g/bhp-hr and ϕ was 1.01.

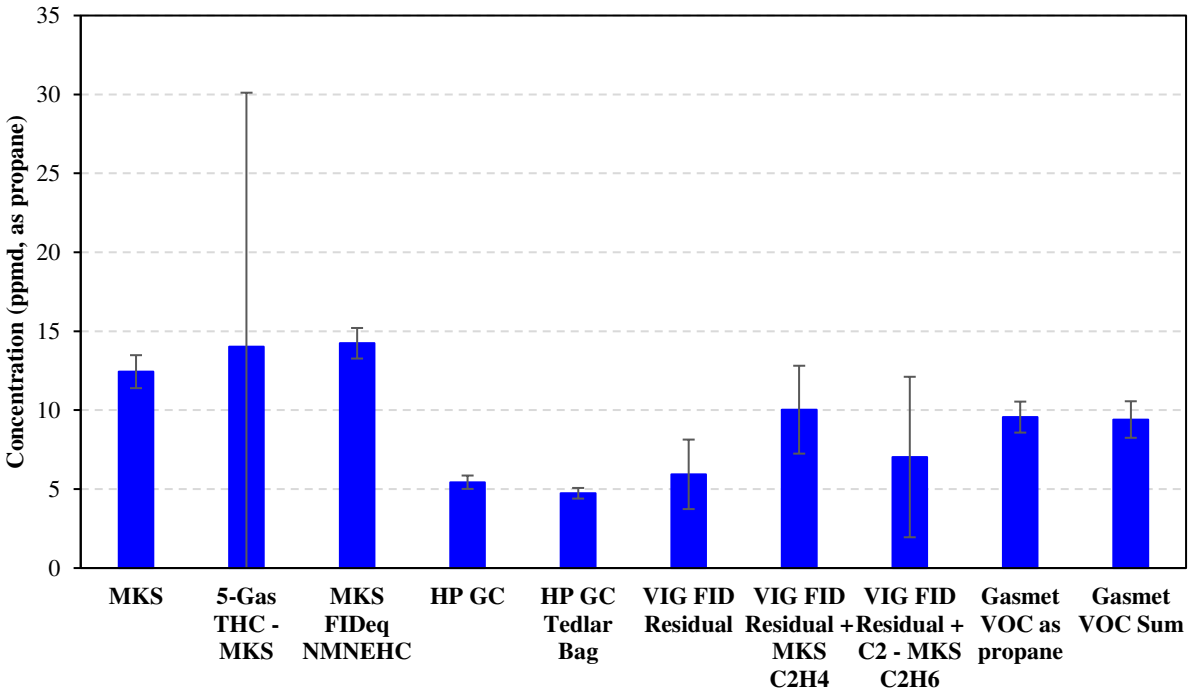

Figure B-38. Total VOC concentrations reported using different analyzers/methods for Data Point 37.

HP GC Chromatograms

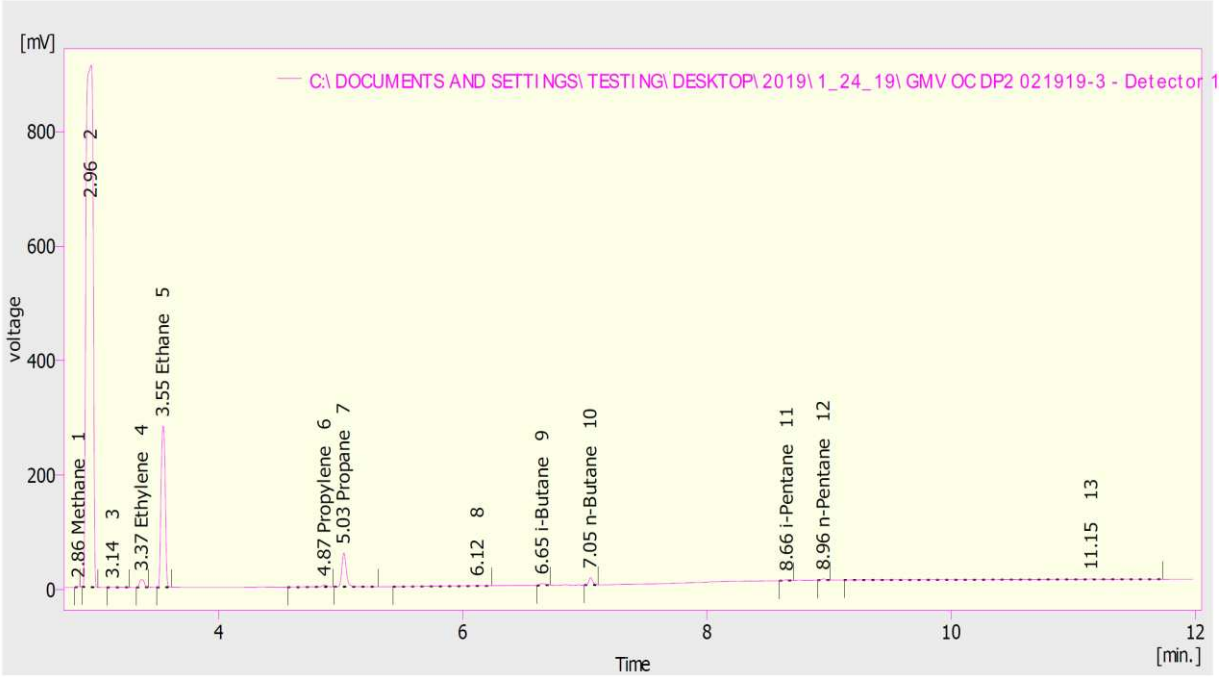

Figure B-39. Sample chromatogram depicting response peaks detected by the HP GC during Data Point 2 for the GMV-4 lean burn, open chamber configuration.

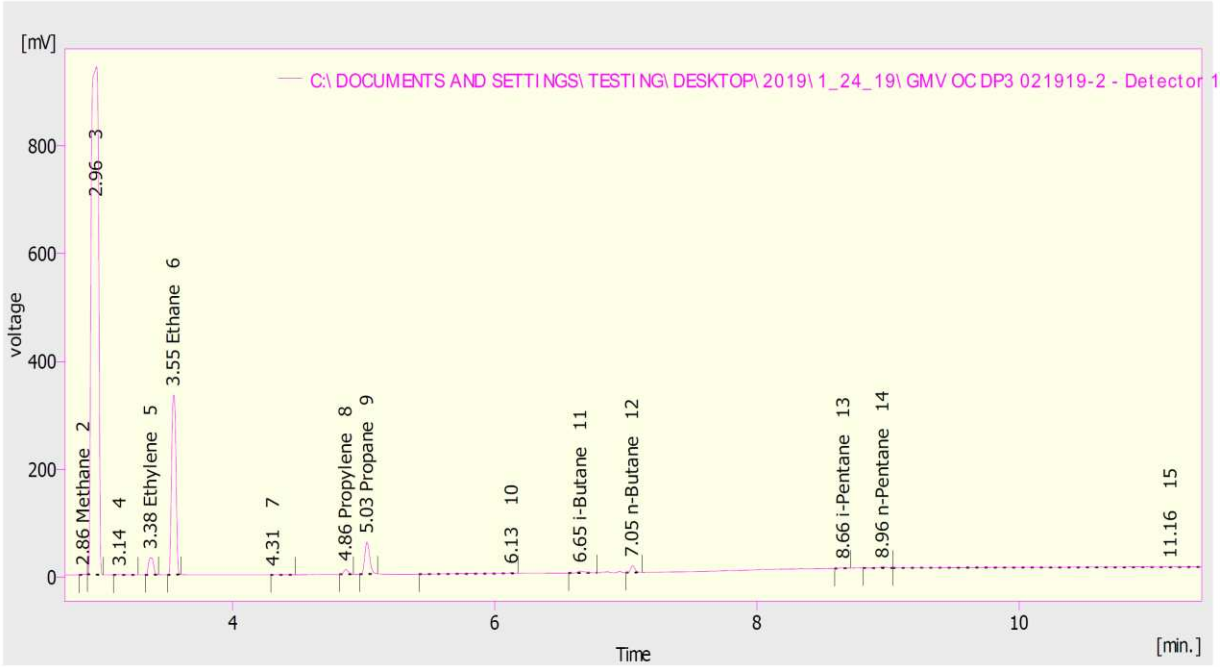

Figure B-40. Sample chromatogram depicting response peaks detected by the HP GC during Data Point 3 for the GMV-4 lean burn, open chamber configuration.

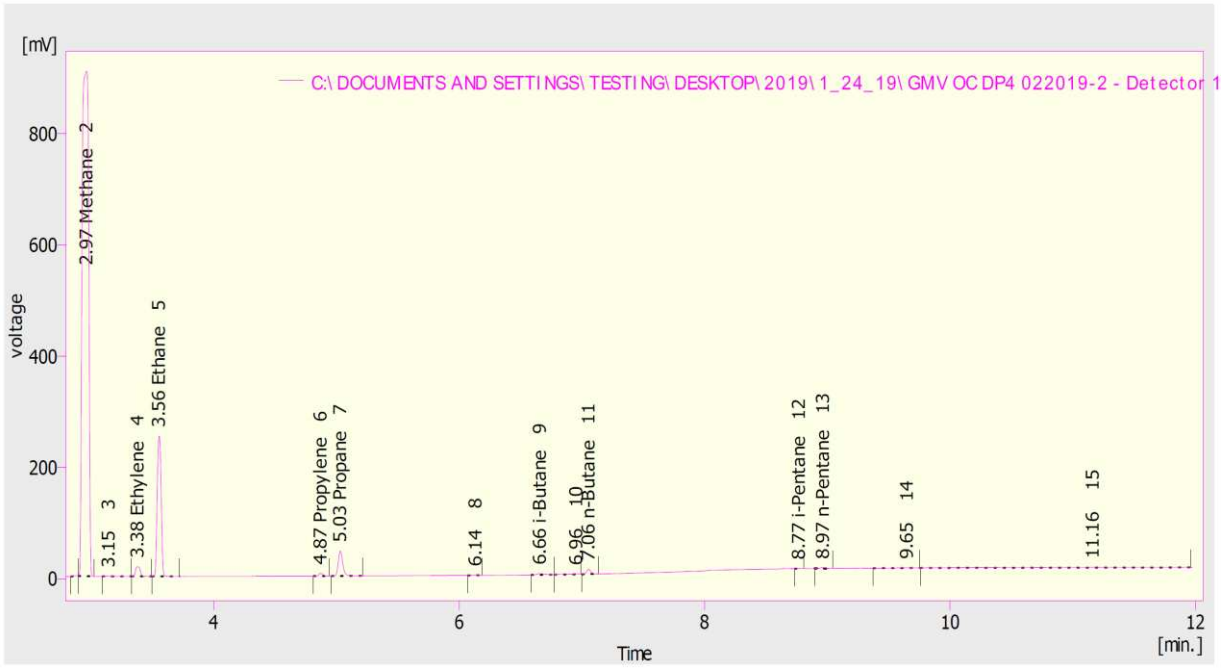

Figure B-41. Sample chromatogram depicting response peaks detected by the HP GC during Data Point 4 for the GMV-4 lean burn, open chamber configuration.

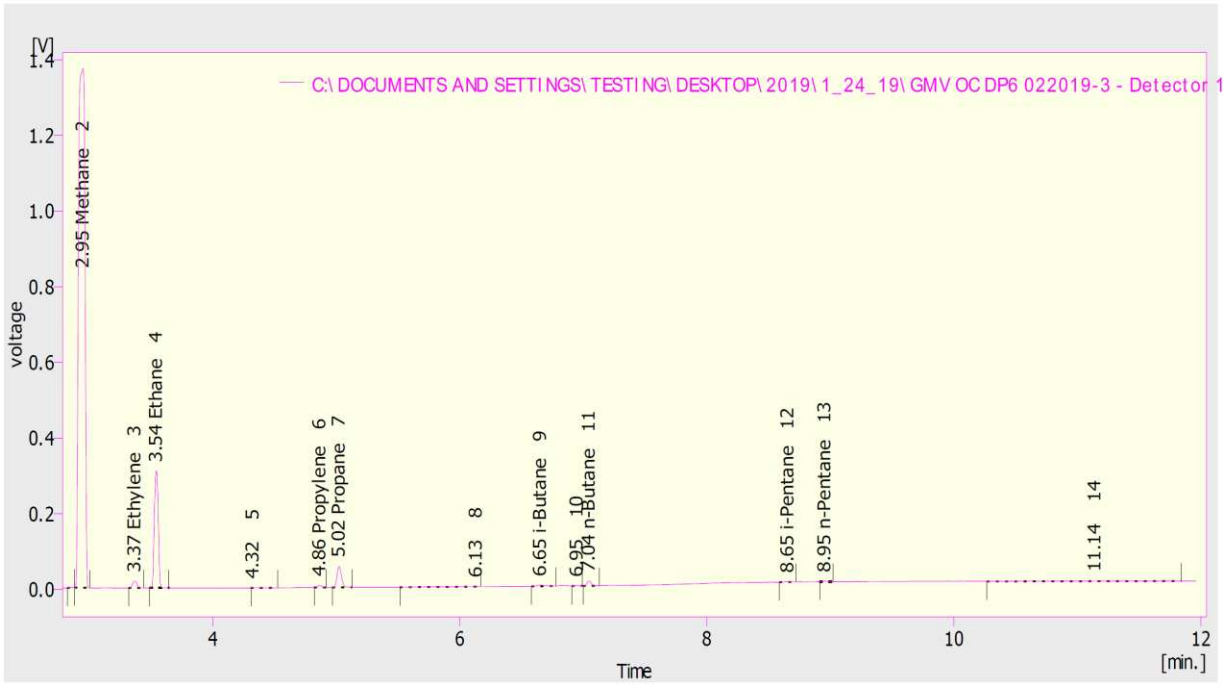

Figure B-42. Sample chromatogram depicting response peaks detected by the HP GC during Data Point 6 for the GMV-4 lean burn, open chamber configuration.

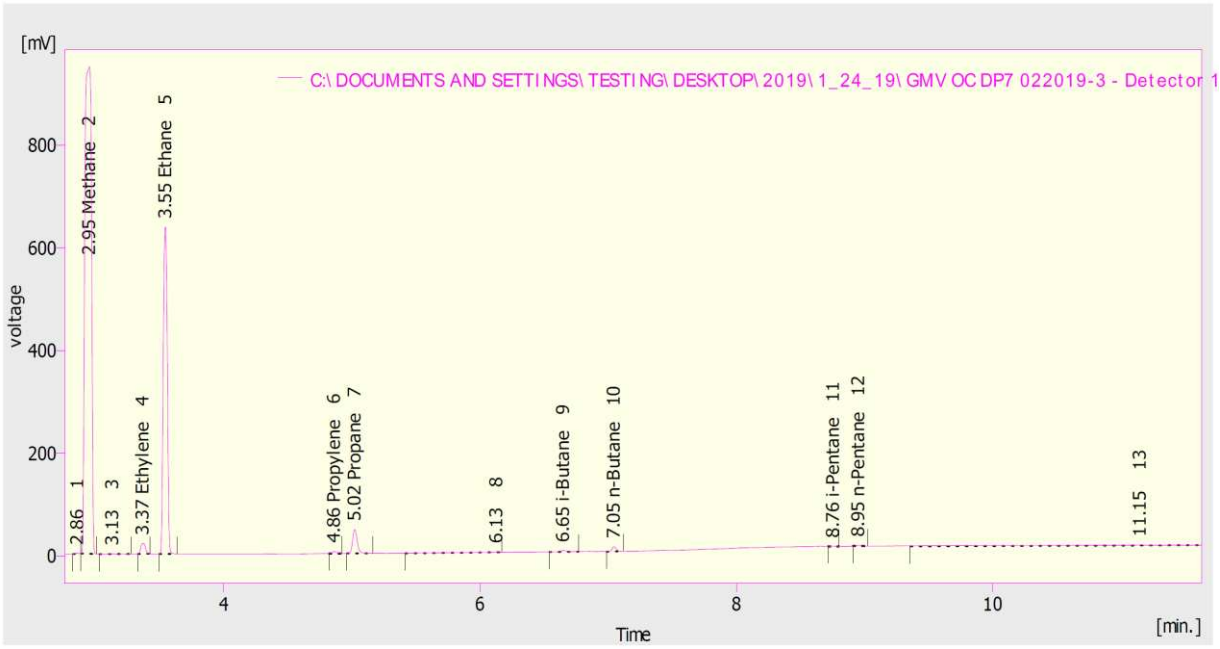

Figure B-43. Sample chromatogram depicting response peaks detected by the HP GC during Data Point 7 for the GMV-4 lean burn, open chamber configuration.

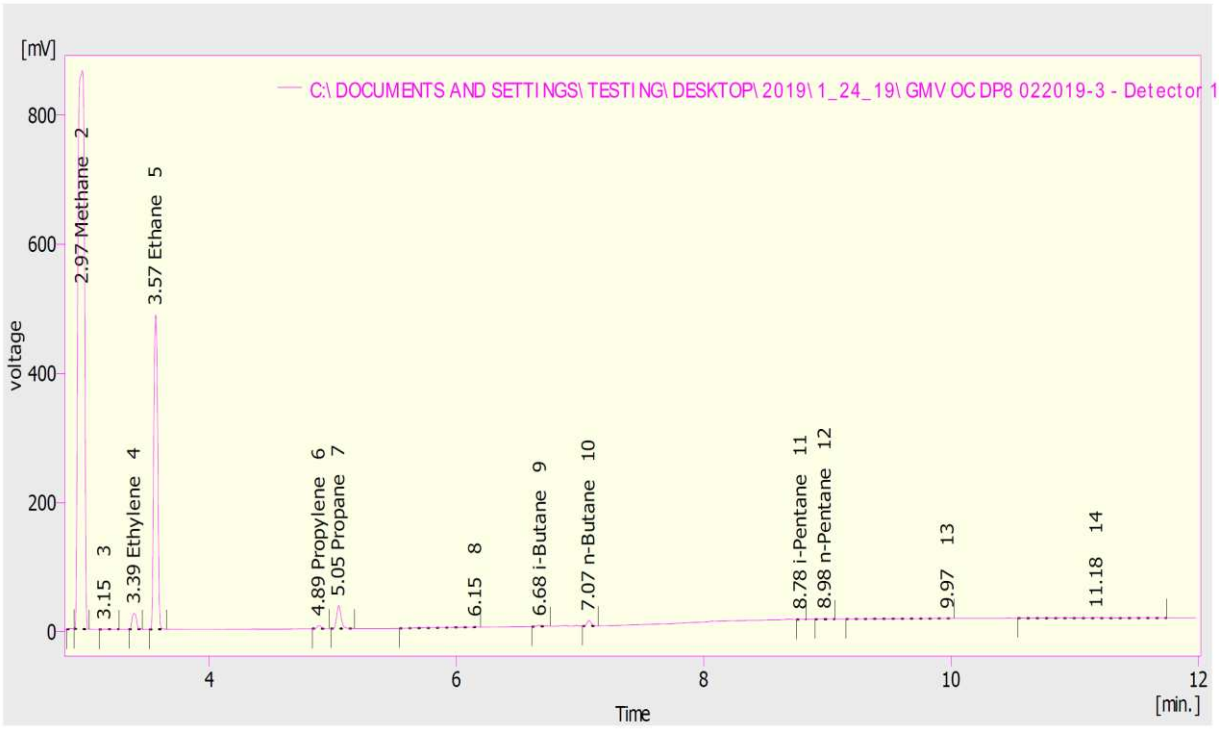

Figure B-44. Sample chromatogram depicting response peaks detected by the HP GC during Data Point 8 for the GMV-4 lean burn, open chamber configuration.

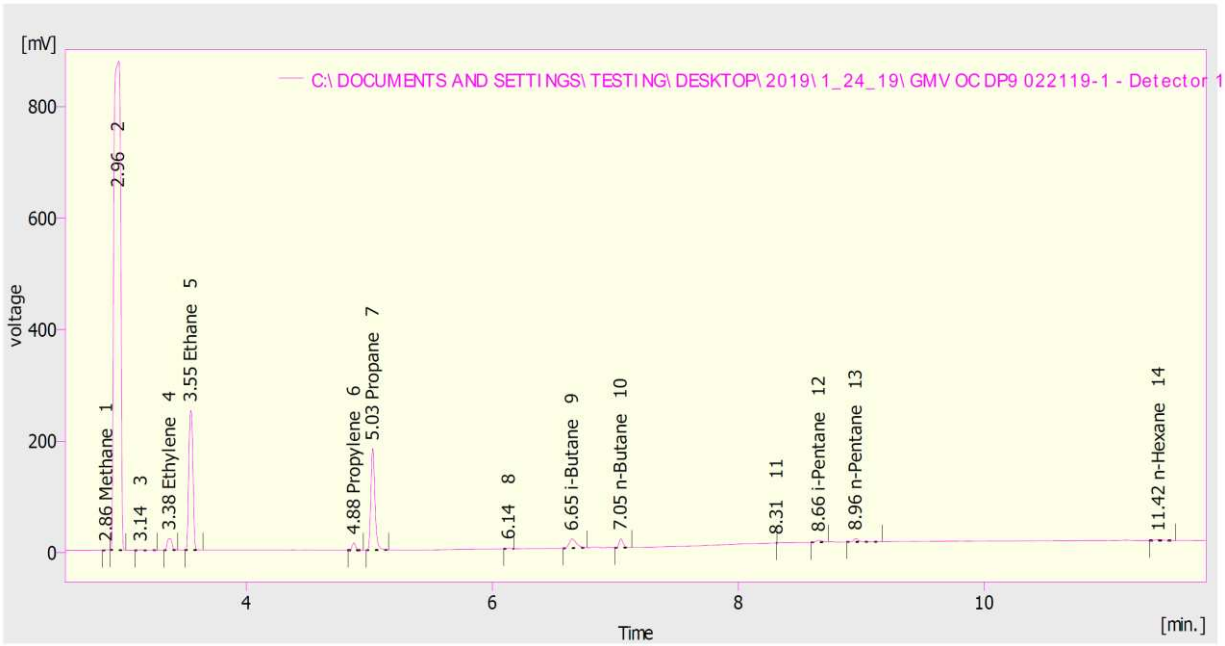

Figure B-45. Sample chromatogram depicting response peaks detected by the HP GC during Data Point 9/10 for the GMV-4 lean burn, open chamber configuration.

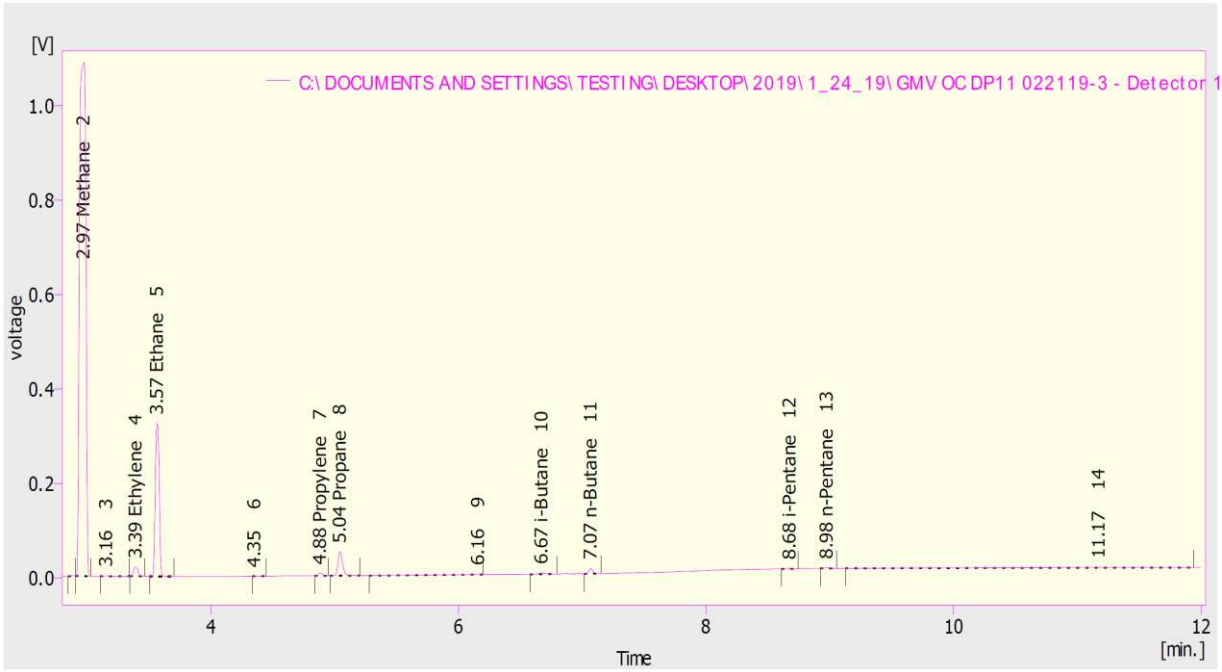

Figure B-46. Sample chromatogram depicting response peaks detected by the HP GC during Data Point 11 for the GMV-4 lean burn, open chamber configuration.

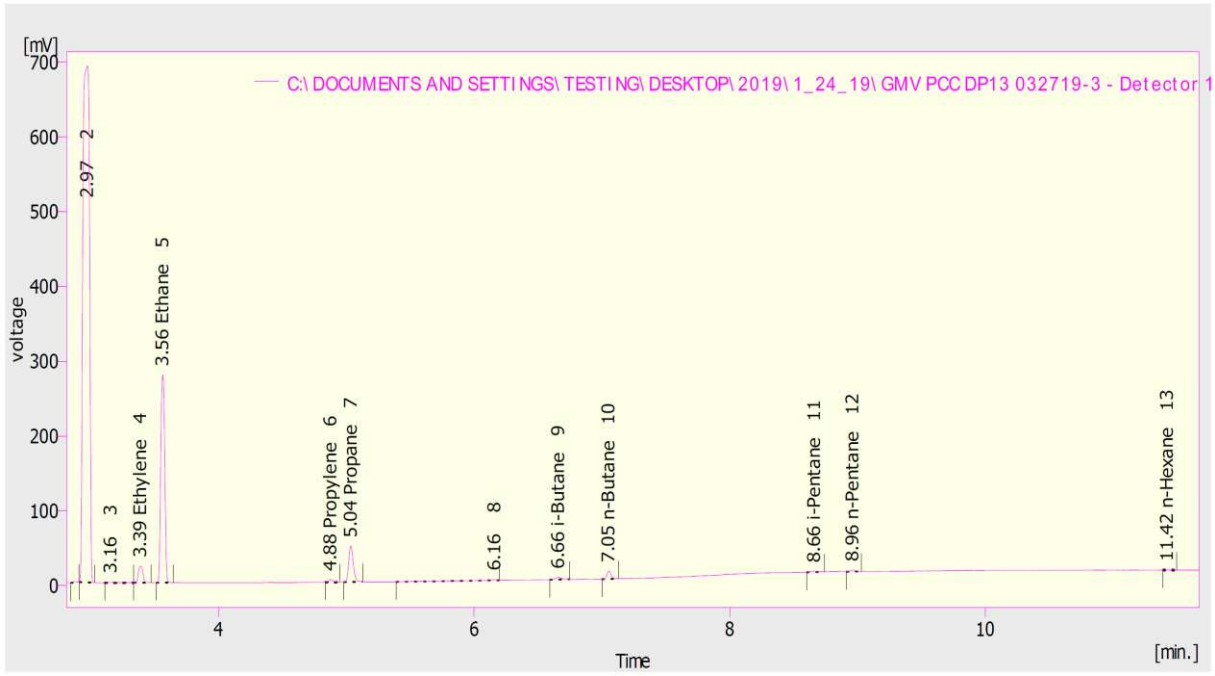

Figure B-47. Sample chromatogram depicting response peaks detected by the HP GC during Data Point 13 for the GMV-4 lean burn, PCC ignition configuration.

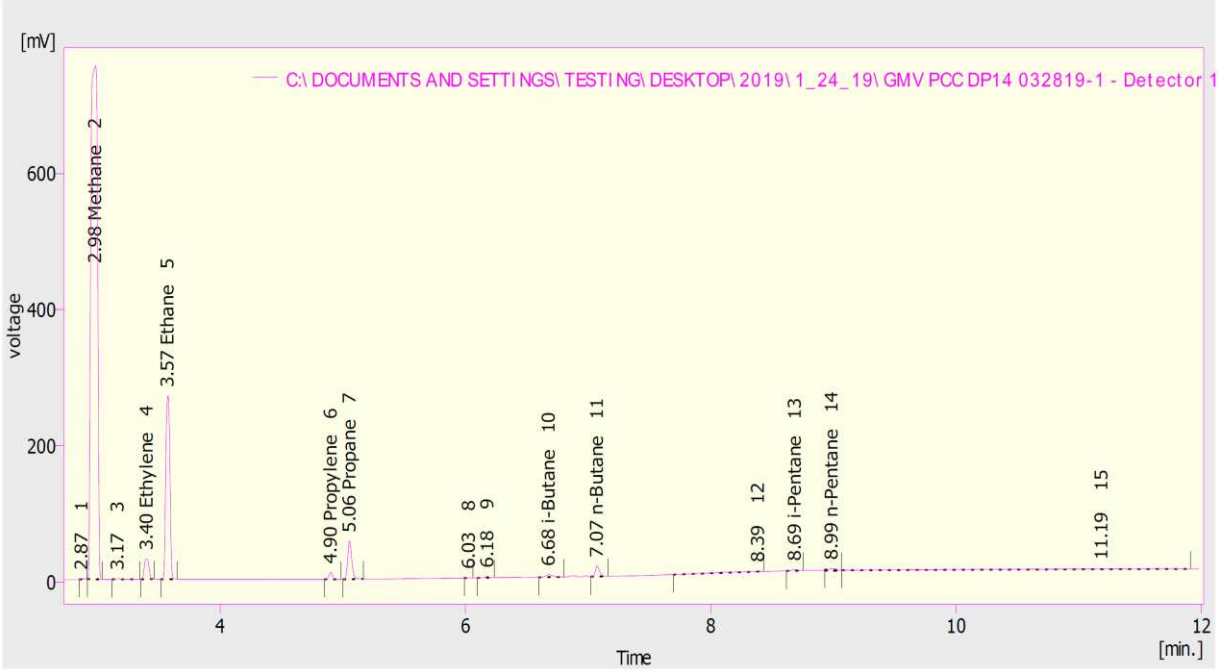

Figure B-48. Sample chromatogram depicting response peaks detected by the HP GC during Data Point 14 for the GMV-4 lean burn, PCC ignition configuration.

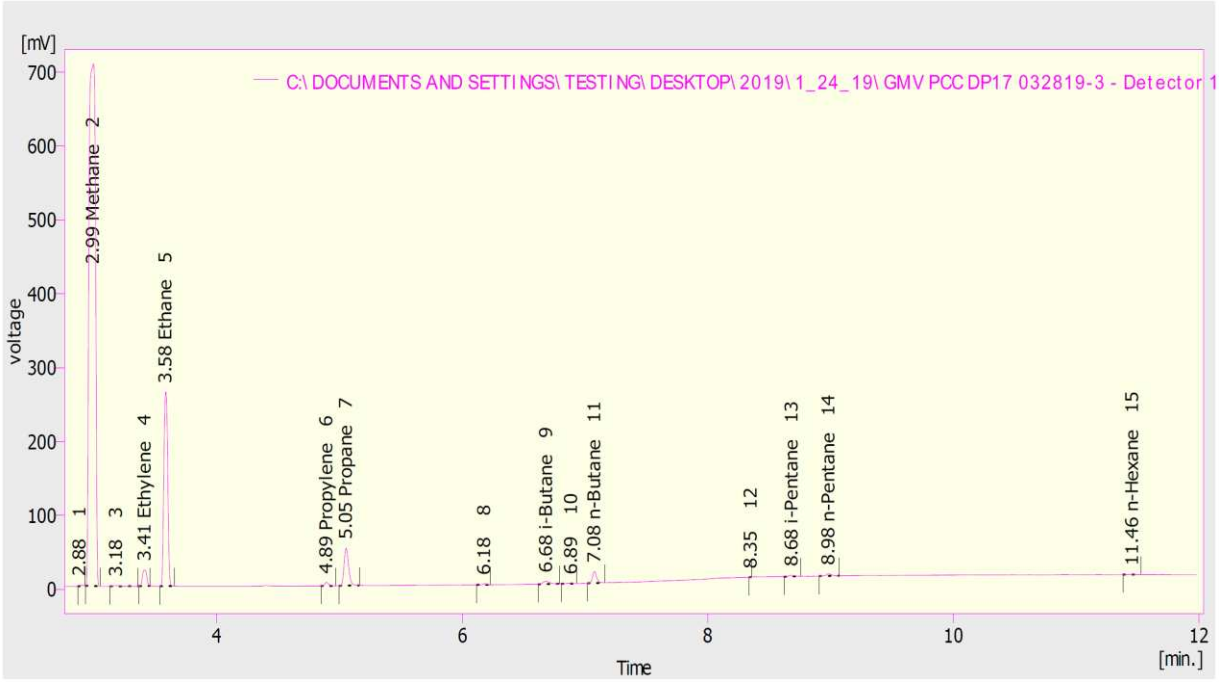

Figure B-49. Sample chromatogram depicting response peaks detected by the HP GC during Data Point 17 for the GMV-4 lean burn, PCC ignition configuration.

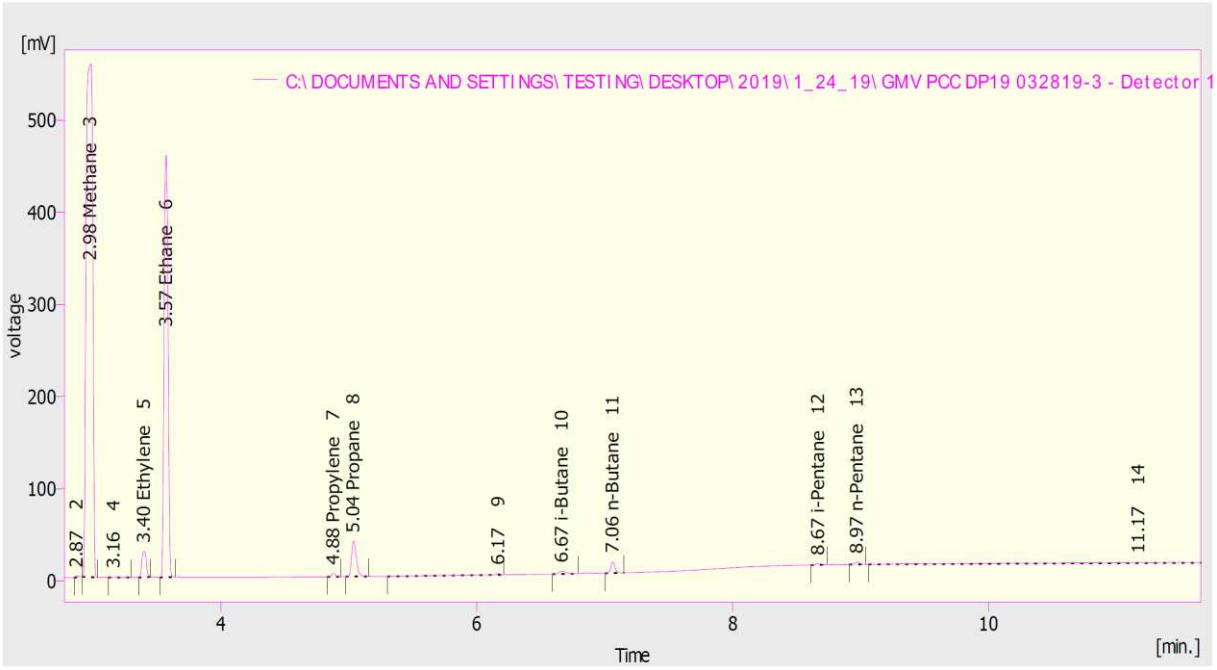

Figure B-50. Sample chromatogram depicting response peaks detected by the HP GC during Data Point 18/19 for the GMV-4 lean burn, PCC ignition configuration.

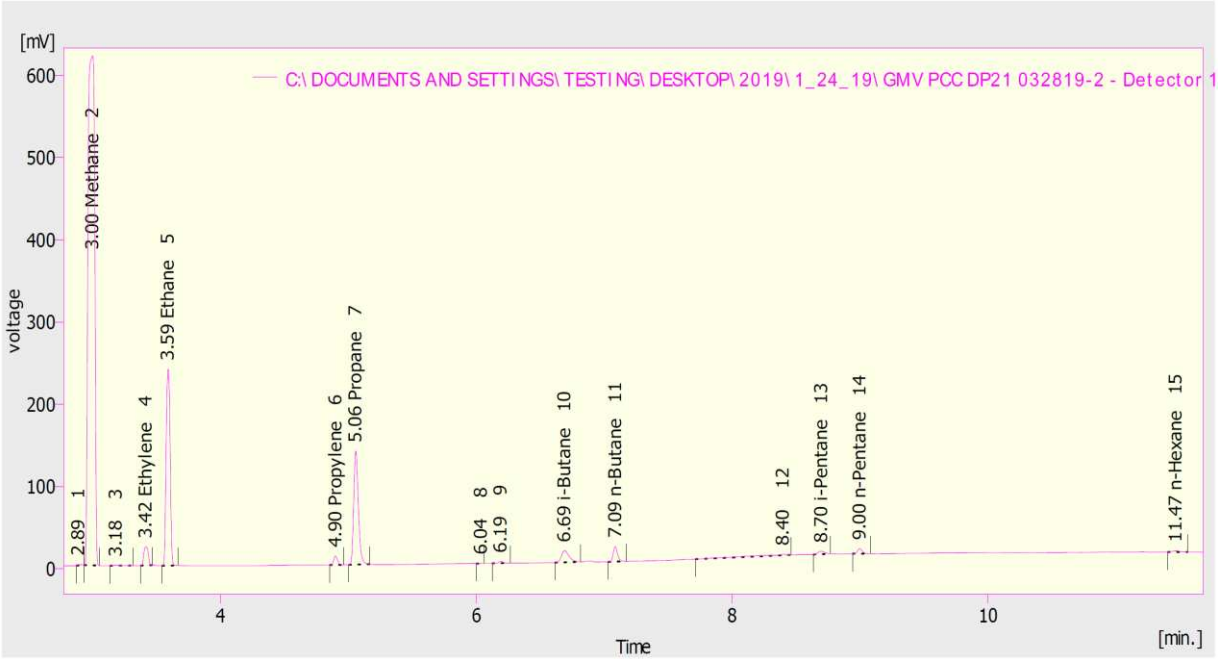

Figure B-51. Sample chromatogram depicting response peaks detected by the HP GC during Data Point 20/21 for the GMV-4 lean burn, PCC ignition configuration.

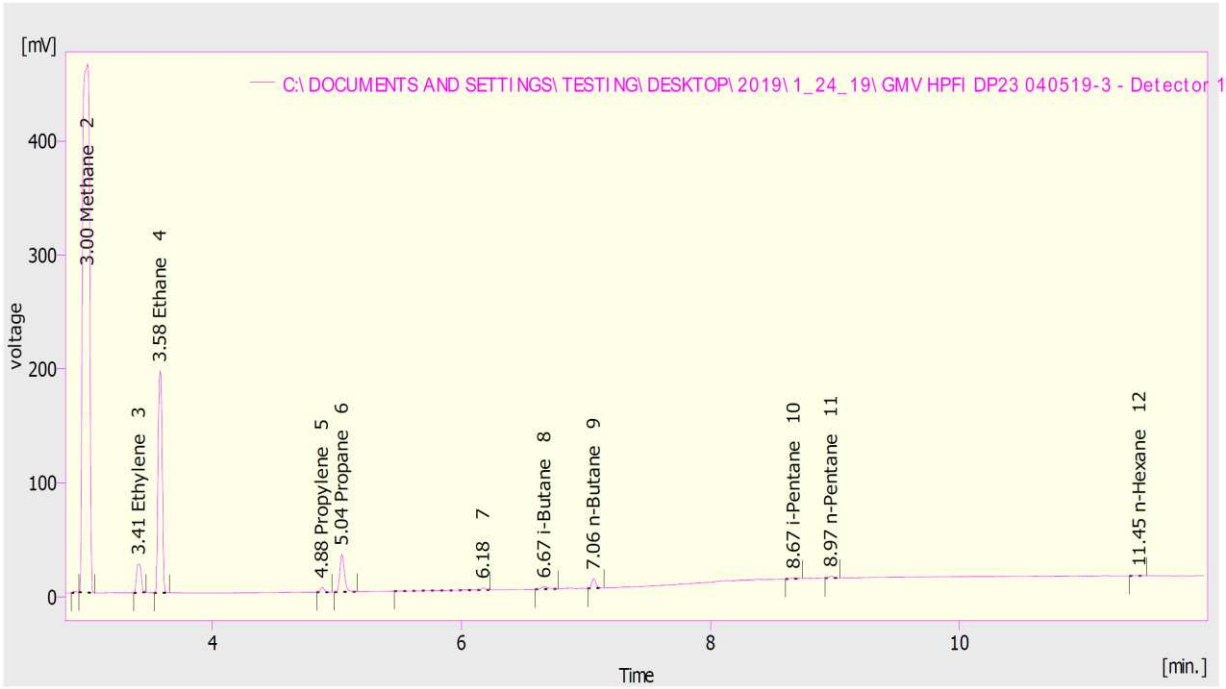

Figure B-52. Sample chromatogram depicting response peaks detected by the HP GC during Data Point 23 for the GMV-4 lean burn, HPFI PCC ignition configuration.

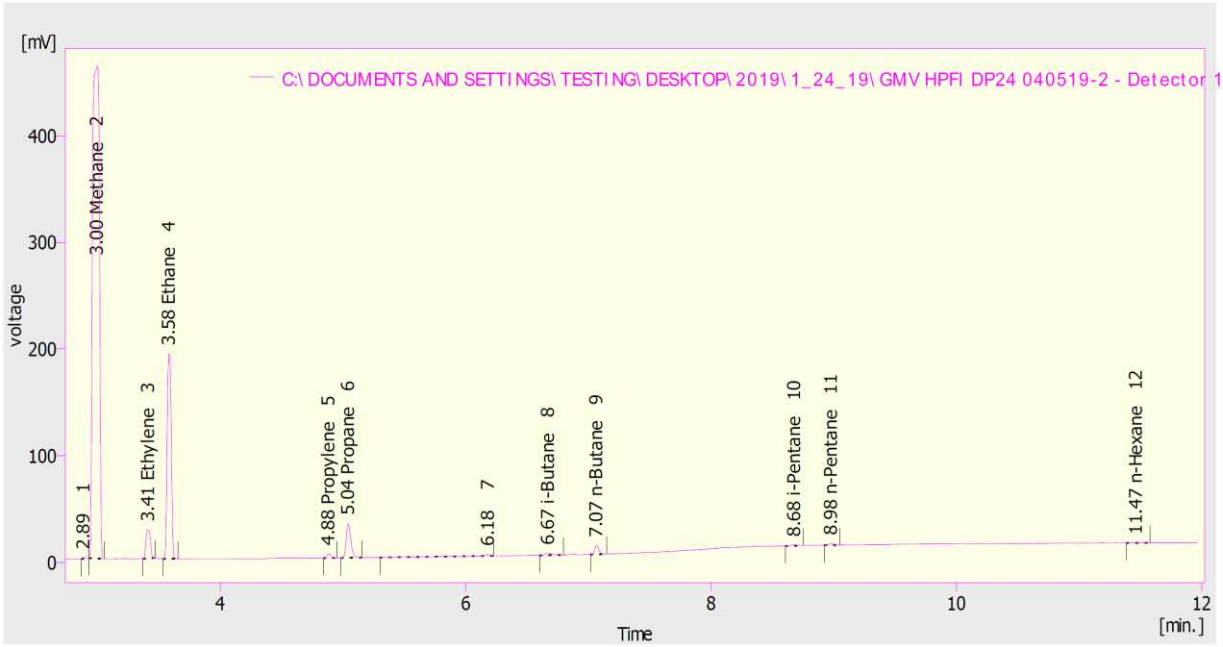

Figure B-53. Sample chromatogram depicting response peaks detected by the HP GC during Data Point 24 for the GMV-4 lean burn, HPFI PCC ignition configuration.

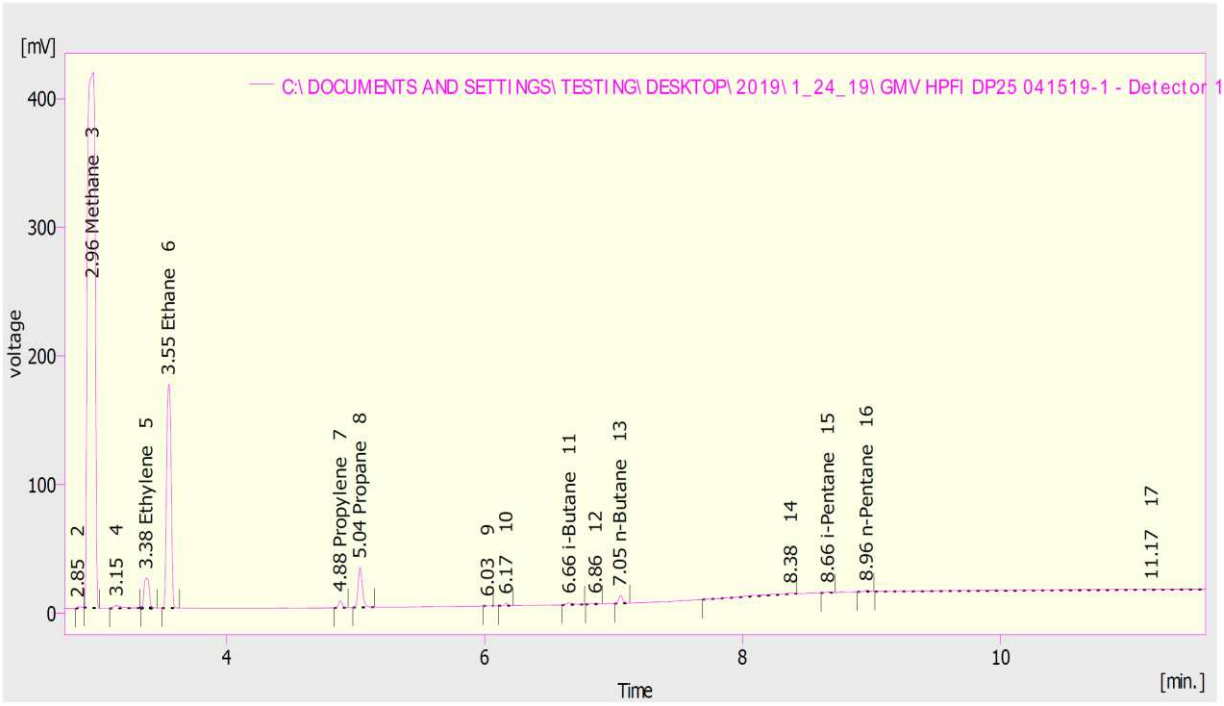

Figure B-54. Sample chromatogram depicting response peaks detected by the HP GC during Data Point 25 for the GMV-4 lean burn, HPFI PCC ignition configuration.

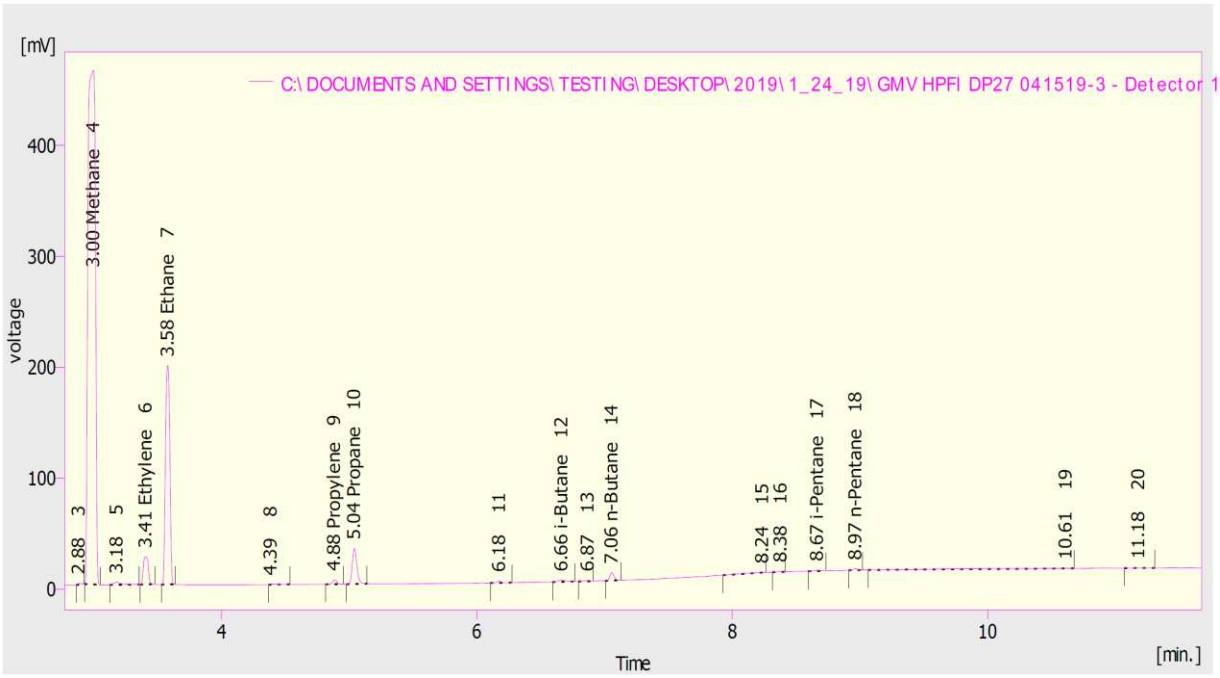

Figure B-55. Sample chromatogram depicting response peaks detected by the HP GC during Data Point 27 for the GMV-4 lean burn, HPFI PCC ignition configuration.

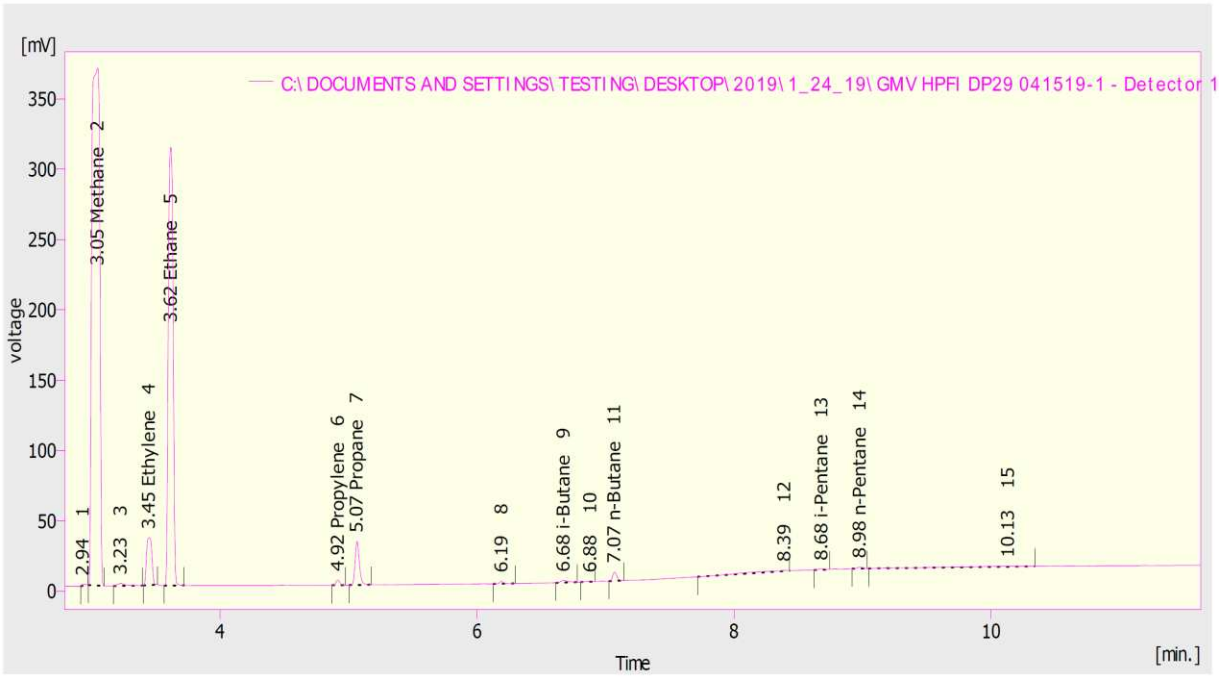

Figure B-56. Sample chromatogram depicting response peaks detected by the HP GC during Data Point 28/29 for the GMV-4 lean burn, HPFI PCC ignition configuration.

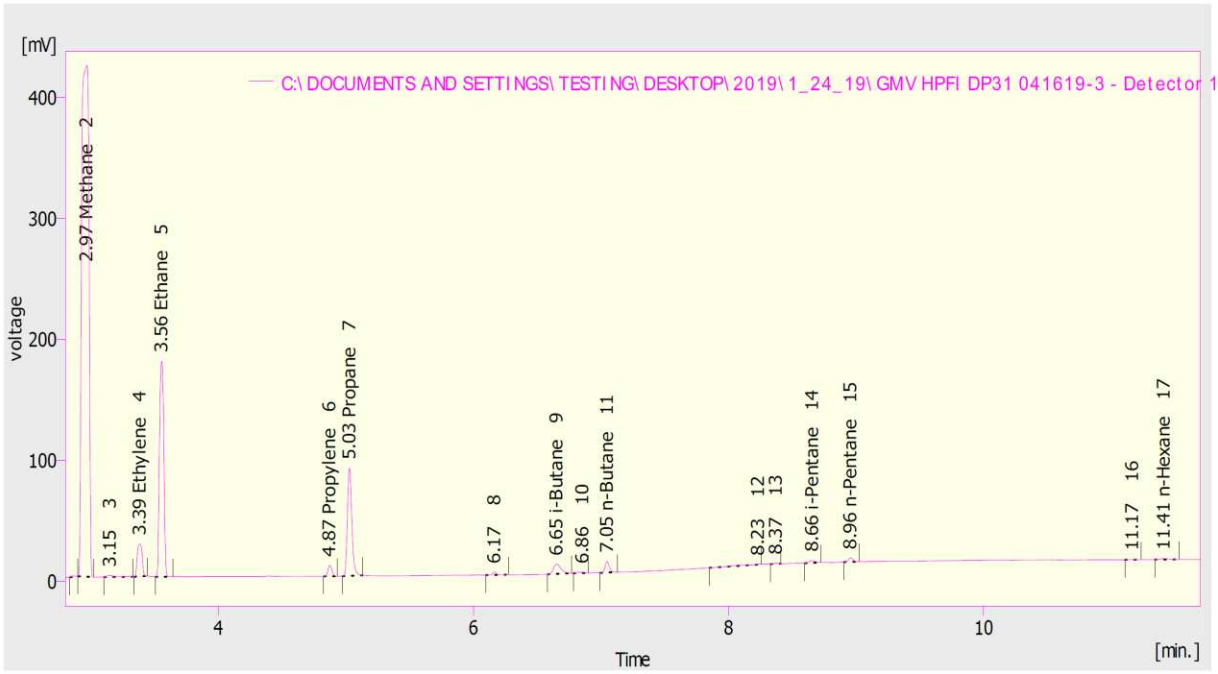

Figure B-57. Sample chromatogram depicting response peaks detected by the HP GC during Data Point 30/31 for the GMV-4 lean burn, HPFI PCC ignition configuration.

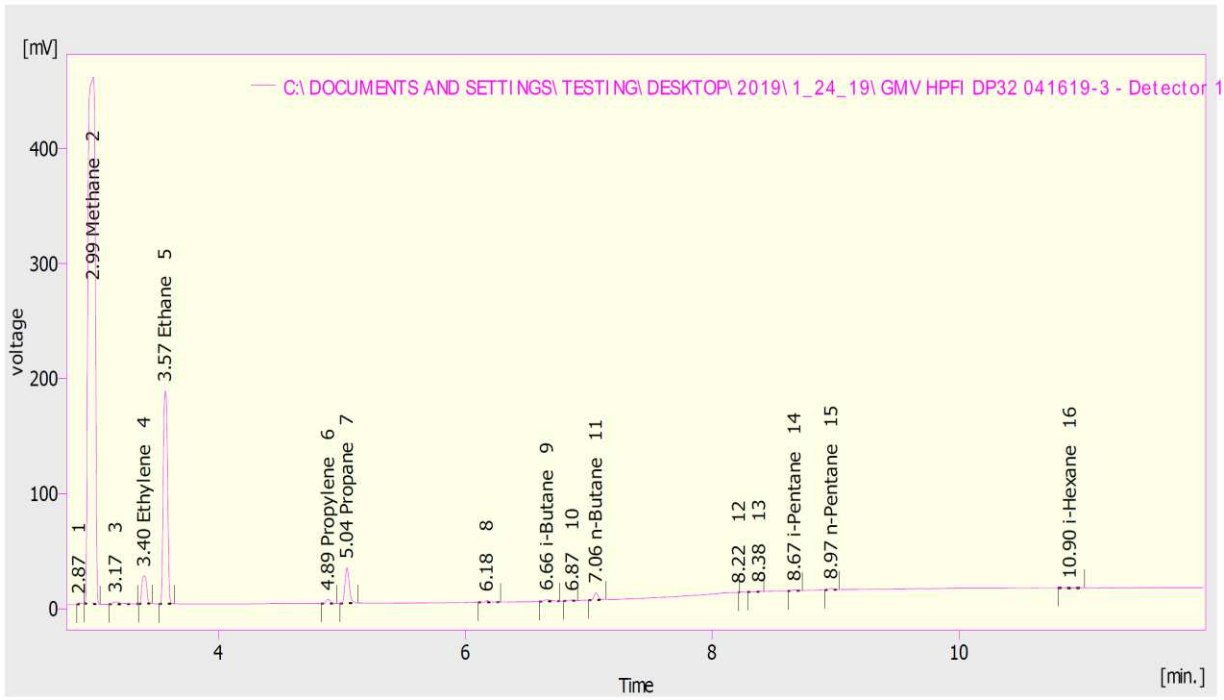

Figure B-58. Sample chromatogram depicting response peaks detected by the HP GC during Data Point 32 for the GMV-4 lean burn, HPFI PCC ignition configuration.

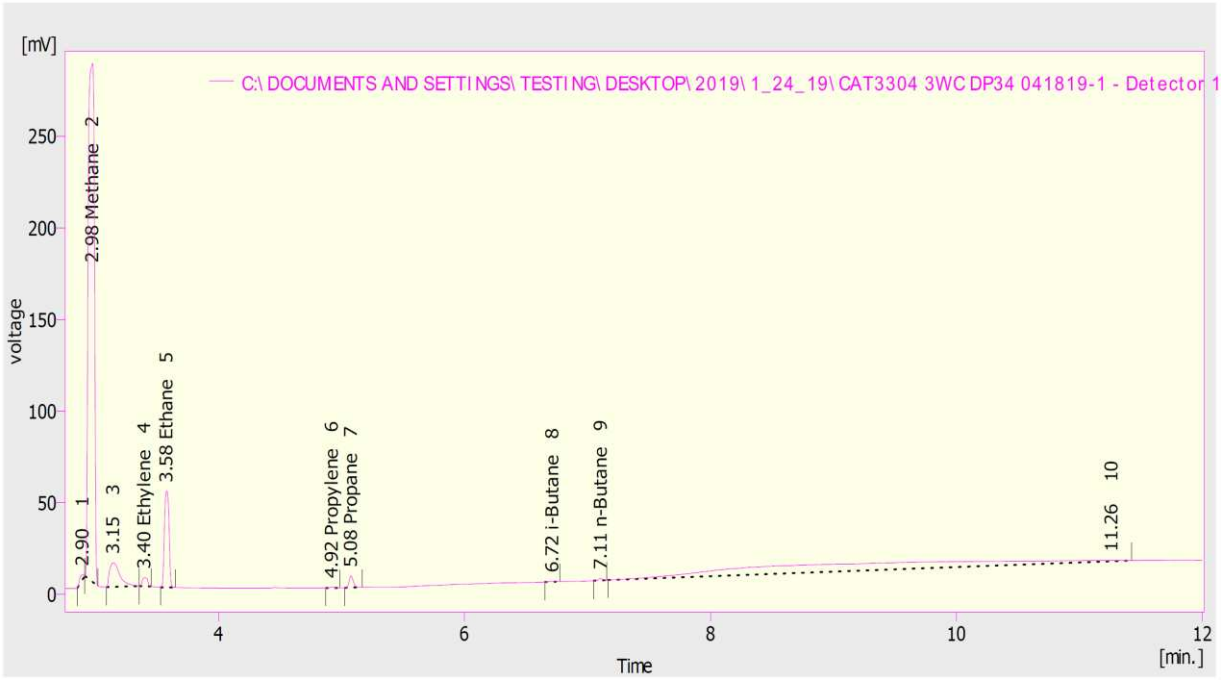

Figure B-59. Sample chromatogram depicting response peaks detected by the HP GC during Data Point 34 for the Caterpillar rich burn with a 3-way catalyst configuration.

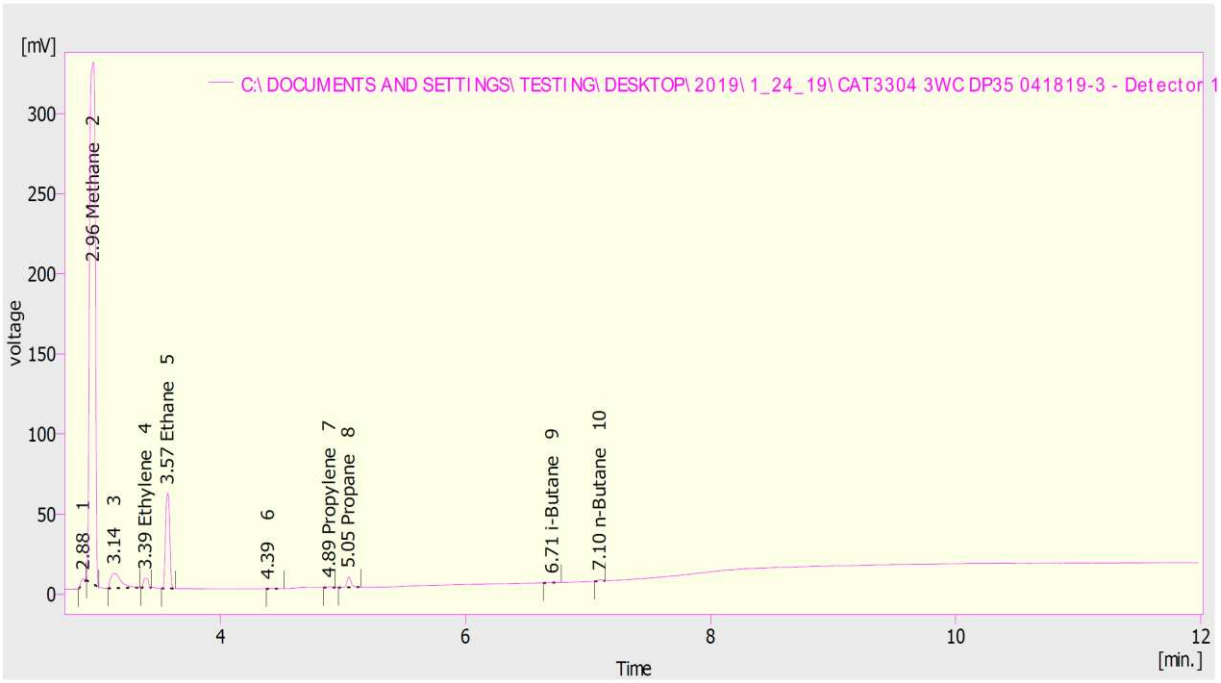

Figure B-60. Sample chromatogram depicting response peaks detected by the HP GC during Data Point 35 for the Caterpillar rich burn with a 3-way catalyst configuration.

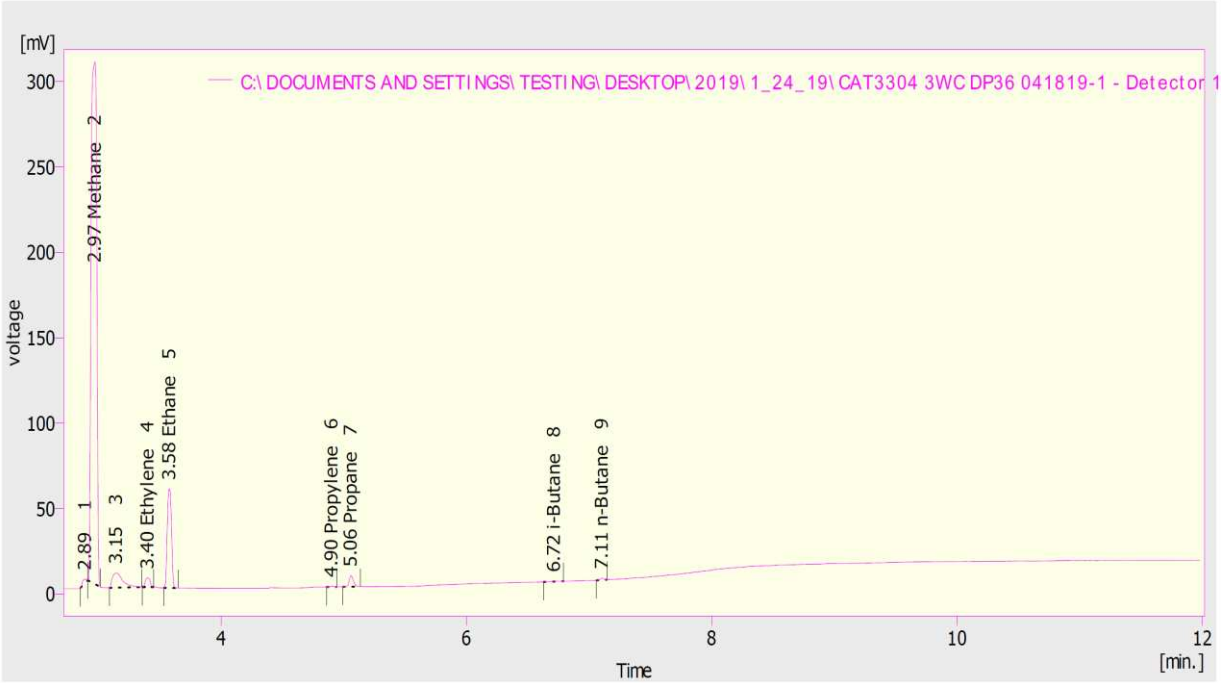

Figure B-61. Sample chromatogram depicting response peaks detected by the HP GC during Data Point 36 for the Caterpillar rich burn with a 3-way catalyst configuration.

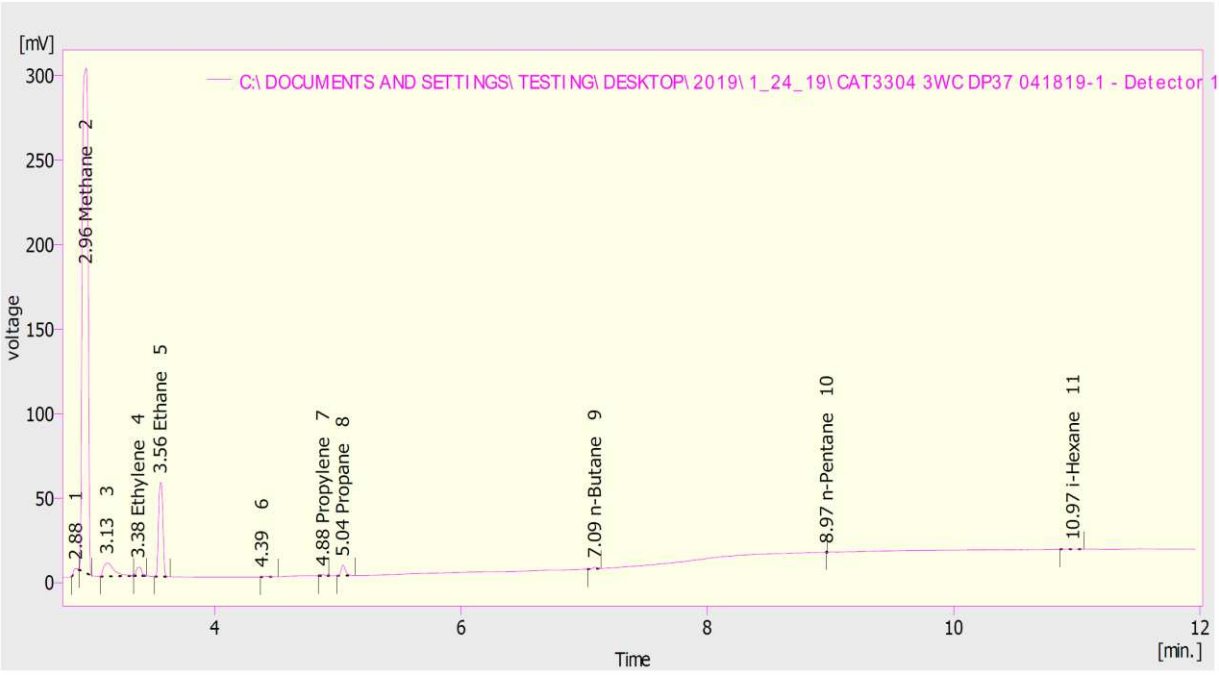

Figure B-62. Sample chromatogram depicting response peaks detected by the HP GC during Data Point 37 for the Caterpillar rich burn with a 3-way catalyst configuration.

Table B-1. Total VOC concentration in units of ppmd, as propane calculated using each method for every data point taken on the GMV-4 and Caterpillar 3304 engine programs.

Data Point	MKS	5-Gas THC-MKS	MKS FIDeq NMNEHC	HP GC	HP GC Tedlar Bag	VIG Residual	VIG FID Residual + MKS C2H4	VIG FID Residual + C2 - MKS C2H6	Gasmet VOC as propane	Gasmet VOC Sum
1	42.6	116	44.1	39.8	39.2	33.8	40.2	32.5	39.7	39.6
2	39.5	41.8	41.7	39.2	34.5	24.3	28.5	38.4	41.1	41.1
3	44.3	69.4	45.8	44.3	38.1	39.0	49.3	46.6	43.1	42.9
4	35.9	28.4	37.5	28.6	33.9	29.2	35.0	12.7	36.4	36.3
6	32.7	45.6	34.1	31.2	30.7	27.6	33.4	13.7	35.3	35.2
7	29.3	51.1	30.4	27.7	27.4	25.0	32.3	7.72	31.7	31.5
8	30.9	66.5	31.8	24.6	28.9	24.5	33.5	5.43	32.9	32.8
9/10	115	171	121	106	103	76.9	84.2	51.0	109	109
11	33.5	64.9	34.9	33.6	31.2	24.5	30.9	-1.84	35.1	35.0
12	38.7	89.8	40.3	33.4	32.9	26.4	34.9	32.9	N/A	N/A
13	34.9	82.1	36.2	29.6	30.9	26.3	34.2	31.8	N/A	N/A
14	43.0	84.8	44.4	37.7	37.5	28.8	39.2	33.0	N/A	N/A
17	40.8	78.7	42.6	36.5	35.6	28.6	36.4	32.4	N/A	N/A
18/19	36.5	74.4	37.9	32.0	32.2	24.3	34.2	36.4	N/A	N/A
20/21	82.6	125	87.2	76.3	77.0	68.6	77.1	73.9	N/A	N/A
23	30.6	52.2	32.2	26.5	25.6	20.0	28.9	25.0	35.6	35.4
24	31.6	51.1	33.3	27.4	26.6	20.4	30.3	24.1	30.8	30.6
25	27.5	52.4	28.7	22.7	21.0	17.5	26.2	21.6	27.9	27.8
27	28.9	56.5	30.4	26.0	23.0	17.9	27.0	22.5	27.4	27.3
28/29	28.2	51.8	29.6	25.4	23.3	16.3	28.1	23.6	27.0	26.8
30/31	55.3	77.5	58.6	49.7	46.4	42.6	52.3	44.9	27.7	27.5
32	29.8	51.3	31.3	24.0	24.2	18.2	27.4	21.1	33.5	33.3
33	12.8	10.7	14.5	5.63	4.78	5.68	9.91	7.08	6.77	6.68
34	12.2	14.6	14.1	5.26	4.67	6.27	10.3	7.06	6.45	6.34
35	12.7	14.9	14.5	5.57	4.73	5.86	10.2	6.83	10.3	10.1
36	12.6	14.4	14.3	5.34	4.78	6.02	10.1	7.25	10.7	10.1
37	12.4	14.0	14.2	5.44	4.74	5.94	10.0	7.03	9.56	9.41

Table B-2. Brake specific total VOC concentration in units of g/bhp-hr calculated using each method for every data point taken on the GMV-4 and Caterpillar 3304 engine programs.

Data Point	MKS	5-Gas THC-MKS	MKS FIDeq NMNEHC	HP GC	HP GC Tedlar Bag	VIG Residual	VIG FID Residual + MKS C2H4	VIG FID Residual + C2 - MKS C2H6	Gasmet VOC as propane	Gasmet Sum
1	0.593	1.619	0.614	0.555	0.545	0.471	0.560	0.452	0.551	0.549
2	0.508	0.539	0.536	0.505	0.444	0.313	0.367	0.495	0.528	0.527
3	0.548	0.858	0.566	0.547	0.471	0.482	0.609	0.576	0.530	0.527
4	0.525	0.415	0.549	0.419	0.496	0.428	0.512	0.186	0.531	0.529
6	0.486	0.677	0.506	0.462	0.456	0.409	0.496	0.203	0.521	0.519
7	0.398	0.692	0.411	0.376	0.371	0.338	0.437	0.105	0.428	0.426
8	0.425	0.916	0.439	0.339	0.398	0.337	0.462	0.075	0.452	0.450
9/10	1.290	1.923	1.365	1.192	1.159	0.864	0.946	0.573	1.227	1.222
11	0.389	0.753	0.404	0.390	0.361	0.284	0.358	-0.021	0.405	0.403
12	0.552	1.281	0.575	0.476	0.469	0.377	0.497	0.469	N/A	N/A
13	0.502	1.181	0.521	0.426	0.445	0.379	0.492	0.457	N/A	N/A
14	0.624	1.230	0.644	0.547	0.543	0.417	0.569	0.479	N/A	N/A
17	0.608	1.175	0.636	0.544	0.531	0.427	0.543	0.483	N/A	N/A
18/19	0.528	1.076	0.548	0.463	0.465	0.351	0.494	0.527	N/A	N/A
20/21	1.191	1.799	1.257	1.100	1.110	0.989	1.111	1.065	N/A	N/A
23	0.394	0.671	0.415	0.341	0.329	0.258	0.372	0.322	0.457	0.454
24	0.408	0.660	0.430	0.354	0.343	0.263	0.392	0.311	0.397	0.395
25	0.445	0.849	0.464	0.367	0.341	0.284	0.424	0.350	0.451	0.448
27	0.486	0.950	0.511	0.437	0.388	0.302	0.455	0.379	0.462	0.459
28/29	0.466	0.855	0.488	0.418	0.384	0.270	0.463	0.389	0.444	0.441
30/31	0.710	0.995	0.752	0.638	0.596	0.547	0.672	0.577	0.355	0.353
32	0.394	0.677	0.413	0.317	0.319	0.241	0.362	0.278	0.441	0.438
33	0.037	0.031	0.042	0.016	0.014	0.016	0.029	0.020	0.019	0.019
34	0.035	0.042	0.041	0.015	0.013	0.018	0.030	0.020	0.019	0.018
35	0.037	0.044	0.042	0.016	0.014	0.017	0.030	0.020	0.030	0.029
36	0.036	0.042	0.041	0.015	0.014	0.017	0.029	0.021	0.031	0.029
37	0.036	0.041	0.041	0.016	0.014	0.017	0.029	0.020	0.028	0.027

Table B-3. Percent relative measurement difference of each method compared to the HP GC for every data point taken on the GMV-4 and Caterpillar 3304 engine programs.

Data Point	MKS	5-Gas THC-MKS	MKS FIDeq NMNEHC	HP GC	HP GC Tedlar Bag	VIG Residual	VIG FID Residual + MKS C2H4	VIG FID Residual + C2 - MKS C2H6	Gasmet VOC as propane	Gasmet Sum
1	6.89	192	10.7	0.00	-1.68	-15.1	0.965	-18.5	-0.664	-0.977
2	0.63	6.67	6.24	0.00	-12.0	-38.1	-27.4	-2.04	4.49	4.30
3	0.12	56.8	3.41	0.00	-14.0	-12.0	11.3	5.23	-3.13	-3.59
4	25.26	-0.941	30.9	0.00	18.4	2.03	22.1	-55.5	26.7	26.3
6	5.09	46.3	9.50	0.00	-1.37	-11.5	7.36	-56.2	12.6	12.2
7	5.85	84.2	9.51	0.00	-1.22	-9.92	16.4	-72.2	13.9	13.4
8	25.2	170	29.2	0.00	17.2	-0.732	36.0	-77.9	33.2	32.5
9/10	8.16	61.3	14.5	0.00	-2.85	-27.5	-20.7	-52.0	2.89	2.47
11	-0.27	93.1	3.71	0.00	-7.27	-27.2	-8.17	-105	3.80	3.46
12	16.0	169	20.9	0.00	-1.33	-20.8	4.57	-1.43	N/A	N/A
13	17.8	177	22.1	0.00	4.45	-11.1	15.3	7.22	N/A	N/A
14	14.0	125	17.7	0.00	-0.626	-23.8	3.95	-12.5	N/A	N/A
17	11.7	116	16.8	0.00	-2.37	-21.6	-0.241	-11.2	N/A	N/A
18/19	14.1	132	18.5	0.00	0.511	-24.1	6.73	13.8	N/A	N/A
20/21	8.29	63.6	14.3	0.00	0.926	-10.1	1.04	-3.16	N/A	N/A
23	15.6	96.9	21.6	0.00	-3.56	-24.4	9.09	-5.70	34.1	33.2
24	15.4	86.8	21.7	0.00	-2.98	-25.7	10.8	-12.0	12.2	11.6
25	21.3	131	26.4	0.00	-7.20	-22.7	15.4	-4.54	22.9	22.1
27	11.3	117	16.9	0.00	-11.4	-31.0	3.98	-13.4	5.54	4.86
28/29	11.4	104	16.6	0.00	-8.28	-35.5	10.7	-6.88	6.11	5.42
30/31	11.3	56.0	17.8	0.00	-6.62	-14.3	5.26	-9.57	-44.4	-44.7
32	24.1	113	30.1	0.00	0.443	-24.1	14.1	-12.4	38.9	38.1
33	127	90.7	158	0.00	-15.1	1.06	76.1	25.9	20.0	18.4
34	133	177	167	0.00	-11.3	19.1	96.4	34.2	22.2	20.1
35	129	168	161	0.00	-15.0	5.23	82.6	22.8	84.1	81.0
36	135	169	168	0.00	-10.4	12.7	89.9	35.8	99.0	87.9
37	129	158	162	0.00	-12.9	9.20	84.5	29.4	75.4	72.5

Table B-4. Uncertainty of total VOC concentration for each method in units of ppmd, as propane for every data point taken on the GMV-4 and Caterpillar 3304 engine programs.

Data Point	MKS	5-Gas THC-MKS	MKS FIDeq NMNEHC	HP GC	HP GC Tedlar Bag	VIG Residual	VIG FID Residual + MKS C2H4	VIG FID Residual + C2 - MKS C2H6	Gasmet VOC as propane	Gasmet Sum
1	8.35	285	7.30	5.89	3.59	5.41	7.21	38.3	2.12	2.75
2	9.10	177	6.22	9.24	5.19	2.22	5.37	42.0	1.68	2.40
3	12.7	235	6.30	12.4	8.87	2.35	14.47	63.3	1.88	2.41
4	7.60	179	6.24	4.99	3.80	4.41	6.59	36.1	1.18	2.06
6	12.2	322	4.83	9.07	9.58	3.59	13.58	57.9	1.19	1.76
7	10.6	258	3.83	8.90	8.76	2.79	12.69	133	2.23	2.58
8	10.8	281	4.03	7.10	8.97	3.92	13.40	128	0.92	1.34
9/10	30.9	172	22.4	23.4	17.0	2.70	3.12	29.5	8.06	7.73
11	7.16	172	5.23	5.92	4.33	2.79	5.85	35.2	1.18	1.83
12	2.57	33.4	2.29	1.98	2.27	5.42	6.23	14.0	1.21	1.07
13	2.45	31.5	2.27	2.67	1.77	3.15	3.89	11.6	N/A	N/A
14	2.82	39.9	2.05	3.06	2.44	3.22	4.47	12.8	N/A	N/A
17	4.00	51.7	1.95	3.42	3.30	3.44	5.44	16.5	N/A	N/A
18/19	3.00	40.8	1.79	2.61	2.38	3.03	4.48	25.2	N/A	N/A
20/21	8.49	40.1	5.13	6.97	6.54	3.76	8.45	14.8	N/A	N/A
23	2.03	24.5	1.51	1.83	1.72	2.34	3.25	9.27	3.15	2.82
24	1.71	21.1	1.55	2.03	1.31	2.54	3.18	7.44	1.66	2.16
25	1.38	16.8	1.42	1.04	0.98	2.26	2.74	6.10	0.27	0.77
27	1.95	26.0	1.57	2.10	1.40	2.47	3.25	9.28	0.87	1.14
28/29	2.23	26.0	1.47	2.20	1.79	2.35	3.47	16.8	0.34	0.73
30/31	4.50	25.5	2.37	3.88	3.65	4.06	6.31	10.6	0.36	0.73
32	3.13	40.4	1.81	2.56	2.44	3.48	4.96	14.9	2.48	2.31
33	1.06	16.3	0.94	0.36	0.38	2.41	3.04	4.90	3.10	2.24
34	1.06	15.8	0.93	0.42	0.42	2.22	2.83	4.81	1.21	1.07
35	1.08	18.7	0.94	0.38	0.36	2.50	3.15	6.64	0.58	0.99
36	1.04	15.7	0.96	0.38	0.38	2.31	2.92	6.07	1.95	0.96
37	1.04	16.1	0.97	0.42	0.34	2.20	2.78	5.08	0.98	1.16

Table B-5. Uncertainty of total VOC concentration as a percentage of the total VOC concentration calculated for each method for every data point taken on the GMV-4 and Caterpillar 3304 engine programs.

Data Point	MKS	5-Gas THC-MKS	MKS FIDeq NMNEHC	HP GC	HP GC Tedlar Bag	VIG Residual	VIG FID Residual + MKS C2H4	VIG FID Residual + C2 - MKS C2H6	Gasmet VOC as propane	Gasmet Sum
1	19.62	245.24	16.55	14.77	9.16	16.00	17.93	117.98	5.33	6.95
2	23.07	422.14	14.93	23.57	15.05	9.14	18.87	109.40	4.08	5.84
3	28.58	337.82	13.75	27.98	23.27	6.03	29.34	135.81	4.35	5.62
4	21.20	632.81	16.65	17.41	11.20	15.11	18.85	283.22	3.23	5.66
6	37.32	705.40	14.15	29.13	31.17	13.03	40.61	424.03	3.38	4.99
7	35.97	504.26	12.62	32.11	31.97	11.18	39.32	1727.63	7.04	8.18
8	35.07	422.01	12.64	28.82	31.05	16.02	39.98	2352.74	2.80	4.10
9/10	26.95	100.53	18.46	22.04	16.51	3.50	3.71	57.79	7.37	7.09
11	21.35	264.86	14.98	17.61	13.90	11.37	18.95	-1916.52	3.36	5.24
12	6.66	37.14	5.69	5.93	6.90	20.51	17.88	42.74	N/A	N/A
13	7.01	38.39	6.28	9.02	5.72	11.96	11.38	36.51	N/A	N/A
14	6.57	47.08	4.61	8.10	6.51	11.21	11.41	38.90	N/A	N/A
17	9.82	65.66	4.58	9.36	9.25	12.03	14.94	51.00	N/A	N/A
18/19	8.22	54.80	4.72	8.14	7.41	12.47	13.10	69.03	N/A	N/A
20/21	10.27	32.16	5.88	9.13	8.49	5.49	10.96	20.07	N/A	N/A
23	6.62	46.98	4.68	6.90	6.72	11.68	11.25	37.12	8.85	7.96
24	5.42	41.28	4.65	7.42	4.95	12.47	10.49	30.87	5.40	7.05
25	5.03	32.11	4.95	4.60	4.66	12.90	10.48	28.19	0.97	2.79
27	6.75	46.11	5.18	8.06	6.06	13.78	12.01	41.21	3.17	4.19
28/29	7.90	50.14	4.96	8.67	7.70	14.38	12.37	71.06	1.25	2.74
30/31	8.14	32.90	4.04	7.81	7.87	9.52	12.05	23.57	1.29	2.67
32	10.49	78.80	5.79	10.63	10.10	19.07	18.07	70.84	7.41	6.92
33	8.31	151.66	6.46	6.46	7.91	42.34	30.71	69.23	45.79	33.57
34	8.63	108.22	6.64	7.91	8.91	35.50	27.35	68.05	18.80	16.88
35	8.49	125.58	6.50	6.85	7.65	42.67	30.97	97.13	5.64	9.82
36	8.26	108.94	6.70	7.19	7.88	38.44	28.81	83.63	18.30	9.51
37	8.39	114.73	6.79	7.80	7.11	37.07	27.75	72.27	10.26	12.30

Table B-6. Destruction efficiency of hydrocarbons for all data points taken on the GMV-4 and Caterpillar 3304 engines.

Data Point	Methane (%)	Ethane (%)	Propane (%)	i-Butane (%)	n-Butane (%)	i-Pentane (%)	n-Pentane (%)	n-Hexane (%)
1	94.0	94.3	95.9	98.4	95.9	98.3	97.7	100
2	93.5	93.7	95.3	96.6	95.5	98.1	97.7	100
3	94.6	94.2	96.0	97.1	96.3	98.7	97.8	100
4	94.8	95.0	96.3	97.3	96.4	98.6	97.9	100
6	94.2	94.4	95.9	97.0	96.1	98.6	98.4	100
7	94.7	95.0	96.2	97.3	96.4	99.1	98.2	100
8	95.7	96.1	97.1	98.0	97.1	99.3	98.6	100
9/10	94.2	94.5	95.8	95.7	96.7	98.3	98.7	100
11	94.5	94.7	95.9	96.2	96.7	98.5	98.8	100
12	95.3	95.6	96.6	97.3	97.0	99.0	98.7	100
13	95.4	95.8	97.1	97.8	97.6	99.1	99.0	100
14	96.0	96.3	97.3	97.9	97.5	97.9	98.6	100
17	95.4	95.6	96.7	97.6	97.0	97.7	98.5	100
18/19	95.7	95.9	96.9	97.7	97.1	97.9	98.8	100
20/21	95.5	95.8	96.8	97.4	97.0	97.4	98.5	100
23	96.7	97.0	97.9	98.2	98.0	98.7	99.0	100
24	96.5	96.9	97.8	98.0	97.9	98.3	98.8	100
25	97.0	97.3	98.1	98.5	98.3	99.3	98.9	100
27	96.4	96.7	97.7	98.0	97.8	98.3	98.7	100
28/29	96.6	97.0	97.8	98.2	98.0	98.6	98.8	100
30/31	96.9	97.1	98.1	98.1	98.0	98.5	98.8	100
32	96.8	97.2	98.1	98.5	98.3	98.9	99.1	100
33	99.4	99.7	99.9	99.9	99.9	99.9	100	100
34	99.5	99.7	99.9	99.9	99.9	100	100	100
35	99.4	99.7	99.9	99.9	99.9	100	100	100
36	99.5	99.7	99.9	99.9	99.9	100	100	100
37	99.4	99.7	99.9	100	99.9	100	100	100